HYDROGEOLOGIC CHARACTERISATION OF CRYSTALLINE BASEMENT AQUIFERS OF PART OF IBARAPA AREA, SOUTHWESTERN NIGERIA

BY

OLANREWAJU AKINFEMIWA AKANBI
B.Sc. (Hon.), M.Sc. Geology (Ibadan)

MATRIC. No. : 69594

A thesis in the Department of Geology submitted to the Faculty of Science in partial fulfilment of the requirement for the award of the degree of

DOCTOR OF PHILOSOPHY

of the

UNIVERSITY OF IBADAN

APRIL, 2017

ABSTRACT

Globally, nearly half of human population relies on groundwater for various uses. However, the occurrences of this vital resource are usually constrained in areas underlain by crystalline bedrocks. This is more critical in the southwestern Nigeria (SN), where about half of the landmass is underlain by crystalline bedrocks; hence the need for proper hydrogeological characterisation of crystalline basement aquifers. Therefore, this study was designed to focus on geological, geomorphological, geophysical and hydraulic characterisations of the crystalline basement aquifers of part of Ibarapa area located in the SN in order to determine the groundwater potential and ensure sustainable groundwater development.

The study utilised geological, remote sensing, Vertical Electrical Sounding (VES) and pumping test methods. The geological approach involved geological field mapping, while the remote sensing method included the use of Radar and Landsat imageries from which thematic maps (drainage, elevation, lineament/fracture, and vegetation index) processed with ArcGIS and Erdas imagine software were generated. Eighty-five VES were carried out using Schlumberger array. The field data were processed by partial curve matching and computer iteration using Winresist 1.0 software. Longitudinal conductance derivatives were estimated for assessment of recharge potential from the VES data. Single-well pumping tests with constant discharge and corresponding recovery tests were carried out on twenty-three boreholes for the determination of hydraulic (transmissivity and hydraulic conductivity) parameters.

Amphibolite, gneisses, migmatite and porphyritic granite were the underlying rock units delineated. Weathering potential was higher in amphibolite and gneisses due to foliation and abundance of ferromagnesian minerals. Geomorphological characterisation revealed two hydro-geomorphic units: the high-lying areas underlain by migmatite (characterised by ridges and inselbergs of porphyritic granite) and the low-lying areas underlain by gneisses and amphibolite representing groundwater discharge zones. The dominant VES curve types were three-layer H-type (91.5%), characterised by moderate to thick weathered regolith with thickness >18m in

amphibolite and gneisses terrains, compared to <13m in migmatite and porphyritic granite areas. The corresponding resistivity (Ωm) for the weathered layers were 9.1 – 225.2, 18.8 – 810.6, 28.1 – 565.5 and 26.5 – 294.0 for amphibolite, gneisses, migmatite and porphyritic granite, respectively. The estimated total longitudinal conductance (Ω^{-1}) was 0.02 – 0.60 in migmatite and porphyritic granite, and 0.01 – 1.42 in amphibolite and gneisses which is an indication of thicker clayey weathered units. The estimated transmissivities (m^2/day) were 0.25 – 11.65 in amphibolite and gneisses area; and 0.56 – 2.95 in migmatite and granite terrains. The corresponding hydraulic conductivities (m/day) were 0.54 – 66.80 × 10^{-2} and 2.31 – 19.69 ×10^{-2}. These hydraulic results indicated that boreholes in amphibolite and gneisses terrains have good water transmission capacity. Thirty-five percent of all the tested boreholes attained dynamic equilibrium water level at low drawdown during pumping; an indication of higher yield of the penetrated fractured bedrock and rock contacts especially in gneisses and amphibolite terrains.

Areas underlain by amphibolite and gneisses in Ibarapa region were characterised by good hydrogeological attributes that may guarantee sustainable productive boreholes, while areas underlain by migmatite and porphyritic granite exhibit low groundwater potential that can only sustain hand-dug wells.

Keywords: Bedrock delineation, Hydro-geomorphic, Longitudinal conductance, Hydraulic parameters, Fractured bedrock

Word count: 491

DEDICATION

This work is dedicated to all the saints of our LORD, who through patience and endurance possess the promise of GOD- the Father of our Lord and Saviour Jesus Christ.

''For as the sufferings of Christ abound in us, so also our consolation also abounded by Christ''- 2 Corinthians 1:5.

''For I reckon that the sufferings of this present time are not worthy to be compared with the glory which shall be reveal*ed in us''*- Romans 8:18.

I also dedicate this work to my wife who stood by me, through all the challenging moments. Oluwatosin you are amazing!

CERTIFICATION

I certify that this work was carried out by Mr. O.A. Akanbi in the Department of Geology of University of Ibadan-Ibadan Nigeria.

……

Supervisor

Moshood 'Niyi Tijani

B.Sc., (Ilorin), M.Sc., (Ibadan), PhD (Muester)

Professor of Hydrogeology and Environmental Geology

University of Ibadan, Nigeria

ACKNOWLEGEMENTS

First and foremost, I sincerely acknowledge God's Grace and interventions for the completion of this research in University of Ibadan.

I am grateful to my research Supervisor- Professor Tijani N. Moshood for his support, assistance and for sparing his time to read through the thesis. I also appreciate his generosity for the free utilization of his personal equipment - the depth sounder/water level indicator which is a crucial tool employed for hydraulic investigation. Thank you sir and God bless you.

I acknowledge the people of Ibarapa region, particularly those at Igboora, Idere, Ayete, and Tapa Towns and the adjoining villages. I salute the Directors of works of Ibarapa North and Ibarapa Central LGAs of Oyo State between 2010 and 2013 during the period of my field data collation. I also acknowledge the assistance of the WATSAN Coordinators of these LGAs. I am also grateful to the hired crew that went along with me during the hydraulic data collations, namely Mr. Iyiola, Mr. Oguntoye, Jelili, Demola, and Kunle. Additionally, I also appreciate the various security outfits for their cooperation at the time when field tests and investigations were conducted.

I thank all the academic staff of the Department of Geology, University of Ibadan. I am grateful to the Head of Department- Professor O.A. Ehinola. I also appreciate all my Teachers, especially Professor A.I. Olayinka- the current Vice-Chancellor of University of Ibadan and Dr. A.T. Bolarinwa for their personal interests and support, which eventually facilitated the completion of this work. I am also grateful to Professor G. O. Adeyemi for his encouragement and good wishes. Additionally, I also wish to thank Dr. M.A. Oladunjoye for his contribution in the interpretation of the geophysical data and Dr. S.A. Olatunji (the Postgraduate Coordinator) for his advice and admirable contributions to this work. Professor Okunlola, (the immediate past President of NMGS) for his input in the modifications of the geological map of the study area.

I salute the entire staff of the Department of Earth sciences of Ajayi Crowther University, Oyo, where I am presently lecturing. I am grateful to the pioneer Head of Department- Prof. S.S. Dada who recognized the need for granting day-off when necessary for academic staff on research programme to facilitate speedy completion of their research works. I am also thankful to my present Head of Department- Professor O. Oshin, for relieving me of the duty of Departmental examination Officer in order to complete my research degree. My appreciation also goes to other Ex. HOD, including Prof. D.R. Adeleye and Dr. O. Lawal for their assistance in reaching out to all necessary contacts for the completion of this work. I need to mention the credible affectionate kindness shown to me by Mr. J.A. Aderogbin and Dr. (Mrs.) E.E. Umoh for taking up the teaching of my courses during the period I went for data collation at Ibarapa.

I also wish to acknowledge G.P. Kruseman and N.A. de Ridder for free online download of their book titled 'Analysis and evaluation of pumping test data' that assisted me in analysing the groundwater hydraulic data. Though, these Authors were acknowledged in the list of references, they deserve special recognition for their liberality.

I also appreciate the inputs of Mr. Oluwatola Adedeji for his expertise in GIS and remote sensing applications. Also, Mr. Joseph of the Department of Geography of University of Ibadan for my Cartographic works.

I also acknowledge Mr. Ayoade- the owner of Joy Crown Hotel at Igboora for granting me a discount during my long stay at Igboora for the field mapping and data collation exercises. Thank you and God bless you.

I thank my Father, Papa Timothy Akanbi and my Parents-in-law Papa and Mama Shotonade for their prayers and good wishes. My Sister, Mrs. Bunmi Oyedemi with her husband Pastor Tope Oyedemi for their intercessions and encouragement. Also, my gratitude to Papa and Mama Ojo at Awe Town, Bro. Amos Sublim, Pastor Remi Adejumobi, and Evangelist Israel Olulowo for their concerns, prayers and good wishes. You will not miss your reward.

I also wish to acknowledge and appreciate all my Examiners for their assessments and contributions to this work.

Lastly, I thank my wife and our daughters Inioluwa and Toluwa for their understanding, cooperation and support. You are my inspiration for holding on till the end. Thank you all.

TABLE OF CONTENTS

LIST OF FIGURES

LIST OF TABLES

LIST OF PLATES

LIST OF APPENDICES

CHAPTER 1

1.0 INTRODUCTION

1.1 General Statement

Water is essential for life on Earth. Apart from oxygen, fresh water is the next most indispensable natural resource for man and other living things. Fresh water is found as gas in the atmosphere and as solids in glaciers, ice caps and snow. Also, fresh water occurs in liquid form in inland surface water bodies such as streams, rivers, and lakes. Similarly, fresh water is found in underground environment in soils and rocks and in other geological structural units such as fractures, faults as well as other rock discontinuities. However, the degree of water saturation varies within the subsurface environment and any geological unit that is fully saturated is called an aquifer; and the enclosed water is known as groundwater.

Comparatively, out of all fresh water sources, groundwater is more desirable in respect of quality and availability. This is because groundwater is concealed in underground environment; hence, it is less exposed to pathogens and less vulnerable to contamination. Additionally, groundwater is renewable and it is readily more accessible than most of other fresh water sources (Heath, 1983; Edmund and Smedley, 2005; MacDonald, *et. al.* 2005; Healy, et al. 2007; Tijani, 2016). Also, groundwater temperature is constant and not affected by weather conditions, unlike surface waters that are largely influenced by changes in land temperatures. Consequently, approximately 50% of world citizens relies on groundwater for domestic, industrial and agricultural utilisation (Siebert, 2010). This proportion is larger in developing countries such as sub-Sahara Africa and parts of Asia, where there is continual increase in human population, as well as in agricultural and industrial growths. These growths create the need for expansion of social amenities such as water supply and electricity. Due to this need for the increase in the supply of fresh water, crystalline

basement terrains where potentials for groundwater occurrences are low (Heath, 1983; Danskin, 1998) are now being investigated in detail for groundwater development.

Crystalline basement terrains are underlain by igneous and metamorphic rocks that ordinarily cannot store nor transmit groundwater. Crystalline basement terrains are also associated with complex structural framework and abrupt change in rock lithology. This is unlike sedimentary environments where rocks are more continuous. Also, sedimentary rocks are characterised by development of primary porosity that can be up to 45% for unconsolidated coarse sands, whereas the porosity of most unweathered crystalline rocks such as granite and gneiss could be as low as 0.01% (Freeze and Cherry, 1979, Driscoll, 1986). Nevertheless, considerable groundwater zones can develop in basement terrains when the impermeable crystalline bedrocks undergo intense weathering and fracturing. Hence, in basement terrains groundwater bearing units are found within the fractures zones or where significant regolith thickness develops on the fresh crystalline rocks. Singhal and Gupta (1999) emphasized that, if there is a good and a perennial source of recharge; thick and extensive weathered regolith on fresh basement rocks can form potential aquifers, and a thin regolith layer of 5-7m thickness can be a good source of groundwater supply.

In this regard, many groundwater investigations have been undertaken in the basement terrains of Nigeria to delineate groundwater potential zones (Olorunfemi and Olorunniwo, 1985, 1990; Ako et al., 1990; Malomo et al., 1991; Olayinka and Mbachi, 1992; Olorunfemi and Okhue, 1992; Philip and Singhal, 1992; Abimbola et al., 1999; Singhal and Gupta, 1999; Olayinka and Olayiwola, 2001; Tijani and Abimbola, 2003; Oseji, et.al., 2005; Tijani et al., 2006; Oladapo and Akintorinwa, 2007; Alile *et. al.*, 2008). Most of these investigations in crystalline basement areas described the lithology of the weathered-fractured zones from geophysical point of view, and chemical evolution of the enclosed water. However, studies in respect of hydraulic characterisation of crystalline aquifers are scantily reported and documented in developing nations such as Nigeria. Furthermore, the attributes of groundwater occurrences in crystalline basement terrains have been described to be erratic, localized and shallow. Also, groundwater recharge seasonal and mainly from precipitation (Jones and Hockey, 1964; Egboka, 1987; Tijani and Abimbola, 2003; Oladapo and Akintorinwa, 2006; Jayeoba and Oladunjoye, 2013; Tijani, 2016; Akanbi,

2016). These hydrological attributes pose great challenges for groundwater sustainability in areas underlain by basement rocks.

Hence, as a result of the complexity in groundwater occurrences in basement terrains; methods involving the integration of remote sensing and geographic information systems are also integrated to delineate groundwater potential zones across a large area coverage (Teme, S.C. and Oni, S.F. 1991; Talabi and Tijani, 2011; Fashae *et. al.* 2014). Nevertheless, comprehensive investigations of the crystalline water bearing zones in basement areas of Nigeria are still inadequate, and lack of understanding of the occurrence, movement and recharge processes of groundwater in basement terrain have frequently contributed to the failure of many boreholes in basement terrains (UNESCO, 1984a; Chilton and Foster, 1995; Holland, 2011; Akanbi, 2016).

In the light of this, detail studies such as hydro-geomorphic investigations, as well as hydrologic and hydraulic characterisations of crystalline aquifer units need to be incorporated. This is required for complete understanding of the groundwater dynamics of basement areas of Nigeria. Furthermore, the hydraulic characterisations of the water bearing zones will provide a comprehensive understanding of the possible yield and sustainability of the groundwater supply in crystalline basement areas. This can be achieved from the estimations of the aquifer properties from pumping tests, and from the understanding of the groundwater recharge processes. These comprehensive studies are crucial in Nigeria where about half of the landmass is underlain by crystalline basement crust (Oyawoye, 1972; Dada, 1998; Offodile, 2002). Additionally, presently in Nigeria, there is gross inefficiency and break-down of conventional piped water supply schemes. This is due to lack of maintenance culture and failure of the government to expand the existing social amenities. Hence, groundwater has become substitute to the municipal town water scheme in many cities and rural communities where such water scheme is grossly unavailable. This has resulted in increase in reliance on groundwater for various usage (Tijani, 2016). Consequently, as a result of increase in demand for water, it has been estimated that by 2030 there will be a deficit of over 17 billion litre/day in water supply in Nigeria (Ojo *et al.* 2004).

Therefore, the present investigation incorporates geological, structural and geomorphological approaches as well as geophysical characterisation for the

understanding of the weathered-fractured units to study the groundwater occurrence and distribution of Ibarapa region within the Basement Complex of southwestern Nigeria. In addition; hydraulic characterisation of the water-bearing zones of Ibarapa region will be integrated to provide tangible understanding on the yield, groundwater sustainability and recharge processes of this basement area. This will be a great contribution to groundwater development and sustainable management, especially in many rural and urban communities in Nigeria where weathered/fractured basement aquifers are being exploited for water supply scheme.

1.2 Aim and Objectives of the Present Work

The overall aim of the present research work is to characterise the hydrogeological settings of the crystalline bedrock aquifer systems of Ibarapa areas of SW Nigeria for sustainable groundwater development. This will involve the use of integrated application of geological and structural methods as well as geomorphological, geophysical and hydraulic approaches. To execute this, the following integral objectives will be carried out:

1. To study and delineate the study area into the various bedrock and fracture distribution units.
2. To generate hydro-geomorphological units and develop groundwater indication (thematic) maps.
3. To determine the lateral and vertical extents of weathering and the degree of development of bedrock fracturing from the primary geo-electric parameters, and to deduce the recharge potential across the study area from the secondary geo-electric parameters.
4. To characterise the aquifer system using the groundwater flow diagnostic plots and quantify the estimable hydrological and hydraulic parameters.

1.3 Scope

To accomplish the above itemized objectives, the scope of the present studies entails the following systematic approaches:

1. Geological and fracture characterisation will require conventional geological field mapping of the outcropping rocks with the purpose of generating rock boundaries and lineament distributions for the entire study area. Review of existing topographical and geological maps covering the study area will serve as guide for generating the geographical and geological data for the present work.
2. The geomorphological studies will incorporate the application of geographical information system (GIS) and the principles of remote sensing method for studying the landforms and the hydro-geomorphological features across the area. Hence, Landsat and Radar satellites images of appropriate bands and resolution covering the entire study area will be used to produce the essential hydro-geomorphological units (HGU) including digital elevation models (DEM) and the Normalized Difference Vegetation Index (NDVI) that indicate groundwater occurrence and recharge potentials from which thematic maps such as surface drainage network, relief/contour, elevation/landform and lineament distributions across the study area are to be generated. Rock boundary delineation and structural attributes from field geological mapping are to serve as control for the application of the remote sensing method in generating the aforementioned thematic maps.
3. Subsurface mapping of the weathering development and distribution across the varied bedrock boundaries in the study area will include the application of geophysical method such as vertical electrical sounding (VES). From the results of electrical soundings, the primary geo-electric parameters i.e. the layers' resistivities and thicknesses of each geo-electric sequence will be interpreted. Spatial spread of viable lithological geo-section profiles with respective lithological thicknesses will be outlined and mapped across the various bedrocks that underlie the study area. Also, the lithology of the weathered layer and the nature of the bedrock that succeed the weathered layers are to be characterised across the study area. Additionally, secondary geo-electric parameters, otherwise known as Dar-Zarrouk variables will also be calculated from the VES results to deduce the water conductance attributes of the regolith units and generate the groundwater potential map across the study area.
4. Hydraulic parameters of the water-bearing zones as well as the sustainability of the groundwater supply will be carried out by conducting single-well pumping tests (and corresponding recovery tests) on the existing suitable boreholes that penetrate the various bedrocks of the study area. The choice of appropriate method of

analyses of the pumping tests depends on the type of flow regime deciphered from the diagnostic plots of the pumping test data. From the trend of the time-drawdown curves of the flow regime, aquifer types and the boundary conditions of the water bearing zones are to be interpreted. Additionally, the recovery phase of the pumping tests are pointers to the recharging rate, from which the sustainability of the groundwater supply can be discussed in conjunction with hydraulic properties obtained from the pumping operations.

5. Data evaluation of the present work involved the processing and digitalizing of both the field and remotely sensed data and imageries to produce tables, diagrams, charts and maps. These graphic illustrations were produced using Microsoft office packages and appropriate GIS techniques and software that included ArcGIS, Edas Imagine, Surfer -10, Global Mapper and Map Source. For instance, various thematic maps are to be produced from the satellite imageries. Also, statistical evaluations and other mathematical operations will be done to produce charts, plots and tables for the estimations and appraisals of data variables. Additionally, interpretation of true geo-electric parameters will involve curve matching techniques and computer iteration using win-resist software and Surfer-10 for the generation of iso-resistivity and isopach maps.

1.4 The Study Area

1.4.1 Location, Extent and Accessibility

Ibarapa region is located within the southwestern part of Nigeria, bounded in the east by Ibadan- the capital city of Oyo State, Benin Republic at the west, Abeokuta at the south and Oke-Ogun at the North. Presently, Ibarapa region is made up of three political local government areas, namely-Ibarapa East, Ibarapa North, and Ibarapa central. The study area covered a total of 711.17 km^2 landmass area of Ibarapa region (Figure 1.1), on coordinates- 7^0 21' to 7^0 37'N and 3^0 07' to 3^o 21'E and, covering most parts of Ibarapa Central and Ibarapa North Local Government Areas of Oyo State of Federal Republic of Nigeria. Major township areas within the study area are Igboora, Idere, Ayete and Tapa; with their adjoining communities and villages. The major towns are fairly accessible and are connected by asphalted major road networks that link bigger Towns and cities such as Ibadan, Abeokuta and Iseyin. The adjoining hamlets and villages are however, poorly connected and are mostly accessible by

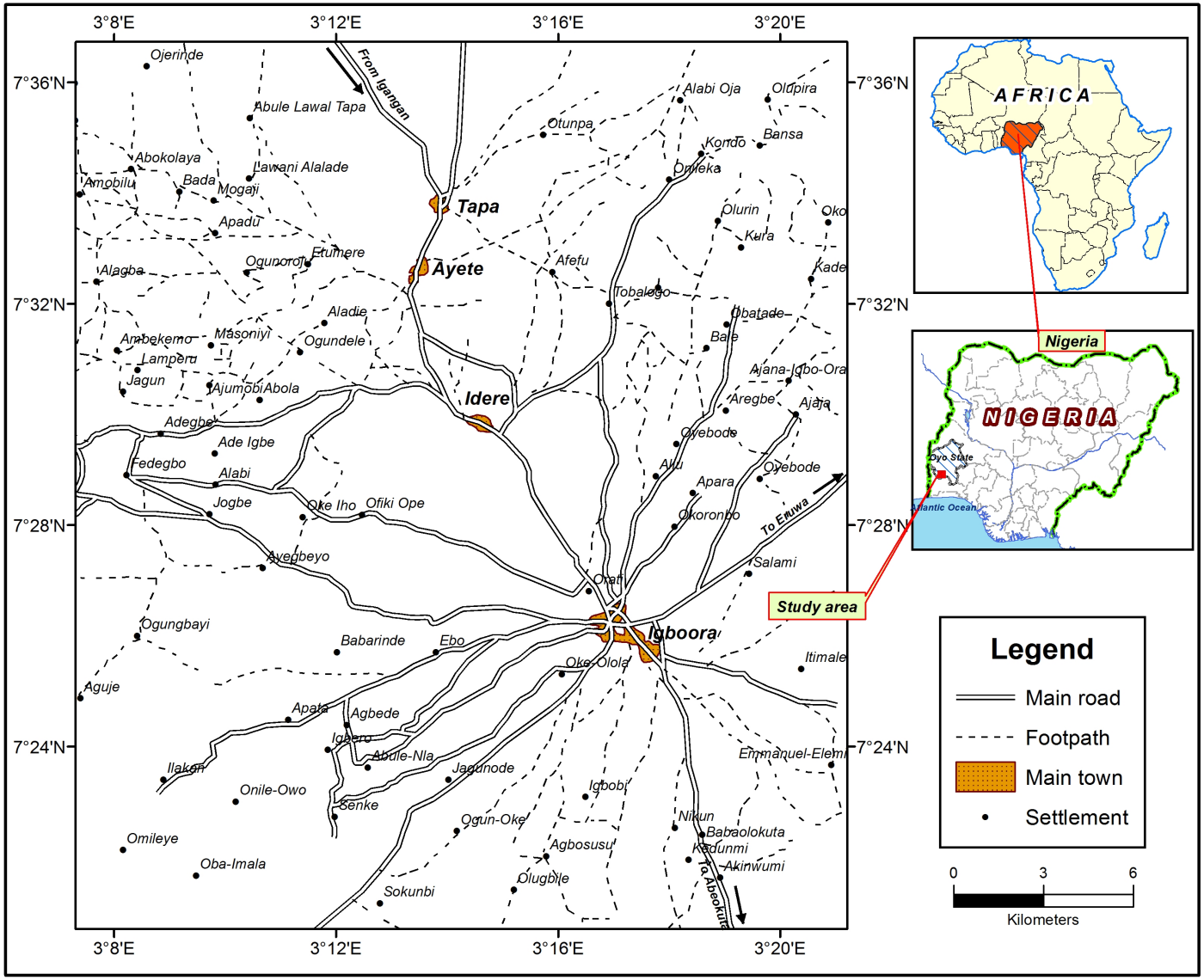

Figure 1.1: Location map of the Study Area

motorcycles, and by 4- wheel vehicles where the untarred roads are wide enough.

1.4.2 Climate and Vegetation

The study area lies within the tropical climatic zone, marked by two distinct seasons: wet and dry seasons. The dry season extends from November to March with an average monthly precipitation of less than 25mm. The wet season peaks around June and September with monthly rainfall exceeding 100mm. The total annual rainfall in the area ranges from 813 to 1853mm, while the annual temperature ranges from 24^0 to 29^0C. When compared to an average rainfall of 1541mm/yr for the entire SW Nigeria, the study area has lower average precipitation and higher average temperature (Munaserei, 1979; Daly, *et. al.*, 1981; David, 1988; Tijani, 2016). Hence, it is expected that the vegetal cover will not be as thick, compared to other parts of SW Nigeria. The vegetal cover is more of derived savannah forested land marked by scattered- scanty small trees and shrubs, sandwiched by tall grasses. It lies between the transition zone of lowland rain forest of southern areas of Nigeria and the savannah zone of the further northern areas of Oyo state. The vegetation index as groundwater indicator is discussed in latter sections of this work.

1.4.3 Relief

The relief of the study area is characterised by frequent rising and falling in elevations. Figure 1.2 shows the relief contours, with elevations above the mean sea level spanning from 90m in the flood plain area at the south-west boundary to 240m at the central hilly portion. However, Figure 1.3 is a 3-dimensional illustration of the relief of the area produced from elevation data obtained from the field revealed the highlands and intermediate valleys. The central portion of the area is mainly made up ridges extending from Igboora to the northern end of the study area.

1.4.4 Drainage and Watershed

The drainage pattern is dendritic (Figure 1.4) as typical of basement areas marked by high contrast in relief of inselbergs and hills. In a dendritic drainage pattern, tributary streams generally join at an acute angle forming Y-shaped junctions.The river network consists of primary rivers, namely Iworo, Ayin, Afo-Ape, Opeki, and Aboluku sourced from the highlands terrain underlain by crystalline rocks. River Ofiki is the major river

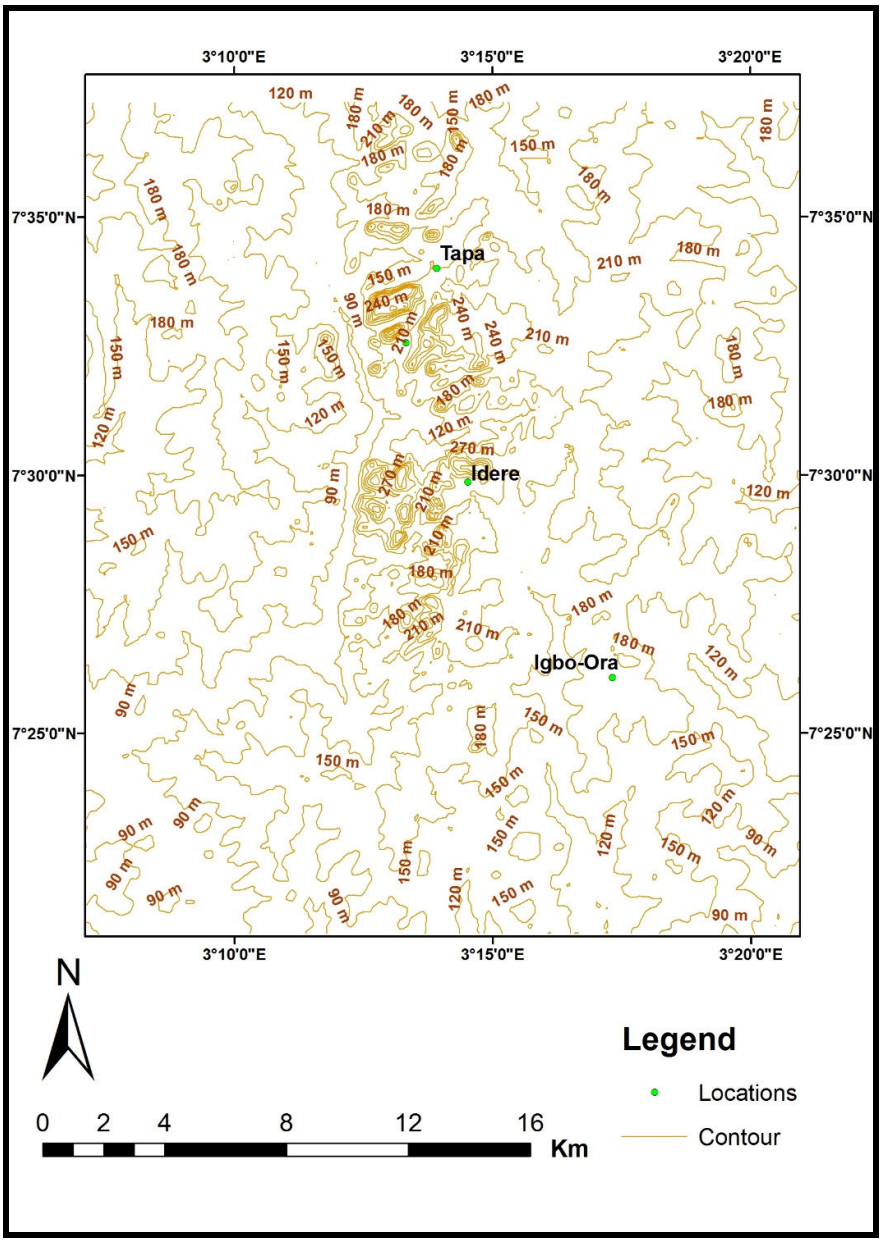

Figure 1.2: Topographical map of the Study Area

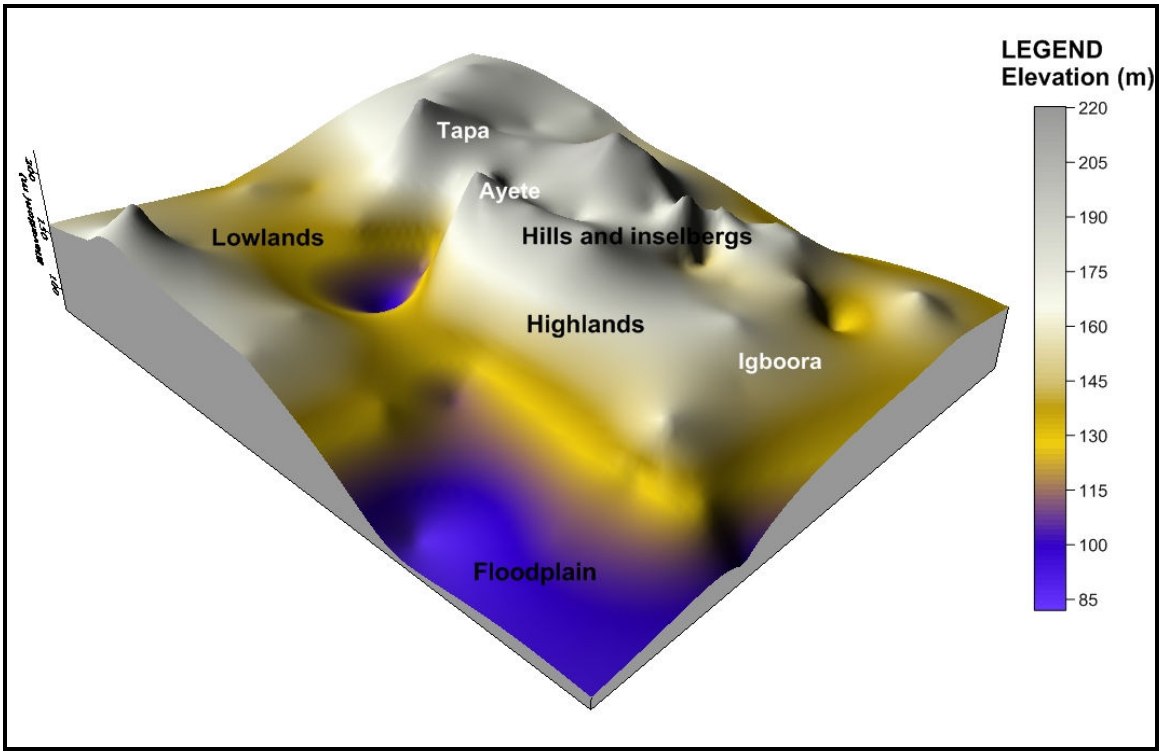

Figure 1.3 : 3D Surface landform expression, showing the contrast in Relief across the study area

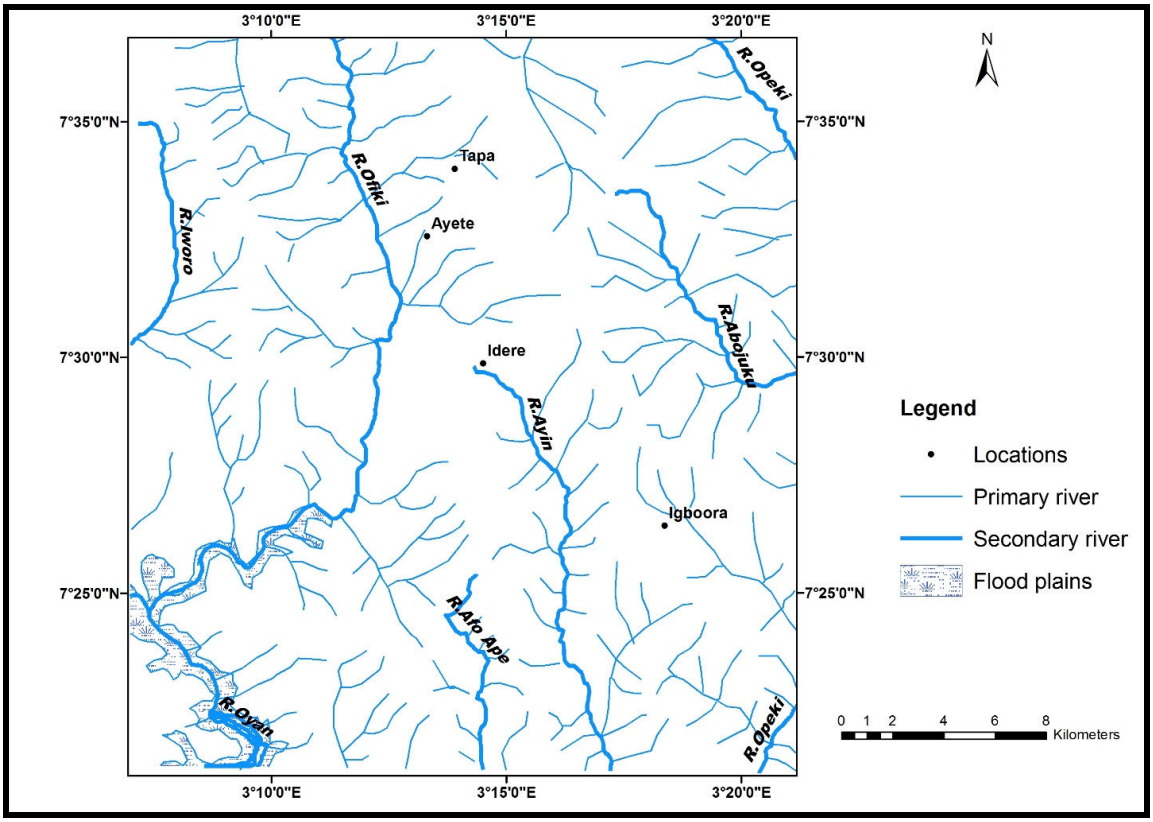

Figure 1.4: Drainage pattern of the study area

that drains the gneissic and granitic terrains and it runs into River Ayin (Secondary River) at the SW region. It is remarkable to note that the primary rivers in the area run along the rock boundaries and coincide with the major structural NNW-SSE and NNE-SSW trends development in the area. Other streams are intermittently connected to the primary rivers forming in orthogonal and oblique manners. This drainage pattern is more or less a design that separates the entire study area into interfluves.

Each interfluve can be regarded as an eroded upland area sandwiched in between two adjacent streams. By connecting interfluves that sourced from the same primary river, the entire area can be partitioned into six watershed units named after the primal river draining the area. These include Iworo at the NW, Ofiki central west, Afo-Ape at the south central, Ayin at the south central east and lastly the Aboluku-Opeki watershed extending from the eastern to the north-eastern. These watershed units can then be integrated with geological and geomorphological data to discuss the variations in hydrogeological attributes of the entire area. The various water-shed units that are recognised within the study area are discussed below.

The Iworo Watershed: This watershed is underlain by banded biotite gneiss steeply dipping west. The primary river draining this region (Iworo) aligns in N-S trend, along the strike of the rock foliation (Figure 1.4). Villages located within this catchment include, Akamo, Alaagba and Ajegunle.

The Ofiki Watershed: Ofiki watershed consists of the major river namely Ofiki. River Ofiki which is the longest and the most prominent river in the entire study area runs along the granitic and gneissic boundary and drains into River Oyan at the SW end. The tributaries of River Ofiki drain most part of inland regions of Oye-Igangan, Tapa, Ayete and Idere towns. This watershed has the most contrasting relief, ranging from the centrally ridged upland areas that are made up of mainly porphyritic granite and porphyroblastic gneiss hills and inselbergs, that peaked at approximately 350m above the sea level (with adjacent lower-relief areas) to the lowland of 57m which serve as the river course.

The Afo-Ape Watershed: This is a minor watershed located at the central southern part of the study area, underlain by porphyritic granitic. It is notably a lowland, with

elevation below 150m above sea level. However, the central portion is dominated by inselbergs with elevations that can be up to 300m above sea level.

The Ayin Watershed: This watershed unit covers the main township of Igboora and Idere with their adjoining areas. This region is the most complex in terms of rock types. Idere town and environ are noted by porphyritic granite hills, with preferred alignment of the feldspathic porphyries toward the western part. The rock type changes abruptly at the west to migmatite and to amphibolite at the SW. Though, Igboora town is mainly underlain by amphibolite, there are quartzite/quartz veins intercalations along the exposed sections. The major river that drains this region i.e. River Ayin runs along the boundaries of these rock types.

The Aboluku- Opeki Watershed: This watershed consists of a lot of rural settlements, among which are Tobalogbo, Kondo, Alabi-Ilumo, Alabi-Oja, and Olowolayemo. This watershed is underlain by migmatite. There are few scattered inselbergs which are the highest point in the area. The region is mainly uplands with relief lying approximately between 190m and 250m above sea level.

1.5 Justification of the Present Work

The entire region of Ibarapa lies within the southwestern basement terrain and is completely underlain by 'hard', brittle crystalline rocks of Pre-Cambrian Era (Weerawarnakula, 1986; David, 1988; NGSA, 2009). Like many towns and rural settlements in Nigeria; the town water supply scheme, which is largely sourced from surface water has long been abandoned and houses are not connected with piped water facilities. Therefore, for domestic water needs; and even for agricultural purposes, residents of Ibarapa areas rely on groundwater supply tapped from hundreds of hand-pump boreholes that were drilled for the communities across the area. These groundwater supply structures were mainly funded by the government of Japan under the water supply and sanitation aid for rural communities development (WATSAN) scheme and by the Oyo State Community and Social Development Agency (CSDA), formerly known as LEEMP. However; even with these provisions, availability of potable water is still inadequate, largely due to the unsustainable yield of many of the functioning boreholes and the frequent mechanical failure of the installed hand-pump facilities.

This scenario is further complicated, due to increasing human population associated with many developing nations such as Nigeria, with an attending increasing demand for fresh water supply for domestic, industrial and agricultural utilisations. This demand has made it mandatory to explore for groundwater in areas such as Ibarapa region that is entirely underlain by crystalline basement rocks, which ordinarily have little or no potential for groundwater except where there are significant regolith thickness and/or occurrences of fractured bedrocks. Additionally; in comparison, groundwater is more accessible and less vulnerable to contamination than other fresh water bodies. However, the occurrence and distribution of groundwater resource in crystalline basement environments are rather complex as a result of geological and structural complexities associated with crystalline basement terrains.

Furthermore; about half of Nigeria land surface is underlain by crystalline rocks. Due to the need to ensure adequate provision of fresh water supply all year round; there is need for detail characterisation of groundwater potential, even in areas that are regarded to exhibit low groundwater potential.

Therefore, the characterisation of the crystalline aquifer system of Ibarapa region of southwestern Nigeria, from the geological, geomorphological, geophysical and hydraulic perspectives will provide information on the sustainable groundwater development, which will be a great contribution to scientific knowledge of groundwater resource in areas that are known to exhibit poor groundwater potential such as Ibarapa region of SW Nigeria.

1.6 Literature Review

Geological and hydrological methods were the earliest scientific approach for describing groundwater potential of an area. The associated rock types and the occurrences of surface water bodies in an area has been linked to groundwater occurrence and movement in the subsurface environment (Daubee, 1887; Slichter, 1899; Thiem, 1906; Sheppard, 1917, Theis, 1935). The use of aerial photos were also incorporated for tracing geological fractures and lineaments, and for landforms demarcations; from which hydrogeological attributes are interpreted (Lattman, 1958; Lattman and Parizek, 1964). Later on due to advancement in space technology, satellite imageries are now being used to study the hydrology and inferred the

hydrogeological attributes of the subsurface environment. According to Ellyett and Pratt 1975, some natural features such as topography, landforms, drainage characteristics, depth of weathering, lithology, lineaments, and soil moisture that are either direct or indirect indicators of groundwater occurrence can now be inferred from satellite imageries/remote sensing techniques (RST). Emphasis on the use of RST for studying the hydrogeology of crystalline rocks was given by Waters *et al.*, (1990).

To a large extent, the application of remote sensing techniques (RST) for hydro-geomorphological studies of various landforms have been undertaken in more advanced nations (Phillip and Singhal, 1992; Sreedevi *et al*., 2005) and it is now becoming popular in developing nations within African continent. The use of RST in Africa are more associated to studies that involve water management, particularly in regions that are underlain by crystalline basement rock units. The sole aim in most of these nations is to increase the available fresh water resources from groundwater source. Sander (2007) linked the increased in borehole success rate, and reduction in the costs of groundwater exploration in Ghana to the application of RST for lineament interpretation. Also, air-photos and radar images have been used for lineament studies in siting wells at the south-eastern Nigeria (Teme and Oni, 1991; Edet, et al. 1998). More recently; in Nigeria, integrated GIS techniques and remote sensing methods were employed for delineation of groundwater potential zones over large basement area in SW-Nigeria for reliable and cost effective groundwater exploration (Talabi and Tijani, 2011; Fashae *et al*. 2014).

However, no matter how crucial the remote sensing methods are, probe of the subsurface environment using geophysical methods are much more valid for delineation of groundwater potential zones particularly in basement terrains. Geophysical methods are known to reveal important water bearing fractures that are not even represented or detected by remote sensing method (Hazell *et al*., 1992). The applications of geophysical methods are readily applicable for groundwater exploration due to the localised nature of groundwater occurrence in basement terrains. In Nigeria, the applications of electrical resistivity geophysical methods have been used for decades in lithological characterisation of the overburden units and bedrock fractures. Olorunfemi and Olorunniwo (1985, 1990) used vertical electrical sounding (VES) geophysical method to study the geo-electric parameters and aquifer characteristics of

the residual overburden developed on different crystalline rocks underlying some areas in SW Nigeria. These studies revealed that overburden thickness was higher in areas underlain by gneiss and meta-sediment bedrocks, compared to locations underlain by granite. The studies further established that there is overlap in resistivity of the overburden units across various parent rocks, though the resistivity of residual clays was put between 5-150Ωm. However, David (1988) went further to study the lithological characteristics and water saturation, and other hydrological properties of regolith and the underlying bedrock unit that bear direct groundwater significance across various crystalline bedrocks around Idere in Ibarapa region. From the resistivity soundings, these works revealed that the dominant vertical weathering profile associated with these basement environments can be grouped into three major units or layers; namely: the topsoil that is normally regarded as alluvium with wide range in resistivity values, the intermediate middle layers that are classified as either clayey, sandy or lateritised clayey units with resistivity values that may be up to 600 Ωm and lastly, the last layer which can be massive, weathered or fractured depending on the resistivity. The comparative resistivities of the earlier workers are presented in Table 1.1.

Also, secondary geo-electric parameters known as the Dar-Zarrouk variables that included the longitudinal conductance, the traverse resistance and the coefficient of anisotropy can equally be employed for spatial characterisation of hydrogeological attributes of the weathered regolith. The concepts of longitudinal unit conductance and transverse unit resistance were derived from the integration of primary geo-electric parameters (i.e. the layer thicknesses and their corresponding true resistivities). The Dar Zarrouk variables were first introduced by Maillet, 1947 and Sabnavis and Patangay (2006) likened the passage of electric current across and parallel to the geo-electric boundaries to water passage through subsurface layers. More recent research works such as Oladapo and Akintorinwa, 2007; Abiola *et. al.*, 2009; Aweto; 2011; Jayeoba and Oladunjoye, 2013; and Akanbi, 2016; used these variables to demarcate areas into various groundwater potential zones and for estimation of the protective capacity of the overburden unit for groundwater vulnerability assessment.

Rocks heterogeneities due to disparities in mineral content, and in textures and structures, even within the same rock types were also believed to bring about much inconsistence of weathering pattern and bedrock topography. This in effect bears

Table 1.1. Comparison of Range of Geo-Electric Layers Resistivities of Subsurface Materials of Similar Crystalline Rocks of SW-Nigeria

Geo-electric layer	Olorunfemi and Olorunniwo (1985)		David 1988	Environmental conditions		
	Lithology	**Ωm**	**Lithology**	**Dry Ωm**	**Wet Ωm**	**Saturated Ωm**
Topsoil	Alluvium	37-5000	Topsoil	300-2400	45-300	
	Alluvium- sandy	<1000				
	Laterites and compacted sand	>1000				
Intermediate	Clay with little or no sand	0 - 60	Duricrust (Hardpan) Clay	400-1600	270-380	15-50
	Sandy clay	60-150	Sandy clay			50-100
	Clayey sand/sand	151-600	Clayey sand			100-175
Fractured or highly weathered bedrock		< 600				228-1800
Massive bedrock			≥ 1800			

imprints on the hydraulic characteristics of the water bearing zones of the crystalline rock units (Akanbi, 2016).

The hydraulic properties of crystalline rocks guide the storage and flow of water in the weathered-fractured components. Such properties include but not limited to the following: porosity, permeability, void ratio, hydraulic conductivity, yield, transmissivity and storativity. These properties can be estimated by various methods either in the field or in the laboratory. Singhal and Gupta (1999) have proved that field methods provide a better estimate of hydraulic characteristics, since a larger volume of material of the water-bearing units is tested. Field methods or in-situ measurement of hydraulic properties are pumping test and slug test. The former is more useful and has been used as the conventional field method for hydraulic characterisation of water bearing zones, including those in crystalline basement. However, there are few reports or published work on hydraulic characterisation, the available ones are restricted to developed nations and are rare for crystalline basement. In basement terrains of Europe, Carlsson and Carlstedt, (1977); and Carvalho (1993), obtained transmissivity ranges of 0.01- 0.1 and 0.2 - 160 in m^2/day for Swedish granite-gneiss bedrock aquifers and Portuguese Hercynian Massif respectively, while Banks *et. al.*, (1992) estimated a range of $10^{-6} – 10^{-8}$ md^{-1} as hydraulic conductivity for Precambrian granitic aquifers in Norway. In North America, UNESCO, (1972, 1975) and Sidle and Lee (1995), obtained hydraulic conductivity as low as 10^{-12} in crystalline metasedimentary aquifers in the USA. Notwithstanding, in Africa, better hydraulic conductivity and transmissivity value ranges of 0.01 – 2.8 md^{-1} and 0.5 – 101 m^2/day respectively were obtained for fractured gneiss – granite rock units in Zimbabwe (Wright, 1992).

In Nigeria, documentation of hydraulic parameters of basement aquifers are few, and when found the assessments are mainly based on well yield. Records of aquifer properties such as the transmissivity and hydraulic conductivity are scarcely available. Notwithstanding, Fashae, et al. (2014) and Tijani, (2016) delineated SW Nigeria into areas of low, moderate and high groundwater potential zones using groundwater yield alone. The study revealed that areas underlain by migmatite, banded and augen gneisses were within the low potential zones with capacity of producing <75 m^3/day (or < 75,000 liters daily) of groundwater, while terrains underlain by metasediments such as schist, amphibolite and quartzite were categorized as moderate zones with yield capacity between 75 and 150 m^3/day. Areas underlain by granitic rocks were the

only terrains that fall under high potential zones with >150 m^3/day yield.

From these studies, there is evidence of information gap, in linking groundwater potential of basement area with aquifer properties. Hence, the need for the present studies of characterising the groundwater occurrence and recharge potentials of various crystalline bedrocks from geological, geomorphological and geophysical approaches; and evaluating the hydrological and hydraulic properties of the associated water-bearing zones of the weathered-fractured components. This information will ensure sustainable groundwater development in crystalline basement terrains.

CHAPTER 2

2.0 REVIEW OF THE REGIONAL GEOLOGICAL AND HYDROGEOLOGICAL SETTINGS OF THE STUDY AREA

2.1 Regional Geological and Structural Settings of Basement Complex of Southwestern Nigeria

The geological settings of the Basement Complex of southwestern Nigeria have been widely reported and documented for decades. The earliest reports on the crystalline basement rock units were mostly associated with mineral explorations and national infrastructural development such as those carried out by the Mineral Survey of Southern Nigeria in-between 1905 and 1908 (Dustan 1910a, 1911). These reports covered large areas for preliminary reconnaissance survey for possible occurrences of valuable minerals within the crystalline rocks of southern Nigeria. Also, after the establishment of the Geological survey of Nigeria, a survey for the construction of western railway was carried out and this extended for about 16km (10 miles) strip of the landmass at each side of the railway. The map scale was 1:250,000 (Wilson, 1922). From the studies, the earliest crystalline rocks mapped were the quartzites, quartz-schists, and some biotite-gneisses that exist only as discontinuous relics. These rock units were described to be the oldest rocks of the Basement Complex by Wilson (1922). However, systematic geological mapping on a scale of 1:100,000 was carried out by Jones and Hockey (1964) using aerial photographs and topographical maps as base maps in the preparation of the geological maps.

Accordingly, Jones and Hockey (1964) showed that the crystalline rocks of the southwestern Nigeria form a part of the African crystalline shield which consist predominantly of folded gneisses, schists and quartzites. Granitic and basic intrusions were emplaced into these rocks, with the latter being on a minor extent. Several principal rock members were grouped under three main Basement Complex rocks as presented in Table 2.1. The Gneiss Complex rocks that were interpreted as the oldest

Table 2.1: Generalized Groups of Basement Rock Units (Jones And Hockey, 1964)

	MAIN GROUP OF BASEMENT ROCKS	PRINCIPAL MEMBERS
1	OLDER GRANITE	Olivine-dolerite dykes
		Pegmatite, aplite, and quartz-veins Migmatite, and porphyroblastic gneiss Fine-and medium-grained granite Granite-gneiss Coarse- porphyritic granite and syenite Granodiorite and quartz-diorite
2	CHARNOCKITIC INTRUSIVES	Pyroxene-diorite and metagabbro
3	GNEISS COMPLEX	Biotite-and biotite-hornblende-gneiss Quartzite and quartz-schist Amphibole-schist and amphibolite Mica-schist Granulitic gneiss Marble and calc-silicate rocks

rocks were considered to be a bedded series, predominantly of sedimentary origin, but migmatised to a variable extent. Rocks categorized as the Older Granites also constitute a major group which mainly comprised granitic rocks that have been emplaced by intrusion and replacement in the Gneiss Complex.

Much of the migmatisation of the Gneiss Complex is associated with the later phases of the Older Granite activity but there is evidence that the onset of intrusive activity found the Gneiss Complex already highly metamorphosed.

Later geological mappings were more detailed, more widened and restructured the earlier crystalline rocks groups. For example, Rahaman (1976) proposed the following classification of the crystalline rocks of the southwestern Basement Complex as:

1. Migmatite - Gneiss - Quartzite Complex comprising biotite - hornblende gneisses, quartzites and quartz schists.
2. Schist belt of slightly migmatised to unmigmatised paraschists. This consists of pelitic schists, quartzites, amphibolite, talcose rocks, metaconglomerates, marble and calc-silicate rocks.
3. Charnockitic rocks
4. Older granite, which include granite, granodiorite, diorites and potassic syenites
5. Unmetamorphosed doleritic dykes which are considered as the youngest rock in Basement Complex.

Additionally, recent geological map of Nigeria produced by the Nigerian Geological Survey Agency (NGSA, 2009) on scale 1:1,000,000 illustrated the various crystalline rocks of the Basement Complex of southwestern Nigeria (Figure 2.1). Principal crystalline rock members were also classified under three major rock groups namely:

a. The Older Granite series; which comprises pegmatite (as the youngest rock unit in the series), granodiorite, syenite, porphyritic granite, granite gneiss, undifferentiated granite gneiss and migmatite, diorite, charnockite and charnockitic rock, and meta-diorite.

b. The Meta-sedimentary and Meta-volcanic Complex; which includes amphibole schists and amphibolite, talc-schists, biotite garnet gneiss and schists, marble,

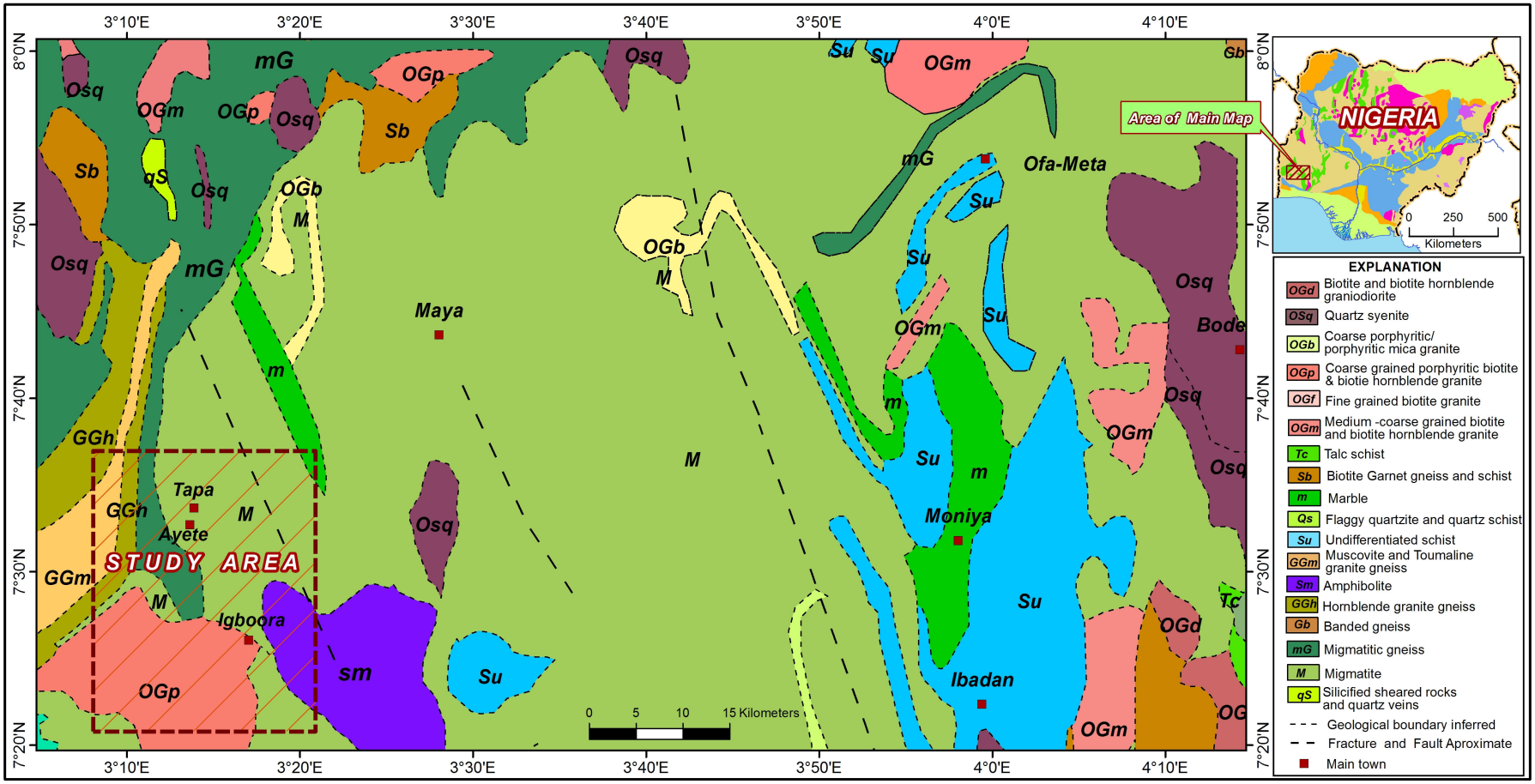

Figure 2.1: Geological map of the Basement Complex of some parts of southwestern Nigeria (modified after NGSA, 2009)

quartzite and quartz-schist, and undifferentiated schist.

c. Lastly, the Gneiss-Migmatite Complex; porphyroblastic gneiss, muscovite and tourmaline granite-gneiss, hornblende granite-gneiss, granite-gneiss, quartz feldspathic granulite and gneiss, muscovite schist, banded gneiss, migmatitic augen gneiss, migmatitic gneiss, migmatite, silicified sheared rocks and quartz veins, and rhyolite. The crystalline rocks of the Basement Complex of southwestern Nigeria have been dated to be of Pre-Cambrian age (Jones and Hockey, 1964; Dada 1998).

Conversely, the petrology and geochemistry of the crystalline rocks of Ibarapa area has been reported by Weerawarnakula (1986). Six major rock groups that underlain the area were outlined as: the Migmatite-Gneiss-Quartzites Complex, Granitic and augen gneisses, Biotite schists and paragneisses (younger meta-sediments), Charnockitic rocks, Older Granite Complex, and lastly Pegmatites, aplites and quartz veins (Figure 2.2).

The Migmatite-Gneiss-Quartzites Complex included the early biotite gneisses, amphibolite and migmatite. The early biotite gneisses are interbedded with quartzites and migmatite gneisses. Quartzites are folded with the migmatite and early biotite gneisses, and are often graded into micaceous quartzites. The Older Granite Complex composed mainly of porphyritic biotite granite and homogenous fine to medium grained biotite granite. Augen gneisses occur in close contact with Older Granite and as isolated dyke-shaped bodies in the migmatite-gneiss-quarzite Complex. The youngest rock units in the area are the pegmatites, aplites and quartz veins which intruded all other rock bodies in the area (Figure 2.2).

Aside the migmatite rock units, porphyritic granite is the next most widely occurring bedrock in the entire Ibarapa region. It intruded the most parts of the western axis of Ibarapa, extending from the northern boundary underlying major towns such as Tapa, Idere, Ayete, to the southern part of the study area. Porphyritic granite is also conspicuously underlying the larger parts of Lanlate and Eruwa at the eastern axis of the study area. The amphibolite is restricted to Igboora and biotite gneiss is dominant at the west.

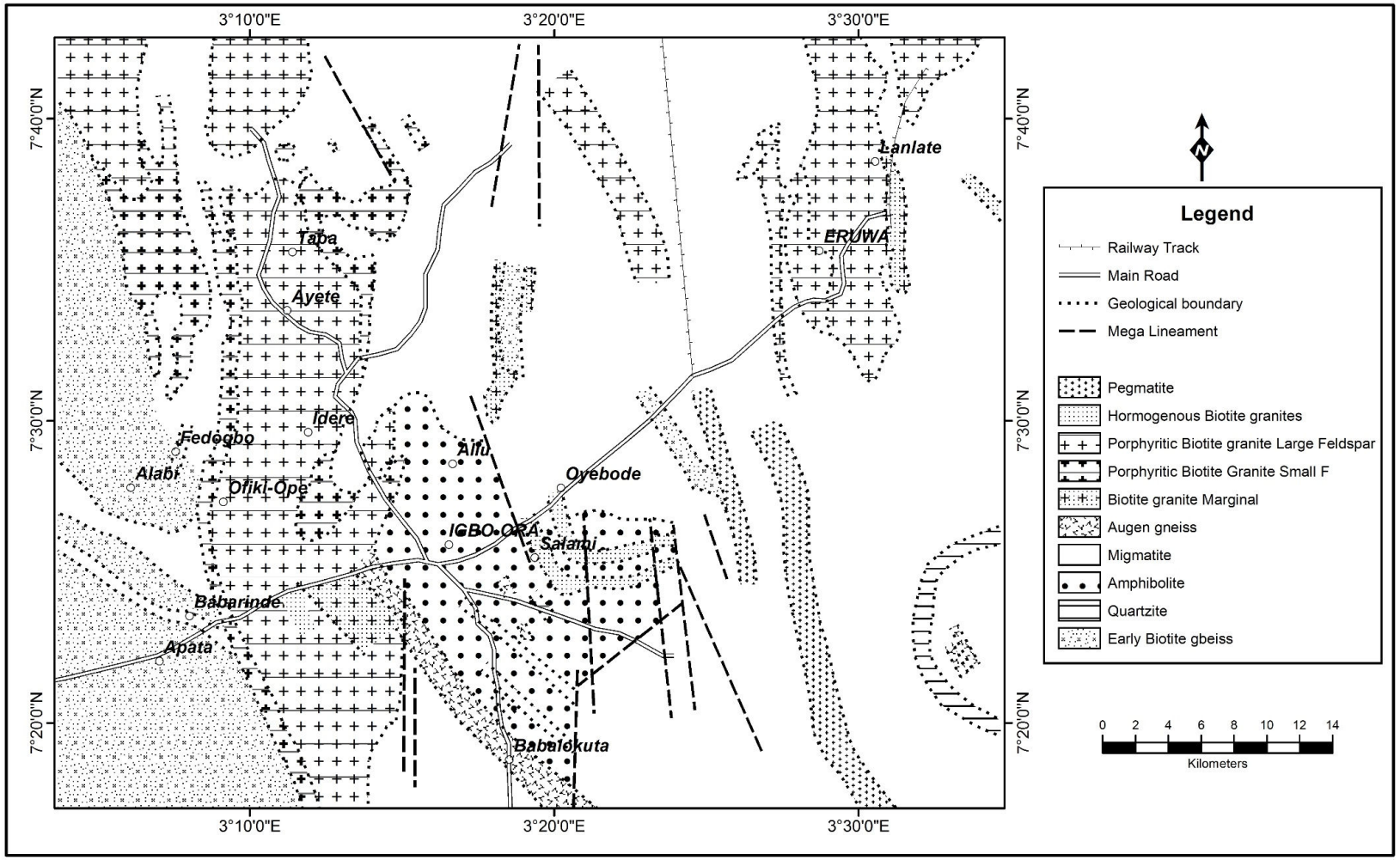

Figure 2.2: Geological Map of Ibarapa Region (Weerawarnakula, 1986)

2.2 Hydrogeological Setting of Crystalline Basement

Crystalline basement rock units have negligible porosity and permeability and can neither store nor transmit water. Nonetheless, secondary conduits or discontinuities mostly from epigenetic geological occurrences can develop within the impermeable crystalline rock units. Such crystalline rock discontinuities of hydrogeological importance are rock boundary, foliation, fractures and faults. These discontinuities are regarded as lineaments, and most times they have surface expression that are mappable on the outcropping rock sections which could be traced out by application of remote sensing methods for regional overview over a large terrain. The characteristics of the linear features such as the orientation, density and interconnectivity are crucial factors determining their effectiveness to groundwater storage and transmission.

In addition, the breakdown of crystalline rocks by physical and chemical weathering lead to formation of soil or development of matrix (granular) units that can have substantial water storage and transmission properties. Hence, the hydrological properties of crystalline rocks present a dual complex nature of weathered-fractured components.

In the light of this, many authors (Chilton and Smith-Carington, 1984; Rushton and Weller, 1985; Sekhar *et al*., 1994; Taylor and Howard, 2000; Van Tonder *et al*., 2002; Gonthier, 2009) have indicated that crystalline basement aquifers are usually semi-confined in nature with a water-table matrix (regolith layer) situated on top of the fractured bedrock. This represents a dual aquifer nature, where the components are hydraulically interconnected and cannot be treated separately. Hence, under favourable hydraulic conditions, the weathered layers are regarded as the unconsolidated porous medium through which water can be stored and transmitted to the fractured bedrock which represents the consolidated conduit system. In this regard, there is guarantee of replenishment of the groundwater resources through infiltration from meteoric and other surface water sources.

Therefore, the extent and the degree of saturation of the weathered units, as well as the amount and the interconnectivity of bedrock fractures are the major determinants of the complexity of groundwater supply in the basement terrains. However, these two complex components which largely influence the crystalline rocks potential for

groundwater supply depends on a number of independent and interrelated factors such as geology, climatic conditions, landform and topographic features of the area that may be on a regional and local scale.

According to Wright and Burgess (1992); the common viewpoint for long-term borehole productivity in crystalline basement aquifers is that there should be presence of weathered material overlying either the fractured rock or an alternative source of recharge such as a river or associated alluvium. Consequently, in more arid environment underlain by crystalline rocks characterised by lack of surface water resources and development of thin weathered overburden, then the interest of hydrogeologists is predominantly on the dominant fissure/fracture flow.

According to Wright (1992), there are some restraints to groundwater development in basement areas of Africa. These include:

a. High frequency of borehole failures, at the rate of 10 to 40%. The higher failure rates are associated to dry regions and places where the regolith are thin.
b. Vulnerability of basement aquifers to surface environment contamination due to shallow occurrence of the water-bearing zones.
c. Low storativity potential of basement aquifers that can lead to groundwater depletion during prolonged dry season.
d. Sensitivity of recharge to changes in land use changes, particularly in desert areas.

In this regard, geophysical and geomorphological studies of large basement areas are crucial for groundwater development in Nigeria for studying the weathered-fractured components of the crystalline bedrocks, and for characterising the landforms of the area and their respective hydro-geomorphic attributes.

Generally, groundwater occurrence in areas underlain by crystalline basement are normally characterised by shallow water level conditions, associated with seasonal and disconnected water occurrence and the water yield is usually low in hand-dug wells tapping such bedrock settings. The improvement in exploration techniques in recent times has increased the understanding of the hydrology of the weathered-fractured

aquifer system in crystalline basement. Consequently, constructions of boreholes with good water yield are now feasible in crystalline basement (Offodile, 2002).

2.2.1 Hydraulic Properties of Crystalline Aquifers

Hydraulic properties of basement aquifers are essential parameters for characterising groundwater storage and transmission attributes within the water-bearing zones. These properties include, porosity, permeability, hydraulic conductivity, transmissivity and storativity.

Dense crystalline rocks are normally characterised by low hydraulic properties, compared to sedimentary formations (Table 2.2). These values are even relatively lower when dealing with massive or fresh metamorphic and intrusive igneous rocks where the porosity (n) is mostly below 1.0 percent, and permeability is commonly between 10^{-5} and 10^{-8} m/day, unlike sedimentary formations such as sandstone and gravels with permeability of up to scores of thousands of m/day. However, the porosity of weathered basement rock can be up to 45% and the permeability up to over 70 m/day (Davis and De Weist, 1966; Todd, 1980; Driscoll, 1986; Singhal and Gupta, 1999). On the other hand, the porosity of fractured crystalline basement commonly ranges between 5 and 10 %, which is considerably lower than the overlying regolith.

The actual amount of water that is released under the influence of gravity to the nearby well or spring by water-bearing zones is referred to as the specific yield (S_y) or the effective porosity. In crystalline basement aquifers, the effective porosity is usually less than the total porosity of the medium. This is because unconnected fractures are not relevant for groundwater flow and it is only connected fractures that can transmit water effectively within basement aquifers. Hence, in all cases the effective porosity is usually less than the actual porosity. The actual porosity is the percentage of the total fractures in crystalline rocks. In respect of effective porosity, the regolith is also characterised by higher specific yield range of 10 to 20% than 2 to 5% associated with fractured basement, while both the actual and the effective porosity in fresh basement can be as low as 0% (Table 2.2).

Also, hydraulic conductivity (K) is a crucial aquifer property as well. Hydraulic conductivity is a measure of the ability of a formation to transmit water and it

Table 2.2. Representative Values of Some Hydraulic Properties in Selected Geological Formations (modified after Morris and Johnson, 1967; Hamil and Bell, 1986; Singhal and Gupta, 1999)

Geological formation	**Porosity (n) %**	**Specific yield/ effective porosity (S_y) %**	**Hydraulic Conductivity (K) m/s**	**Relative Groundwater potential**
Gravel	28 - 34	15 – 30	$1 – 10^{-3}$	Very high
Sand/sandstone	15 - 50	5 – 30	$10^{-2} – 10^{-7}$	Very high to moderate
Clay	40 - 60	1 - 5	$10^{-6} – 10^{-9}$	Moderate - low
Fresh crystalline rocks	0 - 5	0 - 3	$10^{-9} – 10^{-13}$	Very low
Weathered Basement	20 - 40	10 - 20	$10^{-4} – 10^{-9}$	Moderate to low
Fractured Basement	5 - 10	2 - 5	$10^{-4} – 10^{-9}$	Moderate to low

governed by both the aquifer and groundwater properties. In crystalline rocks, K depends on the density, size and fractures interconnections. The K values for fresh crystalline rocks are less than 10^{-8}m/s, classified as having low to very low groundwater potential. Fresh bedrocks are normally categorized as having very poor or negligible groundwater potential. However, weathered and fractured components are characterised by moderate potential for groundwater with K values commonly exceeding 10^{-8}m/s (Morris and Johnson, 1967; Hamil and Bell, 1986; Singhal and Gupta, 1999).

Reliable estimates of hydraulic parameters are essential for the management and protection of groundwater resources. This is more so in crystalline basement terrains, where the uniformities of the geo-hydrological properties of rocks are expected to be large as a result of spatial changes in geological/structural features. For instance, depth variations of hydraulic properties in the weathered-fractured components of crystalline basement terrains of Africa has been estimated by many authors. These included Jones, 1985; Acworth, 1987; Chilton and Foster 1995, Singhal and Gupta 1999 and Holland, 2011. The results revealed that the hydraulic properties in relation to depth were inconsistent and widely varied as illustrated in Figure 2.3. These variations are discussed below under the respective lithological units associated with basement terrains within the tropical climatic environment of sub- Sahara Africa:

a. The topsoil unit which composed of highly weathered residual and/or transported reddish coloured, quartz rich alluvium, with thickness mostly <5m. The top soil can consist of highly variable grain sizes. The effective porosity and the permeability/hydraulic conductivity are fairly large, and the transmissivity is equally large as well.

b. The saprolite unit, which is made up of massive accumulation of mainly secondary clay minerals and may also consist of sandy grains. The thickness of the saprolite may be up to 30m, and sometimes 50m. Water flow is characterised by high porosity and fairly large transmissivity but relatively low permeability.

c. The saprock which preserves the relics of the structures and Petrographical features of the underlying fresh rock. It is made up of partially weathered bedrocks

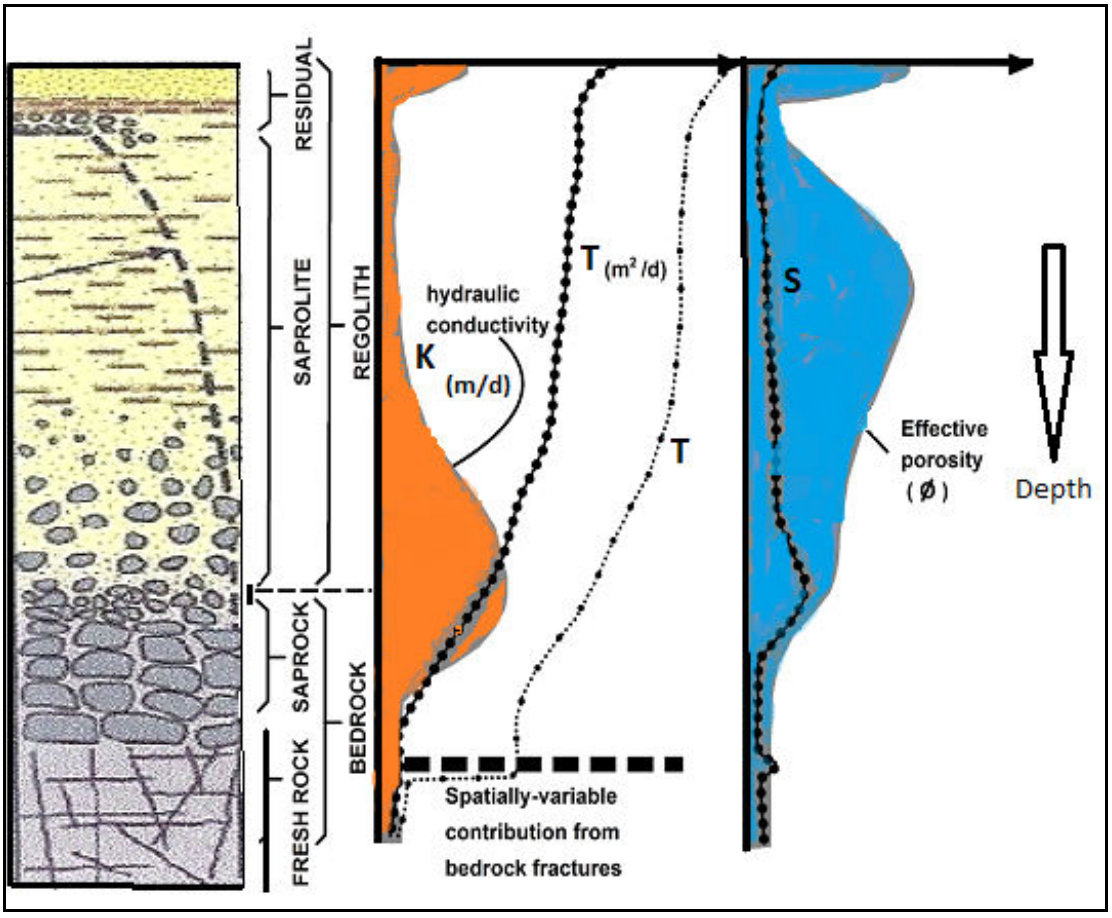

Figure 2.3: Variation of geo-hydrological properties of basement terrain with depth (Modified after Chilton and Foster, 1995; Singhal and Gupta, 1999; and Holland, 2011)

and the thickness lies between 20 and 30m. This unit is characterised by relatively lower porosity and storativity, but fairly high permeability and medium transmissivity that reduces downward.

d. Fresh rock zone. This is an infinite unit that is characterised by very low or negligible hydraulic properties, except when fractured in which it may be characterised by reasonable hydraulic properties, but the water storage potential is low.

Generally, weathering is more rapid in tropical parts of Africa due to favourable climatic condition of repeatedly alternating wetness and dryness. The overlying regolith is composed of unconsolidated material derived from prolonged in-situ decomposition of bedrock having a negligible thickness to as thick as a few tens of meters. The weathered layer, otherwise known as the regolith usually has a high porosity and a low permeability. The low permeability is due to clay-rich material and when saturated, the weathered layer constitutes the reservoir or the aquifer.

However, the porosity of the weathered profile generally decreases with depth, along with clay content, until fresh rock is reached. This is because the fractured-weathered layer is generally characterized by decrease in fracture density with depth, which is related to cooling stresses in the magma following tectonic activity (Houston and Lewis, 1988) or litho-static decompression processes (Wright, 1992). The horizon of fracturing between the fresh rock and the regolith frequently has a higher permeability, due to a number of factors such as the extent of fracturing and the presence of clay in the fractures. This layer mainly assumes the transmission function in the aquifer and is pumped by most of the wells drilled in hard-rock areas (Marechal *et al*., 2007). The fresh basement which is the un-weathered bedrock is permeable only locally where deep tectonic fractures are present.

Therefore, rock weathering and structural features of the basement are extremely variable in nature (Gustafson and Krasny, 1994). Likewise, the hydraulic properties of the water-bearing zones within the basement terrains are expected to be variable. More so, methods of estimation of hydraulic properties should take into account the double-porosity behaviour of the basement aquifer system (Taylor and Howard, 2000), which comprises an overlying conductive porous overburden units or a matrix component on

the bedrock units that may be either partially weathered, fractured or fresh.

The hydraulic properties of aquifers can either be estimated in the laboratory (by analyzing the rock/soil samples) or in the field by conducting field tests such as slug or pumping tests in wells. Though, the laboratory investigations are relatively inexpensive and less time consuming, they do not often represent the actual field situations. The field tests; though, are more cumbersome and laborious are known to be more reliable and dependable (Singhal and Gupta, 1999). For instance, pumping tests can yield enough information for evaluating the safe yield of an aquifer. This is in addition for being a reliable techniques for obtaining hydraulic properties such as transmissivity (T), hydraulic conductivity (K) and the storativity or storage coefficient (S) of the water-bearing zones. Holland (2011) noted that a short-term duration pumping test could be sufficient to predict the sustainability of water discharge in low permeable formation such as crystalline aquifers. The intention of a pumping test is to stress an aquifer by pumping water out of the well and to note the drawdown over space and/or time, from which the characteristics of the aquifer can be estimated under special considerations.

The hydrogeology of the present study area, which is entirely underlain by crystalline basement rock is expected to be largely defined by the weathered-fractured units that are expected to vary across the area. Although, there are hundreds of drilled wells within the main towns and adjoining villages, the long queue for water at the borehole points has raised questions on the sustainability of the groundwater system within these localities. More so, there are no records of both the pre-drilling and the well logs data in the archives of the agencies that drilled the boreholes, and not even with the end users and the overseeing Local Government Area (LGAs) Councils within the study area. Consequently, there is need for hydrogeological characterisation of the water – bearing zones that developed within the crystalline basement rock units in this part of Ibarapa region. People of Ibarapa areas solely relies on groundwater supply for domestic needs, and to some extent for agricultural purposes during the dry season. The local hydrogeologic settings of the area are not known to have been reported but may be inferred from the integrated applications of relevant studies such as geological, structural studies, and even from the geomorphological characterisation of the landforms. Also, the studies of the weathered-fractured components on the basement terrains should also be incorporated from geophysical studies.

CHAPTER 3

3.0 MATERIALS AND METHODS

The present research on hydrogeologic characterisation of crystalline aquifers of Ibarapa area involved geological (and structural), geomorphological, geophysical and hydraulic approaches. These studies are aimed at describing the groundwater potential; and, evaluating the hydrologic and hydraulic parameters of the groundwater bearing zones under the various bedrocks that underlain the study area. The flowchart of the research methodology and basic outlines of the main objectives are highlighted in Figure 3.1.

3.1 Geological and Structural Approach

The geological approach involved the traditional field mapping and rock boundaries delineation and mineral identification by petrographical studies. Fresh samples obtained during the field mapping were cut into thin sections and studied with the aid of petrological microscope and photomicrographs taken. The petrographical studies were conducted in the Petrological Laboratory of the Department of Earth sciences of Ajayi Crowther University Oyo, Oyo Nigeria.

The existing topographical and recent geological and mineral resources maps of NGSA, (2006, 2009), and that of Weerawarnakula (1986) were used as reconnaissance geological maps. These maps were upgraded by more precise fixing of rock boundaries and lineament features as well as inclusions of other rock types as studied during the field mapping exercise. Hence, new geological map with bigger scale was generated from the present studies.

For rock boundary delineation, rocks colour codes of Nigerian Geological Survey Agency (NGSA, 2006) were used as symbols for respective bedrock units across the study area. Field photographs and photomicrographs were presented in Appendices IA

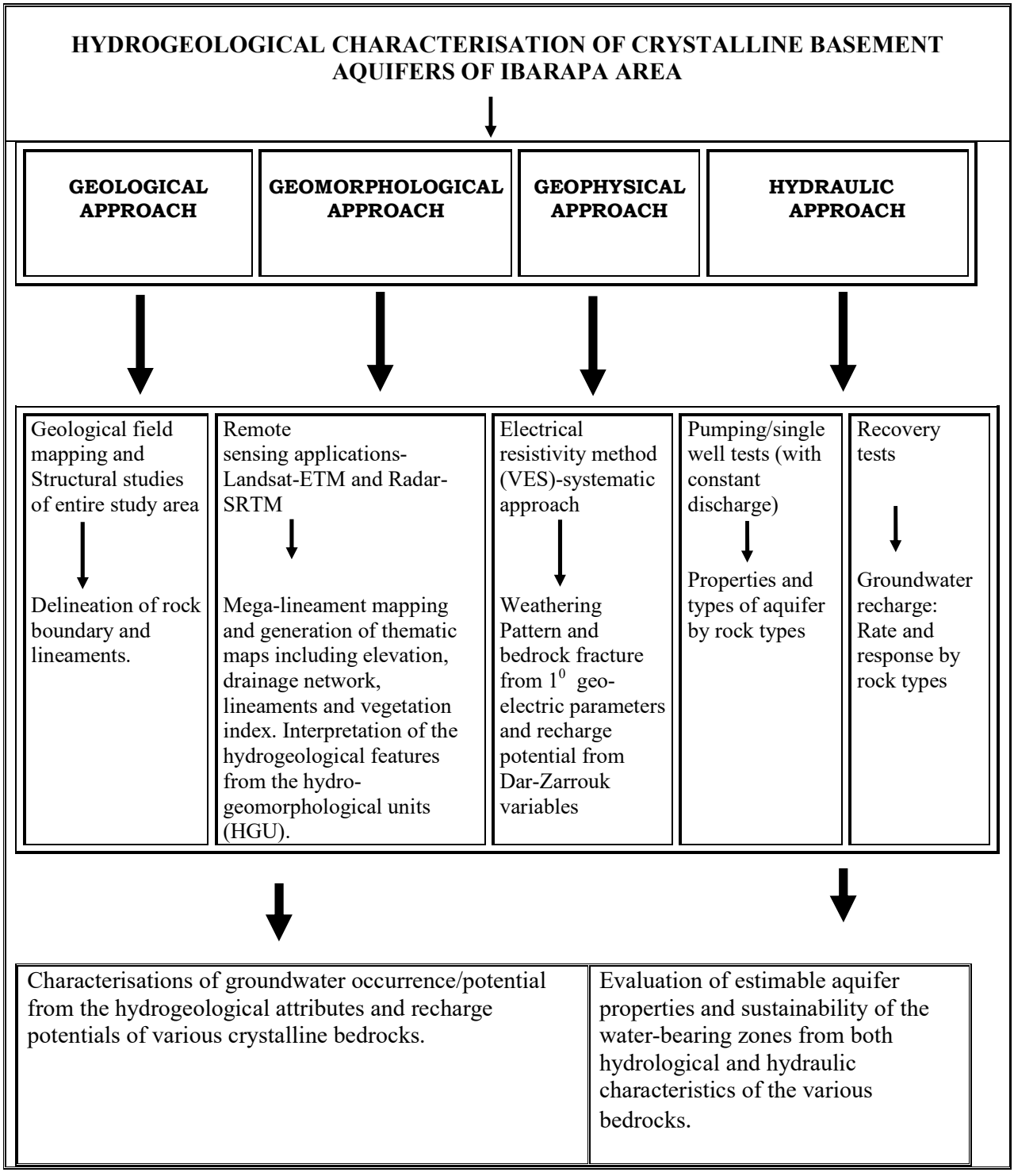

Figure 3.1 Flowchart of Research Methodology

and II respectively, while some pungent examples were cited and included at the appropriate sections of this report.

Geological approach was also involved in fracture characterisation. All mappable natural discontinuities of hydrogeological importance collectively referred to a lineaments or fractures in this study; such as fractures, faults, foliations and, even rock contacts were studied, measured and mapped on the outcropping rock sections in the field. These linear features do indicate groundwater occurrences because lineaments are important for storing and transmitting groundwater in any basement terrains. Hence, most often; fracture density and orientations on outcropping sections do indicate the occurrences and the direction of flow of underground water in basement areas.

Additionally, integration of remote sensing and GIS method was also employed for studying lineament attributes such as direction, density and persistence or continuity. Hence, the Thermal-InfraRed (TIR) bands of Landsat TM (thematic mapper) satellite imagery was also used for wider spatial studies of linear features. This satellite imagery is applicable for delineating structural features such as folds, faults, foliation, and layering. Details of the application of the Landsat TM satellite imageries are discussed in Appendix III.

3.2 Geomorphological Approach

The geomorphological approach involved generations of hydro-geomorphological thematic maps for the study area. These maps include, the elevation map, drainage, structural-lineaments and vegetation Index. From these thematic maps, hydrogeological attributes of the different parts of the study area are studied.

For geomorphological studies of the study area, employing field methods to study the hydro-geomorpological features is crucial but not enough for large area coverage. Also, relying on field data alone is inefficient and gives limited information on the spatial distribution and continuities of mega structures and hydro-geomorphical units of interest. Hence, the present study integrated remote sensing methods, field mapping and application of GIS techniques for extracting and inferring the hydro-geomorphological units from available information, maps and imageries.

3.2.1 Remote Sensing Application and Satellite Imageries

The principle of remote sensing revolves around the physical attributes of natural ground objects in response to their distinguishing abilities to reflect, emit and absorb different intensities of radiation at different electromagnetic wavelength ranges.

The application of the principles of remote sensing methods in the present work entailed obtaining and studying the appropriate satellite images. It also involved the applications of geographical information system (GIS) techniques, using Erdras Imagine and ArcGIS softwares for processing and extraction of data from the raw satellite images, and for generating visual and digital thematic maps. Mapped linear features from the integration of geological mapping, remote sensing applications and GIS methods are then superimposed on the geological map to characterise the fracture elements across the bedrock units within the study area.

The following satellites imageries of the study area discussed below were shot by the National Aeronautics and Space Administration (NASA) on February 6, 2000 and were considered appropriate for the present study. The imageries were shot at the peak of dry season in the study area and were employed for hydrogeological interpretation of the crystalline areas of Ibarapa region:

Radar Imageries (SRTM bands): For terrain analysis and generation of the digital elevation model for the study area, the Shuttle Radar Terrain Model (SRTM) bands of radar imageries owned by NASA as employed. The SRTM is a digital elevation Model (DEM) aspect of radar which has strong application to the land surface relief and can give a 3D elevation impression of the study area. The SRTM is employed for a comprehensive hydrogeological evaluation in mapping the associations between lithology, geomorphology/landforms, and elevations of the study area.

Landsat Thematic Mapper (TM): This is employed for structural characterisation of the crystalline rocks through the mapping and delineation of linear features such as folds, faults, fractures and rock boundaries. These lineaments act as conduit for water and will produce contrasting heat variations along the region of groundwater flow which are traceable or mappable as linear features on the processed images with the aid of GIS. The processed image from the Landsat satellite images are the Normalized Difference Vegetation Index (NDVI) and the colour composites.

The DEM are presented in both 2- and 3-dimensional models. These maps provide the platform for geomorphological characterisation of the study area from the various landforms.

On the other hand, the NDVI transform and the colour composite images processed from Landsat ETM satellite image are applicable for generating linear geological structural (the lineament) map of the study area. The colour composite is more helpful and further enhances the images of the hills and the inselbergs located at the central part of the map, while the clustered settlements are also visibly seen as bluish spreads.

Details on the characteristics of these imageries are discussed further in Appendix III.

3.3 Geophysical Approach

Suitable geophysical methods are applicable for more precise and detailed groundwater exploration work. Geophysical surveys are able to provide a more specific hydrogeological assessment of the subsurface geological environment.

The vertical electrical sounding (VES) resistivity geophysical method has been found to be mostly applicable for hydrogeological surveys (Olorunfemi, and Olorunniwo, 1985, 1990; Olayinka and Mbachi, 1992; Olorunfemi, and Okhue 1992; Murali and Patangay, 2006). From Murali and Patangay, 2006, VES is suitable for the following groundwater investigations in crystalline terrains:

a. Study of large groundwater basins including the vertical section, multiple aquifer systems, water quality etc.

b. Tracing potential groundwater zones in hard rocks such as saturated weathered zones, fractures, shear zones etc.,

c. Detecting pollution in groundwater due to different sources.

For this present study, the Schlumberger configuration is employed for sounding. It is less laborious to use and the total electrodes spacing for sounding is smaller, since it does not involved moving the potential electrodes as often as the current electrodes are moved, while the accuracy of the resistivity measurements is not compromised. The maximum AB separation employed was between 200-266m; this is considered appropriate for groundwater investigation in crystalline basement where groundwater

occurs at shallow depths associated with seasonal and disconnected water occurrence (Offodile, 2002). The terrameter brand used was Allied Omega.

The derived geo-electric parameters of the VES surveys were employed in characterising the bedrocks that underlie the areas in respect of the degree and extent of weathering development, textural characteristics of the regolith unit and potential for water recharge. These parameters were important in understanding the hydrogeological situation of the subsurface environment under different bedrock settings underlying the area of study.

The concepts of electrical resistivity geophysical method, including the basic, ground penetration, and the electrode configuration concepts as well as the concepts of the Dar-Zarrouk parameters and field procedures for conducting VES are discussed in Appendix IV.

3.3.1 Interpretation of VES Data

In depicting logical subsurface geological conclusions from the field VES data, quantitative and qualitative methods of interpretation were employed. The quantitative methods involved originating values for the primary geo-electric parameters that include the layers' resistivities and thicknesses either by curve matching or computer techniques. For the present work, integration of partial curve matching and computer iteration was employed. This was done by plotting the apparent resistivities values obtained from the field against the electrode spacing on a log-log chart. The curves obtained were then compared with those of auxiliary curve charts of Orellana-Mooney (1966) to derive the true layer's resistivity and thickness for each geo-electric layer. These were employed as model values in computer iteration using Winresist VES software application.

Qualitative interpretation of VES data normally reveals reasonable hydrogeological deductions. These include curve type, basement topography, apparent resistivity pseudosections, isopach, geo-sections from which both the sub-surface lithological mapping and spatial variations across the study area are studied. For the present study, the qualitative interpretation approach of VES data are provided mainly in form of maps, sections and charts and are made using Surfer 10 software.

Qualitative VES data investigation also included the estimation of the secondary geo-electric parameters, otherwise called the Dar-Zarrouk variables including the longitudinal conductance and the traverse resistance.

When a number of layers are involved in a geo-electric section, their total longitudinal conductance S and total transverse resistance T are quantifiable using the primary geo-electric parameters thus:

$S= S_1 +S_2 + S_3 +....$, where $S_1 = h_1 /\rho_1$, $S_2 = h_2 /\rho_2$ ……..etc, and

$T= T_1+ T_2 + T_3 +....$where $T_1 = h_1*\rho_1$, $T_2 = h_2*\rho_2$ ……etc. where; h1, ρ1, S_1 and

T_1 are the thickness, resistivity, longitudinal conductance and traverse resistance respectively for layer 1 in a geo-electric sequence. Hence, the recharge potentials were inferred from the Dar Zarrouk variables particularly from the longitudinal conductance which is an indication of water conductance across the regolith units.

The details of the qualitative and quantitative methods of interpreting VES data are presented along with the concepts in Appendix IV. The values of the Dar- Zarrouk variables by bedrock units was estimated using Microsoft excel. The modified ranges of resistivities employed for the lithological characterisation of geo-electric layers for the present geophysical studies are presented in Table 3.1. The VES surveys were conducted between March 5 and June 9, 2011.

3.4 Hydraulic Approach

The hydraulic characterisation of the bedrock aquifer system of Ibarapa areas was done by conducting single-well pumping tests and the corresponding recovery tests on twenty - three (23) suitable existing boreholes that penetrated the various bedrocks across the study areas. Estimable hydraulic properties including transmissivity, hydraulic conductivity, drawdown, specific capacity and other hydrologic parameters were estimated. Also, rates of groundwater recovery were estimated from the corresponding recovery and together with pumping test data, the groundwater sustainability was described. Recovery tests also serve as back-up data in single-well test, to eliminate skin effects when encountered during pumping.

Table 3.1: Range of Resistivity for Lithological Characterisation of the Saprolite and Bedrock Description (Modified after Olorunfemi and Olorunniwo, 1985; and David, 1988)

s/n	Resistivity range Ωm	Lithological description of the saprolite	Last/ infinite layer Ωm	Description of the bedrock
1	0-60	clay	<500	Fractured bedrock
2	61-150	Sandy clay	500-1800	Weak/slightly weathered
3	151-400	Clayey sand/sandy	>1800	Fresh bedrock
4	401-1600	Compacted sand or clay, hardpan		

Seven wells were tested in terrains underlain by amphibolite, six in gneisses, and five each in areas underlain by both migmatite and porphyritic granite. With the exception of two recently drilled boreholes located at Idere and at Alabi-Oja, all other tested wells were existing boreholes. All the existing wells tested were hand pump (manually operated) boreholes fitted with submersible hydraulic plunger (Figure 3.2a). The plunger is connected to the stem rod that extends to the surface and is connected to the drive chain. The typical installation structure of the hand-pump boreholes tested in Ibarapa is illustrated in Figure 3.2b.

To avoid changes in field measurements due to weather condition, all the pumping and recovery tests were carried out within the same season in the month of November, 2011. At this time, the rain season just ends, and aquifer systems are fully recharged. Also, by this time (that is the beginning of dry season), field measurements will not be affected by rainfall, and measurements made will be true representation of the water-bearing zones. The following materials were employed for hydraulic characterisation:

3.4.1 Materials and Tools for Single-well Pumping and Recovery Tests

The following tools and materials were employed for the conduct of pumping test.

a. **Submersible Pump:** For the hydraulic testing in basement terrain, where the aquifer yield is expected to be low, a 0.5 Horse Power Sigma model 4'' submersible pump was employed. The submersible pump requires a 0.37Kw, 220/50 and 3.3A power supply (Plate 3.1A).

b. **Riser Pipes:** PVC riser pipes with one inch diameter were employed for the testing. This is considered suitable for aquifer testing of low permeable formations such as crystalline aquifers. The first riser pipe was connected to the electrically powered submersible pump. Other pipes were screwed one after the other as the submersible pump is lowered into the borehole. The screwed ends were made water tight using Nastro professional Tenuta filetti ribbon to avoid water loss through leaking during pumping. The water flow meter was installed along the pipe-line for measurements of discharge (Plate 3.1B).

c. **Water Flow Meters:** For every water level measurement taken during the pumping test, the corresponding volume of water pumped from the well was

Figure 3.2a: Typical manually operated well at Ibarapa

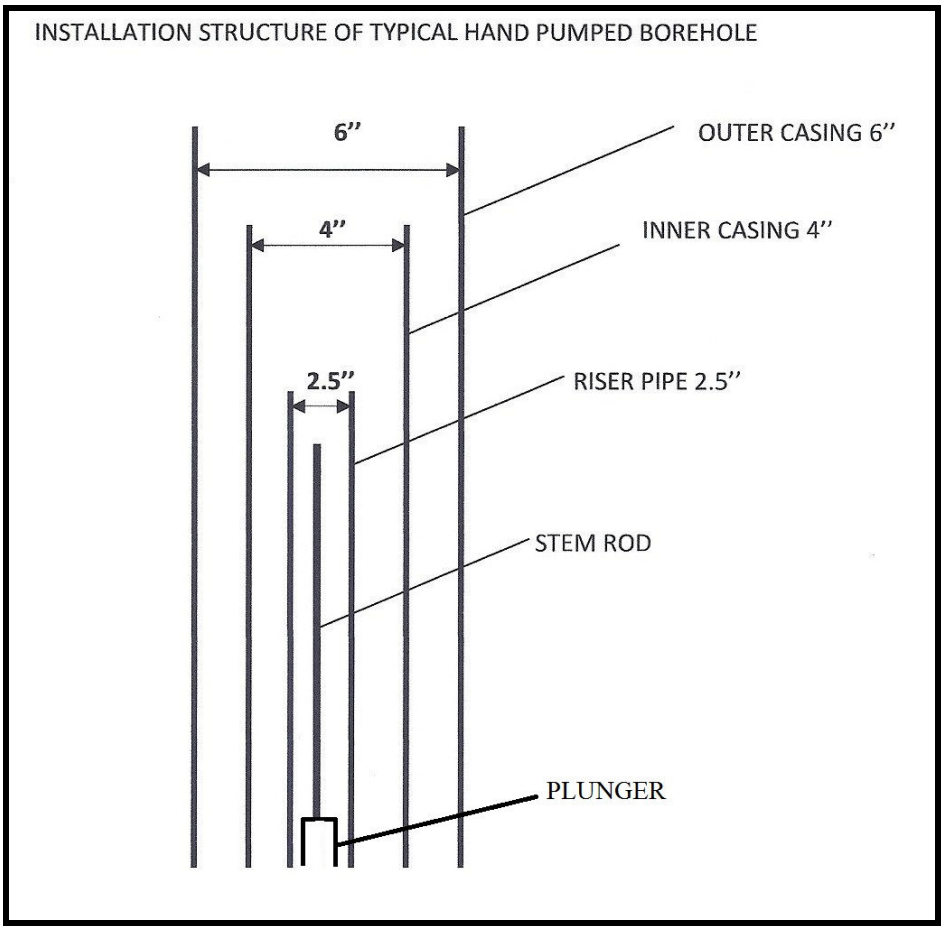

Figure 3.2b: Typical installation structure of the manually operated borehole in Ibarapa

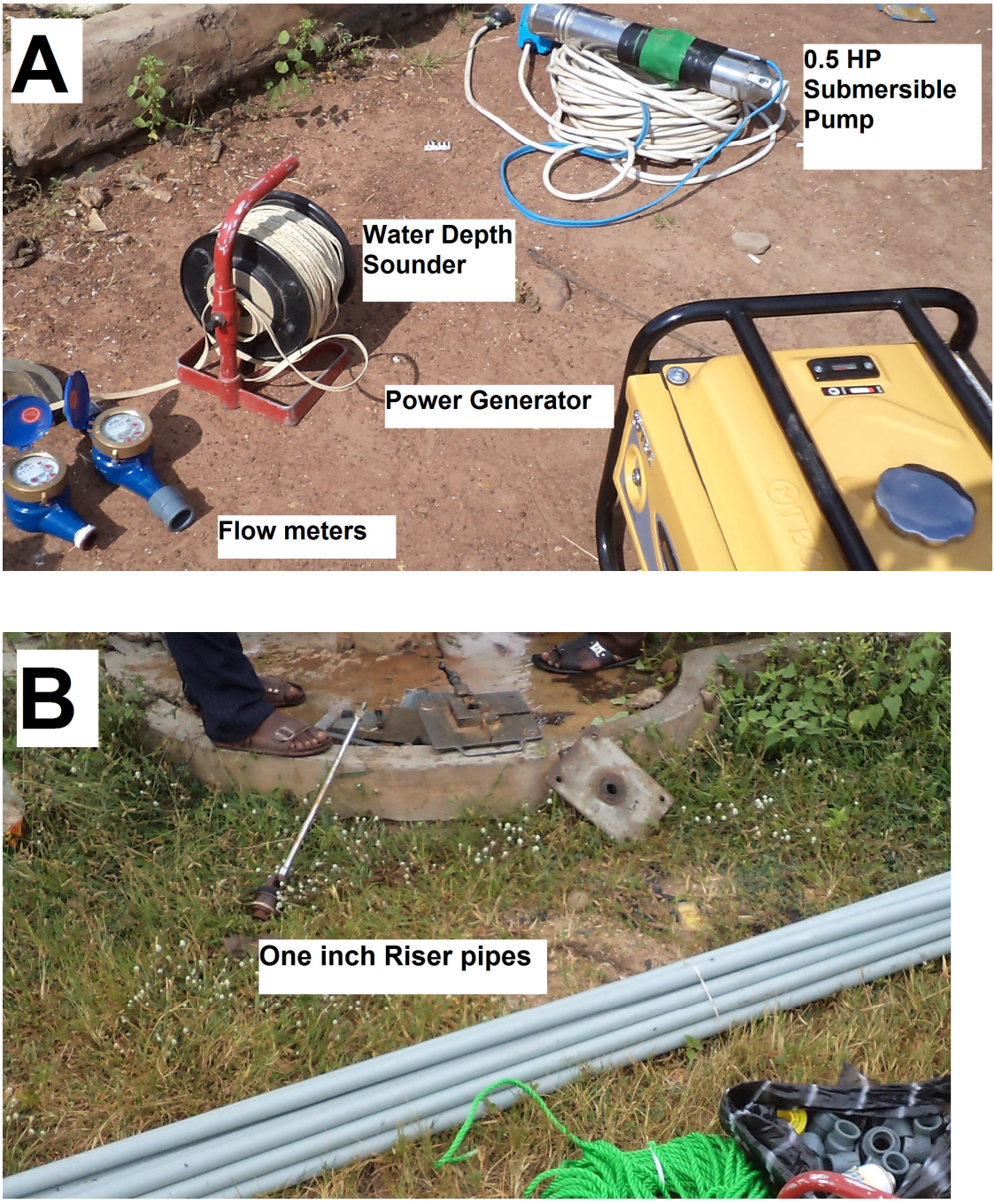

Plates 3.1: Equipment for the conduct of Pumping and Recovery tests at Ibarapa

also measured using ISO 4064 DN20 water meter (Plate 3.1C) with the accuracy of 0.0001m^3 (or 0.1 litre).

d. **Water Level/Depth Indicator:** All water level and borehole depth measurements were done using a measuring rubber tape fitted with an automatic water level and depth light bulb indicator.

e. **Uninterrupted Electrical Power Supply:** To ensure an uninterrupted power supply during pumping, a portable 2.2 KW generator was procured for this exercise. Aside guiding against the erratic power supply often experience in this part of the world, most boreholes tested were located in remote villages that are not yet connected to the National electrical power supply, hence the need to provide a portable power source for the pumping test is non-negotiable (Plate 3.1A).

f. **Garmin Etrex GPS:** All the field observations of interest including the boreholes locations were represented in the appropriate maps in the course of this study, using Garmin Etrex GPS with an accuracy of ±3m. The Garmin etrex GPS was used to take three coordinates including the longitude, latitude and the elevations of all boreholes cited and tested in the field.

Prior to the conduct of the pumping tests, the pre-pumping level, the depth of the well and the saturated column were normally measured to establish the worth of the boreholes for testing.

3.4.2 Field Measurements and Precautions

Four kinds of measurements were taken during the pumping and recovery tests:

a. **Water Discharge Q**: This is the pumping rate and it is the quantity of water discharged per unit time. The unit of the quantity of water discharged can be in cubic meter or smaller units such as liter, gallon etc. Time measurement can also range from seconds to days. To obtain the actual volume of water discharge per unit time by the aquifer through the well, the initial reading was subtracted from the reading obtained for that particular time. For the present study water discharge is measured in both m^3/day (where, 1000 liter = 1m^3) depending on the emphasis at each section of the work. The tool used for

Plates 3.1 cont.: Equipment for the conduct of Pumping and Recovery tests at Ibarapa, **C**- showing water-flow meter. **D**: showing installation of submersible pump at Tapa.

measuring the groundwater discharge is the water flow meter ISO 4064 DN20 (Plate 3.1C) with an accuracy of 0.0001m^3 (or 0.1 litre).

This is the well discharge denoted by Q which is used in estimating other hydraulic parameters such as the transmissivity. The discharge is expressed as m^3/time, while time could be in any unit of time like in seconds, or days. It is mandatory to monitor the discharge on specific time intervals (per minute) during pumping to monitor the pumping rate. It is impossible to maintain a uniform pumping rate throughout the duration of the test even when a constant discharge method is used as noted by Kruseman and de Ridder, (2000). This was also the case in this present work, where the estimated pumping rate in m^3/min varied over the test due to variation in water pressure. The average pumping rate is always used as the representative constant discharge.

b. **Static Water Level and Well Depth**: The pre-pumping water level represents the water level at non-pumping state of the well. It is also the depth to water level in the well. The static water level and the depths of individual boreholes were measured in metre using automatic water level indicator. The depth of the well is useful in estimating the saturated water column and also applicable to deducting other points of hydrogeological importance. The pre-pumping water level and the total depth of the well were always the first to be measured prior to pumping. The pre-pumping water level has to be taken prior to the installation of the submersible pump and riser pipes and re-taken after the installation. The original water table is represented by the first measurements, while the second measurement is employable for the processing of the pumping test data. It is customary that the pre-pumping water level should be measured after the installation of pumping test facility in the borehole, since all other drawdown measurements have to be taken likewise.

c. **Drawdowns**: During the constant discharge pumping tests, water levels in the well were measured at specific time intervals many times during each test, with as much accuracy as possible. The difference between two respective water-level measurements during pumping for a specific period of time is the drawdown. Measurements were taken in most cases at every 30seconds for the first five minutes of the test because water levels are dropping fast at initial

stage. The time intervals were increased as pumping continues. The boreholes tested were pumped continuously till steady state condition were reached or water discharge ceased during pumping. In case where there is outright cessation of water, it means the aquifer yield could no longer support the rate of discharge.

The essence of water level measurements during pumping phase is to derive the drawdown at every given time. The time-drawdown curves are very valuable in plotting the diagnostic curves that are used to recognize the aquifer type that the pumped well is penetrating.

d. **Measurement of Water Level during Recovery Phase:** After pump cessation the recovery phase of the test begins. Water level measurements can assume the same time interval as the pumping phase, since the water levels in the well will start to rise; rapidly at first, but more slowly afterwards. These rises can be measured in what is known as a recovery test. The recovery is measure in Litre/time.

e. **Saturated Water Column (Apparent Saturated Aquifer Thickness)**: The saturated water column is the length of the water column in the well. It is calculated as the difference between the total depth of the well and the pre-pumping water level i.e. Apparent saturated aquifer thickness = Total depth of the well – Pre-pumping water level. It is also known as the pressure head. The saturated water column is important in estimating the hydraulic conductivity. For weathered-fractured aquifers which are largely unconfined or semi-confined in nature, the saturated water column in the borehole is taken as the apparent saturated aquifer thickness, *b*' used to estimate the hydraulic conductivity from T = Kb' as long as the transmissivity is known.

3.4.3 Estimable Aquifer Properties from Single-well Tests

The estimable hydraulic properties of the aquifer system using single-well test are the discharge, drawdown, transmissivity, hydraulic conductivity and specific capacity of the wells. Other measurable hydrologic parameters of interest are the well elevation, static water level (water table), well depth and the saturated water column which is the apparent thickness of the aquifer.

a. **Transmissivity**: For the present work, aquifer transmissivity was estimated using Jacob's straight line method (Cooper –Jacob method, 1946). Theis recovery method was employed to analysis Time-drawdowns affected by skin. These methods were described below and appropriately in Appendix VA. However, storage coefficient could not be analysed since no observation well(s) are used. The unit of measurement of transmissivity was m^2/day.

b. **Hydraulic Conductivity**: The hydraulic conductivity was derived from the equation T = Kb', where T is the estimated transmissivity, K is the hydraulic conductivity and b' is the apparent saturated thickness of the aquifer which is synonymous to the saturated column. Information on the actual saturated thickness of the aquifers are not available, hence the saturated thickness is taken as the apparent saturated thickness of the aquifer. Also, since no observation well is used in single well test, K cannot be directly estimated from the pumping test as transmissivity. Therefore, the hydraulic conductivity is then the ratio of the transmissivity to the saturated column. The unit of measurement was m/day.

c. **Specific Capacity**: this was derived from the ratio of the average pumping rate or water discharge to the total drawdown in the well during the entire pumping period, i.e. Specific capacity = discharge/total drawdown

   The specific capacity of is used to estimate the efficiency of the well. The units of measurement of specific capacity for the present work were m^3/day/m and litre/minute/metre.

Description of details of principles and procedures for hydraulic characterisations are presented in Appendix VA and the corresponding illustrative pictures in Appendix IB. Methods of control of water infiltration within the vicinities of tested wells during pumping phase are presented in Plate 3.2.

3.4.4 Data Processing

3.4.4.1 Drawdown Curves and Response of Aquifer to Pumping

An aquifer system is initially an unknown system prior to the plots of drawdown curves. The drawdown plots are crucial in estimating the hydraulic characteristics of

aquifer system, and there are two types of drawdown curves; namely, the Time-drawdown and the Distance-drawdown curves. Distance-drawdown curve require use of observation wells, and are not applicable to single-well pumping test, that was employed for hydraulic characterisation in the present study. The time –drawdown curve, can clearly identifies the four parameters that define water flow regimes commonly associated with any aquifer system. These are influences due to water in the well-bore, skin, aquifer and aquifer boundary conditions as illustrated in Figure 3.3. For the first few minutes, the flow is dominated by the stagnant water in the well, known as the water storage effect. This effect is exclusive in time-drawdown analysis, since it does not represent aquifer response to pumping.

Typical aquifer boundary conditions have been defined from the Time-drawdown curves by various workers such as Kruseman and de Ridder, (2000); Singhal and Gupta (1999) and Phillippe *et. al.* (2008). Hence, Time drawdown curves were used to identify the boundary situations of the crystalline water-bearing zones of Ibarapa areas.

3.4.4.2 Analyses of Time-drawdown Data

For the present work, two methods are applicable for the analysis of single –well pumping test and the residual Time-drawdown field data. These are; the Jacob's straight line and the Theis-Recovery methods. The latter method is used to analyse wells with skin effects.

Jacob's straight line method for analysis of Time drawdown semi-log plots employed the Cooper –Jacob method (1946) equation for estimating the transmissivity of the aquifer. From the straight line plot, obtained from the semi-log graph of drawdowns (vertical/arithmetic axis) versus time (horizontal/logarithmic axis) the transmissivity, T and storage coefficient, S are given as:

$$T = 2.3Q/4\pi\Delta s, \text{ and}$$

$$S = 2.25Tt_0/r^2$$

Where,

Q = pumping rate, proportional to the slope of the straight line.

Δs = drawdown across one log cycle

t_0 = point of intersection of the straight line to the zero drawdown line

Plates 3.2: Methods of control of water infiltration from groundwater discharge within the vicinities of tested wells. **A**- Groundwater flow being collected in water containers at Ayete. **B**- Groundwater flow being drained into concrete drain-line at Igboole in Igboora.

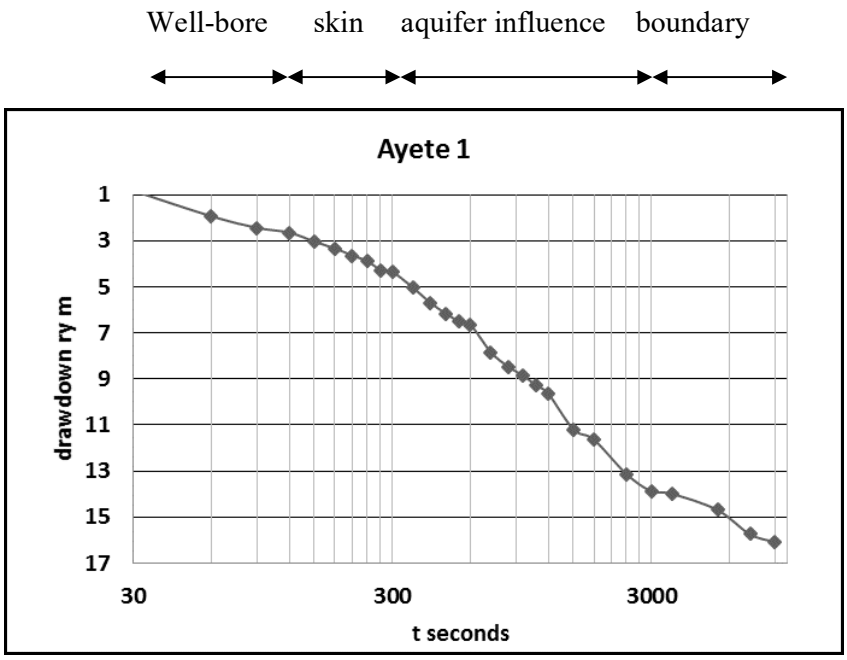

Figure 3.3: Typical Time-Drawdown semi-log plot obtained at Ayete, showing the four flow segments

r = distance of the observation well to pumping well

The Cooper-Jacob method is quite useful in identifying the heterogeneity of an aquifer. In the analysis of multiple wells, the transmissivity or storage coefficient can be calculated from the time drawdown graph of any of the wells, since the results would be the same, if the aquifer were homogeneous and isotropic. However, since no observation wells were used in the single-well test, r could not be determined. Hence, storage coefficient could not be estimated.

The recovery method employed residual drawdown from recovery test, and according to Theis (1935), transmissivity obtainable from a plot of s^1 versus t/t^1 on semi-log paper (t/t^1 on logarithmic scale) will yield a straight line. The slope of the line is

$$\Delta s^1 = \frac{2.30Q}{4\pi T}$$

Where $\Delta s'$ is the residual drawdown difference per log cycle of t/t^1. If Δs^1 and Q are known, then the transmissivity is:

$$T = \frac{2.30Q}{4\pi \Delta s^1}$$

where; s^1= residual drawdown in m; T = transmissivity of the aquifer in m^2/d; t = time in days since the start of pumping; t^1 = time in days since the cessation of pumping, and Q= rate of recharge = rate of discharge in m^3/d.

In this regard, for the present study, the transmissivities of the aquifer systems were estimated from the semi-log plots using both Jacob's straight line and Theis recovery methods. Other hydraulic properties such as total drawdown, drawdown per log cycle, hydraulic conductivity and specific capacity were estimated as stated above.

3.5 Groundwater Recovery and Sustainability

Alley *et al.* (1999) defines groundwater sustainability as the development and the use of groundwater in a manner that can be maintained for an indefinite time without causing unacceptable environmental, economic, or social consequences.

Most of the tested wells were left to recharge to over 90% of the pre-pumping water level. From the recovery tests conducted along with pumping tests, an attempt was made to estimate the quantity of water coming into the well through the weathered and

fractured zones and it is presented in Appendix VB. However, since the rates of water recharge were different from well to well, and in order to visualize the disparity in changes in rates of groundwater recharge during recovery, smaller unit in litre per minutes (litre/min.) was estimated using the recovery data. Three rates of groundwater recharge were examined and their average values (i.e. average rates) in minutes/liter by bedrocks was compared using recovery data for the first and the second 15minutes of recharge, as well as for the entire recovery phase. The three phases of rates of groundwater recharge in wells and mathematical operations employed for analysis are presented in Appendix VB.

Details of the principles of single well pumping and recovery tests, procedures for analysis and data processing techniques as well as the various interpretation models are also presented in Appendix VA&B.

From these approaches of study, groundwater potential data were generated and theoretical models of the hydrogeological settings of the basement aquifers of the study area were then postulated.

CHAPTER 4

4.0 RESULTS, INTERPRETATION AND DISCUSSION

4.1 Geological and Structural Settings

4.1.1 Rock Units Underlying the Study Area

The present work covered a total area of 711.17 km^2 of Ibarapa region in south-western Nigeria. The principal rock units that underlie this area include: Porphyritic biotite granite; homogeneous medium grained granite; gneisses that comprise biotite-hornblende gneiss, biotite-garnet gneiss and augen gneiss, amphibolite and migmatite. Minor occurrences of porphyroblastic gneiss, quartzites, quartz veins, and pegmatites rock units are also found to be associated with the major rock units in the area. The distribution of the major rock units in the study area is presented in Figure 4.1a. Details of the bedrock units are discussed below.

a. Coarse Porphyritic Biotite Granite

The outcrop exposures of porphyritic biotite granite occupy about one-third of the entire study area. It is the dominant bedrock along a N-S trend at the middle section of the study area. The landforms formed by granitic outcrops are ridges and inselbergs with intermediate low-lying areas. A cross section along profile A-B (Figure 4.1b) showed the relative elevated landform of porphyritic granite in the stusy area.. Porphyritic biotite granite is the major rock units at Idere, Ayete and Tapa. The porphyritic biotite granite composed mainly of quartz, biotite and conspicuously large-sized (or phenocrysts) of potassic feldspar (Plate 4.1A). The mineral grains of both quartz and feldspars are coarse and interlocking and their sizes range from one outcrop to another rocks; though that of feldspar is conspicuously large. Biotite mineral exhibits a platy texture in nature and not massive as those of quartz and feldspars. The lengths of some of the porphyries of feldspars are up to about 10.0cm but some could be as small as 3.0cm. The shape of the porphyries are mostly cylindrical but on few occasion shapes are irregular.

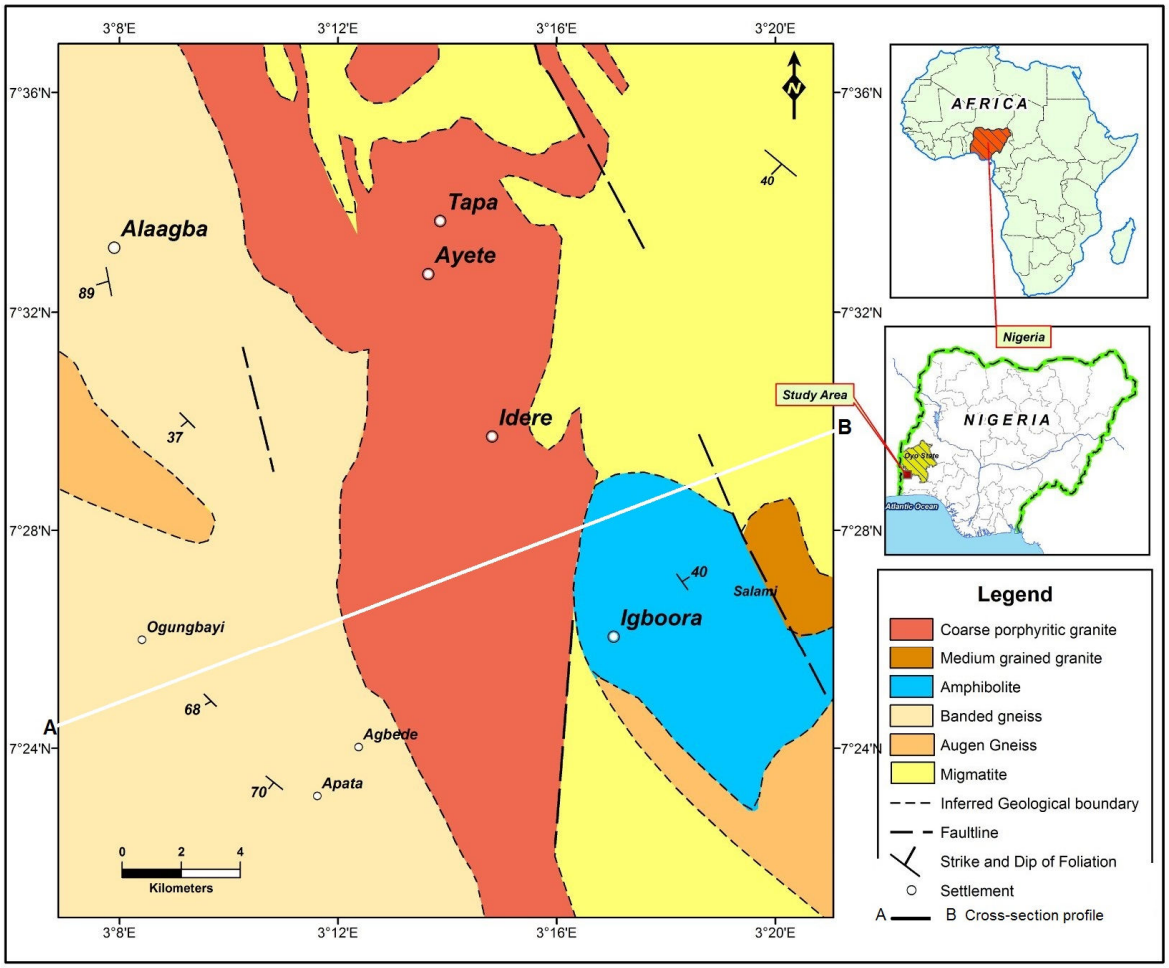

Figure 4.1a: Geological map of the study area (Updated after Weerawarnakula, 1986)

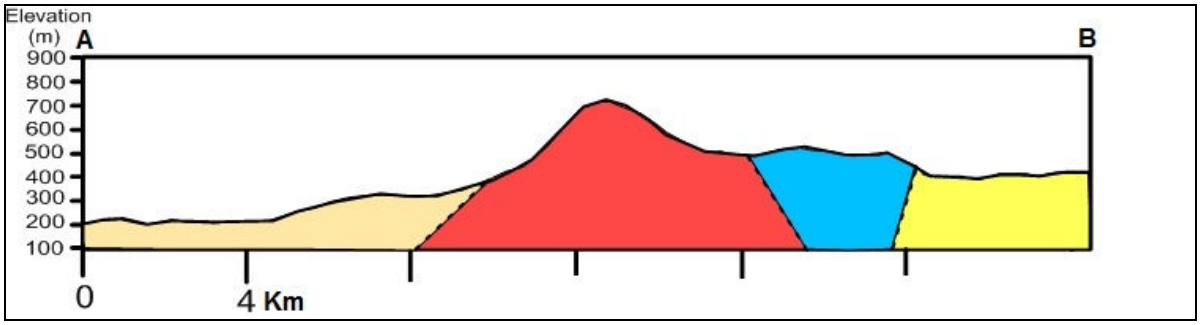

Figure 4.1b: Cross-section showing relative corresponding elevations of bedrocks across profile A-B.

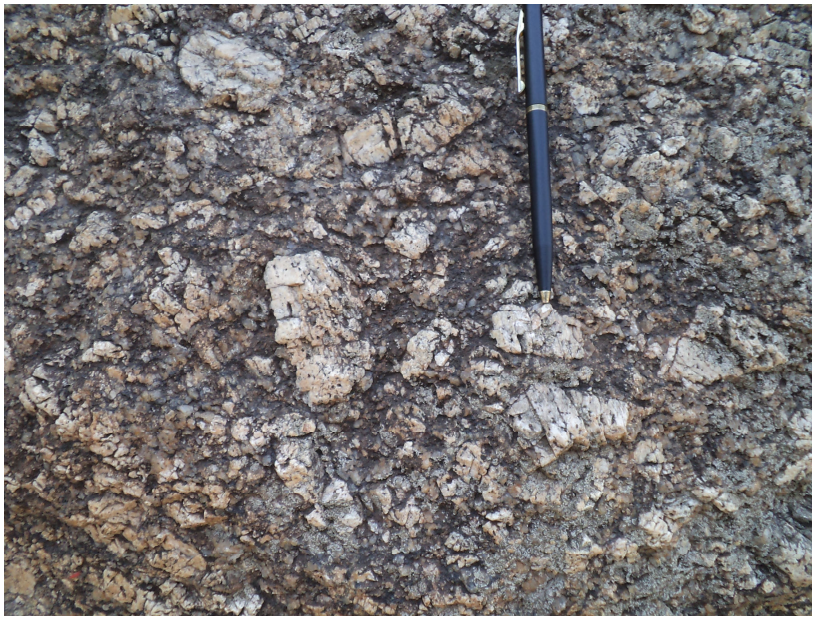

A

B

Plates 4.1: **A**- Showing the conspicuous large grains of K-feldspars in Porphyritic granite, Location: Idere. **B** - Elongated feldspar grains of coarse porphyritic biotite granite, Location: Tapa.

On many of the outcrops, the porphyries are aligned in preferred orientation (Plate 4.1B). At Idere the feldspathic porphyries are aligned on NE orientation ranging from 010^0 to 044^0, while at Tapa the orientations are mostly in NW trend ranging from 308^0 to 347^0. There are occasions when the alignments are not uniform on the same outcrop, where the measured strikes of the porphyries are widely trending between NE-SW.

The coarse porphyritic biotite granite are felsic rocks, due to large amount of leucocratic minerals. Loose mineral grains of quartz and feldspar conspicuously dotted the erosion pathways and are angularly shaped. This suggests that these minerals (particularly quartz) are more resistance to weathering than biotite. Hence, quartz and feldspar grains are more common in the soil unit than biotite. Biotite easily become unstable and is not preserved within the soil horizon.

b. Medium Grained Granite

Isolated outcrops of medium grained granite are common and are confined to small section at the eastern part of the study area. This rock occurs as intrusion in other principal rock units in the area. The mineral grains in medium grained granite are interlocking, homogeneous and massive. Identifiable prominent minerals in hand specimen are quartz, K-feldspar and biotite. The rock is generally felsic and the biotite concentration is small.

c. Amphibolite

Amphibolite outcrops are found as disjointed low-lying boulder sized units (Plates 4.2) across Igboora Town. It is the main bedrock that underlies Igboora. In respect of textural attribute, the amphibolite is fine to medium grained melanocractic rock. Two varieties of amphibolite are found at Igboora due to textural difference. These are the massive and the schistose varieties (Plates 4.3). The schistose structures are clearly seen in most outcrops, the massive variety is associated with inclusions of felsic minerals such as quartz and feldspars that occur as bands within the amphibolite. Occasionally, massive and schistose varieties do occur together on the same outcrops. In most of the mapped outcrops, lineation trend ranges from 093^0 to 124^0 in NWW-SEE direction, while the foliation plane dips between 38^0 to 44^0W

A

B

Plates 4.2: **A**- Fragmented low-lying amphibolite outcrop at Pako-Igboora.

B- Outcrop of amphibolite with hammer resting on the foliation plane which is dipping between 38 and 42^{0}W at Akede-Igboora.

A

B

Plates 4.3: **A**- massive amphibolite with an inclusion of quartz vein at Apata-Giri Igboora. **B**- Schistose foliated amphibolite at Pako-Igboora

C

Plate 4.3 cont. C: Weathered ampibolite with resistant quartzite intercalations, Location: Itaagbe-Igboora

(Plate 4.3B). However, at Apata Giri within Igboora, the foliation is aligned and plunged at an average of $050^0/50^0$W.

In respect of mineralogical assemblage, this melanocratic rock is rich in hornblende, plagioclase feldspar and biotite. In most locations, amphibolite occurs in association with quartzite and quartz schist. Intercalations of quartzite with fresh and weathered amphibolite were respectively mapped at Apata-Giri and Itaagbe within Igboora Township (Plates 4.3A and 4.3C).

d. Gneisses

Varieties of gneissic rock units mapped include banded gneiss, augen gneiss and porphyroblastic gneiss. Depending on mineral enrichment, banded gneiss are subdivided into banded biotite-garnet gneiss and hornblende –biotite gneiss. For ease of description in the present work, the banded gneissic rock units are undifferentiated in the geological map.

i. **Banded Biotite-Garnet Gneiss:** The outcrops of biotite-garnet gneiss largely dominate the southwestern part of the area. The outcrops are not very conspicuous and they extend over small areas where they are found and are mostly truncated by augen gneiss in many locations. Garnet grains occur as pebbles and are randomly distributed within the banded gneiss. When fresh, garnet is dark-red in colour, when weathered they look pale-brown in hand specimen. Garnet inclusions are more prominent within outcrops at Apata areas where the diameter ranges between 0.1 and 1.0 cm (Plate 4.4A).

   Mineral foliation strike is NNW with ranging between 339^0-360^0 while the foliation plane dips between 36^0 and 40^0E.

ii. **Hornblende-Biotite Gneiss:** The hornblende-biotite banded gneiss occurs as low-lying outcrops. The fresh sections are not commonly seen like other principal rock units found in the study area. For example, those mapped at Alaagba have become decolourised while most of the biotite mineral

A

B

Plates 4.4: A- Banded biotite-garnet gneiss with garnet grains inclusions at Apata **B**-Perpendicularly dipping gneiss with hammer resting on the foliation plane at Alaagba

assemblage has been weathered leaving the resistant quartz and K- feldspars. The strike of mineral lineation is NNE-SSW ranging between 004^0 and 028^0. The foliation plane dips between 74^0 and 88^0W, to almost 90^0 at Alaagba (Plate 4.4B).

iii. **Augen Gneiss**

Augen gneiss is characterised by the spindle shaped feldspathic structure otherwise described as eye-like structure. Most outcrops of augen gneiss found are flat-lying and leucocratic, with the quartz and the eye shaped feldspathic grains conspicously displayed. The feldspar grains on outcrop located at Sekere have diameter ranging from 2.2 to 5.0 cm. The feldspathic augen generally orientates in NW trend.

e. Migmatite

The migmatite exposures are mostly restricted to the adjoining villages such as Kondo, Obatade, Tobalogbo and Alabi Oja at the north-eastern part but terminated at Idere where they are intruded upon by the porphyritic granite. Migmatisation occurred as a result of the effects of latter intrusions of granitic materials on the earlier formed rock units typified by mixtures of pegmatites or fine grained granitic materials and older rocks such as the gneisses and porphyritic granite. The outcrops of migmatite preserved a lot of structural post-crystallization structural events like folds and fractures in the areas.

f. Minor Rock Units

The minor rock units are classified as the rock group whose outcrops are not prevalent and that covers a very small area in the study area. It also included rocks that occur as intrusions and veins truncating the principal rock units in the area. Hence, these rocks are only reported and are not included in the geological map due to their negligible area coverage.

Pegmatites, Quartzites and Quartz Veins: These rock units occur largely as intrusions into the principal rocks in the area. Quartzite occurs in close association with amphibolite in many locations, most especially within Igboora town (Plates 4.3A and 4.3C). Isolated quarzite ridges (outcrops) are hardly encountered in the

area, except the cobbles and pebbly sized grains that dominate the erosional pathways in some areas, most especially at Agbede village.

Pegmatites are associated with migmatite and represent the latter magmatic intrusion that is responsible for the migmatisation of the pre-existing rocks in the area. The pegmatites are felsic rocks composed of mainly orthoclase feldspar and quartz and are very coarse-grained.

4.1.2 Petrographical Study of the Crystalline Rocks of the Study area

Petrographical study of the crystalline rocks was restricted to mineral identification under the optical microscope. The photomicrographs of the thin sections of samples obtained in the field are presented in Plates 4.5. Study of the thin section was limited to amphibolite and the fine grained intrusions within gneisses and porphyritic granite. Mineral grains in amphibolites are fine and could not be easily identified by unaided eye, whereas those within porphyritic granite and most gneisses are coarse to medium grained.

Plates 4.5A-B represent sections through the samples of amphibolite under cross polarised light at X40 magnification showing the brown and green varieties of hornblende. Hornblende is commonly identified under optical microscope by cross-cutting cleavages at about 60^0 and 120^0, Plate 4.5C clearly shows the cleavage orientation of hornblende under plane and cross polarised light for samples at Akede within Igboora town. Other prominent minerals present in amphibolite are plagioclase feldspars, and biotite. Furthermore, the section through the gneiss sample obtained at Abola close to Ayete revealed that the mafic components composed mainly of hornblende and biotite minerals, as shown in Plates 4.5D. Hornblende grains are not just abundant like other mafic minerals, its grain sizes are also larger than others as seen in Plate 4.5D under cross polarised light at X40 magnification.

The major intrusion that cuts through the Alaagba gneiss is a medium grained melanocratic rock in hand specimen. The photomicrographs of this rock revealed that biotite and plagioclase feldspars are abundant and low in quartz (Plates 4.5E and F). This mineral assemblage typified those of intermediate igneous rocks, namely diorite. The biotite appears brownish under plane polarised light at X100 magnification (Plate 4.5E), while the plagioclase feldspar grains are well distinguishable under cross

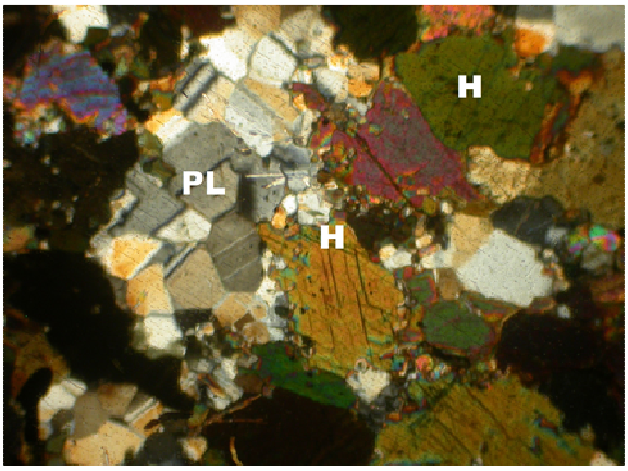

A

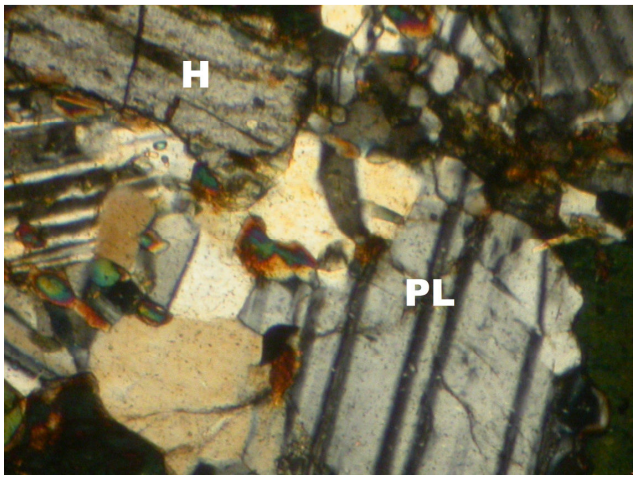

B

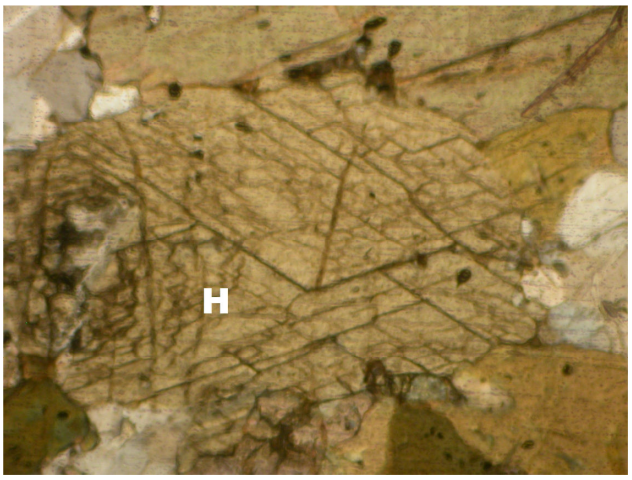

C

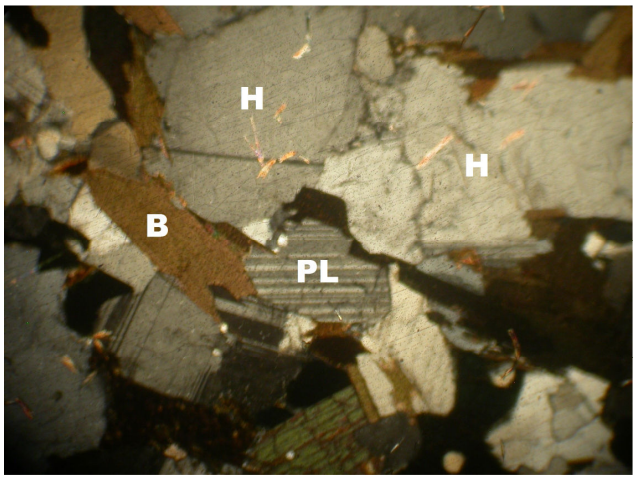

D

Plates 4.5: Photomicrographs sections through amphibolites, showing the brown and green varieties of hornblende (H), plagioclase feldspars (PL) and biotite (B**)** under **A**: cross polarised light and **B**. X40 magnification at Akede, and Apata-Giri. **C**: section through amphibolite revealing the cleavages crossing of hornblende mineral crystals at 60^0 and 120^0 under plane polarised light at X40 magnification Location: Akede. **D** sections through Hornblende-Biotite Gneiss, showing hornblende (H) and biotite (B) as the major mafic minerals under cross polarized light at X40 magnification. Location: Abola.

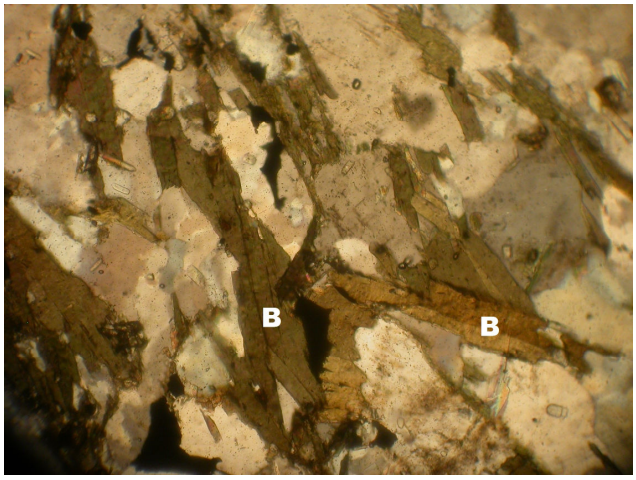

E

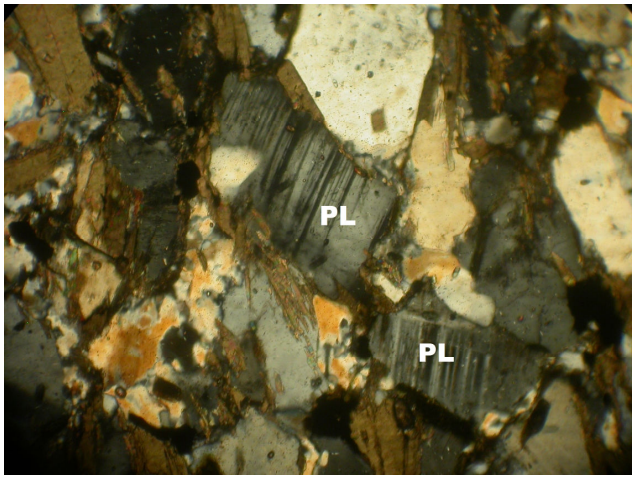

F

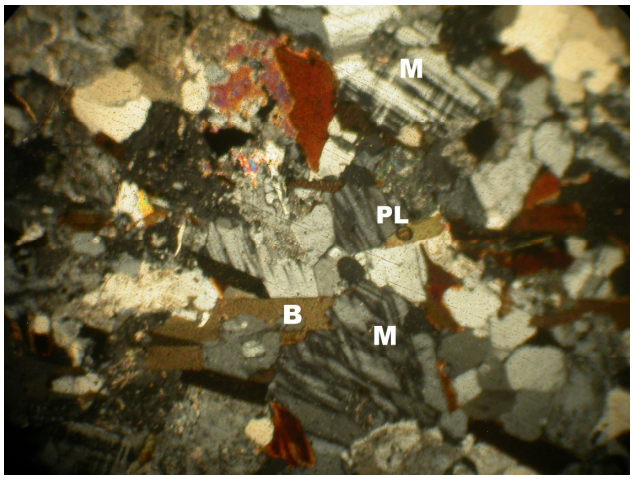

G

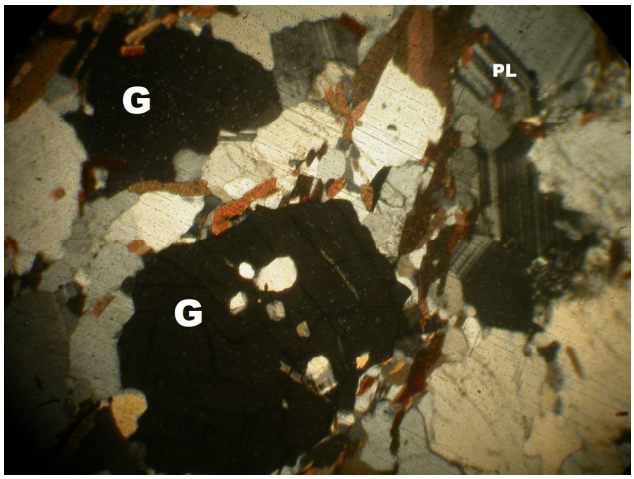

H

Plates 4.5 cont.: Photomicrographs of sections through the fine grained melanocratic rock that intruded into the banded biotite gneiss, **E:** Showing biotite (B) and **F:** Plagioclase feldspars (PL) as prominent minerals under plane and cross polarised light and at X100 magnification respectively. Location: Alaagba. **G:** Section through fine grained leucocratic granitic rock that intruded into the porphyritic granite, showing microcline feldspars (M) as abundant minerals. Location: Idere. **H:** Section through biotite-garnet gneiss, showing garnet grain (G) with feldspar inclusions under cross polarised light and X40 magnification. Location: Apata.

polarised light and at X100 magnification by their characteristic lamellar twinning (Plate 4.5F). Conversely, sections through the felsic, fine grained intrusive rock that intruded the porphyritic granite at Idere revealed abundant microcline, small amount of biotite and quartz mineral assemblage (Plate 4.5G), characteristic of granitic composition.

The garnet inclusions in banded gneiss sampled at Apata village appeared black under cross polarised light at X40 magnification (Plate 4.5H) and are sandwiched by biotite and plagioclase feldspars. Some of the garnet grains contain feldspathic inclusions as seen in Plate 4.5H.

Lastly, from the geological studies, the study area can be broadly delineated into four main bedrocks units, namely; porphyritic granite that underlain the central region; migmatite found at the NE and SE parts; amphibolites bedrocks that are restricted to the SE region and gneisses that dominate the entire landmass at the western axis of the study area. The gneissic bedrocks are mainly banded gneiss with biotite and hornblende varieties. Augen gneiss is also fairly represented (Figure 4.1a).

4.2 Geomorphological Characterisation

4.2.1 Thematic Maps

Thematic maps are essential hydro-geomorphological units (HGU) that are viable tools for hydrogeological interpretations of the study area, and are indicators of occurrence of groundwater, either directly or indirectly.

From the SRTM satellite imagery, thematic 2-D and 3-D digital elevation model (DEM) maps of the study area are correspondingly presented in Figures 4.2a and 4.2b.

4.2.1.1 Landforms

The geomorphology of the area is characterised by wide landform disparity of hills and inselbergs, highlands, lowlands and floodplains (Figures 4.2). The landforms of the area can be categorised into two main hydro-geomorphic units, namely; the high-lying and low-lying areas. The highland areas are characterised by granitic ridges and

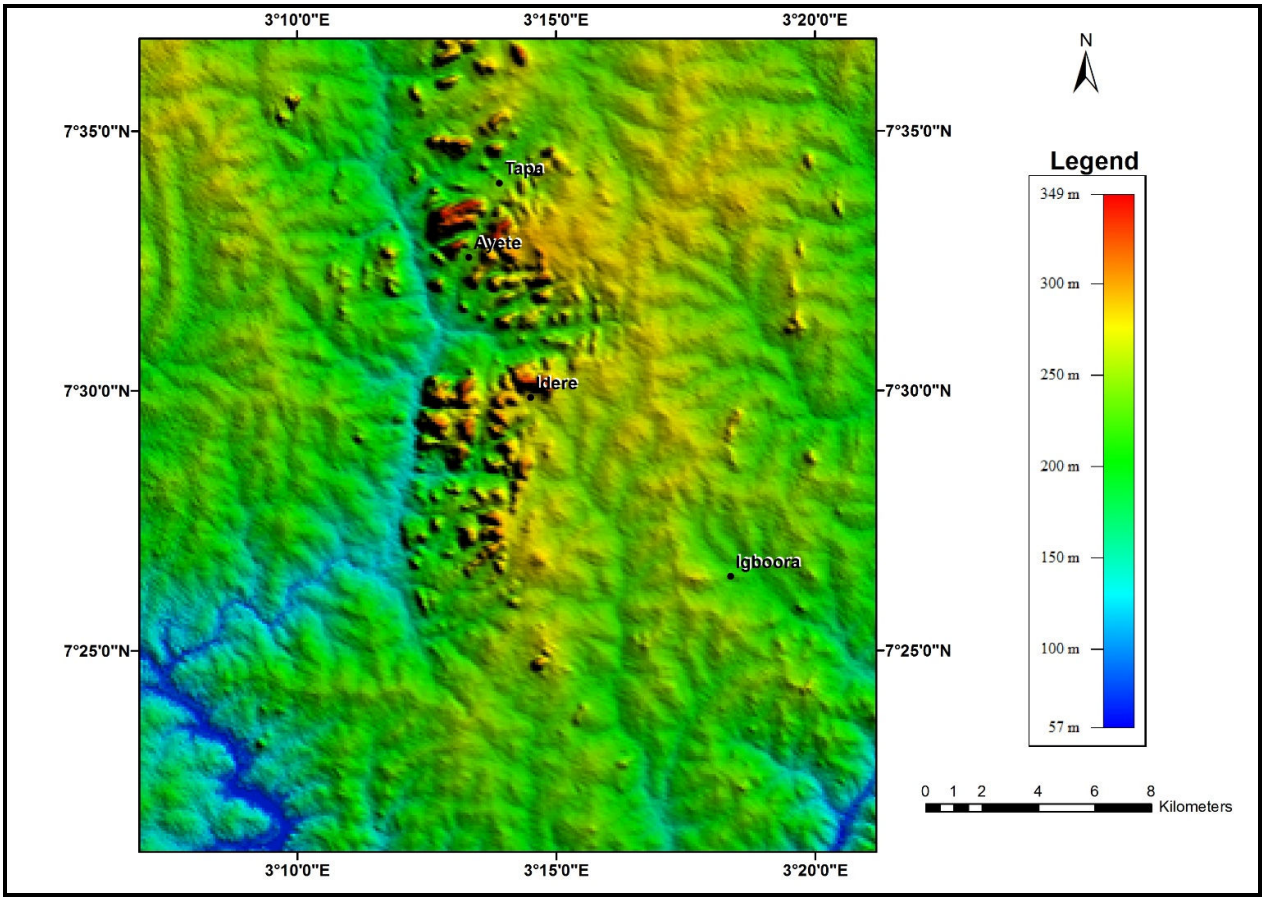

Figure 4.2a: Digital elevation model showing the spatial distribution of the various landforms over the study area

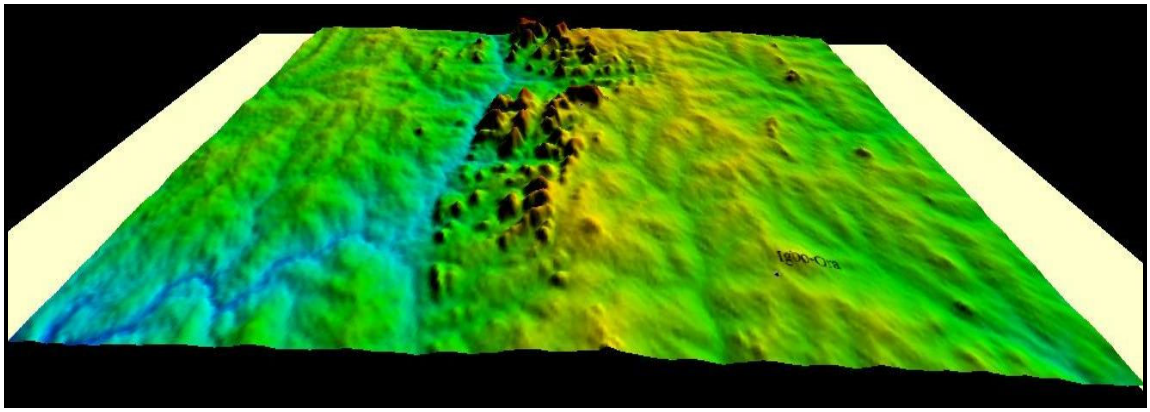

Figure 4.2b: 3-dimensional DEM image of the study area, showing the relative elevations of the various landform

inselbergs that spanned from the Mid-central to northern end of the study area; and this unit also included terrains underlain by migmatite at the north-east. The low-lying areas are made up of the lowlands and the floodplains.

These two major landforms are further discussed under four main headings:

a. **Hills, Ridges and Inselbergs**: these cover the central upper-middle portion of the study area, covering most of the main towns, namely Oye, Tapa, Ayete and Idere. These areas are typically characterised by hills and inselbergs with linear incisions in-between. The elevation peaks at 349m. The linear incisions are the valleys and obviously the only flashpoint for groundwater occurrence. Though, this is a function of development of sufficient weathering products (and possibly fractured basement). Most of these hills are porphyritic granite at Tapa, Ayete and part of Idere. Inselbergs are also in the eastern part of the study area. The ridges and inselbergs extend northward to Oye-Igangan at the northern boundary of the area.

b. **Highlands and Moderate-Highlands:** These terrains are mainly constrained to the NE parts, mainly underlain by migmatite. Most parts of the study area are moderate-highlands, including the valley incisions in between the hills and inselbergs. Areas underlain by gneisses and amphibolite are mainly medium-highlands terrain, characterised by gentle slopes which ends at Idere. These areas covered Igboora Township and NW areas correspondingly underlain by amphibolite and biotite gneiss. Most mappable linear features (including fractures, rock contacts etc) are also within the range of this relief.

c. **Lowlands**: this is the lowest parts of the study area characterised by river courses. It can be said to provide the major pathways that drain the area. This is the pathway for the major River- Ofiki that drains the area. The river cuts through the valley incisions between porphyritic granite and biotite gneiss at the upper western through augen gneiss to the floodplain at the SW, where it breaks into secondary River Oyan.

d. **Floodplain**: there are the areas of the lowest relief, which are prone to flooding and liable to thick sediment deposition. The major floodplain in the area is at the SW part of the study area underlain by banded gneiss.

4.2.1.2 Vegetation Index

The Vegetation Index map is presented in Figures 4.3. Groundwater occurrence from the geological and geomorphological studies can be validated from the Vegetation Index processed from Landsat ETM image, since vegetation response to water occurrence in the subsurface environment. The generation of vegetation index is critical in identifying zones of lush vegetation, seen as light tone on the NDVI and green colour on the colour composite transform (Figures 4.3a and 4.3b). The nature of vegetation in respect of orientation and lushness on the ground are indications of fracture trend, and availability of water in such fractures. For instance, fractures with water will support vegetation in dry season and generation of lush vegetation and presence of riparian vegetation along the lineament are indications of water-laden fractures and water seepage into subsurface environment along the river/stream channels.

4.2.1.3 Structural Lineaments

The SRTM and the Vegetation Index were employed for generating structural lineaments map that is presented in Figure 4.4. The superimposed linear features on the geology map is presented in Figure 4.5

Rock foliations are obvious in banded gneiss and in some outcrops of amphibolites (Plates 4.3B). Discriminatory alignment of the felsic and mafic minerals in gneisses facilitates differential mineral weathering and the eventual breakdown of the rock material. Additionally, amphibolite being a fine grained metamorphic rock that is particularly rich in dark coloured minerals such as hornblende and biotite (Plates 4.5), readily weathered to clayey/silty regolith when exposed to surface environment. Susceptibility of amphibolite to weathering is high as seen at Itaagbe in Igboora, where the weathered amphibolite is intercalating with disjointed resistant quartzite (Plate 4.3C). Also, differential weathering of unstable mafic minerals such as biotite and hornblende in gneisses and amphibolite further enhances the potential of these bedrocks to store and conduct groundwater. This is more so, when such openings are penetrative. Differential weathering of mafic minerals will increase the intensive of weathering of the rock mass.

In respect of fracture characterisation, it is known that all rock discontinuities of hydrogeological importance such as fractures, faults, and even rock contacts; apart

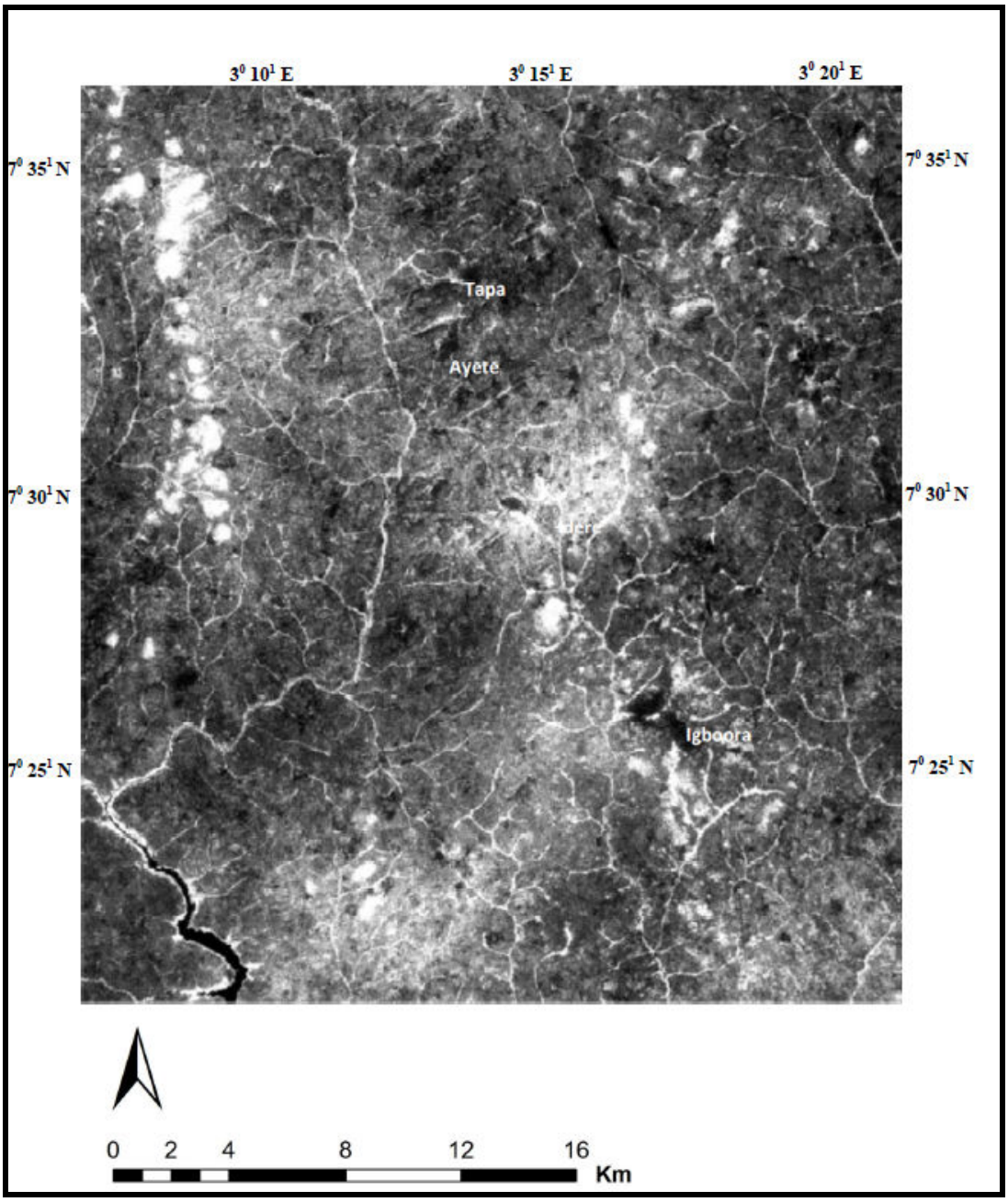

Figure 4.3a: Normalized Difference Vegetation Index (NDVI) of the Study Area

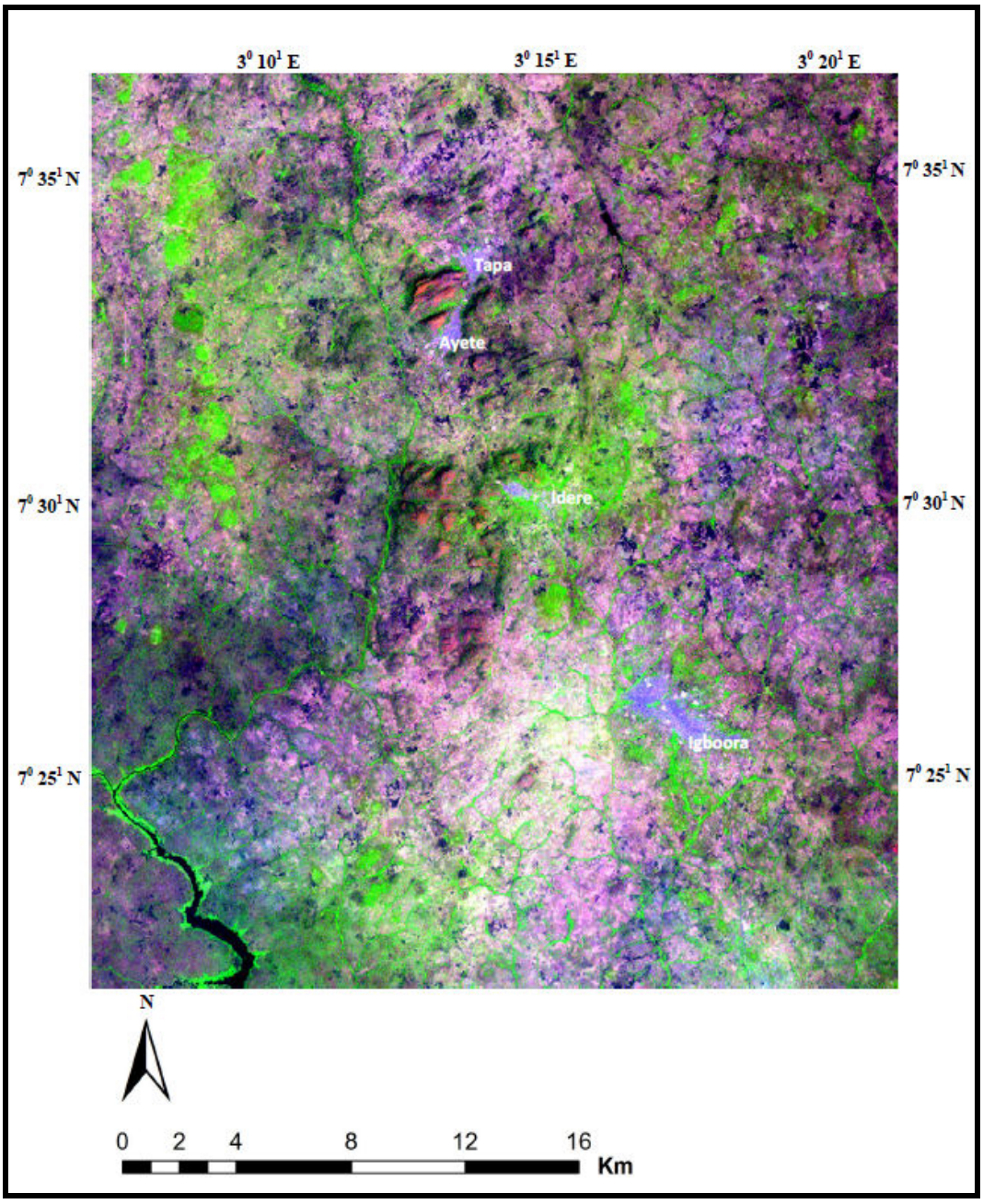

Figure 4.3b: Colour composite image (NDVI transform) of the study area

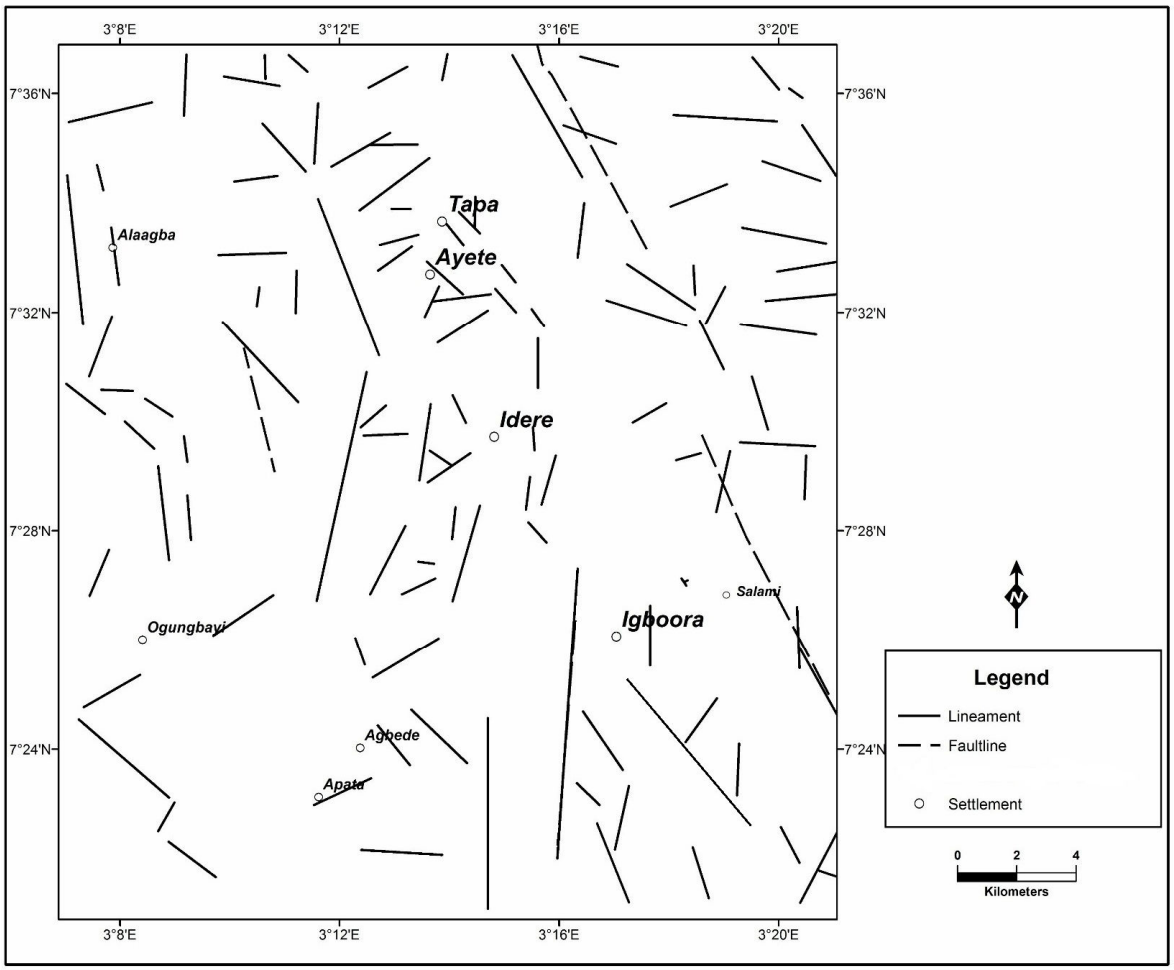

Figure 4.4: Structural map of the study area

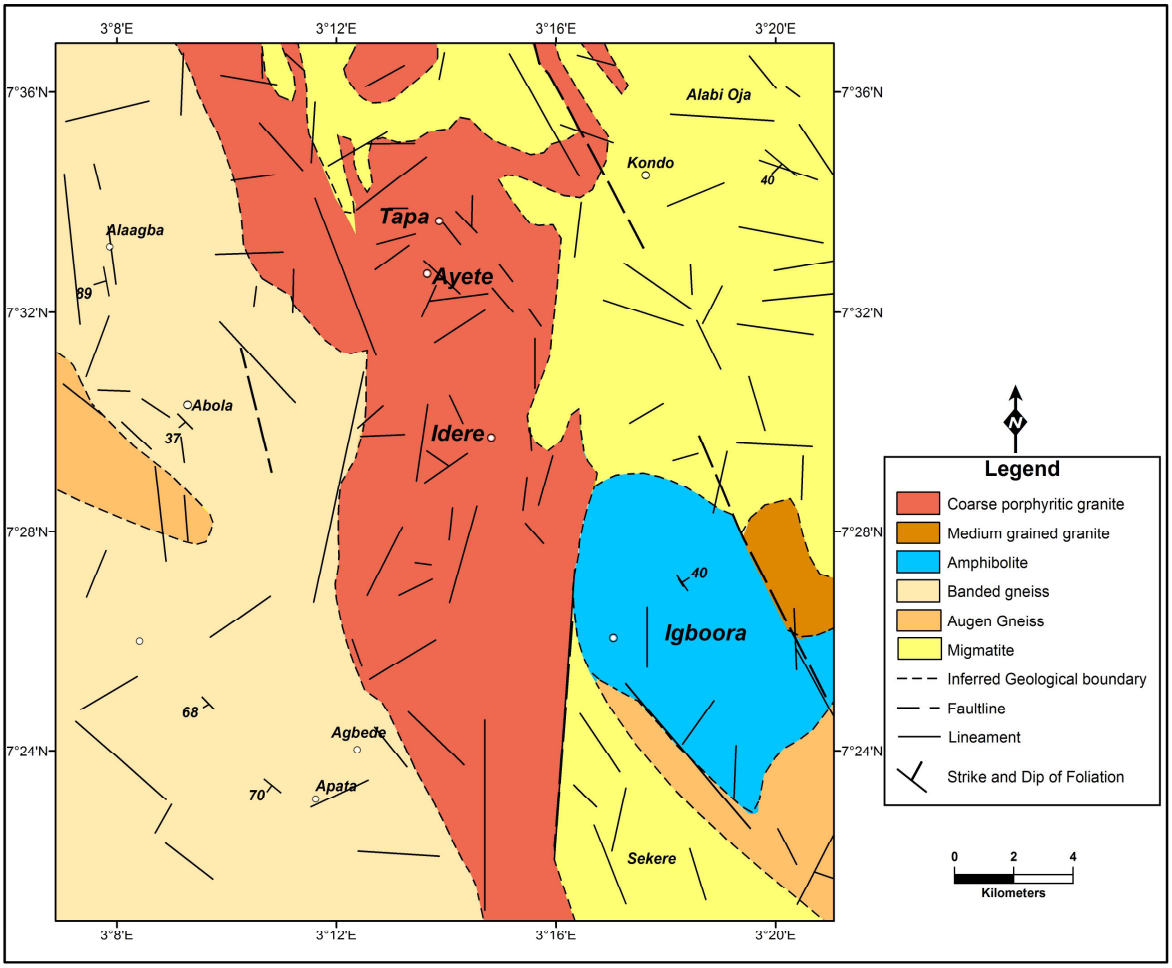

Figure 4.5: Lineaments superimposed on the geology map of the study area

from the weathered units, serve as storage and conduits for water in Basement Complex terrains.

Notably, there are spatial disparities in the directions, density and extent (or continuity) of these fractures across the study area. Conspicuously, the degree of rock brittleness is more intense at the central region underlain by porphyritic granite. This high-lying region of mainly granitic hills and ridges was characterised by more numerous, but short-length fractures with density of 0.25 km^{-2}, compared to other parts of the study area (Figure 4.2). Notwithstanding, the migmatite and gneisses terrains at the northern areas were dominated by more extensive and penetrative fractures, and close fracture density of 0.18km^{-2} and 0.17km^{-2} respectively. At the southern parts of the study area, the porphyritic granite terrains at the south-central portion is also having more spatial concentration of fracture (0.14 km^{-2}), compared to 0.06 km^{-2} and 0.10 km^{-2} obtained for south-west and south-east; underlain by gneisses and amphibolite respectively.

Furthermore, the superimposition of the linear features on the geological map in Figure 4.5, revealed that most of the mega fractures occurred at rock contacts. Infact River Ofiki that is the major river that drains the study area traverses the boundary between porphyritic granite and gneisses at the western part (Figures 1.4, 4.2 and 4.3). Also, at the eastern area, mega-linear features occurrences were associated with rock contacts between porphyritic granite and migmatite at the north, and in-between porphyritic granite, migmatite and amphibolite at the south-east area.

The low spatial density of about 0.10 km^{-2} in amphibolite terrains may not be the true representation of the fracture development in the area. This is due to the fact that Igboora Township is the most populated and most active in respect of infrastructural development and has the largest concentration of man-made structures in the entire region of study. Also, the outcropping amphibolite occurred mostly as boulder- size and is not that resistant to weathering. This crippled the effective application of remote sensing techniques for studying the lineament for that area. However, from the complimentary data obtained from NDVI thematic map (Figure 4.3a&b) amphibolite terrains were characterised by pockets of linear riparian forests, which is an indication of presence of fractures- containing water.

In terms of fracture continuity, porphyritic granitic terrains are associated with more

densely disjointed and least pronounced fracture development, compared to gneisses and migmatite bedrocks, except at rock boundaries locations as noted above.

The orientations of the structural features on bedrocks (Figure 4.6) revealed multiple prominent mega-lineament trends on bedrocks, except on amphibolite where the major fractures trend is mainly along NW. In gneisses, the prominent fracture trends are NNW, NW, and NE. Likewise, migmatite bedrocks were characterised by three major linear trends: E-W, NW and NNE; and porphyritic granitic by two major trends, along NW and NE.

The fractures are mainly rectilinear. This connotes the brittle nature of the 'hard' rocks that underlie the area. However evidence of ductile behaviour represented by curvilinear fractures existed at Alaagba within the NNW part of the study area which is underlain by biotite gneiss where foliation planes dip almost vertically (Figure 4.1a and Plate 4.4B). The regular fractures associated within gneisses and migmatite are oriented in east-west direction striking between 90^0 and 108^0. Faults found in the area are strike-slip and reverse faults.

4.2.2 Groundwater Indication from Geomorphological Characterisations

The hydrogeological interpretations are inferred from the attributes of structural lineaments and groundwater indication from the vegetal index, and inferences were then made to the underlying bedrock units and the landform characteristics of the area.

From Figure 4.7, lush vegetation and riparian forests that represent zones of important hydrogeological attributes that are potential groundwater zones are marked by circles and arrows. These are found as 'pockets' of localised portions across the area.

Generation of riparian forest along the river channels cuts across the area but it is most prominent along river Ofiki which runs along the geological contact of porphyritic granite and gneissic rocks located at the western portions. Also, along this same trend, there is an occurrence of conspicuous linearly arranged lush vegetation (marked by white arrow. The linear forest which trends NW-SE (Figure 4.7) is along the strike of the mega fracture of that location. This structural element is also conspicuous on other thematic maps in Figures 4.1a, 4.3, 4.4, and 4.5 correspondingly for geological, vegetation Index, lineament, and structural map for the study area. Also, the NW-SE

Amphibolite

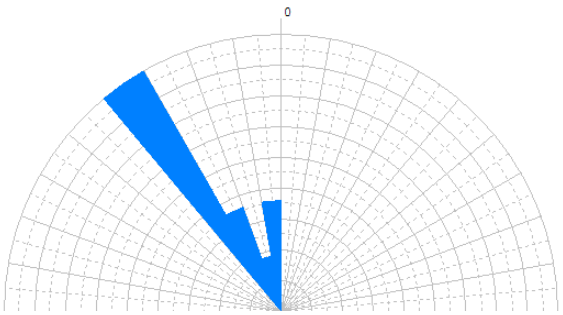

Prominent fracture trend: NW-SE

Gneisses

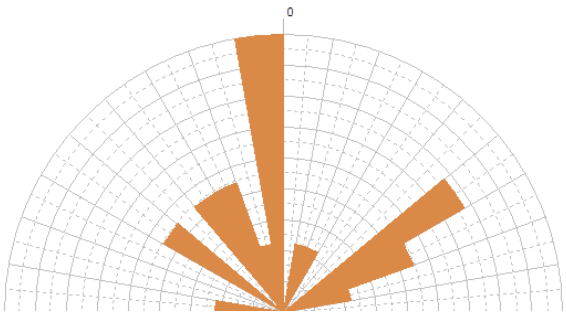

Prominent fracture trends: NNW-SSE, NW-SE and NE-SW.

Migmatite

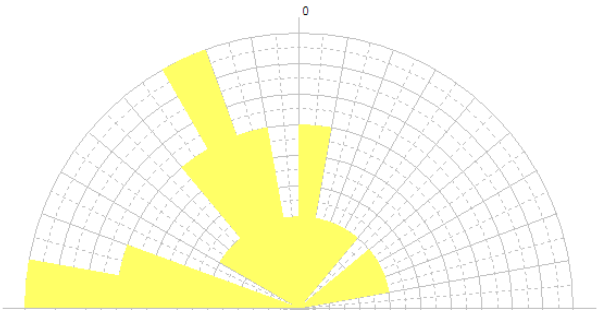

Prominent fracture trends: E-W, NW-SE and NNE-SSW.

Porphyritic Granite

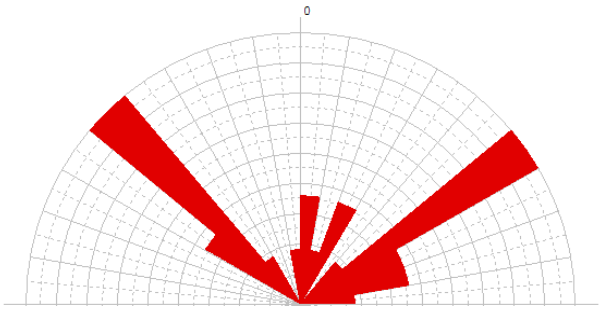

Prominent fracture trends: NW-SE and NE- SW.

Figure 4.6: Rose diagrams of lineaments/fractures obtained for the various bedrocks, illustrating the prominent orientations

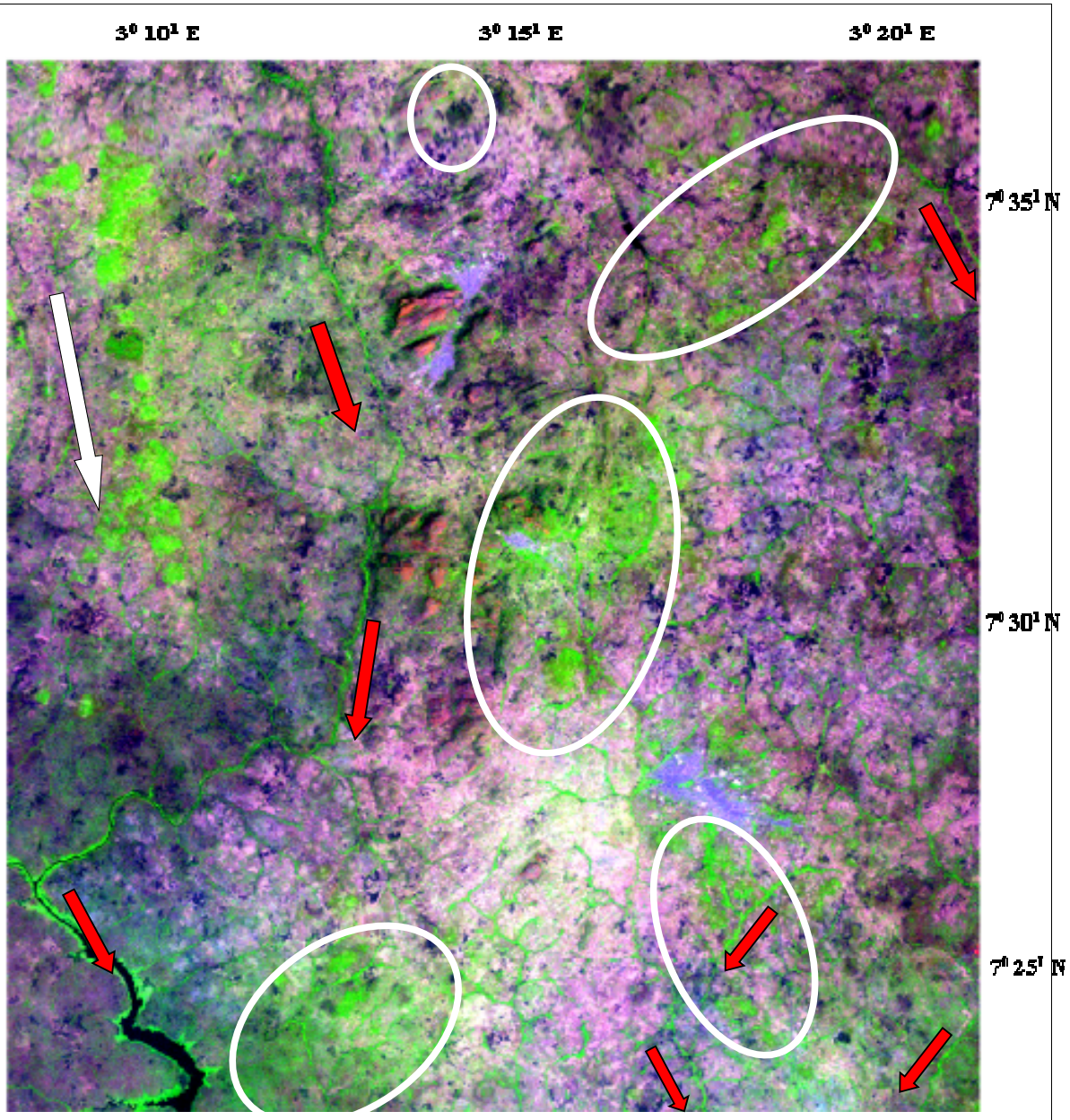

LEGEND

White circles represent clustered lush vegetation which indicates diverse fracture/lineament trends

White arrow indicates linearly oriented lush vegetation, aligned along the direction of the mega fracture/linear feature in that area.

Red arrows indicate riparian forested drainage lines that show that groundwater is present in the fractures/linear features.

Figure 4.7: Groundwater indication map, showing localised zones of water-bearing fractures based on vegetation response.

lineament trend is more abundant than other fracture directions at this region of the study area. This area is underlain by biotite gneiss, and foliation plane is vertically dipping (Plate 4.4B). Locations within this region are Fedegbo, Alaagba, and Bada, which are mainly rural settlements. Other areas with lush vegetation are clustered along the rock boundaries at Idere at the central and southern parts underlain by amphibolite and gneisses (Figure 4.7). However, vegetation response is at the lowest in the hilly and ridged terrains at the central part, while terrains underlain by migmatite are characterised by sparse vegetation occurring as thinly generated riparian forest.

Therefore, potential for groundwater occurrence can be said to be high in 'pockets' of areas. This is marked by lush vegetation occurrences at some locations across the study area particularly on gneissic terrain. However, the blocky nature of the vegetation at rock contact indicates that the rock contacts are viable groundwater zones but of diverse orientations. Also, the highland areas can be regarded as more of run-off zones. Although, fractures are dominant on granitic terrains, these fractures are mostly diverse, fragmented with short-length dimensions that does not favour water seepage. However, gneissic terrains are characterised by more extensive fractures that can be said to be well-connected at the western axis. Terrains at the NE underlain by migmatite are characterised by extensive fractures (Figure 4.4), but the vegetation response is not as dense as those associated with gneissic terrains and rock contacts areas (Figure 4.3). Water indications on migmatite terrain at the NE are characterised by few riparian forest and disseminated small-sized water-bearing fractures. Hence, from geomorphological characterisation, the occurrence of groundwater is low on porphyritic granite and migmatite terrains. The general hydrogeological interpretations under the watershed units of the area underlain by different bedrocks are itemised in Table 4.1.

4.3 Geophysical Characterisation

For geophysical characterisation, a total of eighty-five (85) geo-electric soundings (VES) were conducted in a systematic manner across the various bedrock units. The spreads of the soundings included 25 on amphibolite, 22 on gneisses, 18 on migmatite and 20 on porphyritic granite. Three VES could not be interpreted as a result of bad curve. The sounding locations are presented on the geological map (Figure 4.8).

Table 4.1: Hydrogeological Attributes Interpreted From Geological and Hydro-geomorphic Units (HGU)

s/n	Watershed units	Rock Type	Landform	Lineament characterisation	Vegetation Response	Hydrogeological implication
1	IWORO	Biotite Gneiss	Moderate-highland, strike ridges with adjacent parallel arranged valleys,	NNW-SSE trending fractures, some of which are curvilinear, indicating mega-fold structure	Lush linearly oriented vegetation along the strike of the foliation trend, development of riparian forest	Fractures – containing water aligned along the regional foliation trend. This indicates presence of groundwater along the strike of the local foliation trend.
2	OFIKI **Segment A**	Undifferentiated Augen, Porphyroblastic and Biotite Gneiss (Upper western flank)	Lowland with few inselbergs at the North	Low but lengthy rectilinear fractures, with variable orientations along NEE-SWW, NNE-SSW and NW-SE	Prominence of riparian forested vegetation along the tributary of River Ofiki.	Water seepage along the river channels- an indication of groundwater recharge along the river channel.
3	**Segment B** AFO-APE	Biotite-Gneiss and Quartzite (Lower western flank)	Plain Lowland	Low rectilinear fracture development	Lush clustered vegetation and moderate riparian forest development	Groundwater occurrence in variable directions.

Table 4.1 cont.

s/n	Watershed units	Rock Type	Landform	Lineament characterisation	Vegetation response	Hydrogeological Implication
4	**Segment C**	Porphyritic Granite (Eastern flank)	Upland characterized by hills and inselbergs with adjacent valleys,	Prominent rectilinear fractures, characterised by short-length and variable orientations along the NEE-SWW, NNE-SSW and NE-SW	Sparse vegetation along river bank	High fracture development with low water-bearing fractures indicate that the factures are not penetrative and are poorly connected. With uplands, surface run off is prevalent and groundwater recharge is low.
5	AYIN UPPER SECTION	Rock contacts Porphyritic Granite, Amphibolite and Migmatite	Generally an upland characterized by hills and moderate highland toward the eastern region.	Lengthy fracture along rock boundaries	Lush vegetation at the point of rock contacts and riparian forests along some fractures.	Prominent groundwater zones along rock contacts and along the NNW trending fractures in the area.
6	LOWER SECTION	Rock Contact Rock types as Above	Lowland with sparse small-size inselbergs	Fairly good fracture development within the migmatite terrain toward the eastern flank, with varying structural trends: NE-SW, NW-SE and NNE-SSW.	Low clustered vegetation around the rock contacts and a prominent riparian forest aligned along the river channel.	Fair representation of water-bearing fractures and recharge point.

Table 4.1 cont.

s/n	Watershed units	Rock Type	Landform	Lineament characterisation	Vegetation Response	Hydrogeological Implication
7	ABOLUKU	Predominantly underlain by Migmatite	Moderate highland	The fracture trend is mostly along the NW-SE trend	Scattered, small-sized pockets of vegetation and a prominent riparian forest development along a NW-SE trend	Pockets of disconnected groundwater occurrences and unconnected recharge zones.
8	OPEKI	Predominantly underlain By Amphibolite	Fairly raised lowland	Moderate lineament	Presence of riparian forest and fair lush vegetation	Moderate lineament with fair presence of water-bearing fractures. An evidence of water seepage that indicates fairly good groundwater recharge zone

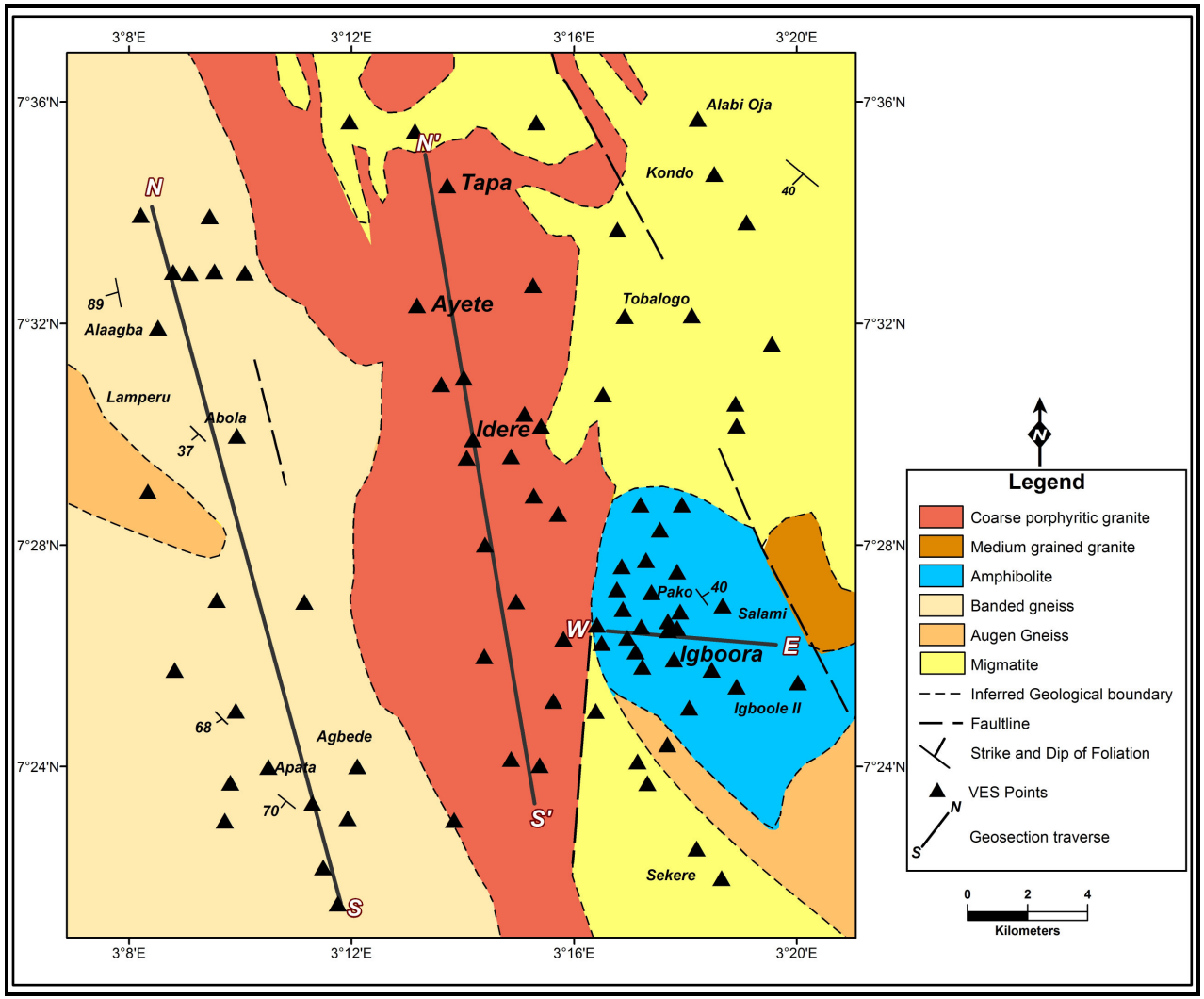

Figure 4.8: Location of VES points on the geology map of the study area

The apparent field resistivities, generated VES curves and primary geo-electric parameters for the eighty-five soundings are presented in Appendices VI, VII and VIII respectively, while the lithological interpretation of the saprolite layer developed upon the various bedrocks is presented in Appendix X. However, the general statistics of the geo-electric parameters are presented in Table 4.2.

4.3.1 The Geo-electric Curves

The dominant VES curve is the 3-layer H type; characterised by relatively more conductive middle layer that terminates on more resistive infinite layer. The infinite layer is partially weathered, fractured or fresh. Only seven curves representing 8.5% of the total VES curves generated were typically characterised by more than 3-layer geo-electric sequence. This included 4-layer KH type generated on VES points 9, 16 and 28, and one each of 4-layer HK and HA types correspondingly on VES-041 at Abokolaiya and VES-017 at Odofin, and two 5-layer HKH type curves located on VES points 30 and 80. Four of these locations were on areas underlain by amphibolite bedrock. One of the 5-layer HKH type curve located on VES-030 at Itaagbe in Igboora was interpreted from the sounding survey taken adjacent to the exposed section of quartzite intercalations within weathered amphibolite bedrock (Plate 4.3C). Examples of typical VES curves obtained in the field are presented in Figure 4.9.

4.3.2 Characterisation of Weathering and Weathering Profile

4.3.2.1 Iso-apparent Resistivity

The variation in weathering with depth was demonstrated by contouring the apparent resistivities for depths corresponding to current electrode distances (ab/2) of 10m, 24m, 55m, 75m and 100m. The iso-resistivity maps of the apparent resistivities are presented in Figures 4.10.

From Figure 4.10, there are clear vertical heterogeneities in weathering, with distinct general decrease in weathering with depth typified by increase in resistivity with depth. The spread of areas with apparent resistivities below 100Ωm which is regarded as highly weathered zone was largest at shallow depth of 10m. Rock decomposition reduces as depth increases. At ab/2 of 10m (Figure 4.10A) depth the intensity of weathering is highly developed upon most of the bedrocks, except on porphyritic

Table 4.2: General Statistics of the Primary Geo-Electric Parameters for Various Bedrocks

Geo-electric parameters	Explanation	Min	Max	Mean	Median	Std dev.
Amphibolite (n = 25)						
ρ1 Ωm	Resistivity of the Topsoil	38.40	3478.00	658.47	407.60	779.16
ρ2 Ωm	Resistivity of Saprolite layer	9.10	225.20	53.10	36.35	53.30
ρ3 Ωm	Resistivity of Bedrock	105.70	5472.70	1515.59	927.00	1531.27
h1 (m)	Thickness of Top soil	0.40	5.80	1.68	1.45	1.22
h2 (m)	Thickness of Saprolite layer	3.80	38.70	16.56	16.00	8.95
H (m)	Total Regolith thickness	4.40	39.40	18.06	17.20	9.12
Gneisses (n = 19)						
ρ1 Ωm	Resistivity of the Topsoil	176.90	4478.20	1343.59	984.30	1054.38
ρ2 Ωm	Resistivity of Saprolite layer	18.80	810.60	117.95	69.00	177.14
ρ3 Ωm	Resistivity of Bedrock	196.60	9601.40	1814.92	934.50	2242.51
h1 (m)	Thickness of Top soil	0.80	2.30	1.51	1.40	0.41
h2 (m)	Thickness of Saprolite layer	4.40	57.70	15.83	12.50	12.09
H (m)	Total Regolith thickness	6.30	59.00	18.49	16.60	11.60
Migmatite (n = 18)						
ρ1 Ωm	Resistivity of the Topsoil	237.20	2331.10	1194.21	965.70	705.00
ρ2 Ωm	Resistivity of Saprolite layer	28.10	565.50	204.39	61.00	442.47
ρ3 Ωm	Resistivity of Bedrock	191.30	6863.30	1488.25	989.15	1628.95
h1 (m)	Thickness of Top soil	0.50	2.80	1.56	1.40	0.62
h2 (m)	Thickness of Saprolite layer	3.40	22.40	11.31	11.85	5.10
H (m)	Total Regolith thickness	4.60	23.60	12.77	12.95	5.18
Porphyritic Granite (n = 20)						
ρ1 Ωm	Resistivity of the Topsoil	110.50	3271.90	1151.57	995.40	887.36
ρ2 Ωm	Resistivity of Saprolite layer	26.50	294.00	93.03	65.55	72.04
ρ3 Ωm	Resistivity of Bedrock	547.20	29903.80	4601.23	2605.35	6494.13
h1 (m)	Thickness of Top soil	0.60	4.50	1.76	1.25	1.06
h2 (m)	Thickness of Saprolite layer	1.80	19.40	9.52	8.30	4.11
H (m)	Total Regolith thickness	2.40	20.80	11.29	10.65	4.59

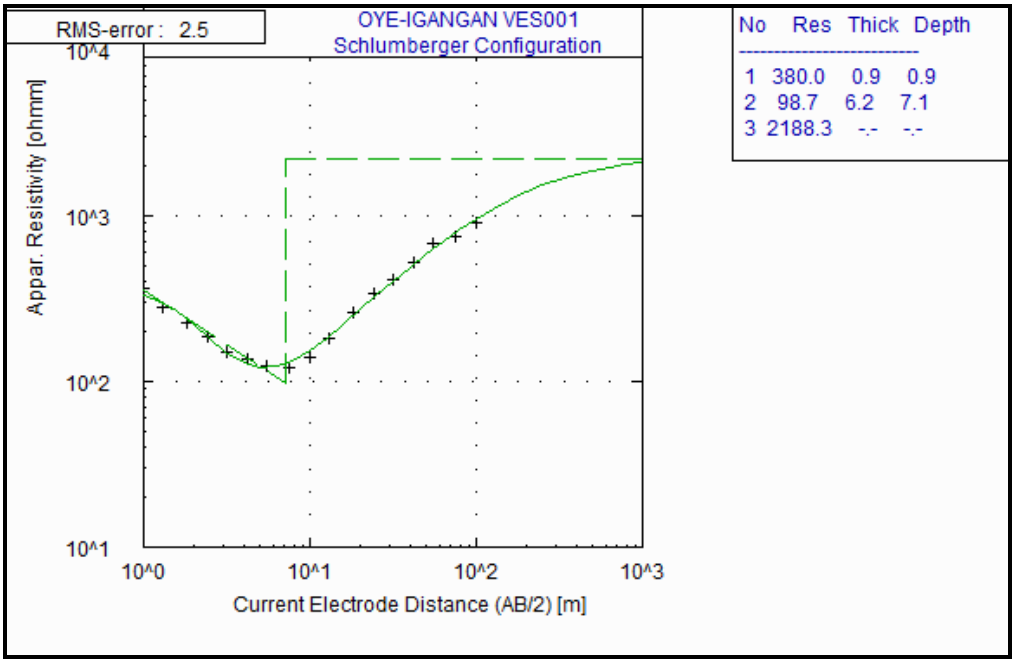

3 layer H-Type curve at Oye-Igangan on VES 001

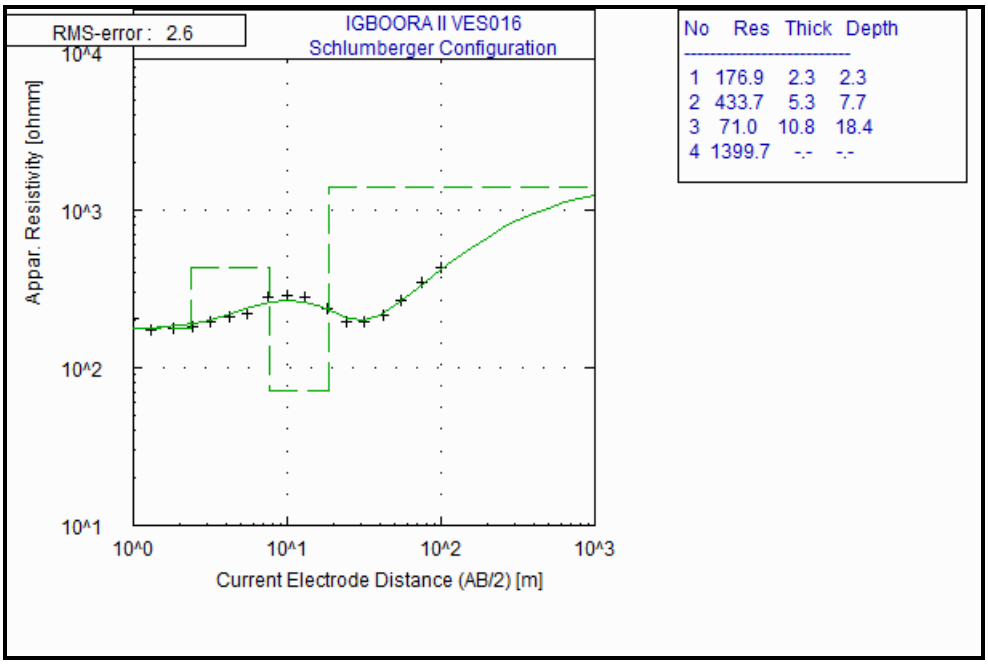

4 layer- KH-type at Igboora on VES016

Figure 4.9: Examples of typical VES curves obtained for the study area

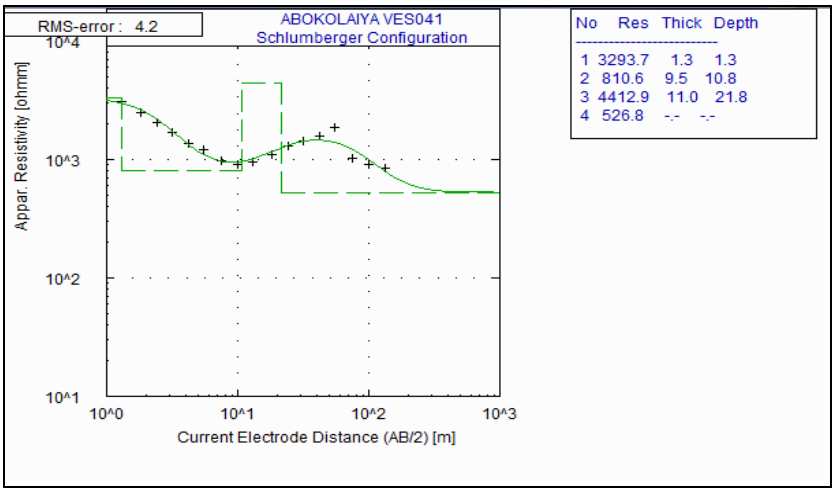

4 layer - HK-type curve at Abokolaiya on VES041

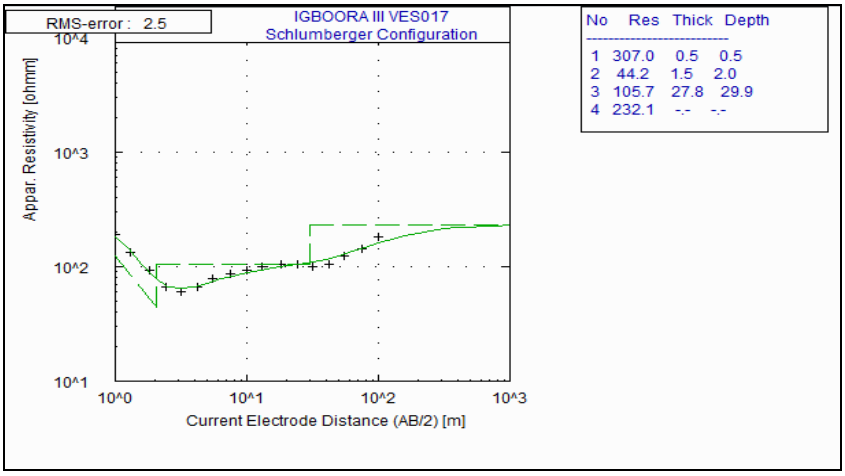

4 layer - HA-Type curve on VES017

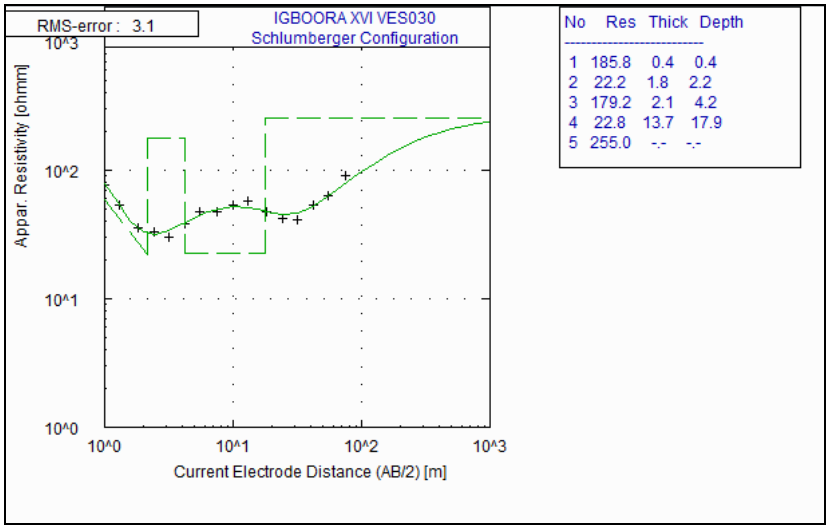

5 layers - HKH Type curve on VES030

Figure 4.9 (cont.): Examples of Typical VES curves obtained for the study area

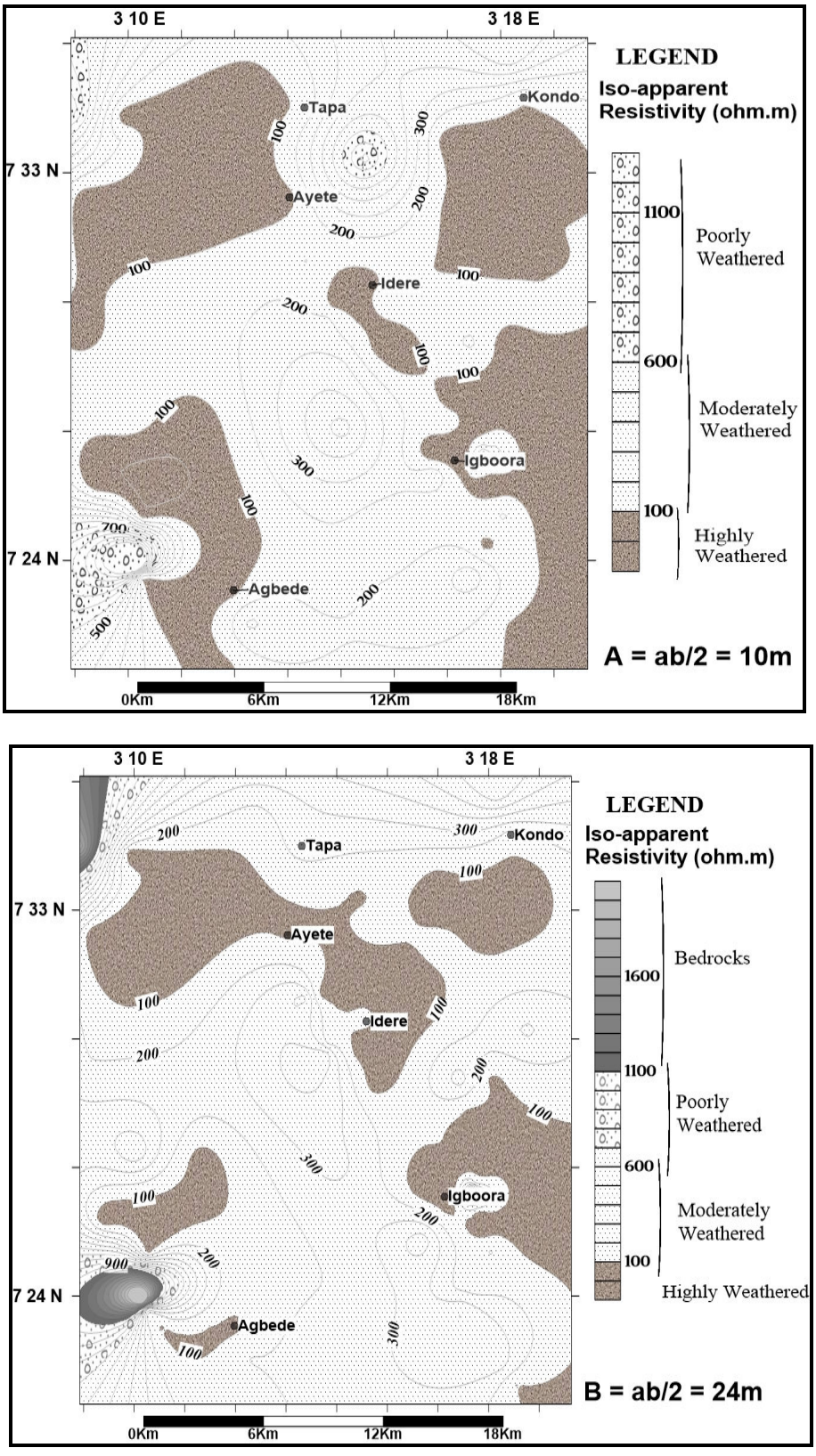

Figure 4.10: Iso-apparent resistivity maps of current electrode distances (ab/2) showing weathering characterisation with depth across the study area

granite, where the only portion classified as highly weathered zone was found at the rock boundaries. However, most area underlain by granite was categorized as moderately weathered horizon. With further increase in depth at ab/2 = 24m (Figure 4.10B), apparent resistivity increases, and zones interpreted as weak bedrocks with apparent resistivities lying between 1000-1800Ωm emerged; although, this is localised at the low relief floodplain area at the SW and NW parts underlain by gneisses. The intensity of the weathering reduces with the thinning out of highly weathered zones with depth and further expansion of the poorly weathered and nearness to massive bedrocks at longer electrode separations. Fresh bedrocks with apparent resistivities above 1800 Ωm are becoming prominent at ab/2 = 42m (Figure 4.10C) but these are mostly restricted to topographically low areas, which mean there is shallow occurrence of bedrocks at the floodplain. Less resistive bedrocks with resistivities range of 1000-1800Ωm are mostly prominent ab/2 depth of 42m. However, even at ab/2 = 75m (Figure 4.10D), large part of the study area are still categorised as being moderately weathered. This is an indication of a fairly deep weathering development with resistivities of 100-600 Ωm across the study area.

4.3.2.2 Weathering Profile

The weathering profile generated from the vertical section of the layered sequence processed from the apparent resistivities VES data revealed the degree of rock decomposition of the subsurface section beneath the survey points. The top soil and the saprolite subsurface horizons are collectively known as the weathered layer or regolith. The thickness of the regolith as well the textural attributes of the regolith materials developed upon the parent rocks in the geo-electric sequence are crucial parameters guiding the groundwater occurrence and movement in the subsurface, apart from the fractures in the subsurface environment. The general weathering profile in the study area irrespective of bedrock-type is three (3) layered sequence; namely the topsoil, the saprolite and the bedrock. These lithological units are discussed below.

a. Topsoil

The resistivity of the topsoil varies, ranging from as low as 38.4 Ωm in amphibolite to as high as 4478.2 Ωm at Alaraba underlain by gneissic bedrock. The mean value of 658.5 Ωm obtained over amphibolite is typically lower as compared to the range

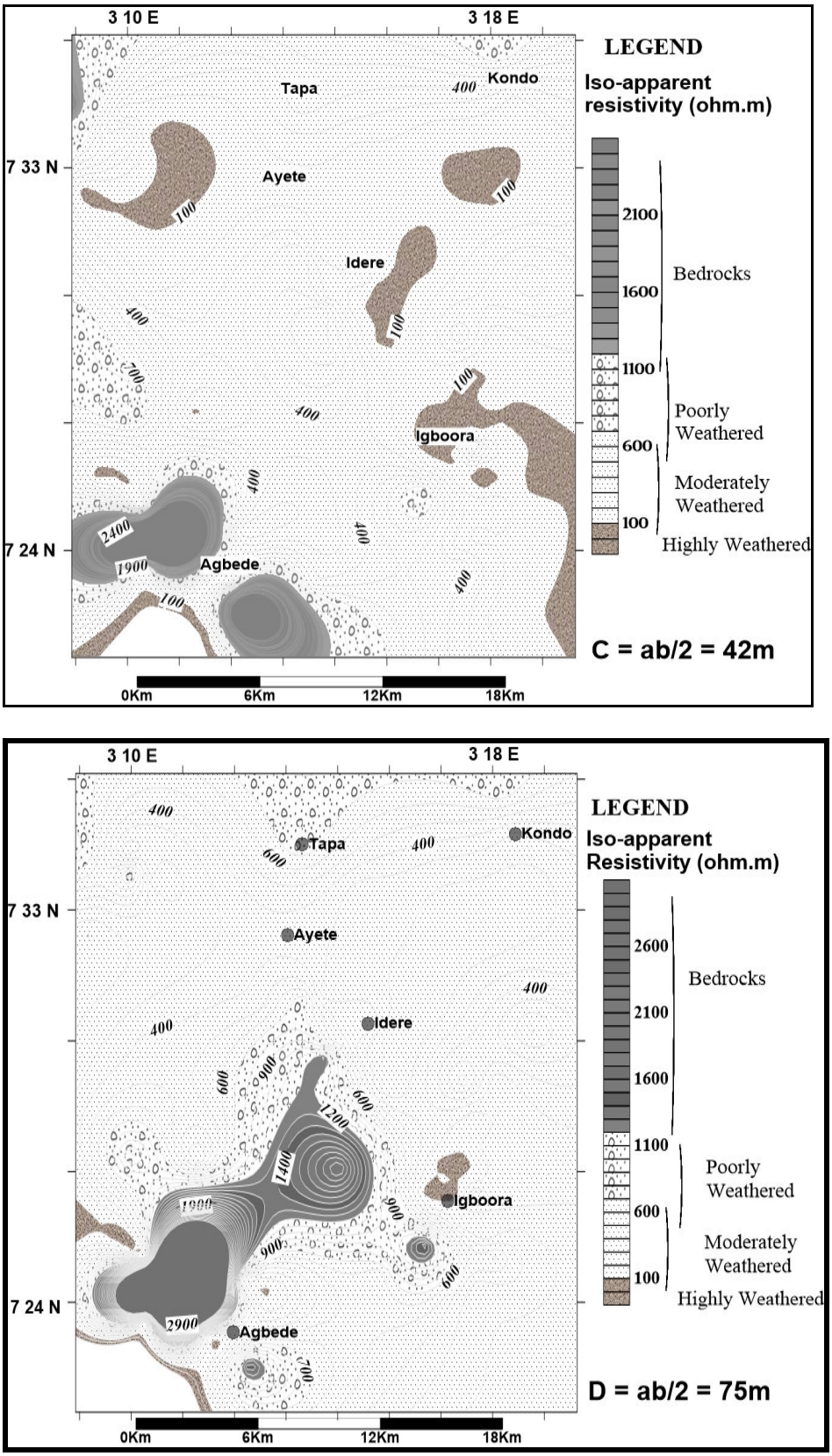

Figure 4.10 (cont.): Iso-apparent resistivity maps of current electrode distances (ab/2) showing weathering characterisation with depth across the study area

of 1152 to 1344 Ωm as average values for other bedrocks. The large variations in resistivity values of top soil are as a result of wide textural characteristics of the constituent grains composing of mixtures of widely varied sizes of eroded alluvium particles and the products of in-situ weathering of the bedrocks. Also, land use pattern of the area such as the use of fertilizers for agricultural purposes and other anthropogenic activities have imprints on the electrical conductivity of the top soil.

The thickness of the top soil is however an important factor for water transmission for direct recharge of the water bearing zones in the subsurface. The thickness of the top soil exceeded 2.0m only in 20 locations and this is more frequent in areas underlain by amphibolite and porphyritic granite. Nonetheless; on the average, the thickness of the top soil is generally less than two metres for all the bedrocks. For most areas, the topsoil layer is shallow, as highlighted in the isopach map of the top soil in Figure 4.11.

The prevalent thickness ranges between 1.0 and 2.0m. Areas with shallow top soil are mostly the low-lying terrains underlain by gneisses and migmatitic bedrocks.

Region having relatively thicker top soil of more than 2.0m are localised. This region extends from the high-lying north central part through rock contacts zones between porphyritic granite, amphibolite and migmatite at the eastern end, to a small area on amphibolite at the south-eastern section. In respect of the geomorphology of the area, it can be said that the high-lying areas susceptible to weathering are characterised by thicker development of top soil, while floodplain areas are associated with thinner top soil overlay.

b. Saprolite

The saprolite is the lower regolith unit which is the middle-layer of the predominantly 3-layer geo-electric sequence obtained in the area. The saprolite could be a prominent water bearing zones in the subsurface. The geo-electric parameters of saprolite are important factors worth considering for evaluating the groundwater potential of areas underlain by crystalline rocks. The contour of the iso-resistivity and isopach (thickness) of the saprolite layer are presented in Figures 4.12a and 4.12b respectively.

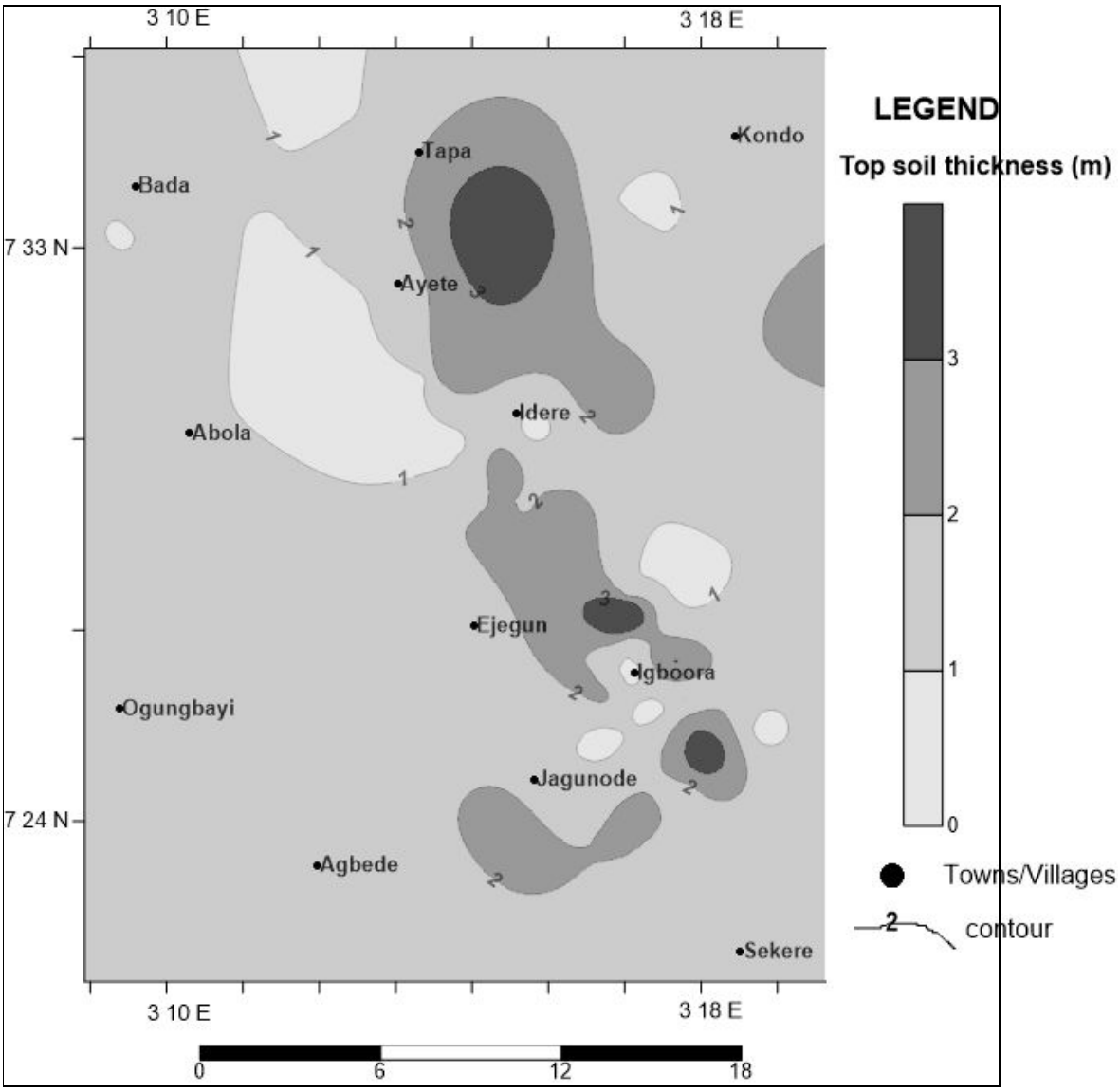

Figure 4.11: Isopach map of the top soil layer across the study area.

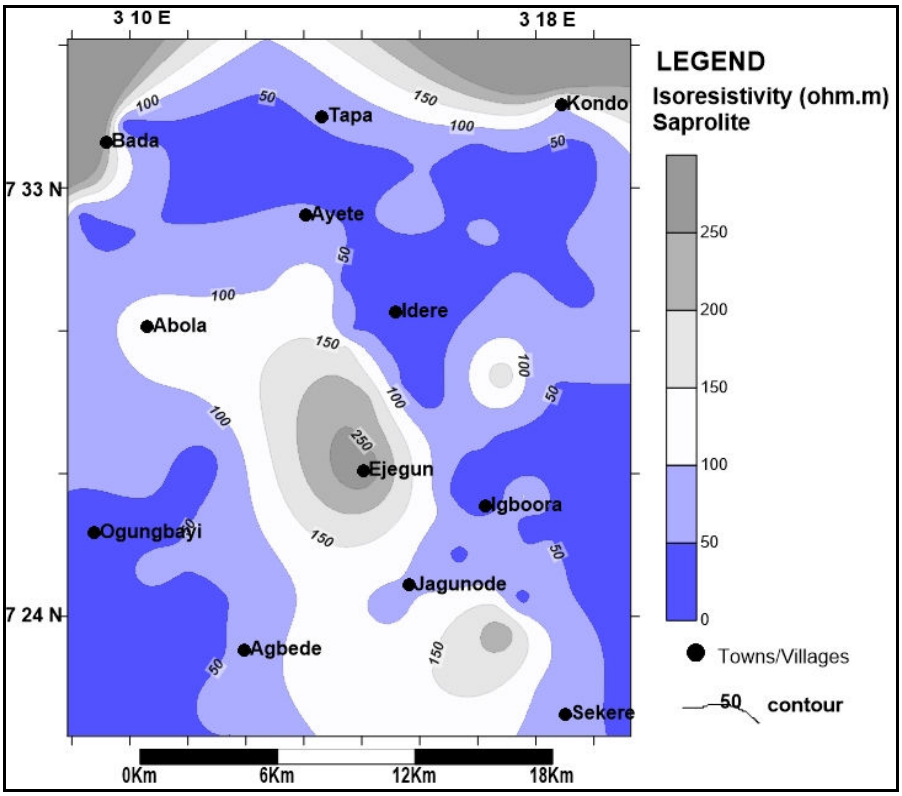

Figure 4.12a: Isoresisitvity map of saprolite layer across the study area

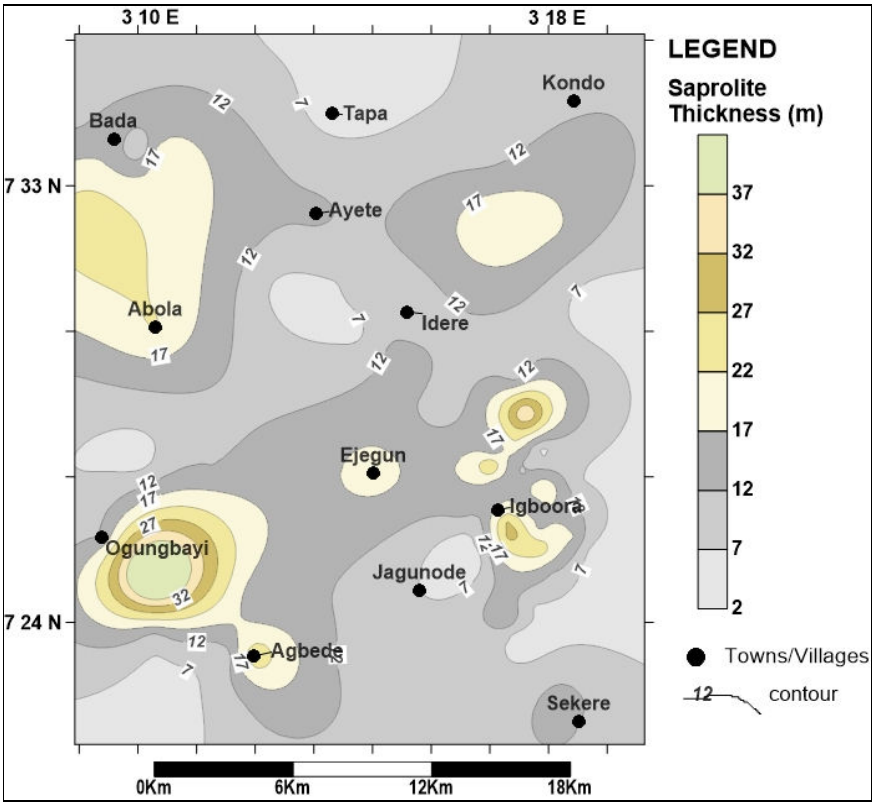

Figure 4.12b: Isopach map of the saprolite across the study area

The general spread of the resistivity of the saprolite across the study area is between 9.1 to 1903 Ωm as presented in Table 4.2. The minimum resistivity obtained for the bedrocks is lowest in amphibolite with 9.1 Ωm and highest in migmatite with 28.1 Ωm. The range of the maximum resistivity is 225.2 to 810.6 Ωm. The mean value of the resistivity of the saprolite is also lowest in areas underlain by amphibolite with 53.1 Ωm, while average resistivities for areas underlain by other bedrocks are higher with values of 93, 118 and 204 Ωm in porphyritic granite, gneisses and migmatite respectively. The resistivity of the saprolite is important parameters from which the lithological interpretation of the constituent matrix could be inferred.

The lithological interpretations of the saprolite layers across the bedrocks are presented Appendix X. The saprolite layer are dominated by fine-to-medium grained soils. Occasionally, there is occurrence of compacted lateritic clay layer, otherwise known as 'hardpan' just below the topsoil. Compacted clay units occurred in four locations across gneisses, migmatite and amphibolite, are associated with very high resistivity 433.7-4412.9 (av. 2252) Ωm.

The saprolite layers were predominantly sandy-clayey as shown by the average resistivity values for the saprolite for all bedrocks (Table 4.2). Just about 11% of saprolite units were sandy and these locations were found across all bedrocks. The decomposition of the bedrocks to fine grained soils could be linked to the mineralogical composition as the bedrocks. From the petrographical studies of the thin sections (Plates 4.5) reasonable amount of ferromagnesian minerals such as biotite and hornblende are present.

The saprolite units that are largely sandy-clayey with average resistivity of 117Ωm, can be exploited for groundwater and where the texture is mainly clayey, the saprolite will impede fluid transmission. This will provide a hydrogeological situation for occurrence of confined aquifers. In this hydrogeological setting, artisan wells can be sited if the bedrocks are fractured.

Aside the lithological characterisation of the saprolite units, the thickness of this zone is another crucial consideration in any groundwater investigation in basement terrain. The thickness of the saprolite ranges from 3.80 to 38.70m (av.16.56m),

4.40 to 57.70m (av.15.83m), 3.40 to 22.40m (av. 11.31m) and 1.80 to 19.40m (av. 9.52m) over amphibolite, gneisses, migmatite and porphyritic granite bedrock settings respectively.

On the average, areas underlain by gneisses and amphibolite are characterised by thicker saprolite unit and deeper weathered layer. The total regolith thicknesses were correspondingly 18.49 and 18.23, compared to 12.77 and 11.29 for migmatite and granitic terrains respectively (Table 4.2).

The most widespread thickness from the isopach map (Figure 4.8b) is within the range of 10 to 15m. This is also reflected in the average thicknesses (Table 4.2) obtained for the bedrock settings. There are also localised deeper weathered zones ranging from 15 to 25m largely found on gneisses and less commonly on amphibolite settings. Location where the saprolite thickness is above 40m is associated with the floodplain part at the south-western portion of the study area.

c. Bedrock

The basement resistivity ranged from 105 to 29903Ωm. The lithological interpretation of the bedrock/ infinite layer resistivities is presented in Appendix XI, while its iso-resistivity contour map showing the relative states of the bedrock across the study area is presented in Figure 4.13. The geo-electric sections that terminate on low resistivity of not more than 500Ωm are indications of the development of fracture zones within the bedrocks. The most promising fracture zones with basement resistivity below 500Ωm lie within the localised portions underlain by banded gneiss at the upper NW central and lower SW, migmatite at the upper NE and small areas underlain by amphibolite at that central lower portion of the study area. The geo-electric sections of most areas underlain by amphibolite and migmatite terminate on resistivity values less than 2000Ωm, while there are high contrasts in the resistivity of areas underlain by gneisses. The bedrock fracturing is least in porphyritic bedrock terrain, mostly characterised by high basement resistivity with an average of 4601Ωm with 80% of the locations having basement resistivity value greater than 2000Ωm.

The state of the infinite layer is a strong determinant of the sustainability of water. Continuous water flow is favoured when the bedrock is fractured and there are

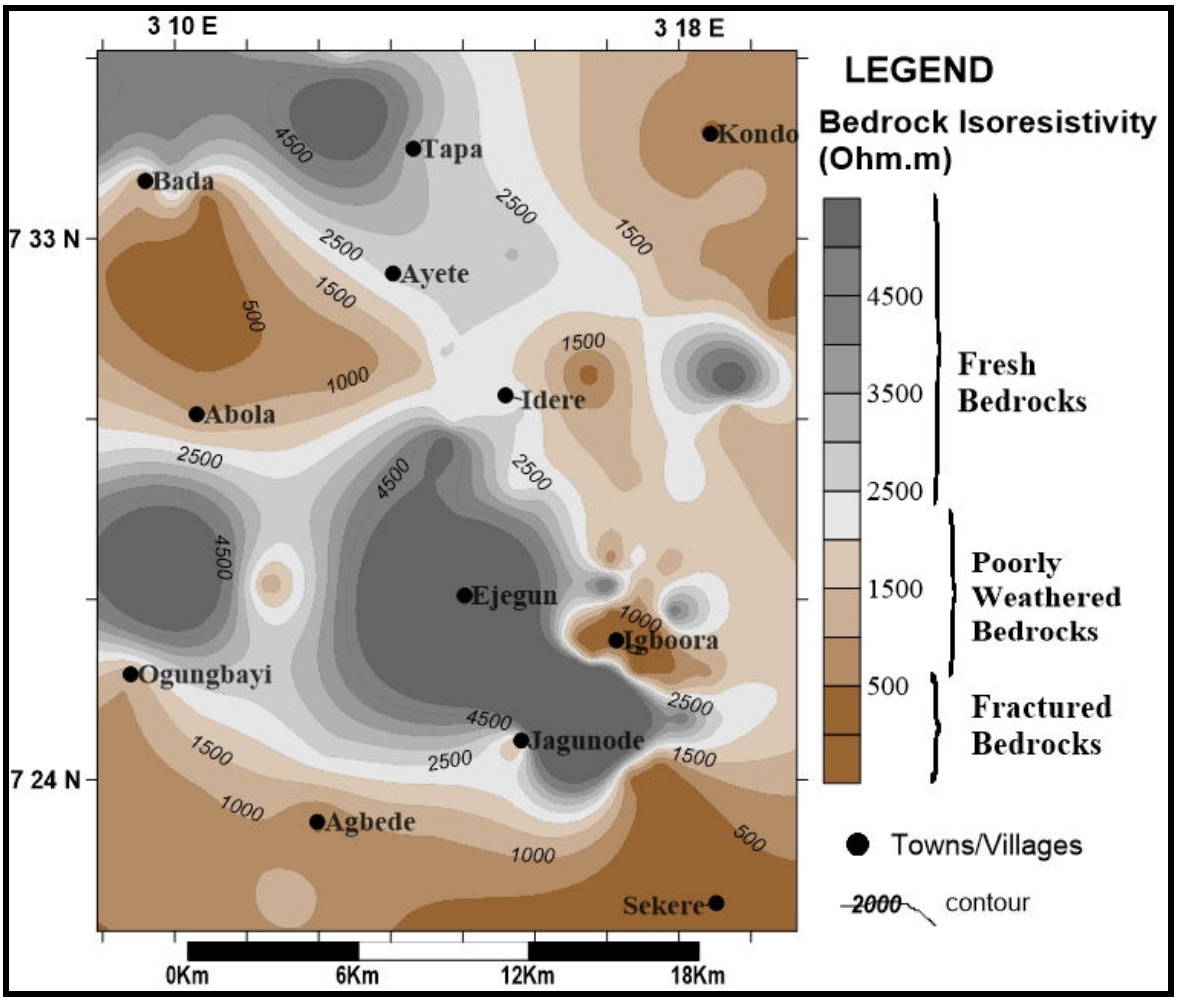

Figure 4.13: Bedrock Iso-resistivity map of the study area

good connections between the fractures and the weathered layer.

From the infinite/last layer resistivities (Appendix XI), fractured bedrock occurred at 24 locations across the various terrains, out of which eleven were found in areas underlain by amphibolite, five in gneissic terrains; and seven locations in migmatite. The bedrock at only one location was fractured within porphyritic granite terrains at Ayete. These fracture zones occurred at different depth ranges of 7.9 to 29.9m (av. 18.3m) in amphibolite terrains, 16.6 to 27.3m (av. 22.3m) on gneisses. Fracture zones were found at relatively shallower depths in migmatite and porphyritic granite with 6.7 to 19.5m (av.13.6m) on migmatite and 5.8m depth at Ayete underlain by porphyritic granite.

4.3.2.3 Spatial Distribution of Weathering Development

Spatial distribution of the weathering profiles across the study area, from one location to another from the geo-electric section traverses are presented in Figures 4.14.

From the vertical sections generated, three distinct weathering profiles are noticeable and are described below.

a. The first type (Type I) is made up of the top soil, with the saprolite layer thicker than 5m, and terminating on fractured or weathered bedrock,

b. The second type (Type II) also composed of the top soil, thick weathered layer (that is saprolite thicker than 5m), and terminates on fresh bedrock.

c. The third-type (Type III) comprises the top soil, with thin weathered layer (that is the thickness of the saprolite layer below 5m) and terminates on fresh bedrock.

There is no profile with thin saprolite and fractures/weathered bedrock.

The three types of weathering profiles are conspicuously represented in locations underlain by amphibolite extending for almost 7km along the west – east axis (Figure 4.14a) from Oja-Oba to Oke-Oyinbo within Igboora Township of the study area. The western terrain which comprises of locations typical of Type I weathering profile is characterised by well-developed regolith unit terminating on weathered or fractured

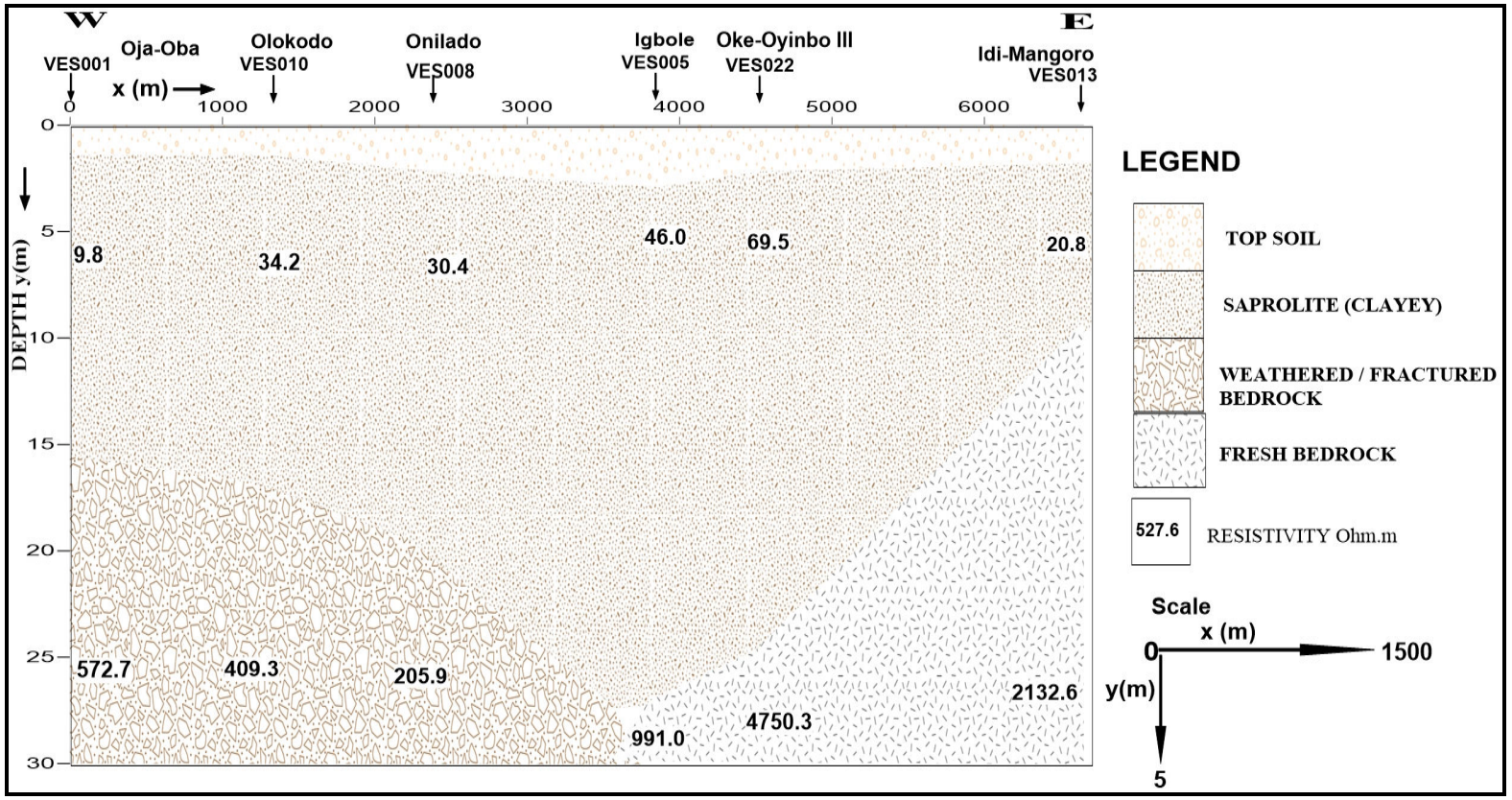

Figure 4.14a: E-W Geo-section traverse on amphibolite terrain within the study area

basement. The thickness of the regolith unit ranged from 15.0m at Olokodo on VES026 to 27.8m on VES020 at Igbole. The saprolite layer is also thickest at Igboole with 25.2m thickness and it is situated at the middle section of the E-W axis. From Igbole towards the eastern part, there is succession of type I weathering profile by Type II and Type III profiles as there is a progressive decrease in the thickness of the regolith layer terminating high resistive basement indicating fresh bedrock. The bedrock is shallowest at Idi-Mangoro on VES029 at the east, occurring at depth 8.8m, while the saprolite thickness at this location is 7.0m.

The basement resistivity at the western section ranged from 205.9 to 572.7Ωm, while those at the eastern region was between 2132.6 and 4750.3Ωm. The topsoil layer is thicker at the middle section of the east-west axis with thickness exceeding 2.0m from Onilado towards Oke-oyinbo. The resistivities of the saprolite layer are mostly well below 50 Ωm along this axis, hence the lithology is interpreted as clayey.

Weathering development in terrains underlain by gneisses generally has thick regolith overburden along the N-S axis (Figure 4.14b). This is particularly noticeable from Fedegbo to Abola which covers a distance of about 8km. Alongside this axis the regolith thicknesses exceeded 20.0m and the saprolite layer is thicker than 15.0m at each location. There is a change in weathering pattern for another distance of about 6km from Araromi on VES038 (near Abola) to Ogungbayi on VES081. This spatial region is characterised by slight decline in the thickness of the regolith from 14.7m to 13.9m and increase in the resistivities of the bedrock. This middle region has the shallowest bedrock occurrence in the area. The last 8km along this N-S section is notably characterised by an uneven overburden development, comprising local sections of deep overburden, including VES080 marked with over 55m regolith thickness which is the location with the deepest weathering extent in the entire study area. On the average, the lithology of the saprolite layer along the N-S trend is sandy clayey.

Areas underlain by porphyritic granite has varying degrees of weathering development from the N-S geo-section traverse stretching over 22km (Figure 4.14c). There is fairly good thick regolith unit development towards the southern end of areas underlain by porphyritic granite. Sections between Tapa and Ayete; and from Idere to Igboora are characterised by well-developed saprolite layer with thickness ranging from 9.4m at

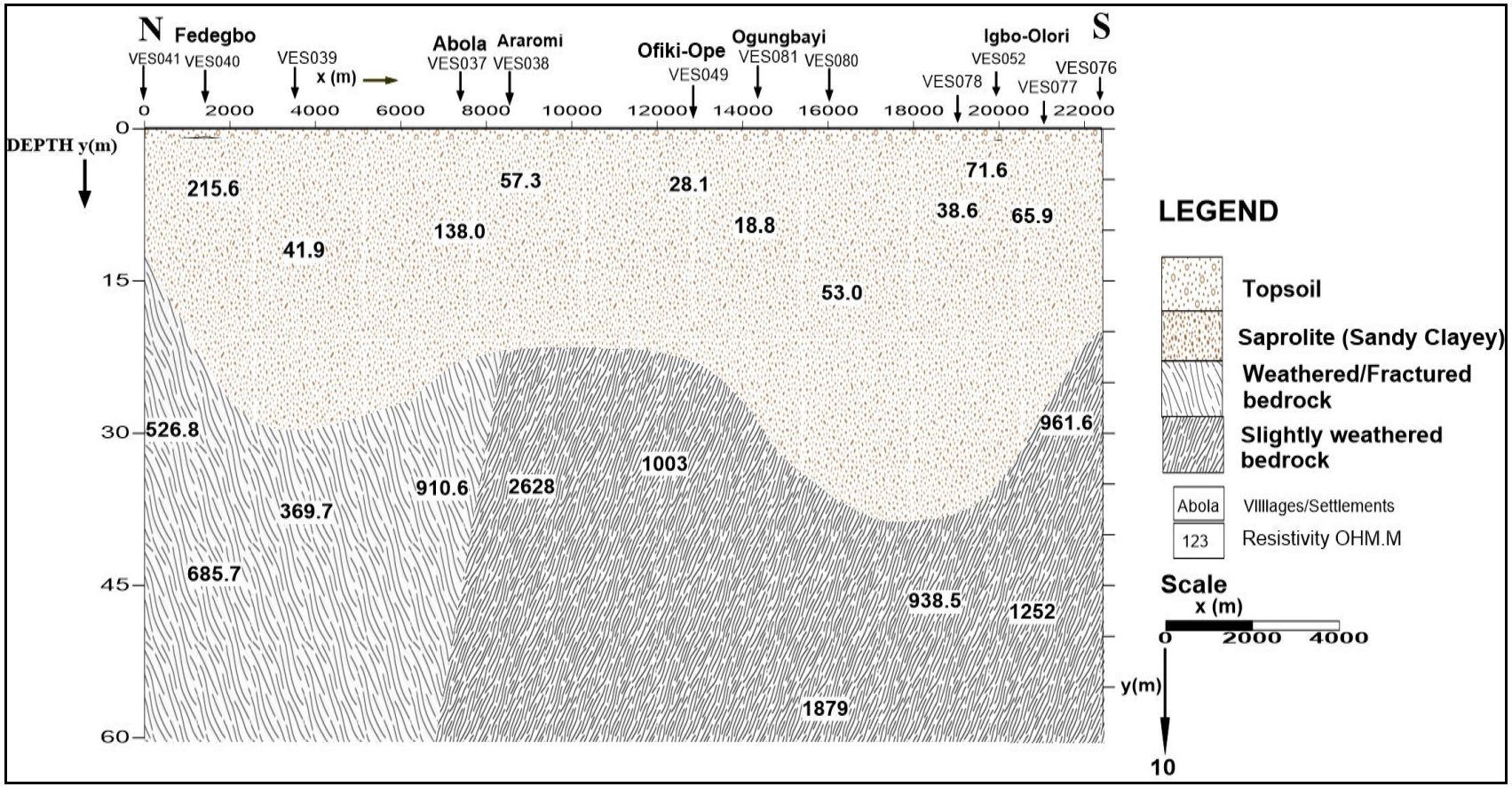

Figure 4.14b: N-S Geo-section traverse on Gneisses terrain within the study area

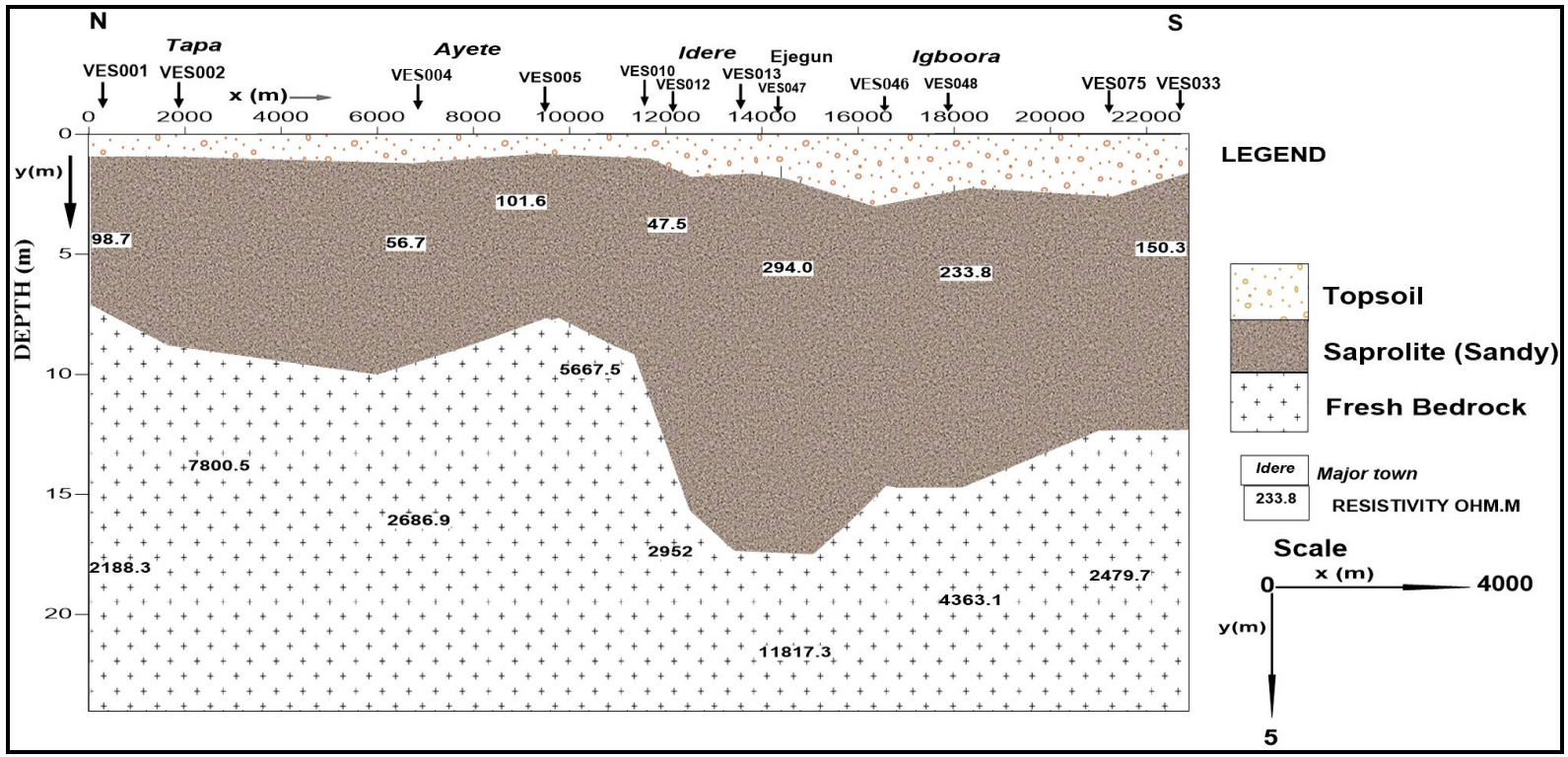

Figure 4.14c: N^{I}-S^{I} Geo-section traverse on Porphyritic Granite terrain within the study area

Oke-Ayin at VES046 to as high as 19.4m at Ejegun. The topsoil units are better developed from Idere towards the southern end of the study area ranging from 1.3m to 4.5m on VES046. Tapa at the far north and the sections between Ayete and Idere are markedly characterised by shallow soil development with topsoil thicknesses mostly below 2.0m and the saprolite layer not exceeding 8.0m, though there is a fairly thick saprolite development of 13.0m at Ayete on VES004. On the other hand, the section is characterised by highly resistive bedrock on a general overview with the bedrock resistivity as high as 11817Ωm at Ejegun on VES 047 near Idere. This is an indication that the regolith units are underlain by fresh granitic bedrocks. The occurrence of the bedrock is shallowest at 5.8m depth at the southern part of Ayete on VES005. Between Idere and Igboora there is development of more weathered regolith and the bedrock occurred between the depth of 15.9m at Idere and 20.6m at Ejegun in Igboora. The resistivity of the saprolite along the N-S section ranged from 47.5 to 294.09 (av. 140.37) which is interpreted as clayey- sandy.

4.3.3 Total Longitudinal Conductance (S) and Recharge Potential

The estimated values of Dar Zarrouk variables for each VES location and the general statistics are presented in Appendix IX and Table 4.3 respectively. Figure 4.15 is the map of longitudinal conductance from which recharge potential of the regolith units are inferred across the study area.

From Table 4.3, the total longitudinal conductance, S ranged from 0.01 to 1.42 Ω^{-1} for all the bedrock settings. Within amphibolite terrains, S ranged from 0.02 to 1.42 Ω^{-1} (av.0.45 Ω^{-1}); for gneisses, 0.01 to 1.06 Ω^{-1} (av.0.28 Ω^{-1}); for migmatite, 0.02 to 0.60 Ω^{-1} (av.0.23 Ω^{-1}) and for porphyritic granite, 0.05 to 0.38 Ω^{-1} (av. 0.15 Ω^{-1}). The potential for water conductance and water transmission across and through the layered sequence are quantified and explained by the Dar Zarrouk parameters, most especially the estimated total longitudinal conductance. The total longitudinal conductance, S typify the potential for groundwater recharge in each VES location through surface water (mostly meteoric) infiltration across the overburden units. Consequently, areas with high S values are locations with low recharge potential and vice-versa for locations with low S values. The relatively higher mean value of S for amphibolite revealed deep weathering condition and as well as development of high amount of fine grained weathering products. However, water transmission in clayey regolith will be

TABLE 4.3: General Statistics of the Dar-Zarrouk Parameters for Various Bedrocks

Dar-Zarrouk parameters	Explanation	Min	Max	Mean	Median	Std dev.
Amphibolite (n = 25)						
H (m)	Thickness of the regolith	4.40	39.40	18.06	17.20	9.12
S (Ω^{-1})	Total longitudinal conductance	0.02	1.42	0.45	0.40	0.33
T (Ωm^2)	Total transverse resistance	57.62	24558.63	3024.78	1917.52	4871.54
λ	Coefficient of anisotropy	0.90	2.89	1.48	1.25	0.49
Gneisses (n = 19)						
H (m)	Thickness of the regolith	6.30	59.00	18.49	16.60	11.60
S (Ω^{-1})	Total longitudinal conductance	0.01	1.06	0.28	0.20	0.26
T (Ωm^2)	Total transverse resistance	1291.30	60524.41	6446.99	3051.44	13228.03
λ	Coefficient of anisotropy	1.03	3.43	1.68	1.36	0.64
Migmatite (n = 18)						
H (m)	Thickness of the regolith	4.60	23.60	12.77	12.95	5.18
S (Ω^{-1})	Total longitudinal conductance	0.02	0.60	0.23	0.18	0.17
T (Ωm^2)	Total transverse resistance	843.90	9141.85	3013.65	2560.87	1934.52
λ	Coefficient of anisotropy	1.08	3.83	1.81	1.77	0.68
Porphyritic Granite (n = 20)						
H (m)	Thickness of the regolith	2.40	20.80	11.29	10.65	4.59
S (Ω^{-1})	Total longitudinal conductance	0.05	0.38	0.15	0.12	0.11
T (Ωm^2)	Total transverse resistance	198.00	10167.57	3344.53	1854.48	3275.69
λ	Coefficient of anisotropy	1.02	3.91	1.65	1.47	0.68

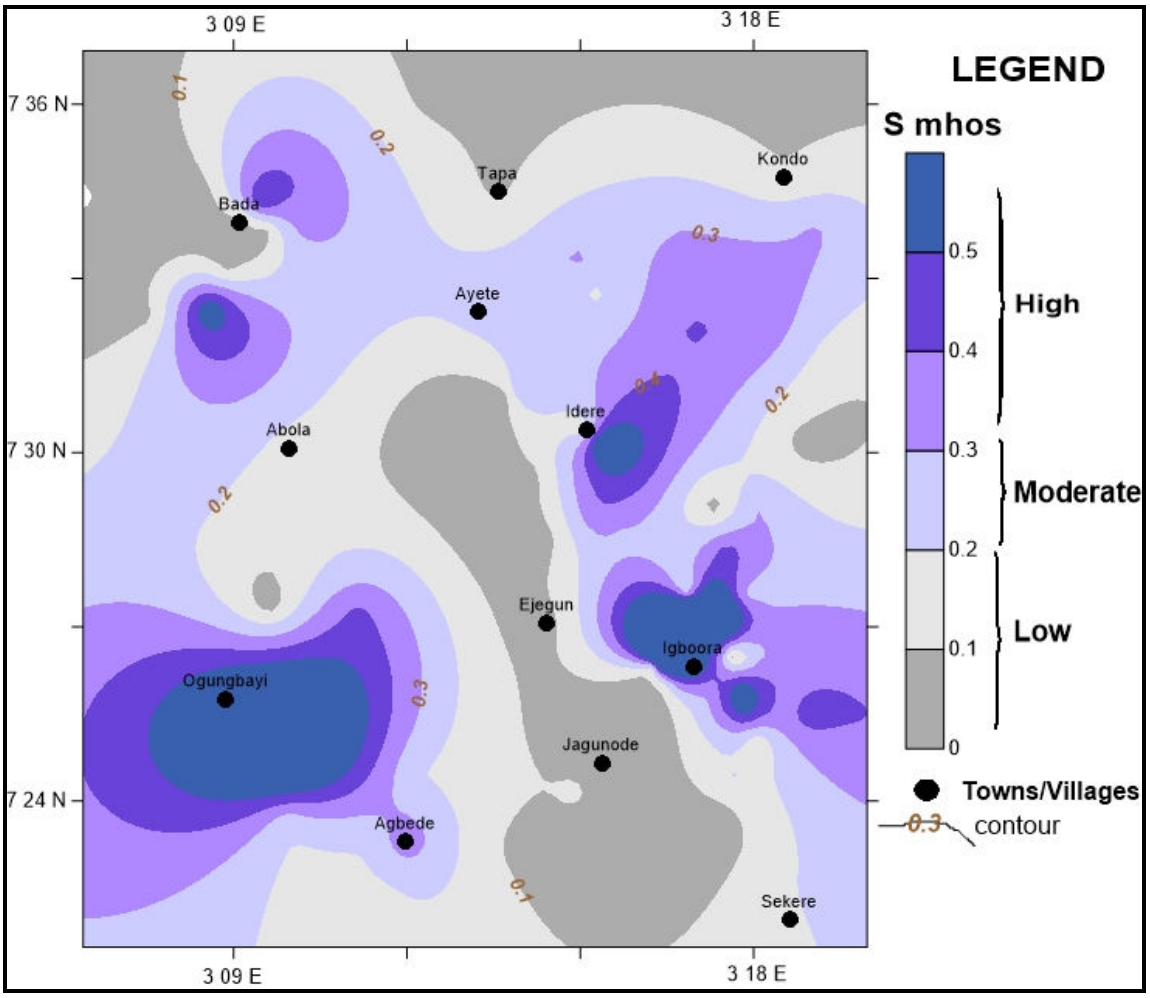

Figure 4.15: Map of total longitudinal conductance (S) of the study area

low, but the reasonable spread of bedrock fractures of about 44% of the area surveyed across amphibolite terrains is a good stand for being regarded as areas with good groundwater potential, coupled with the fact that amphibolite terrains are characterised by thick weathered layer, though largely fine grained. Most terrains within gneisses and migmatite are within moderate conductance with average values of 0.28 and 0.23 respectively. Hence, these terrains can also be considered as having moderate recharge potential.

In respect of electric conductance, saturated clayey units will be good conductor, but in hydrogeological sense, clayey regolith have poor water transmission capacity. Hence, the thicker and more clayey the regolith is, the higher the conductance and the less the ability of the regolith to transmit water. Therefore, areas classified as having moderate to high conductance are more widespread since the weathered units across the study area are mostly clayey, This is more so in locations underlain by amphibolite at Igboora, gneisses at Ogungbayi and rock boundary areas at Idere where S is high.

However, in terms of groundwater recharge from vegetation response (Figure 4.7), areas underlain by gneisses and amphibolite and rock contact locations around Idere have much evidence of water-containing fractures. Hence, this shows that, though most locations within gneisses and amphibolite interpreted as having low recharge potential based on clayey regolith products actually have good water potential. These areas can be said to be the main discharge zones in the entire study areas. Additionally, the fact that there are evidences of water-seepage (through development of riparian forests) along river channels. This is seen along Rivers Ofiki channel on gneissic terrains (Figures 1.4 and 4.7). This also shows that rock contact areas and river channels are crucial recharge zones in the entire study area.

Based on the S value alone, areas underlain by porphyritic granite at the north-central with average conductance of 0.15mhos and other adjoining areas with less than 0.20 mhos can be regarded as having fairly good recharge. Notwithstanding, terrains underlain by porphyritic granite are characterised by shallow regolith and less bedrock fractures (Figure 4.13). Hence, these locations cannot be regarded as having good potential for groundwater since water supply may not be sustainable.

The mean total transverse resistance, T is in decreasing order of 6447 Ωm^2 for

gneisses, 3345 Ωm^2 for porphyritic granite, 3025 Ωm^2 for amphibolite, and 3014 Ωm^2 for migmatite. Transverse resistance, T which expresses the proximity of bedrock to the surface and an impediment to water infiltration is found to be generally low with less than 200 Ωm^2 for most parts of the study area. However; in comparison, areas underlain by porphyritic granite having the lowest mean value of S are also characterised by higher transverse resistance. This is indicative of occurrence of granitic bedrocks at shallow depth.

4.4 Hydraulic Characterisation of the Water-Bearing Zones

The field data of the pumping and the corresponding recovery tests, along with their Time-drawdown plotted curves for all tested boreholes are presented in Appendix XII. The spread of the twenty – three (23) tested boreholes on the geological map of the study area is shown in Figure 4.16. Seven wells tested within amphibolites bedrock terrain, six in gneisses terrain, and five each on both the migmatite and porphyritic granite terrains.

4.4.1 Types of Aquifer Systems Encountered in the Field, and Hydrological and Hydraulic Parameters

Three aquifer categories were identified from the hydraulic characterisation of the water-bearing zones. This classification was based on the nature and the analyses of the Time-drawdown curves of the single-well pumping tests conducted on boreholes across the various bedrocks underlying the study area. The aquifer categories are:

A. Dual aquifer system bounded by high-yielding fractured bedrocks
B. Dual aquifer system bounded by low-yielding fractured bedrocks, and
C. Regolith aquifer system bounded by fresh and un-fractured bedrock.

The measured hydrological parameters and the estimated hydraulic properties by aquifer types are presented in Table 4.4, and the statistical summary is presented in Table 4.5 for each aquifer category.

The estimated hydraulic properties of the various water – bearing zones included the discharge, the drawdown per log cycle, total drawdown, transmissivity, hydraulic

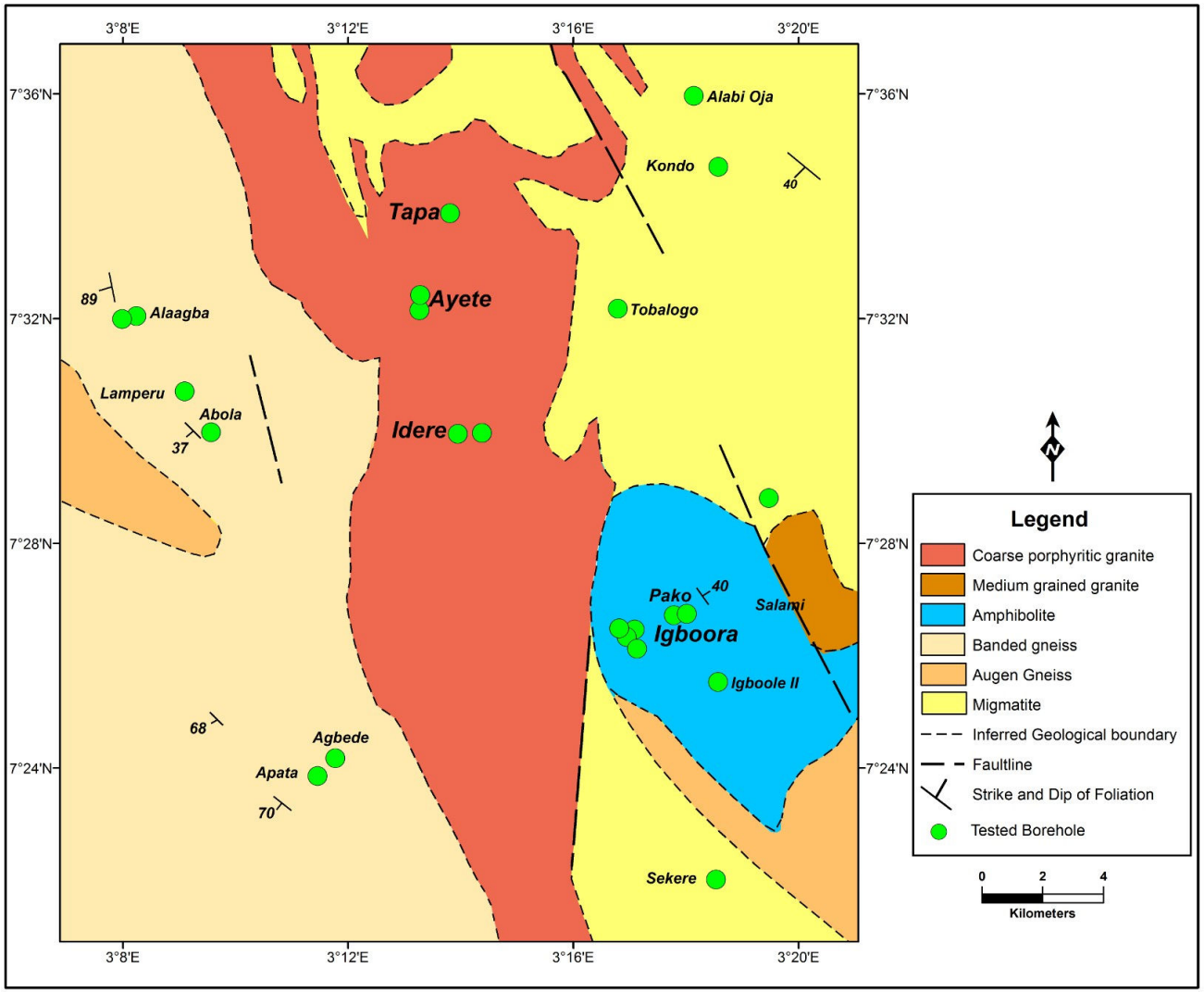

Figure 4.16: Locations of tested boreholes on the geological map

Table 4.4A: Hydrological Parameters and Estimated Hydraulic Properties for Dual Aquifer Systems

s/no	Borehole location	Well Elevation (m)	Well Depth (m)	Water Table (m)	Apparent aquifer thickness (m)	Q (m^3/d)	Δs1 (m)	Δs2 (m)	Total DD (m)	T_1 (m^2/d)	T_2 (m^2/d)	$T_t = T_1 + T_2$ (m^2/d)	K X 10^{-2} (m/d)	Specific Capacity ($m^3/d/m$)	Underlying Bedrock
TYPE I: CHARACTERISED BY HIGH-YIELDING FRACTURED BEDROCK BOUNDARY															
1	Ajegunle	159	18.90	1.46	17.44	93.58	3.80	2.40	8.50	4.51	7.14	11.65	66.80	11.01	Amphibolite
2	Agbede	143	34.60	6.42	28.18	78.92	7.00	2.00	10.03	2.07	7.23	9.30	33.00	7.87	Gneisses
3	Pako	187	31.60	6.40	25.20	73.24	2.00	3.70	7.90	6.71	3.63	10.34	41.03	9.27	Amphibolite
4	Igboole I	170	38.00	4.95	33.05	71.73	4.00	1.60	5.20	3.29	8.23	11.52	34.86	13.79	Amphibolite
5	Igboole II	175	30.40	3.23	27.17	67.92	11.20	1.19	13.51	1.11	10.45	11.56	42.55	5.03	Amphibolite
TYPE II: CHARACTERISED BY LOW-YIELDING FRACTURED OR WEATHERED BEDROCK BOUNDARY															
6	Abola	171	34.1	14.48	19.52	32.78	11.00	2.82	14.82	0.55	2.13	2.68	13.73	2.21	Gneisses
7	Apata	139	38.00	9.40	28.60	37.87	14.50	4.5	22.38	0.48	1.54	2.02	7.06	1.69	Gneisses
8	Ayete I	141	28.00	2.00	26.00	56.81	4.00	8.50	19.70	2.00	0.95	2.95	11.35	2.88	Por. Granite

Table 4.4B: Hydrological Parameters and Estimated Hydraulic Properties for Regolith Aquifer System

s/no	Borehole location	Well Elevation (m)	Well Depth (m)	Water Table (m)	Apparent aquifer thickness (m)	Q (m^3/d)	Δs (m)	Total Drawdown (m)	T (m^2/d)	K X 10^{-2} (m/d)	Sp. cap. ($m^3/d/m$)	Underlying Bedrock
1	Onilado	176	22.90	6.10	16.80	43.56	13.75	12.96	0.58	3.45	3.36	Amphibolite
2	Sagaun	162	22.80	3.30	19.50	98.12	14.00	15.36	1.28	6.56	6.39	Amphibolite
3	Itaagbe	172	27.70	10.70	17.00	55.97	10.60	11.49	1.03	6.06	4.87	Amphibolite
4	Alaagba I	174	43.0	4.15	38.85	40.43	29.50	31.90	0.25	0.64	1.27	Gneisses
5	Alaagba II	164	99.5	2.90	96.60	54.79	19.40	33.50	0.52	0.54	1.64	Gneisses
6	Lamperu	169	30.9	6.68	24.22	75.91	21.50	19.32	0.65	2.68	3.93	Gneisses
7	Alabi-Oja	188	26.36	3.34	23.02	41.91	13.80	18.63	0.56	2.43	2.25	Migmatite
8	Sekere	142	29.10	7.05	22.05	77.04	16.00	18.70	0.88	3.99	4.12	Migmatite
9	Apata-Faju	182	29.72	4.20	25.52	99.79	25.00	21.23	0.73	2.86	4.7	Migmatite
10	Tobalogbo	188	17.80	3.50	14.30	69.48	14.00	11.49	0.91	6.36	6.05	Migmatite
11	Kondo	199	35.60	11.83	23.77	53.15	13.40	18.40	0.71	2.99	2.89	Migmatite
12	Ayete II	140	27.85	3.65	24.20	45.62	15.00	19.91	0.56	2.31	2.29	Por. Granite
13	Tapa	155	36.50	2.05	34.45	57.70	11.00	22.04	0.96	2.79	2.62	Por. Granite
14	Idere I	215	20.30	5.32	14.98	91.10	5.65	9.27	2.94	19.69	9.83	Por. Granite
15	Idere II	209	15.86	6.48	9.38	70.42	10.80	7.00	1.19	12.69	10.06	Por. Granite

Table 4.5: Statistics of Hydrological and Hydraulic Parameters by Aquifer Systems

Aquifer systems	n	Statistics	Well Elevation (m)	Well Depth (m)	Water Table (m)	Apparent aquifer thickness (m)	Discharge Q (m^3/d)	Total drawdown (m)	Transmissivity T (m^2/d)	Hydraulic Conductivity K ($X10^{-2}$) (m/d)	Specific capacity ($m^3/d/m$)
DUAL TYPES											
TYPE I HIGH YIELDING	5	Min	143.00	18.90	1.46	17.44	67.92	5.20	9.30	33.00	5.03
		Max	187.00	38.00	6.42	33.05	93.58	13.51	11.65	66.80	13.79
		Mean	166.80	30.70	4.49	26.21	77.08	9.03	10.87	43.65	9.39
		Std.Dev.	16.68	7.22	2.14	5.69	10.04	3.05	1.03	13.55	3.29
TYPE II LOW YIELDING	3	Min	139.00	28.00	2.00	19.52	32.78	14.82	2.02	7.06	1.69
		Max	171.00	38.00	14.48	28.60	56.81	22.38	2.95	13.73	2.88
		Mean	150.33	33.37	8.63	24.71	42.49	18.97	2.55	10.71	2.26
		Std.Dev.	17.93	5.04	6.28	4.68	12.66	3.83	0.48	3.38	0.60
WEATHERED-REGOLITH	15	Min	140.00	15.86	2.05	9.38	40.43	7.00	0.25	0.54	1.27
		Max	215.00	99.50	11.83	96.60	99.79	33.50	2.95	19.69	10.06
		Mean	175.67	32.39	5.42	26.98	65.00	18.08	0.92	5.07	4.42
		Std.Dev.	21.98	19.92	2.82	20.68	20.10	7.47	0.63	5.04	2.70

conductivity and the specific capacity denoted by Q, Δs, DD, T, K and Sc respectively. The units of measurements for Q is cubic metre/day (m^3/d), Δs and DD were measured in meter (m), T in square meter/day (m^2/d), K in meter/day (m/d) and Sc in cubic metre/day/metre ($m^3/d/m$). The associated hydrological parameters included the well elevation, the well depth, static water table and apparent apparent aquifer thickness measured in metre. Characterisation of the aquifer systems in the field with the associated boundary conditions; and variations of both the hydrological and hydraulic parameters are discussed under subsequent sections below.

4.4.1.1 Dual Aquifer Systems

The Time-drawdown curves of dual aquifer systems are characterised by two distinct flow regimes separated by transition period that is clearly seen on the Time-drawdown curves (Figure 4.17a-b). Each flow regime represents a water-bearing zones that is clearly distinguishable from the other one. The upper water-bearing zone signifies dominant water contribution from the overburden or the weathered layer, whereas the lower aquifer system represents the fractured bedrock zones.

Hence, each flow regime is independently analyzed, since it represented the dominant water-bearing zone at specific intervals of drawdowns in the wells. The total transmissivity of each of the dual aquifer system denoted by T_t will therefore be the sum of the transmissivities of the upper and the lower aquifers (Fetter, 2007) denoted by T_1 and T_2 respectively as given in Table 4.4A.

Wells that penetrated dual aquifer systems can be said to be bounded by recharge boundary that is most likely to be fractured or weathered bedrocks. These wells were generally characterised by longer pumping time with continuous water flow and development of dynamic equilibrium water level during the entire pumping period. The total number of dual aquifer systems were eight (8) representing about thirty-five (35) percent of all the tested wells. Also, dual aquifers were associated with relatively larger transmissivity and hydraulic conductivity (Table 4.5).

However, based on the quantity of groundwater discharged and the rates of drawdown in the wells, there are two categories of dual aquifer systems. Type I represented aquifer systems whose boundaries can be said to have penetrated high-yielding fractured bedrock, while Type II are those whose lower water-bearing zones penetrated

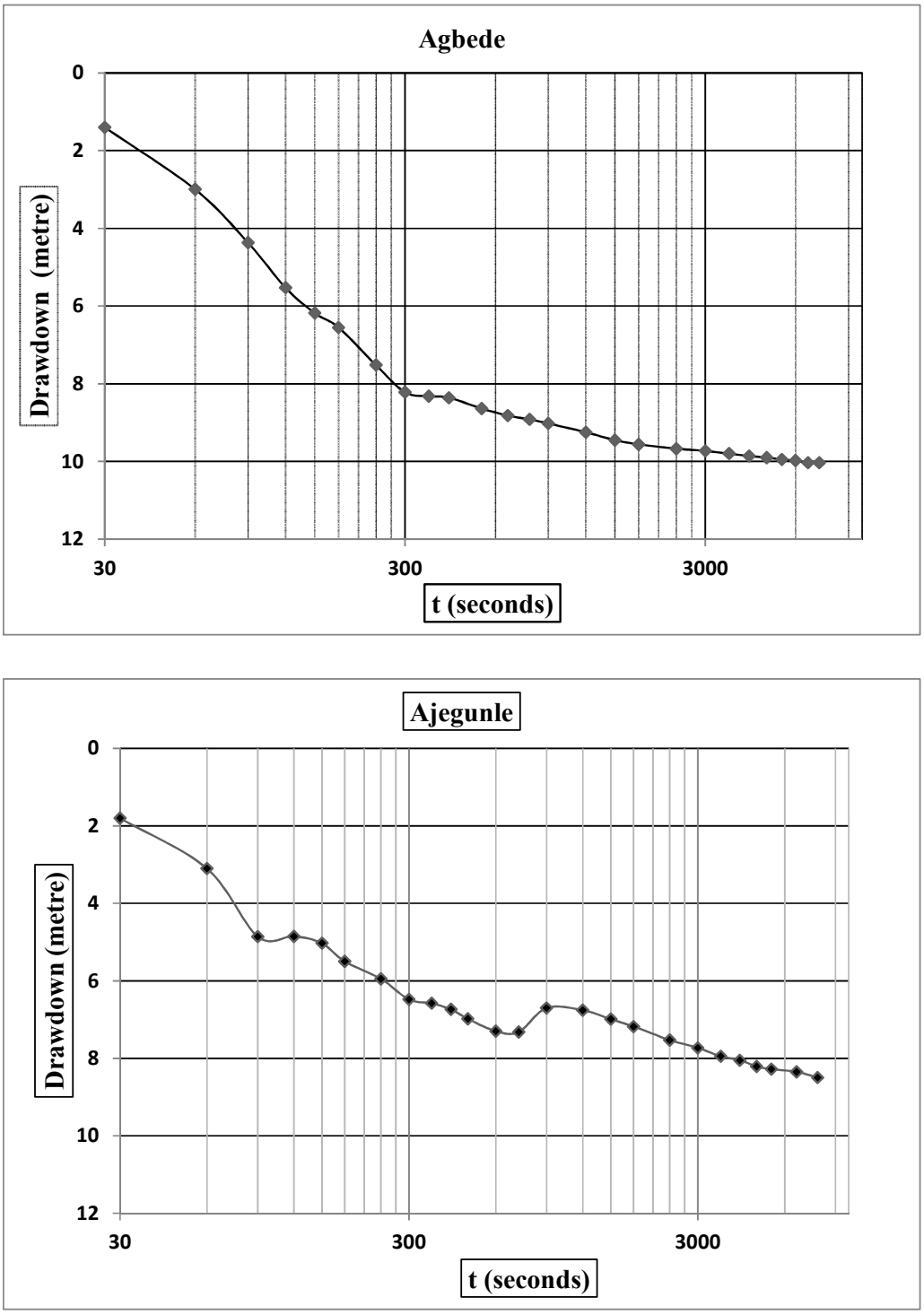

Figure 4.17a: Examples of Time – drawdown for Dual aquifer bounded by high-yielding recharge boundary

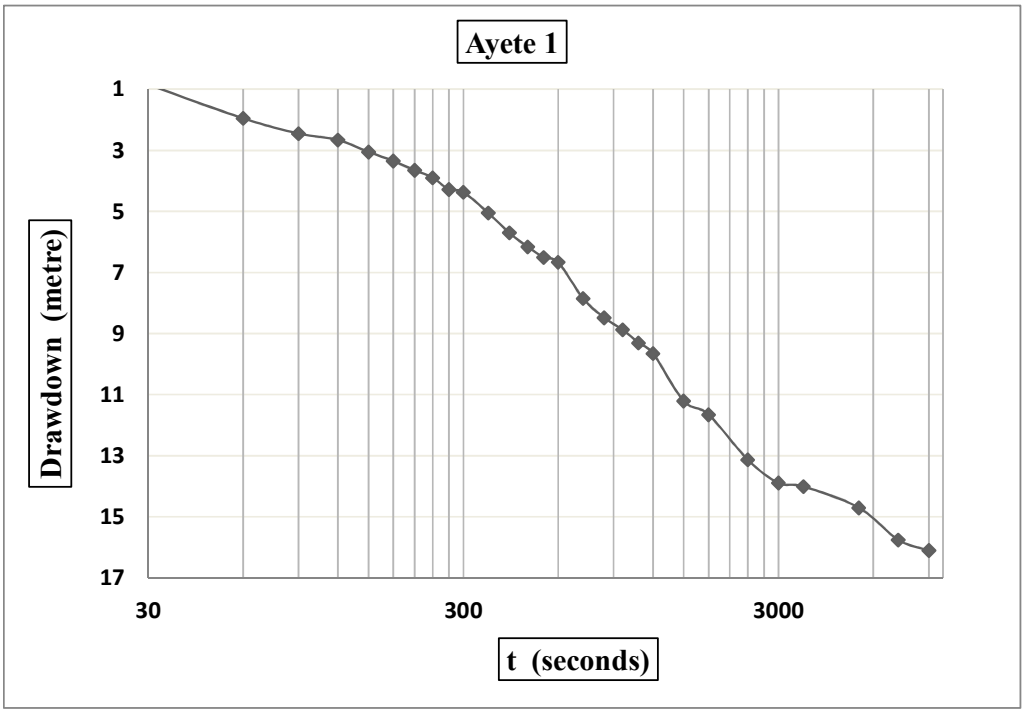

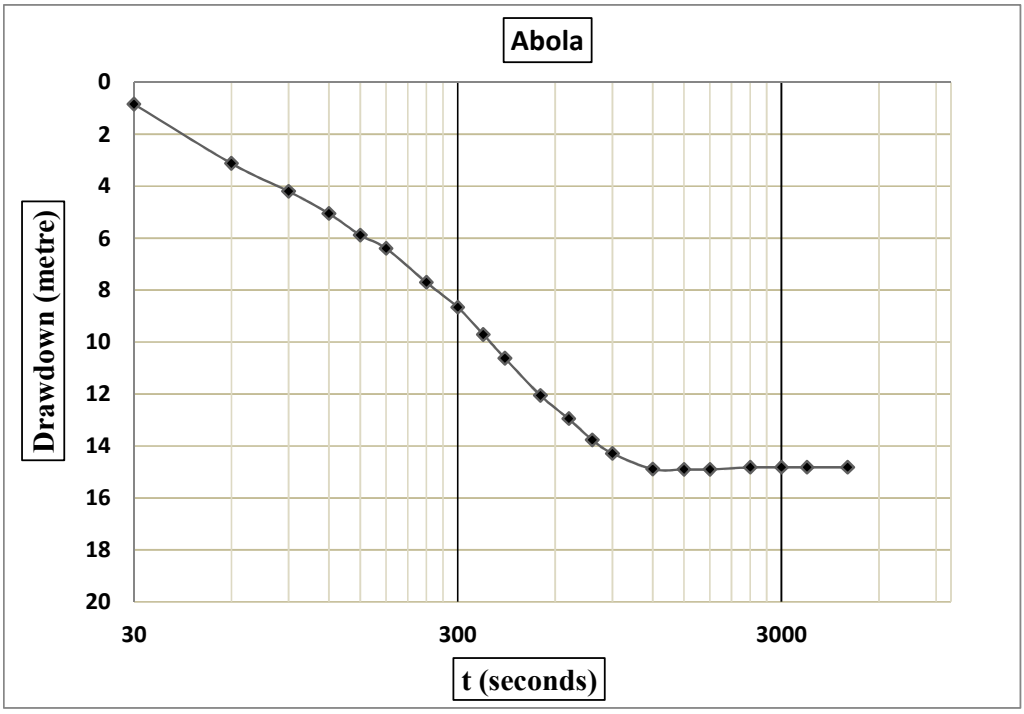

Figure 4.17b: Examples of Time – drawdown semi-log plots for Dual aquifer bounded by low-yielding recharge boundary

low - yielding bedrock fractures or weathered bedrocks with restricted water inputs.

Comparatively, groundwater discharges for Type I aquifer systems were 67.92 to 93.58 (av. 77.08) m^3/day, much larger than those in Type II with 32.78 to 56.81 (av. 42.49) m^3/day. The groundwater yield of Type II wells, which included boreholes located at Abola, Apata and Ayete I reduced as pumping continues; however, the drawdown also stabilized at an average depth of 18.97, even at lower pumping rate average of 42.49 m^3/day (Figure 4.17b, Table 4.5). The larger discharges in Type I wells led to less steep slope of the drawdown intervals for the lower water-bearing zones, which stands for fractured bedrocks (Figure 4.17a).

Consequently, the transmissivities of the lower water-bearing zones/fractured bedrock are larger than those at the upper regolith units, except at Pako and at Ayete I, where the lower aquifers are less productive than the upper ones. Notwithstanding, on the average water transmission, the lower aquifer zones are more productive than the upper weathered units. Also, from the total transmissivity of 9.30 to 11.65 (av. 10.87) m^2/day; Type I dual aquifer systems are much productive than Type II with 2.02 to 2.95 (av. 2.55) m^2/day (Table 4.5).

Invariably, the total drawdown during pumping was relatively smaller (av. 9.03m) in Type I dual aquifer system, compared to 18.97m in Type II. Also, the hydraulic conductivity (K) which describes the rates at which water moves through a porous medium was also much larger in Type I with av. 43.65 $X10^{-2}$m/day, compared to 10.71 $X10^{-2}$ m/day in Type II.

Additionally, the development of steady drawdown state marked by flattened drawdown at the late pumping stage regardless of length of pumping in some of the dual aquifer system including those at Abola (Figure 4.17b), Apata and Igboole II, does not necessarily mean that these aquifers are better productive than other dual aquifer systems. The discharge in Abola and Apata dropped significantly but the drawdown became steady, even at lower discharge. However, it can be deduced that all dual aquifer are bounded by recharge boundaries, whose water input varies from one aquifer system to another, leading to diversity in the values of hydraulic properties.

Generally, from the hydraulic properties and the continuous water discharge throughout the pumping phase, groundwater supply in dual aquifers can be said to be

sustainable. Also, the dual aquifer system revealed that crystalline basement aquifer system can develop a multi-layer water-bearing zones, which is an evidence of water contribution from both the weathered units and the bedrock horizons.

4.4.1.2 Weathered (Regolith) Aquifer System

The regolith aquifer system is the most widespread and it is associated with all bedrock terrains. The number of occurrences of regolith aquifer system was fifteen (15), which is about sixty-five (65) percent of the total number of tested wells. This aquifer category accounts for wells that penetrate and terminates on fresh un-fractured bedrocks with very little or no water input. Hence, recharge input cannot meet the rate of pumping, even with the use of low capacity pump of 0.5HP. The upper matrix/weathered unit was the only water transmitting system in regolith category.

From the Time-drawdown curves, wells in this category were dominated by water from borehole storage at the initial stage; and afterward by flows from the matrix component (or weathered layer, or overburden) units alone. The water input from the overburden units is however not substantial enough. Therefore; the pumping rates fell at the latter stage of pumping. This is marked by sharp decline in drawdown (Δs), as a result of drastic drop in water pressure as the drawdown hits fresh basement, leading to eventual water cessation during pumping (Figure 4.17c).

The yields or discharges from the wells which were 40.43 to 99.79 (av. of 65.00) m^3/day were not sustainable over a long period. Also, the drawdowns in the wells during pumping ranged widely from 7.00 to 33.50m (av. 18.08m) and were characterised by large drawdowns during pumping when compared to Type I dual aquifer category (Table 4.5). The transmissivities, T were 0.25 to 2.95 (av. 0.92) m^2/day. Transmissivities were mostly below 1.50 m^2/day, except at Idere I (Table 4.4B). This shows that the rate of water transmission in regolith units is typically below 2.00 m^2/day and can be said to be generally low. The hydraulic conductivities, K were 0.54 to 19.69 (av. 5.07) m/day (Table 4.5). Based on the lower values of hydraulic properties and the generally short pumping time, regolith aquifer system are not sustainable. Although, with the average transmissivity of 0.92 m^2/day, this aquifer system can be said to be fairly good when compared to other values in similar geological environment in other parts of the world (Davis and DeWeist, 1966).

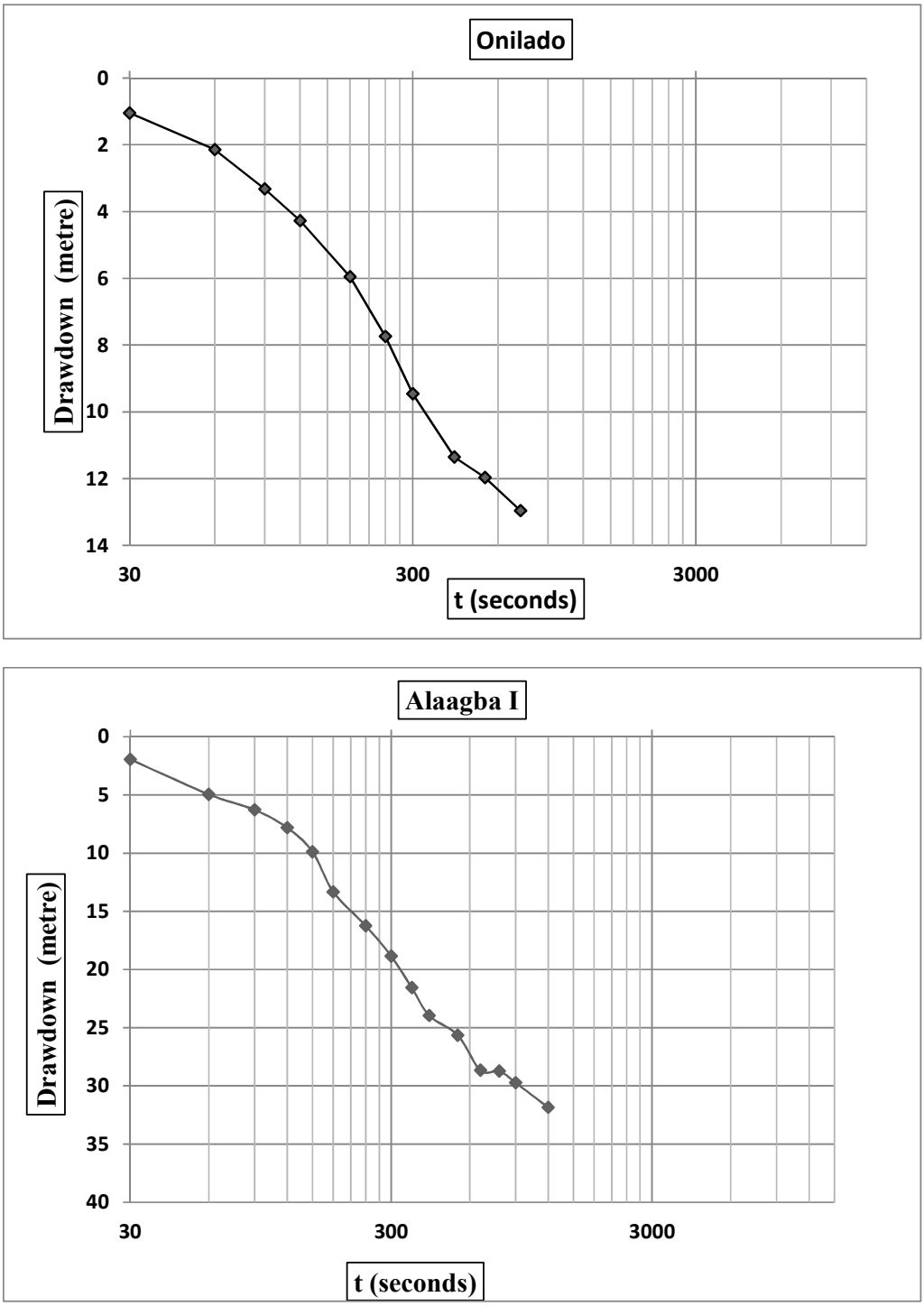

Figure 4.17c: Examples of Time – drawdown semi-log plots for regolith aquifer bounded by fresh bedrocks

The boundary situations of the regolith aquifer are largely fresh (or un-weathered) basement. The bedrocks cannot be said to be fractured as well, and if fractured, then it is either the fractures are dried of largely unconnected.

4.4.1.3 Water – Bearing Zone Largely Affected by Skin

The only well with complex time-drawdown curve was Igboole I (Figure 4.18A). The ambiguity is mostly due to skin effects, in which case the curve is influenced by haphazard contacts in the well and within the water – bearing zones. Notwithstanding, an important precaution taken in the field was to conduct recovery tests immediately after the pump is shut down during pumping test in all cases. Therefore, the recovery data were integrated with the actual drawdown data to produce a residual time-drawdown (Figure 4.18B) curves and the well parameters were appropriately estimated. Aside the skin effects, this well was prolific and marked by continuous discharge for the entire pumping period. However, the original Time-drawdown displays two flow regime from which the hydraulic parameters were analysed and presented in Table 4.4 under Type II dual aquifer system. The total transmissivity was 11.52m^2/day. The well was also characterised by small total drawdown of 5.20m and large hydraulic conductivity of 34.86m/day.

4.4.2 Groundwater Recovery

The Time- recovery curves were presented along with the time-drawdown curves in Appendix XII, but the representative samples are presented in Figures 4.19. The results of the groundwater recovery measured, immediately after pumping was cut off is presented in Table 4.6.

The total recovery time spanned from as short as ten (10) minutes for borehole at Agbede, to as long as 230 minutes at Alaagba. The average recovery time for all the boreholes was 90.87 minutes (Table 4.6). However, the actual rates of recovery that showed the speed at which water recovers in the well spread from 0.55 litre/minutes in borehole at Idere to 7.14 litre/minute at Agbede, while the average recovery rate was 2.03 litre/minute. The well at Alaagba I that was the slowest to recover based on recovery time alone has the second lowest rate of recovery of 0.62 litre/minute, while the well at Agbede with the fastest recovery time of 10 minutes also has the fastest rates of recovery of 7.14 litre/minute (Table 4.6).

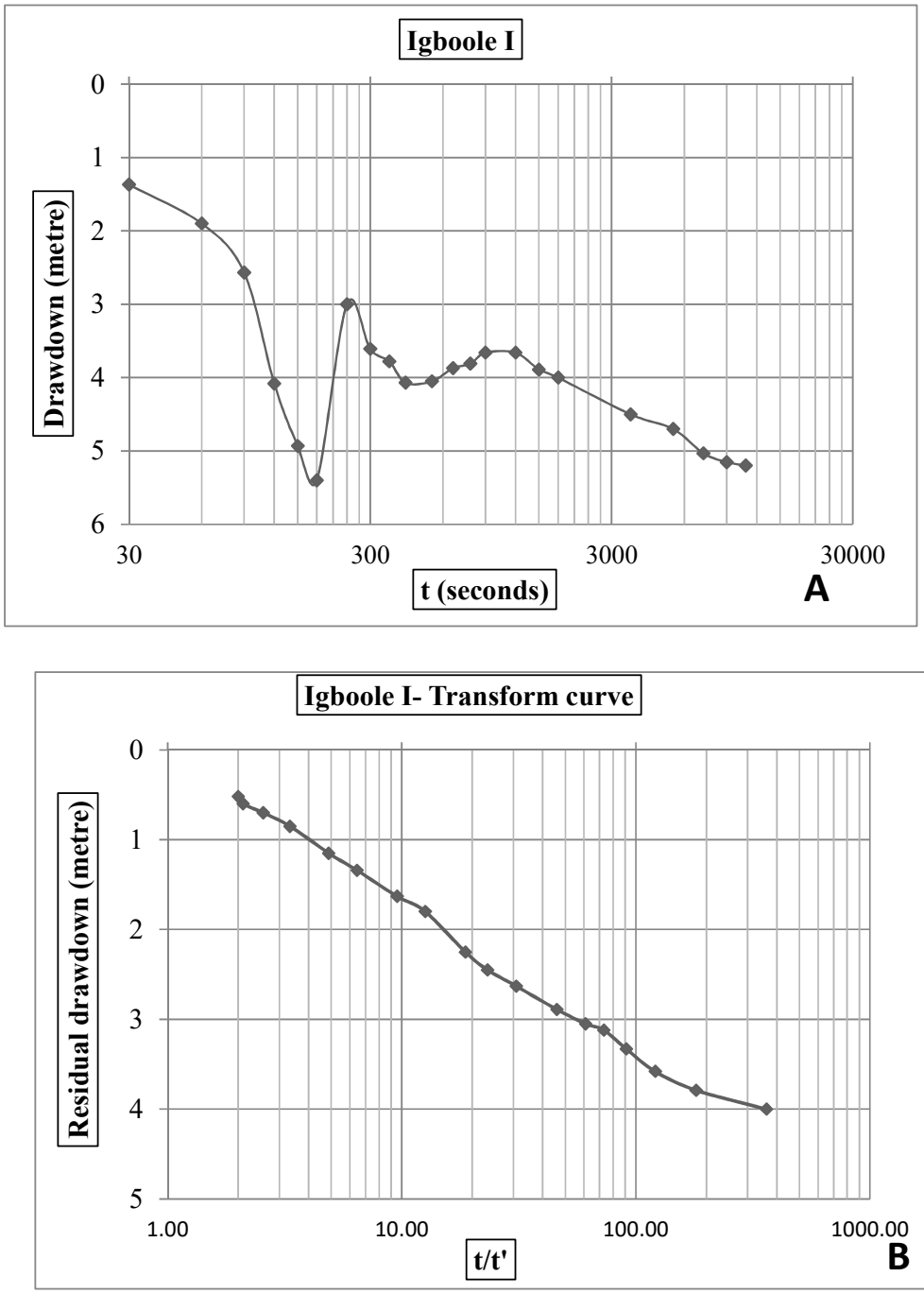

Figure 4.18: A- Original Time-Drawdown Curve largely affected by Skins. **B**-Residual-drawdown 'transform' plot that removed Skin effect from Time- drawdown plots at Igboole I

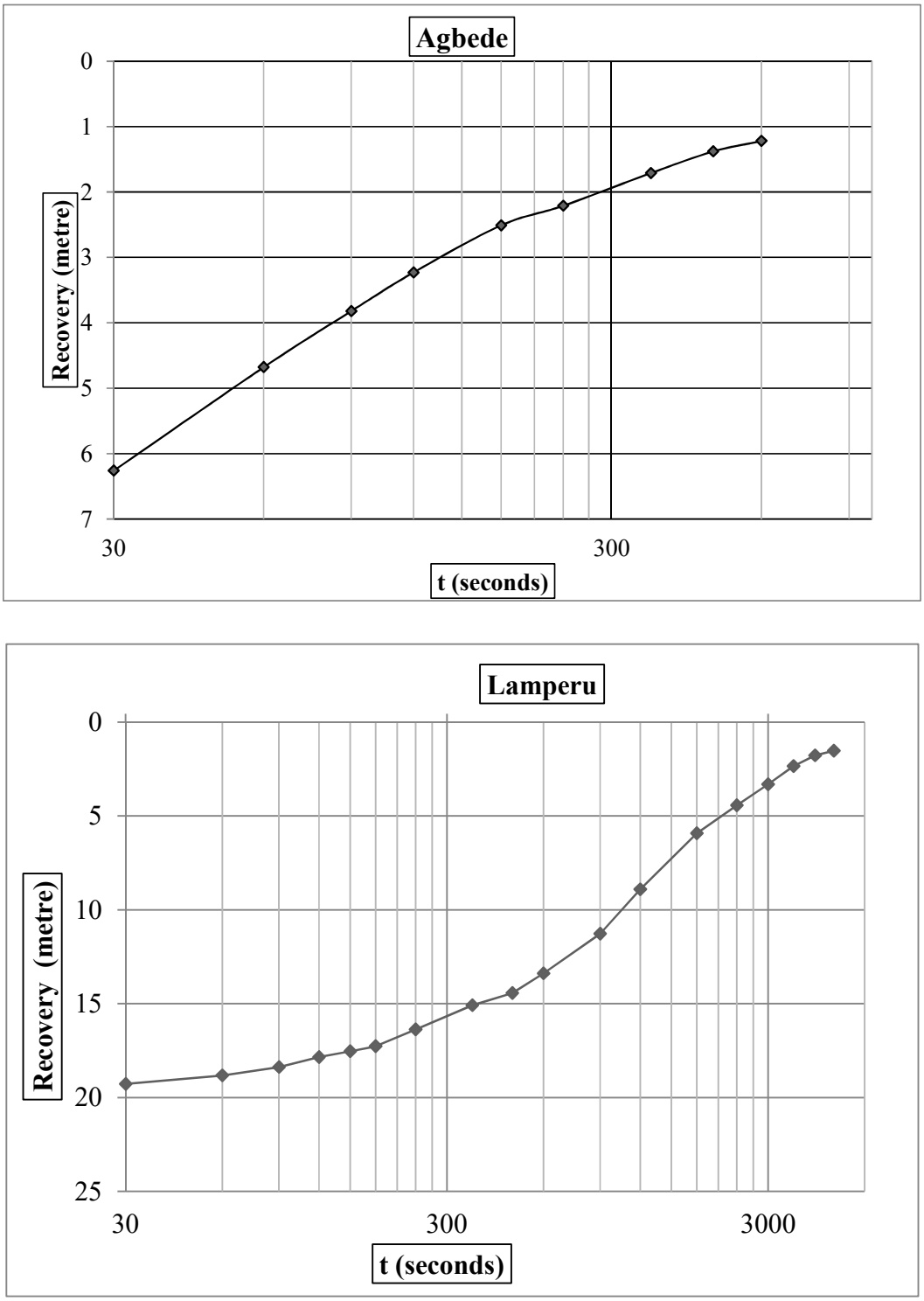

Figure 4.19: Examples of Recovery Curves obtained from the Recovery Tests

Table 4.6: Total and Rates of Groundwater Recovery

Sn.	Borehole Location	Rates of Groundwater Recovery (Liter/min.)	Total Recovery Period (Minutes)
1	Onilado	1.72	180
2	Sagaun	1.87	120
3	Pako	1.03	100
4	Igboole I	0.62	120
5	Igboole II	2.51	40
6	Ajegunle	1.42	40
7	Itaagbe	3.68	25
8	Alaagba I	0.62	230
9	Alaagba II	1.85	160
10	Lamperu	1.80	80
11	Abola	2.03	50
12	Apata	2.35	120
13	Agbede	7.14	10
14	Sekere	1.15	120
15	Tobalogbo	1.43	60
16	Kondo	1.99	60
17	Alabi-Oja	3.35	44
18	Apata-Faju	1.55	110
19	Idere I	0.55	120
20	Idere II	1.11	50
21	Ayete I	1.81	76
22	Ayete II	1.90	120
23	Tapa	3.22	55
	Min.	**0.55**	**10.00**
	Max.	**7.14**	**230.00**
	Mean	**2.03**	**90.87**
	Std. Dev.	**1.39**	**53.40**

The mathematical evaluations of the total recovery time and the rates of groundwater recovery in wells are presented in Appendix VB. The rates of groundwater recovery encompasses both recovery time as well as recovery in well itself. This directly linked the time of recovery with the height of the water column in the well, which varies from well to well due to dissimilarity in depths of all the tested boreholes.

A closer look at recovery parameters by aquifer system, summarized in Table 4.7, revealed that the total recovery time for regolith aquifers were between 25 to 230 minutes, with an average recovery time >100 minutes. These values are rather quite higher compared to 10 to 120 (av. 62) minutes in Dual Type I aquifers and 50 to 120 (av. 82) minute for Dual Type II aquifer systems (Figure 4.20). Also, the rates of recovery in litre/minutes were 0.55 to 3.68 (av. 1.85) for regolith aquifer system; 0.62 – 7.14 (av. 2.54) for Dual aquifer Type I, characterised by high-yielding fractured bedrocks, and 1.81 – 2.35 (2.06) for Dual aquifers Type II bounded by low-yielding recharge boundary (Figure 4.20).

This also showed that wells that penetrated dual aquifer systems and that tapped water from the overburden units and that were bounded by recharge boundaries were characterised by smaller total recovery time, which depicts faster rates of groundwater recovery, compared to wells that only penetrated overburden units alone. However, the dual aquifers Type I system that are typified by high-yielding recharge boundary have the smallest total recovery time as well as the highest rates of recovery (Figure 4.20).

4.4.3 Aquifer Systems and Groundwater Yield

Generally, aquifer systems with good transmission were found in those characterised by dual water-bearing zones. These wells were relatively characterised by smaller drawdown, sustainable water yield, larger transmissivities, hydraulic conductivity and higher specific capacity. Additionally, dual aquifer system has recharge boundary and there is attainment of dynamic equilibrium water-level at the late pumping stage. Dynamic water-level is a situation whereby water recharge is in equilibrium with discharge from the well. Comparatively from the statistical values in Table 4.5, water bearing zones that terminated on fresh bedrocks were characterised by lower transmissivity values with average of 0.92 m^2/day and K of av. 5.07 $X10^{-2}$ m/day, and correspondingly higher total drawdown of av. 18.08m, compared to those which

Table 4.7: Statistics of Groundwater Recovery in Wells by Aquifer Systems

Statistics	Aquifer Systems: Regolith	Dual: Type I	Dual: Type II
Total Recovery time (minutes)			
Min.	25.00	10.00	50.00
Max.	230.00	120.00	120.00
Mean	102.27	62.00	82.00
Std.dev.	56.95	46.04	35.38
Rates of Recovery (litre/minute)			
Min.	0.55	0.62	1.81
Max.	3.68	7.14	2.35
Mean	1.85	2.54	2.06
Std.dev.	0.93	2.66	0.27

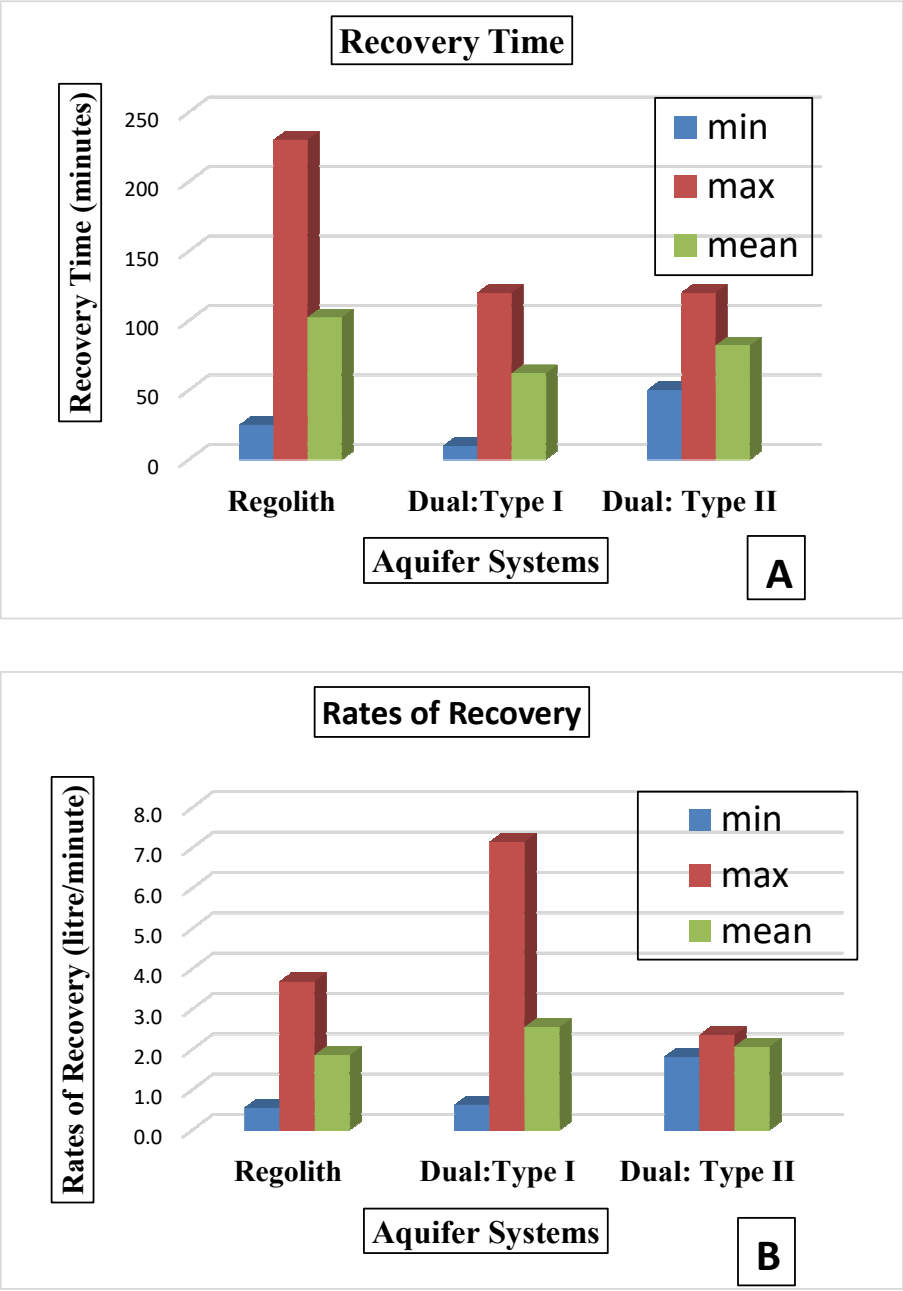

Figure 4.20: Histogram illustrations of variations in: (**A**) Total recovery time, and (**B**) Rates of Recovery in the three aquifer systems

penetrated fractured bedrock with corresponding average transmissivity 6.86 m^2/day and K of av. 27.74 $X10^{-2}$ m/day, and lower total drawdown of av.14.00m.

Wells grouped under dual aquifer systems have enduring continuous water yield, owing to occurrences of recharge boundary with fairly good water discharge and attainment of dynamic water level during pumping. This favours longer pumping time and relatively more steady pumping rates during the pumping tests. Most often, wells that terminate on fresh bedrock boundaries were dominated by large drawdowns.

Furthermore, in respect of discharge alone, borehole yield in water-bearing zones bounded by fresh basement or impermeable units has the second largest average discharge of 65.00m^3/day higher than those in Type II dual aquifer system that were regarded as being prolific. However, the lower discharges in Type II aquifers were sustainable over longer period, whereas the larger pumping rates in regolith aquifers were largely owed to well-bore storage effects, whereby the pumping rates were high initially, but drastically reduced as water head drops in the well as a result of contacts with fresh basement or impermeable boundaries.

From the discussion above, it can be seen that for better hydraulic characterisation, groundwater sustainability is not only a function of the pumping rates (or the well discharge alone). Other hydraulic properties, particularly transmissivity and total drawdown in the wells are essential parameters of evaluation. This is because these properties are parameters that were directly measured in the field. For example the transmissivity of an aquifer is directly controlled by well discharge (Q) and indirectly related to the drawdown in the well. This concept is true from the general overview of these relationships as illustrated by the scatter plots in Figures 4.21A-C. Relationships between the transmissivities of the wells and total drawdowns in the wells are strong and negative existed. This relationship is more significant in dual aquifers with R = -0.86 and less in regolith aquifers with R = - 0.58 (Figure 4.21A). This implies that the transmission capacity of wells that penetrated fractured bedrocks are more enhanced by smaller drawdowns during pumping, than those of regolith aquifers. Additionally, relationships between the transmissivities and well discharges (Figure 4.21B) were positive and strong, but also more significant for dual aquifers with R = 0.87 than for regolith aquifers with R = 0.57.

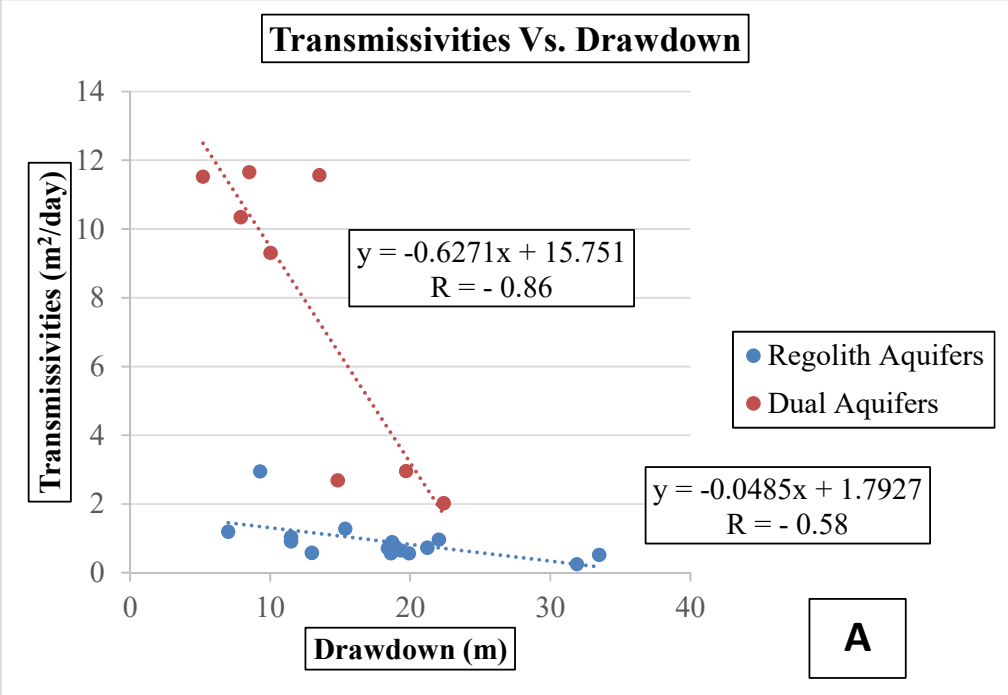

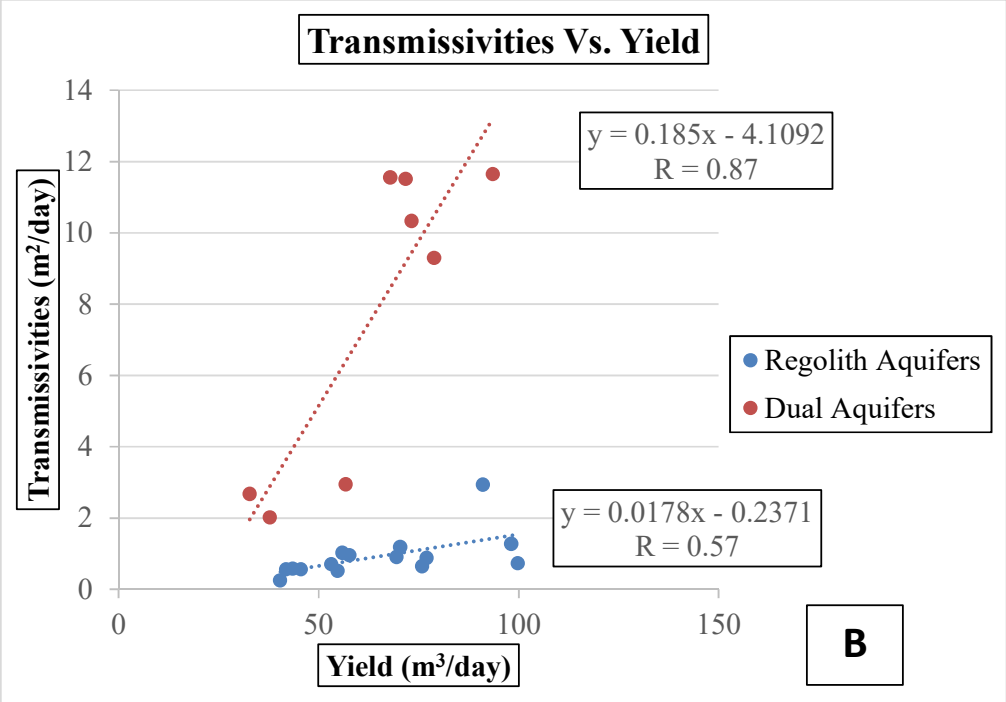

Figure 4.21: Scatter plots of hydraulic parameters. **A-** Transmissivity against drawdown; **B-** Transmissivity against yield

Hence, it can be deduced that the groundwater yield and the level of drawdown in the wells were significant to transmission capacity of aquifers, but the level of significances are more in dual aquifers than in regolith aquifers. The degree of significance of groundwater yield and drawdown in the wells was illustrated in Figure 4.21C. It is seen that the relationships are both negative, but more significant in dual aquifer systems with R = - 0.73 but weak in the regolith aquifers with R = -0.33. The negative relationship mean an indirect association between discharge and drawdown. Generally, well yield has a direct relationship with transmissivity, while drawdown is indirectly associated with the capacity of aquifer to transmit water (Figures 4.21A&B).

4.4.4 Relationships between Hydrological Parameters, Hydraulic Properties and Aquifer Systems

The associated hydrological parameters that were measured in the field prior to hydraulic aquifer testing were; the elevation and the depth of borehole, water table, and apparent aquifer thickness. The data of the four hydrological parameters presented under each aquifer system in Table 4.4 revealed that borehole elevation was between 139m and 215m above mean sea level, while the depths of boreholes were between 18.90m and 99.50m. The depth to water table and the apparent aquifer thickness range from 1.46 to 14.48m and 9.38 to 96.60m respectively. From the assessment of the mean values (Table 4.5), the average values for the borehole depth was between 30.7m in Type I aquifers and 33.37m in Type II aquifers, while the average in regolith aquifers was 32.39m.

The apparent aquifer thickness was 24.71m in Type II dual aquifers and 26.98m in regolith aquifers, while depth to water table is deeper in Type II with an average of 8.63m, compared to 4.49m depth in Type I and 5.42m in regolith aquifers.

The results of correlation analyses, employed in establishing relationships existing between hydrological and hydraulic parameters are presented in Table 4.8. The general correlation of the parameters without aquifer system and bedrock affiliations revealed that there are more occurrences of negative or indirect relationships than direct associations among all the parameters. In all, about thirty-four out of a total of fifty-five (55) relationships were negative or indirect (Table 4.8), which represents

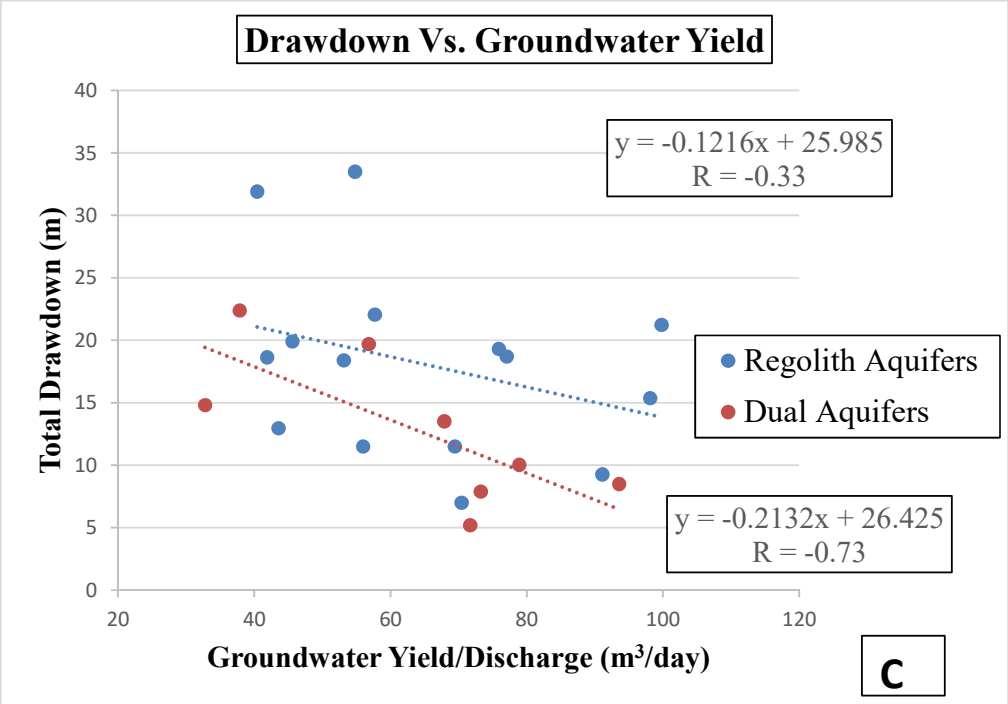

Figure 4.21 cont. C- Plots of drawdown against yield (or well discharge)

Table 4.8: Results of Correlation Analyses of Hydrological and Hydraulic Parameters

Hydrological and Hydraulic Parameters	Well Elevation	Well Depth	Water Table	Apparent aquifer thickness	Yield/ Discharge	Total Drawdown	Transmiss-ivity	Hydraulic conductivity	Specific capacity	Recovery Time	Rate of recovery
Well Elevation	1.00										
Well Depth	-0.21	1.00									
Water Table	0.15	-0.04	1.00								
Apparent aquifer thickness	-0.24	0.98	-0.24	1.00							
Yield/Discharge	0.16	-0.28	-0.37	-0.20	1.00						
Total Drawdown	-0.32	0.66	-0.14	0.67	-0.41	1.00					
Transmissivity	-0.08	-0.09	-0.16	-0.06	0.34	-0.57	1.00				
Hydraulic conductivity	0.00	-0.21	-0.18	-0.17	0.41	-0.62	0.95	1.00			
Specific capacity	0.32	-0.35	-0.15	-0.31	0.65	-0.82	0.67	0.71	1.00		
Recovery Time	-0.04	0.35	-0.18	0.38	-0.17	0.51	-0.31	-0.36	-0.23	1.00	
Rate of recovery	-0.36	0.06	0.12	0.03	-0.10	-0.04	0.12	0.04	-0.16	-0.56	1.00

sixty-four (64) percent of all relationships. In respect of significance of relationships, only twelve (12) associations have their coefficients (R) greater than 0.50. This means that only 22% of the existing relationships have moderate to strong relations that are either direct or indirect. The level of significance of relationships of others (78%) are either weak or insignificant (Table 4.8).

The relationships occurring between the total drawdown in the wells, well depth and apparent aquifer thickness are fairly strongly positive and similar, with R being equal to +0.66 and +0.67 respectively. The relationship is moderately positive with total drawdown and total recovery where R is +0.53. Contrastingly, the relationships between total drawdown with transmissivities T, hydraulic conductivities, K and specific capacity are all indirect. It is very strong with specific capacity with R= -0.82, fairly strong with K, with R= -0.61 and moderate with T with R= -0.57.

Also, the relationships with specific capacity and other hydraulic properties are all positive and strong; with transmissivity, R= +0.67, with hydraulic conductivities, R= +0.70 and with discharge or groundwater yield, R= +0.65. Other significant relationships are those with T and K, where R= +0.95; well depth and apparent aquifer thickness, R = +0.98; and between rates of recovery and total time of recovery, R = +0.56.

However, the degree of associations by aquifer systems affiliation as revealed in Figures 4.22 and 4.23 are more precise. The scatter plots illustrated in Figures 4.22 showed that the levels of significance improved between transmissivities and hydrological parameters by aquifer systems, compared to mostly low significance obtained from the lump correlation in Table 4.8. For instance, the inter-relationship between the transmissivities of the aquifers and other hydrological parameters are comparatively more significant (Figures 4.22) by aquifer systems affiliation. The plot of transmissivities and the borehole elevation (Figure 4.22A) showed a moderate direct relationship with R = 0.53 and 0.49 for dual and regolith aquifers respectively (whereas it was insignificant with R = -0.09 in Table 4.8). This implies that the topography of the borehole location has a direct significance and almost the same influence on the degree of water transmissions in the two aquifer systems.

There is also a similar relationships existing between transmissivities and well depth,

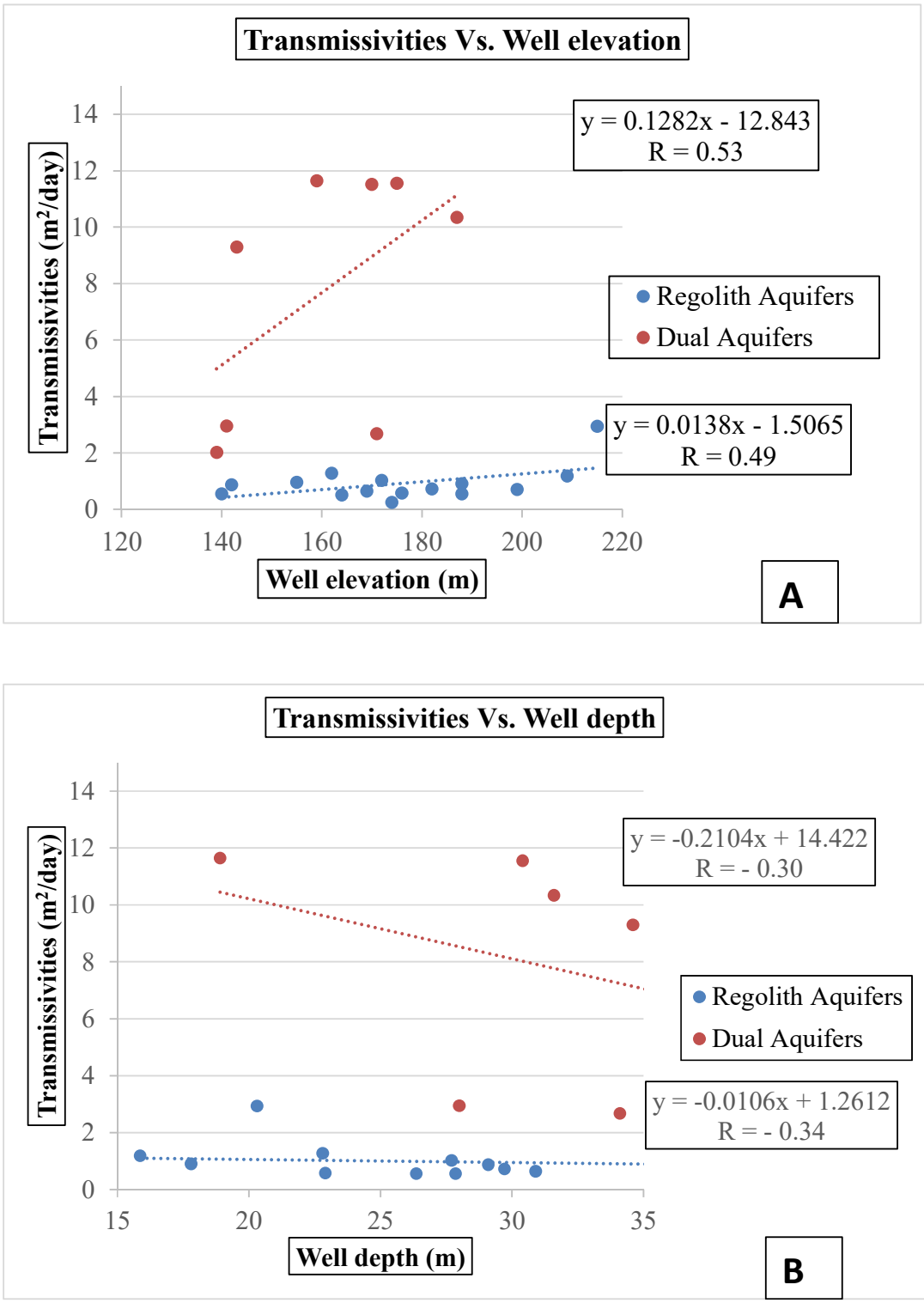

Figure 4.22: Plots of transmissivities against the hydrological parameters, showing varied degree of relationships

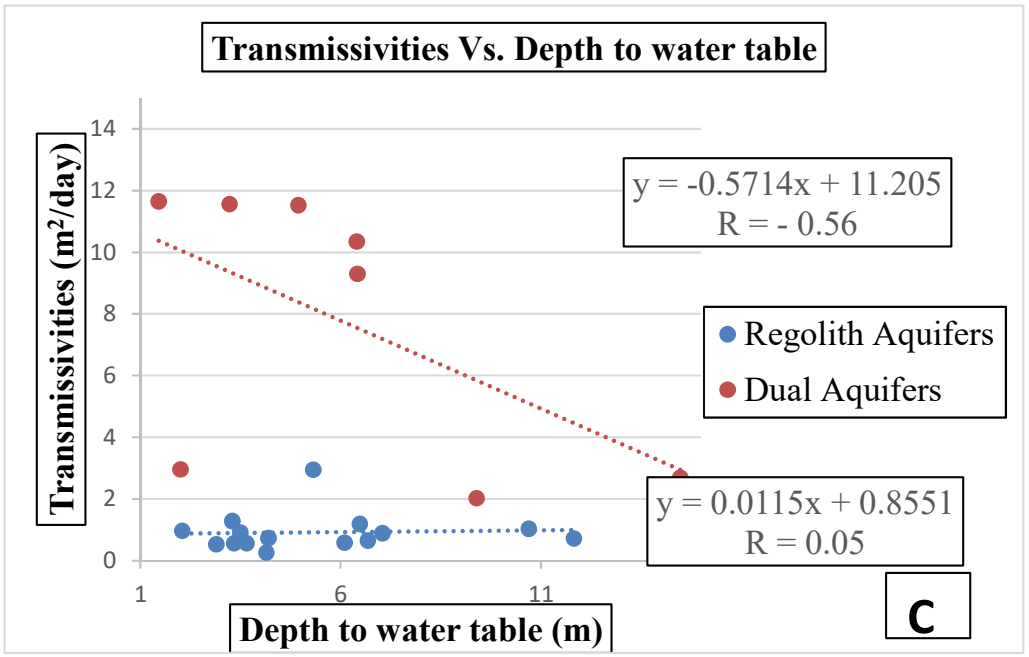

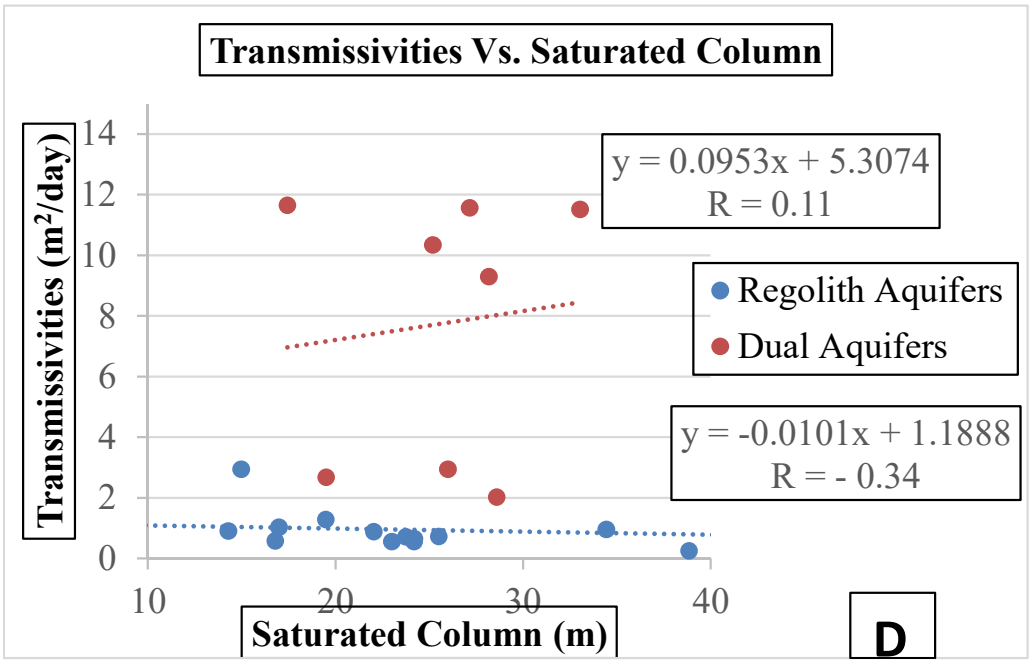

Figure 4.22 (cont.): Plots of transmissivities against the hydrological parameters, showing various levels of relationships

with corresponding R values of -0.30 and -0.34, implying an indirect significance (Figure 4.22B). This means good groundwater yield is not guaranteed in deep wells. Shallow wells are more likely to be more productive- at least to a reasonable degree. This is buttressed by the productivity of the borehole at Ajegunle that has the shallowest depth of 18.9m but the largest transmissivity of 11.65 m^2/day. It also has the highest yield of 93.58m^3/day (Table 4.4) and it is reputed to be the most prolific well tested in the study area. Groundwater level stabilized at the depth of 8.5m and there was continuous flow without water cessation the entire pumping time of over two (2) hours.

There is little or no significance relationship between the transmissivities and the groundwater table for regolith aquifer (R= 0.05), whereas the relationship is strong and indirect with dual aquifer system with R = - 0.56 (Figure 4.22C). This relationship implies that the water table bears little influence on the transmissivities of wells for regolith aquifers, but for dual aquifers bounded by recharge boundary, the influence is fairly high. Lastly, Figure 4.22D showed the degree of association between transmissivities and the thicknesses of aquifer. The relationship is weak but direct in dual aquifers R= 0.11, but indirect and more significant in regolith aquifers, R= - 0.34.

The scattered plots between hydrological parameters in aquifer systems are still low, as obtained in Table 4.8. However, there are demarcations in respect of levels of significance by aquifer system affiliations. The general low levels of significance in relationships between hydrological parameters showed that these variable are not really strongly dependent on one another. However, the degree of inter-dependence of these parameters on one another is fairly higher in regolith aquifers, compared to dual aquifers with R= - 0.27, 0.27, and -0.30 in relationships between well elevation against borehole depth, water table and apparent aquifer thickness. These relationships are insignificant for dual aquifer system with corresponding R values of -0.04, 0.01, and -0.14 (Figures 4.23A-C). This implies that the associated hydrological parameters bear little significance on the aquifer systems, especially on the dual aquifers.

Lastly, relationships between hydraulic parameters that were directly measured in the field were also correlated by aquifer systems and presented in Figures 4.24. These hydraulic properties included the well discharge, drawdown in the well, and

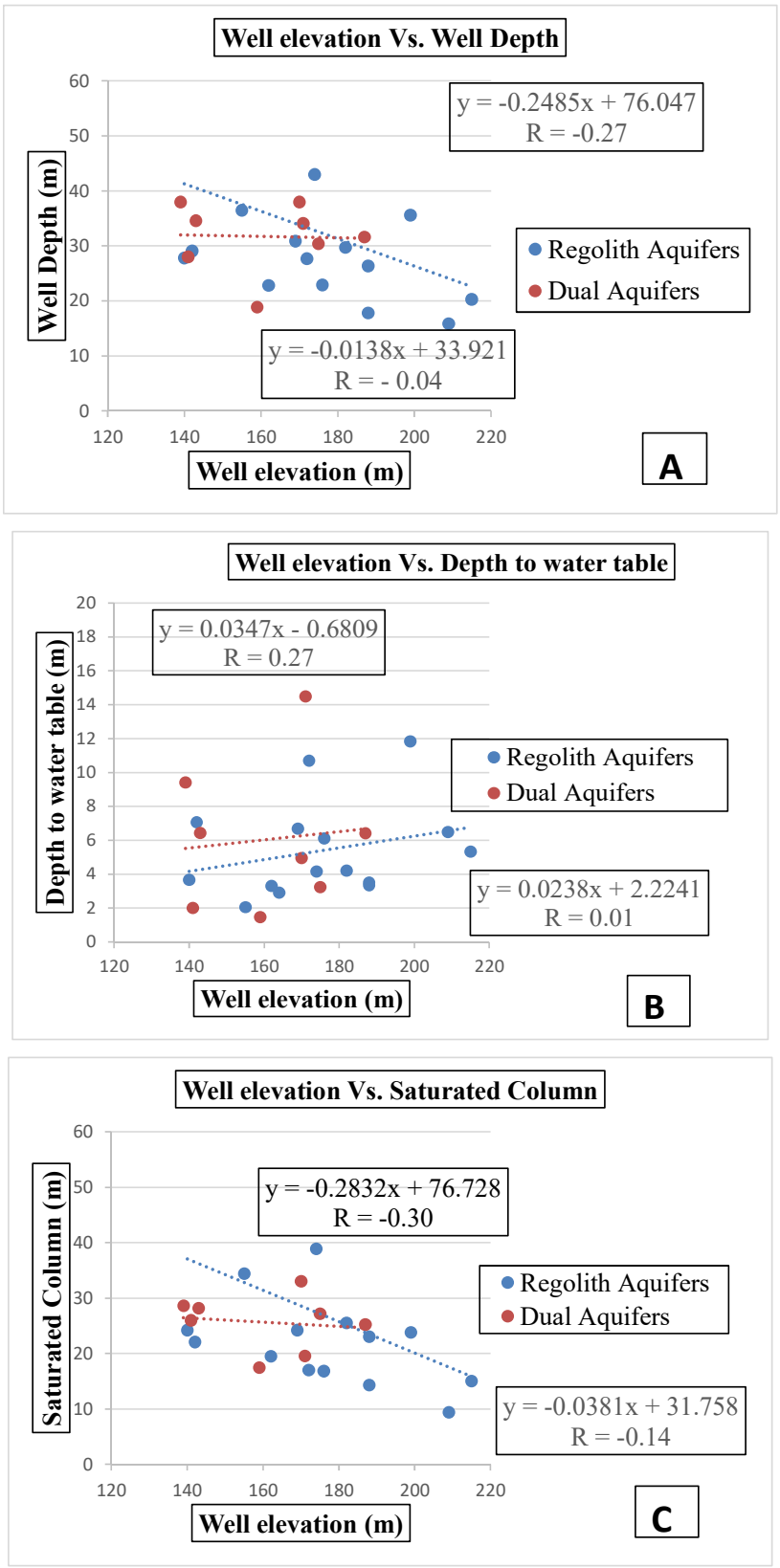

Figure 4.23: Scatter plots showing diverse levels of weak insignificant relationships between the hydrological parameters

groundwater recovery. Relationship between drawdown and recovery time is positive for both aquifer systems (Figure 4.24A), but the significance is moderate for regolith aquifers with R= 0.54 and weak for dual aquifer system, where R= 0.13. On the other hand, association between drawdown and discharge is indirect for both aquifers (Figure 4.24B), but the level of significance is weak for regolith aquifers (R= -0.33) but strong for dual aquifer system (R= -0.73). The strong negative significance for dual aquifer is explained by the development of dynamic water level by which the drawdown stabilizes as pumping continues as a result of occurrences of recharge boundaries. However, the relationship is not strong for regolith aquifer, since water input is through the weathered zone alone and the recharge cannot support the discharge, leading to water cessation during the pumping phase.

The relationship between discharge and recovery time is indirect and weak in both aquifer systems (Figure 4.24C), implying that low yielding aquifers are characterised by longer groundwater recovery time, and vice-versa for high yielding aquifer systems. This is more so for dual aquifer systems with fairly higher significance level of R = -0.33, compared to R= - 0.13 obtained for regolith aquifer systems. Generally, from these plots (Figures 4.24), it is deduced that the degree of impact of drawdown on recovery is more on regolith aquifers, while the influences of discharge on both the drawdown and total recovery time are more significant on dual aquifer systems.

4.5 Synthesis

As earlier emphasized, fresh and un-fractured crystalline bedrocks have no capacity to store or transmit water. However, viable water bearing zones do occur within the weathered and fractured zones. However, the degree and extent of occurrences of weathering and other water - bearing and water - transmitting discontinuities (such as fractures and faults) in crystalline rocks are not uniform across the study area. This is due to diversity in bedrock and structural settings, as well as variations in landforms across the area (Figures 4.1, 4.2, and 4.4). These geological and geomorphic factors are responsible for disparities in bedrock susceptibility to weathering; and variations in the distribution and inter-connectivity of fractures, faults and rock boundaries. These factors play significant role in groundwater occurrence, and are the major deciphers of variations in groundwater potentials across the crystalline basement terrains of Ibarapa.

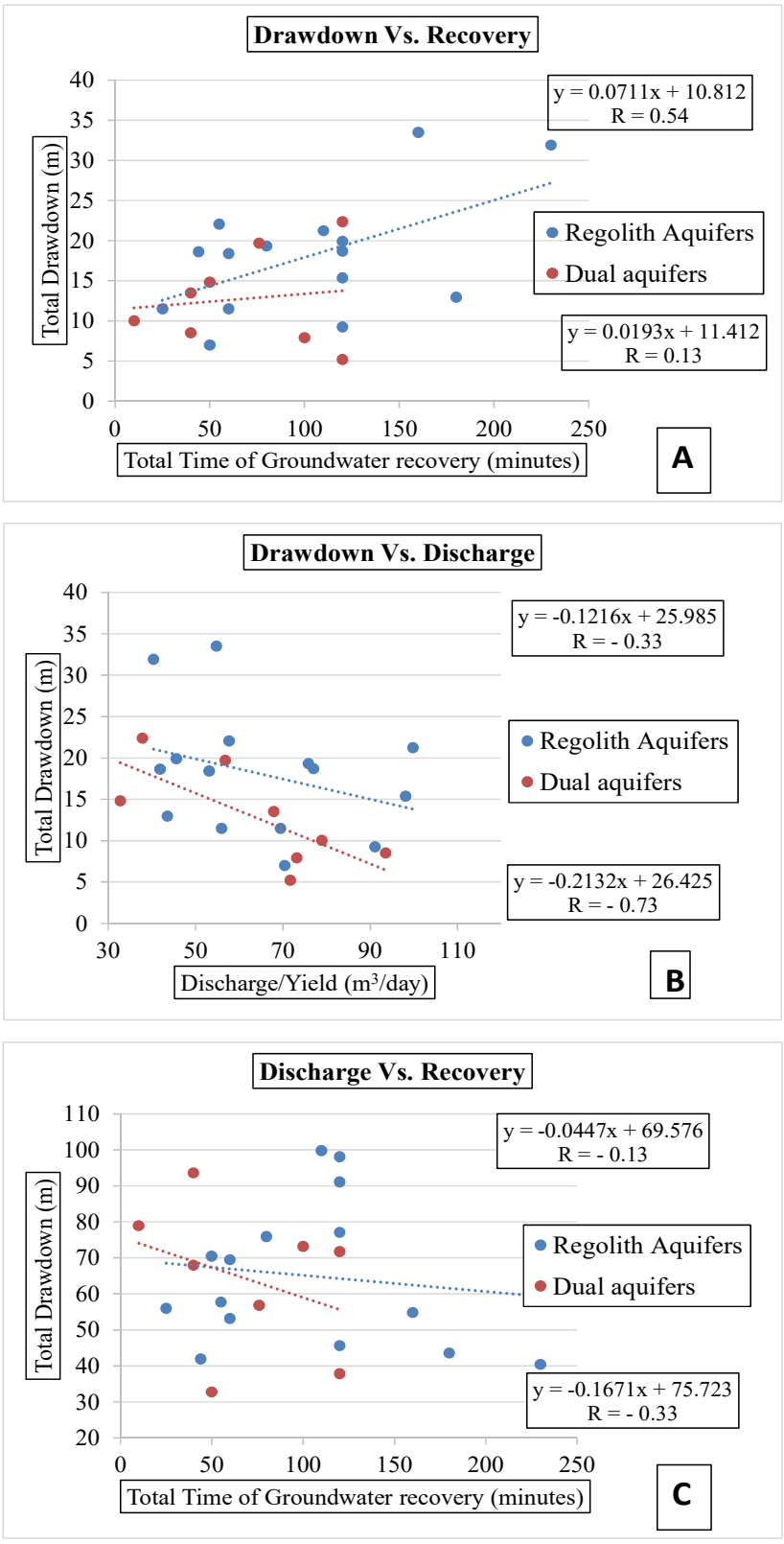

Figure 4.24: Scatter Plots of: **(A)** Drawdown against Groundwater Recovery; **(B)** Drawdown against Discharge and **(C)** Discharge against Recovery.

As stated earlier, groundwater potentials are not consistent across the study area. For example; the extent and intensity of weathering, and occurrences of bedrock fractures vary extensively across the study area. Although, there is close similarity in respect of rock decomposition across same bedrock terrain, there are still variations from one place to another (Tables 4.2, Figures 4.10 – 4.15). Also, there is diversity in the landforms, lineament attributes, and vegetation index from one point to another, even within terrains underlain by same bedrocks (Figures 4.2, 4.3). Hence, the areas are characterised by diverse groundwater occurring indices (Table 4.1, Figures 4.7, 4.15). These inconsistencies in respect to groundwater potential across the study area are integrated and discussed under each bedrock terrain below.

4.5.1 Characterisation of Groundwater Potential by Bedrocks

4.5.1.1 Amphibolite

The total thickness of the regolith units of areas that were mainly underlain by amphibolites were between 4.40 and 39.40m with an average of 18.23m. The middle layer (or the saprolite unit) alone has thickness range of 3.80 to 38.70m at an average of 16.56m. The saprolite units have an average resistivity value of 53.10Ωm and localised zones of high longitudinal conductance (S) occurred within amphibolite terrains (Figure 4.15). The high S values obtained within amphibolite terrains also suggests that the degree and extent of rock weathering is high. This is supported by occurrences of thick weathered units that are largely conductive across the amphibolite bedrock terrains (Figure 4.12a). The development of fine grained regolith is attributable to the high susceptibility of the amphibolite bedrock to weathering, due to large composition of dark coloured ferromagnesian minerals such as hornblende, and biotite (Plates 4.5A-C) in the mineral assemblage of the bedrock. These minerals (i.e. ferromagnesian) are largely unstable at surface environment, since they crystallize at higher melting points. Additionally, the schistose textural attributes of Igboora amphibolites (Plate 4.3B) facilitates easy breakdown of rock by physical processes, and rock mass decomposition by chemical processes. Though, water infiltration capacity is expected to be fairly low, as a result of the mainly fine grained saprolite units, other groundwater potential indices discussed below revealed relatively better groundwater occurrences within amphibolite bedrock terrains, in comparison to other bedrocks.

Groundwater occurrence indices from geomorphological characterisation, revealed that amphibolitic crusts are characterised by features such as clustered vegetation and riparian forest (Figure 4.7 and Table 4.1) which are evidences of water seepage along the river channels and presence of water-containing fractures. So, aside terrains underlain by gneisses at the western parts and rock contacts zones at Idere and the southern end, amphibolite terrains are next in respect of having good water seepage and groundwater potential attributes. More so, coupled with the fact that the landforms are within moderately-high lying to low lying zones (Figures 4.2), and in hydro-geomorphic sense, amphibolite terrains are classified as one of the recharge zones in the study area.

Additionally, aside the fact that the weathering development is well pronounced in areas underlain by amphibolite with >18m average thickness, (though largely fine grained); about eleven (11) locations out of 25 soundings conducted within amphibolite terrains were characterised by bedrock resistivity of <500 Ωm, interpreted as fractured bedrocks. This represents 46% of all fractured bedrock locations (which is the highest compared to fracture occurrences in other bedrocks (Table 4.9, Figure 4.25) across the study area. Generally, 44% of amphibolite bedrocks were fractured, 12% were interpreted as weak or weathered basement while 44% were fresh amphibolite bedrock (Figure 4.26).

Furthermore, aside the fractured bedrocks, another 12% amphibolite bedrocks are weak with resistivity between 500 and 1800Ωm. This weak bedrocks which are already in the process of decomposition will also have good water transmitting capacity. Depths to fractured bedrocks are within 7.9 to 29.9 (av. 18.3m -Table 4.9). The bedrock resistivity of the remaining 44% that are fresh bedrock were less than 2500Ωm, except in Igboole, Oremeji and Oke-Oyinbo III on VES points 19, 67 and 71 respectively. At this locations, bedrock resistivities were within the range of 4500 to 5500Ωm.

The spatial distribution of weathering development as illustrated by the geo-electric sections profiles (Figure 4.10a) revealed that there is increase in the degree of bedrock decomposition from the eastern part towards the western parts of areas underlain by amphibolite. The susceptibility of amphibolite to weathering has surface expressions

Table 4.9: Frequency and Depths of Occurrence of Fractured Bedrocks

Rock units	Total no of VES points	Frequency of occurrence of fractured bedrock in the study area	Depth of occurrence (m)		
		n (%)	Min	Max	Mean
Amphibolite	25	11 (46%)	7.9	29.9	18.3
Gneisses	19	5 (21%)	16.6	27.3	22.5
Migmatite	18	7 (29%)	6.7	19.5	13.7
Porphyritic granite	20	1 (4%)	-	-	-

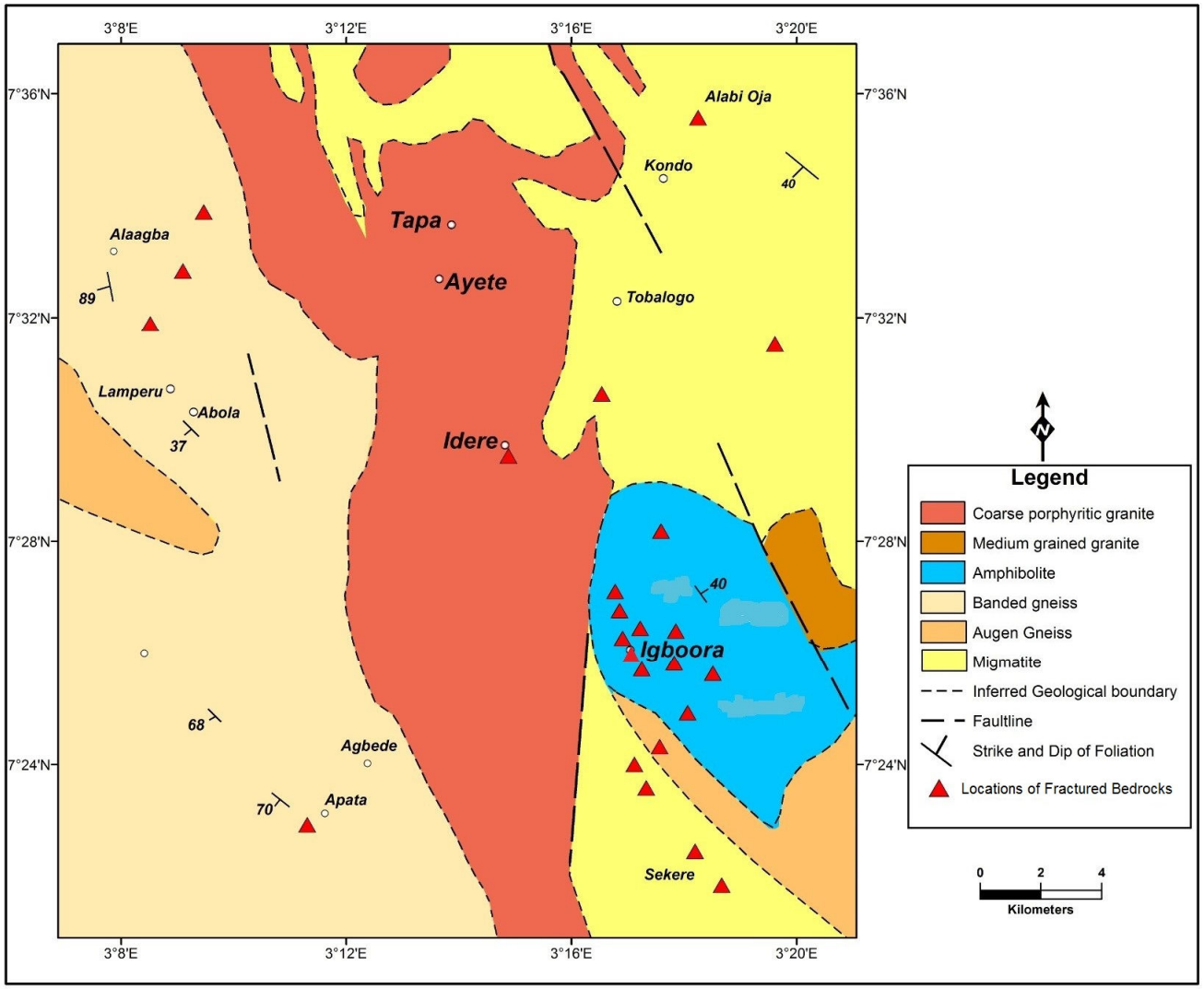

Figure 4.25: Fractured bedrock locations on geological map of the study area.

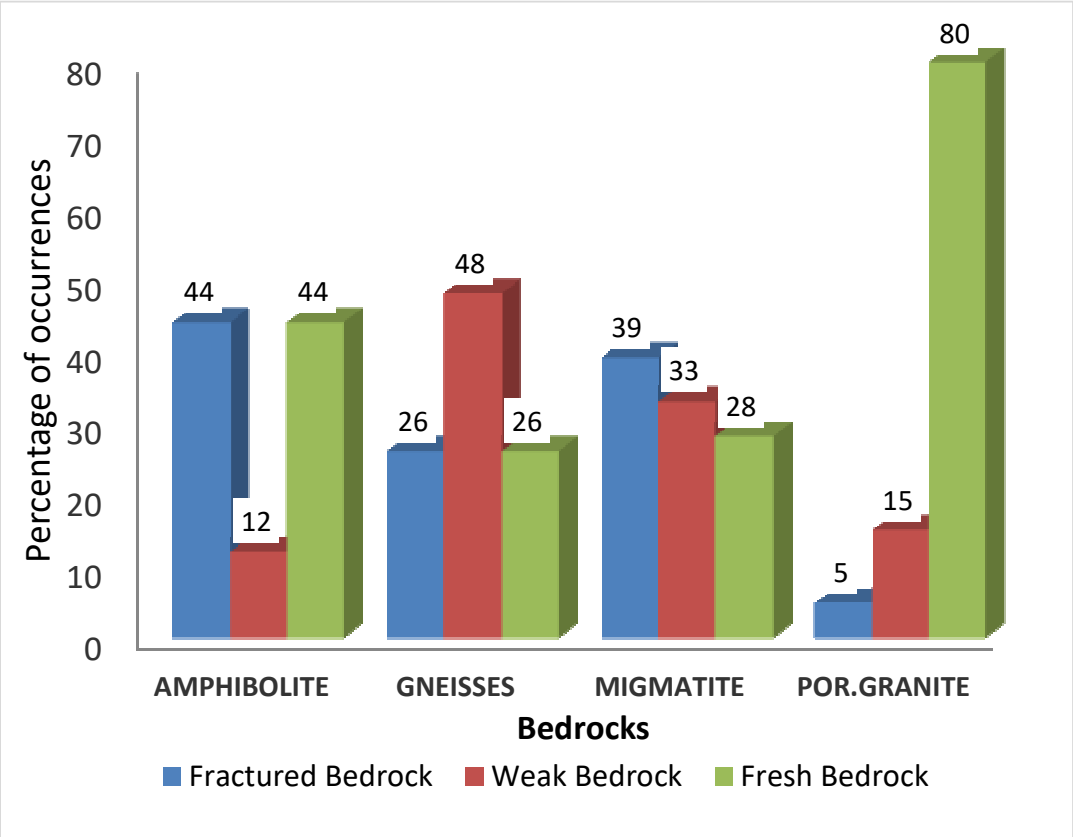

Figure 4.26: Comparative percentage frequencies of the state of the basement in bedrocks

The hydrogeological setting of terrains underlain by amphibolite, as described above, hereby supports generation of artesian aquifer. This is due to widespread occurrence of moderately thick and largely fine grained regolith overlying the largely fractured and weak bedrock. This is more so in the western section of Igboora (Figure 4.14a).

as well, as revealed by the vast fragmented occurrences of outcropping (Plates 4.2). This also explained the susceptibility of the bedrock to fracturing.

On a general evaluation, terrains underlain by amphibolite are classified as high potential zones for groundwater occurrence due to thick and more conductive regolith development. Also, due to generation of good vegetation response to groundwater, abundant occurrence of fractured and weak bedrocks in the area, and favourable landform situation. Additionally, the fine grained texture of the regolith will prevent direct infiltration of pathogens into the aquifer zones. Hence, the groundwater quality is expected to be good. Also, the occurrence of fractured bedrocks which are the main groundwater zones in the area at relatively deeper depth (av. 18.3m) will further enhance the protection of the enclosed groundwater resource in the area.

4.5.1.2 Gneisses

Areas underlain by gneisses were characterised by wide range of landform, including highlands found at the central to NW parts, to low-lying areas and flood plains at the SW (Figures 4.1b and 4.2). These terrains were also characterised by development of thick regolith units: 6.30 to 59.00m (av. 18.49m), which is even a little thicker than those associated with amphibolite terrains. The saprolite units were also fairly well-developed with 4.40 to 57.70m and average of 15.83m (Table 4.2). Though, gneissic terrains were generally marked by thick regolith unit, localised areas of deeper weathering still exist at Fedegbo in NW and at the SW floodplain area, where the thickness of the saprolite units is greater than 22.0m (Figure 4.12b). Possible factors that may favour the development of thick regolith in areas underlain by gneisses are; mineralogical and structural attributes of the gneisses, and wide variations in landforms which facilitates movement of water and soils. Also, rock foliations and abundance of dark coloured minerals such as biotite and hornblende are common features that facilitate rock weathering in areas underlain by gneisses (Plates 4.5E, F &H).

Conversely, the resistivity of the saprolite ranged extensively: 18.80 to 810.60Ωm, and based on the average resistivity of 117.95 Ωm, the regolith units are coarser compared to amphibolite terrains, and are interpreted as sandy-clayey. The coarse sandy components are mainly quartz and potassic feldspar (orthoclase), which are more resistant to weathering processes. However, from geo-traverse across the N-S section (Figure 4.14b), regolith at the northern section are fairly coarser grained compared to those at the southern end. Also, the total longitudinal conductance (av. 0.28 mhos) was markedly lower than those obtained in amphibolite (0.45mhos), which means that the recharge potential of regolith in gneisses are relatively higher compared to amphibolite. Accordingly, the potential for water infiltration through the regolith, inferred from the total longitudinal conductance is better in gneiss terrains than in amphibolite.

Consequently, from geomorphological studies, the processed NDVI transform imageries showed that apart from the rock contact zones, terrains underlain by gneisses are characterised by good development of water-containing fractures. The conspicuous hydro-geomorphic features revealed the evidence of structural control of groundwater occurrences (Figures 4.6, 4.7, and Table 4.1).

Notwithstanding, bedrock resistivities of only five (5) out of nineteen (19) locations were fractured (Figure 4.25). However, the percentage of occurrences of partially weathered basement was (48%) enormous (Figure 4.26). With this, the degree of rock decomposition can also be said to be equally high. However, bedrock fractures occurred at the depth range of 16.6 to 27.3m (av. 22.5m), which is comparably deeper in comparison to other bedrocks (Table 4.9).

Nonetheless, areas underlain by gneisses are expected to have better water transmission ability owing to the thick and the fairly coarser nature of the regolith units. Furthermore, the gneissic foliated structures do not only aid rock decomposition, these foliations are also conduits for groundwater. This is confirmed in Figure 4.7, where groundwater occurrence is aligned along the strike of the major foliation plane close to Alaagba Village at the NW region.

The hydrogeological framework discussed above, will generate a semi-confined aquifer system due to fairly coarser saprolite units overlying the largely weathered

basement. The thick weathered units can serve as both water-bearing zone and a semi-confining unit to the weathered bedrocks, which are expected to have good water bearing capacity. Water quality may be poor in these terrain when tapped from the conductive regolith, whereas water from wells that tap into the relatively deeper fractured bedrocks at an average depth of 22.5m (Table 4.9) may be safer.

4.5.1.3 Migmatite

The thickness of regolith development in areas underlain by migmatite is shallower when compared with terrains underlain by amphibolite and gneisses. The thickness of the regolith was 4.60 to 23.6m (12.77m), while that of the saprolite layer was 3.40 to 22.40 (11.31m). The resistivity of the regolith was 28.10 to 565.50 Ωm (av. 204.39 Ωm). Based on the mean resistivity of 204.39 Ωm, the regolith units are sandy and were characterised by lower longitudinal conductance of 0.02 – 0.60 (av. 0.23) mhos, compared to those within amphibolite and gneisses. Hence, water recharge potential of the regolith units within migmatite terrains is little better than those within gneisses with average of 0.28 mhos and much better than amphibolite terrains (av. 0.45 mhos). Hence, based on S values, areas underlain by migmatite are categorised to have moderate groundwater recharge potential.

However, based on electrical coefficient of anisotropy (λ) mean value of 1.81, the regolith units within migmatite terrains were characterised by broader lithological variation; compared to 1.48 for amphibolites, 1.68 for gneisses and 1.65 for porphyritic granite terrains. The broader lithological differentiation is as a result of the fact that migmatite is a composite rocks of later granitic intrusions into the Older rocks. Hence, it is expected that the petrographical and structural variations will be larger in migmatite than other bedrocks. It is expected that these variations will imprint on the complexity of the weathering processes and bedrock fractures, as well as on the groundwater potential of the area. Oladapo and Akintorinwa (2007); also attributed the high λ values obtained for migmatite terrains in Ogbese area, SW Nigeria as due to high lithological differentiation.

Notwithstanding, seven bedrocks in eighteen of the locations studied were fractured (Table 4.9, Figure 4.25). Bedrock fractures are prominent at Ayanleke, Kondo, Alabi-Oja, Alabi-Ilumo, and Sekere. It is interesting to note that there is a corresponding

relationship between the resistivity of the last layer and the thickness of the regolith layer for these four locations. This means that locations terminating on fracture basement has a rather thicker saprolite zone. However, most locations with fractured bedrocks are localised at the smaller migmatite terrains at the SE. However, fracture bedrock locations in main migmatite bedrock terrains were found scattered and widely spaced from one another. Notwithstanding, 33% of bedrock were classified as weak, which is higher than those found in porphyritic granite and even in amphibolite terrains (Figure 4.26).

Furthermore, the hydro-geomorphic studies revealed that migmatite terrains are characterised by high-lying landform with numerous, extensive fractures. However, from the vegetal response, these fractures are dry, indicative of low groundwater potential. This could be as a result of run-off of water through the largely coarse regolith by force of gravity from the high-lying terrains to adjoining low-lying areas at the central and SE regions underlain by porphyritic granite and amphibolite. More so, at the NE migmatite terrain that was characterised by scanty fractured bedrocks, the bedrocks are largely fresh, and further water transmission through the subsurface are retarded. Additionally, due to the extensive lineament features, coupled with the sandy and relatively shallow regolith units, the groundwater table is highly vulnerable to seasonal weather changes. Consequently, during the wet/rainy season, the water-table rises and wells are recharged, but at the peak of dry season, the wells will be dried as a result of drastic decline in water-table. However, at the smaller migmatite terrain at SE, almost all the bedrocks are fractured and are characterised by thick regolith units ranging from 13.3 to 19.5m. Therefore, the occurrences of groundwater in migmatite terrains are expected to range from low to moderate.

Based on the above, groundwater occurrences within terrains underlain by migmatite bedrock will exist in unconfined state, and the water-table will be exposed to capillary transfer to the vadose zones. More so, the quality of enclosed water will be questionable due to likely direct surface water percolation. Additionally, as a result of occurrences of bedrock fractures at shallower depths of 6.7 to 19.5m (av. 13.7m) and the permeable overlying regolith units in migmatite terrains, groundwater will be liable to contamination.

4.5.1.4 Porphyritic Granite

Terrains underlain by porphyritic granite are the least weathered and the least fractured (Figures 4.25, 4.26 and Table 4.9). The overburden thickness was 1.8 to 19.4m (9.52m), compared to 16.6m, 15.8m, and 11.3m in amphibolite, gneisses and migmatite terrains respectively. Besides, the average thickness of the saprolite was 9.52m, whereas it was 16.6m, 15.8m, and 11.3m correspondingly in other bedrocks (Table 4.2). The extent of weathering development was not only comparatively shallower in terrains underlain by porphyritic granite; the weathered units, also terminate on mainly fresh bedrocks. The porphyritic bedrock resistivity was 547 to 29903Ωm (av. 4601Ωm), in comparison with mean values of 1516Ωm, 1815Ωm, 1488Ωm respectively for other bedrocks. Additionally, bedrock fractures occurred at only one location at Idere, even at a shallow depth of 5.8m (Table 4.9, Figure 4.25), while only three locations were partially weathered, and the rest (that is 80%) are fresh basement (Figure 4.26). Hence, fresh granitic bedrocks occurred at shallow depths, as a result of relatively shallower weathered–regolith development across the terrains. However, areas with fairly thick regolith development were localised at rock boundary zones at Idere, and other few locations where the thickness of the saprolite is higher than 10m.

The resistivity of the saprolite units was 26.5 to 294.0Ωm (av. 93.03Ωm) and largely medium grained silty-sandy-clay units. Based on the average resistivity, the saprolite lithological units in granitic terrains are coarser than those in amphibolite, fairly similar to those in gneisses but finer than those in migmatite terrains. The implication of this is that the comparatively shallower regolith units may not be that permeable to water. Notwithstanding, the mean S value in porphyritic granite was 0.15, compared to 0.45, 0.28 and 0.23 correspondingly for other bedrocks. This indicated that the regolith in granitic terrains will be characterised by better recharge capacity than other bedrocks terrains. Contrastingly, groundwater indication (Figure 4.4) in porphyritic granite terrains is the least; though, these terrains were characterised by much lineaments (Figure 4.5). However, at the boundary intersections with migmatite around Idere area, where there is better development of regolith, there is much groundwater occurrences based on vegetal response. The lush clustered vegetation is indicative of variably occurrences of groundwater in the area.

The comparative poor weathering, bedrock fractures and the eventual low groundwater potential, despite the high lineament density in granitic terrains could be linked to the associated high-lying landforms that characterised the terrains and the fracture characterisation. The valley incisions found between the ridges and the numerous inselbergs are the only deposition centres for the regolith generated from the physical breakdown of many high lying granitic outcropping sections in the area. The breakdown of rocks is largely by physical weathering and there is really no chemical decomposition of rocks. This assertion is illustrated by the fact that porphyritic granite composed mainly of weathered resistance quartz and porphyries of orthoclase sandwiched by less weathering resistive biotite mineral (Plate 4.1B). This is evidenced by the coarseness of the resistance quartz and orthoclase minerals in the loosed regolith along the erosional pathways. Additionally, the fractures could not be said to be interconnected as evidenced by the variations in orientations and their short-length nature.

The development of relatively coarser weathering products porphyritic granite terrains than in amphibolite is owed to the large mineral grains of porphyritic granite (Plates 4.1) and greater abundance of weathering resistance quartz mineral. This will favour good water transmission if the bedrocks are more fractured and the regolith are thicker.

Generally, based on the collaborative assessment of groundwater indicative parameters above, granitic terrains will be characterised by largely unconfined shallow groundwater zones. Groundwater yield is expected to be low and may not sustain long pumping time, as a result of the fact that the only potential groundwater bearing zones is the regolith units, and the fresh bedrock occur at shallow depths. More so, the enclosed groundwater will be very seasonal, and there will be much fluctuation in water Table.

4.5.2 Hydrogeological Characterisation of the Basement Aquifers

The discrepancies in groundwater potentials from one bedrock terrain to another, and from place to place have imprints on the response of the water bearing zones to pumping.

Therefore, hydrogeological characterisation of the study area is discussed under the following sections.

4.5.2.1 Bedrock Influence on Hydrological and Hydraulic Parameters

The statistics of the measured hydrological parameters and the estimated hydraulic properties by bedrocks are presented in Table 4.10. The geological influences on the hydraulic characteristics are discussed under the following sections.

The variations of the hydrological and hydraulic parameters by bedrocks are presented in Table 4.10. It shows that borehole elevation above mean sea level was 159 to 187m (av. 171.6m) within amphibolite bedrock, 139 to 174 (av. 160m) for gneisses, 142 to 199m (180m) for migmatite and 140 to 215 (av. 172m) for porphyritic granite. The corresponding depths of tested boreholes were 18.9 to 38.0m (av. 27.5m), 30.9 to 99.5m (av. 46.7m), 17.8 to 35.6m (27.7m) and 15.7 to 36.5m (av. 25.7m). This showed that well depths are mostly below 30m, except in gneisses where the average borehole depth was 46.68m. The depth to water-table in amphibolite was 1.46 - 10.70m (av. 5.60m), while in gneisses it was between 2.90 to 14.58m (7.36)m, and 3.34 to 11.83 (5.98)m and 2.00 to 6.48 (av. 3.90m) for migmatite and porphyritic granite respectively. The corresponding apparent aquifer thickness which is the saturated water column in the well was within 16.80 and 33.05 (av. 22.31m), 19.52 to 96.60m (av. 39.33m), 14.30 to 25.52m (av. 21.73m), 38 to 34.45 (av. 21.80m).

For estimated hydraulic properties of the crystalline water-bearing zones; discharge in m^3/day for amphibolite was 43.56 to 98.1 (av.72.05), 32.78 to 8.92 (av.53.45) for gneisses, 41.91 to 99.79 (68.27) for migmatite and for porphyritic granite 45.62 to 91.00 (av. 64.33). The total drawdown were 5.20 to 15.36m (av. 10.70m), 10.03 to 33.50 (av. 21.99m), 11.49 to 21.23m (av. 17.69m), and lastly for porphyritic granite, 7.00 to 22.04m (av. 15.58m). The transmissivity (in m^2/day), hydraulic conductivity (X 10^{-2} m/day) and specific capacity (in m^3/d/m) for each bedrock were correspondingly; 0.58 to 11.65 (av. 6.85), 3.45 to 66.80 (av. 28.76), 3.36 to 13.79 (av. 7.67) for amphibolite; for gneisses, 0.25 to 9.30 (av. 2.57), 0.54 to 33.00 (av. 6.91), 1.27 to 7.87 (av. 3.10); and for migmatite, 0.56 to 0.91 (av. 0.76), 2.43 to 6.36 (av. 3.73), 2.25 to 6.05 (av. 4.00), and lastly for porphyritic granite 0.56 - 2.95 (av. 1.72), 2.31 to 19.69 (av. 9.77), 2.29 to 10.06 (av. 5.54).

Graphical illustrations of variations in the statistics of hydraulic properties are presented in Figure 4.27. It is clearly seen that based on the average values,

Table 4.10: Statistics of Hydrological and Hydraulic Parameters by Bedrocks

Bedrock Units	n	Statistics	Well Elevation (m)	Well Depth (m)	Water Table (m)	Aquifer Thickness (m)	Q (m^3/day)	Draw-down (m)	T (m^2/day)	K ($X10^{-2}$) (m/day)	Specific capacity (m^3/d/m)
Amphibolite	7	Min.	159.00	18.90	1.46	16.80	43.56	5.20	0.58	3.45	3.36
		Max.	187.00	38.00	10.70	33.05	98.12	15.36	11.65	66.80	13.79
		Mean	171.57	27.47	5.16	22.31	72.02	10.70	6.85	28.76	7.67
		Std dev.	9.32	6.49	3.00	6.29	19.29	3.61	5.53	24.06	3.79
Gneisses	6	Min.	139.00	30.90	2.90	19.52	32.78	10.03	0.25	0.54	1.27
		Max.	174.00	99.50	14.48	96.60	78.92	33.50	9.30	33.00	7.87
		Mean	160.00	46.68	7.34	39.33	53.45	21.99	2.57	9.61	3.10
		Std dev.	15.13	26.20	4.16	28.78	19.97	9.30	3.43	12.50	2.52
Migmatite	5	Min.	142.00	17.80	3.34	14.30	41.91	11.49	0.56	2.43	2.25
		Max.	199.00	35.60	11.83	25.52	99.79	21.23	0.91	6.36	6.05
		Mean	179.80	27.72	5.98	21.73	68.27	17.69	0.76	3.73	4.00
		Std dev.	22.00	6.49	3.59	4.34	22.33	3.65	0.14	1.58	1.50
Porphyritic Granite	5	Min.	140.00	15.86	2.00	9.38	45.62	7.00	0.56	2.31	2.29
		Max.	215.00	36.50	6.48	34.45	91.10	22.04	2.95	19.69	10.06
		Mean	172.00	25.70	3.90	21.80	64.33	15.58	1.72	9.77	5.54
		Std dev.	37.05	7.95	1.99	9.80	17.35	6.91	1.14	7.31	4.03

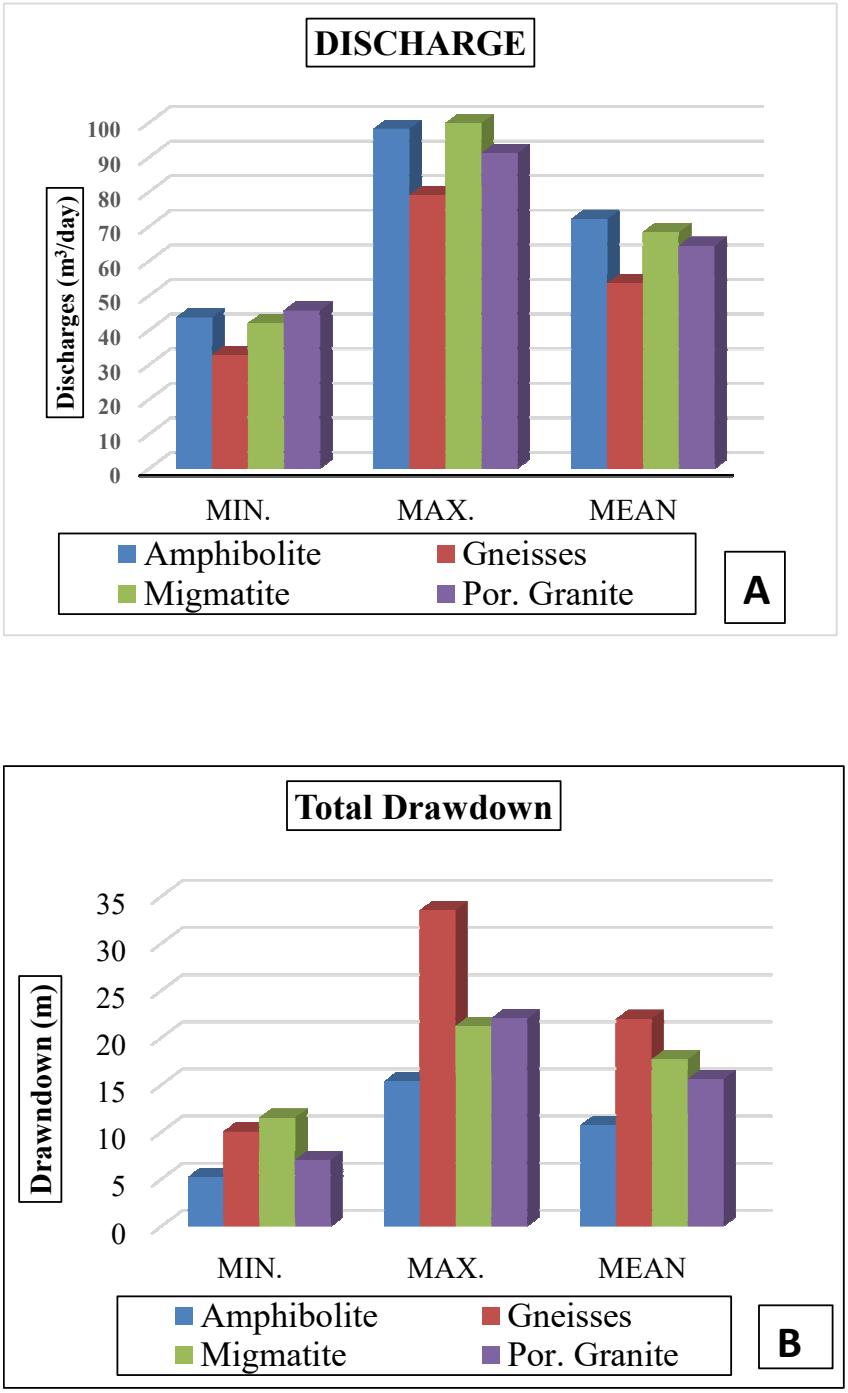

Figure 4.27: Histogram illustrations of hydraulic properties by bedrock

groundwater discharges in wells that penetrated amphibolite, migmatite and porphyritic exceeded 60m^3/day, while those in gneisses have the lowest yield of about 50m^3/day (Figure 4.27A). Consequently, the total drawdown during pumping in wells in gneisses is the largest with the mean exceeding 20m; whereas in other bedrocks, the total drawdowns after pumping are 18m (Figure 4.27B). Although, this may not necessarily mean that wells in gneisses are less productive. The reason is due to the fact that gneisses are characterised by deeper wells as a result of deeper weathering (Table 4.3, Figure 4.26). The transmissivities in amphibolites is above 6.0m^2/day with a range of 0.58 to11.65m^2/day, followed by gneisses with an average transmissivity above 2.5m^2/day (Figure 4.27C). The degree of water transmission in migmatite is the lowest with mean transmissivity less than 1.0m^2/day. The hydraulic conductivity is also largest in amphibolite with mean value close to 30m/day; whereas the values are less than 10m/day in both gneisses and porphyritic granite, and much less in migmatite with < 4.0m/day (Figure 4.27D)

4.5.2.2 Bedrocks, Associated Aquifer Systems and Boundary Conditions

From the frequencies of the associated aquifer systems by bedrocks presented in Figure 4.28, regolith aquifers that is the most abundant 65% occurrence (Figure 4.28a) were found to be associated with all the bedrocks in the study area (Figure 4.28b).

Water-bearing zones within amphibolite were characterised by two aquifer systems. Four wells were found to belong to dual-Type I category with total transmissivity ranging from 11.65 m^2/day for the well tested at Ajegunle to 10.34 m^2/day at Pako. On the other hand, the wells at Onilado, Sagaun and Itaagbe terminated on impermeable boundary. The impermeable boundary may either be an impermeable weathered regolith such as clayey units that are known to have good water storage ability, but poor water transmission capacity. This inference is supported by the fact that the regolith units within amphibolite terrains were mainly clayey (with average saprolite resistivity of 53.1Ωm) as revealed by the geophysical studies and outcropping sections (Appendix X, Table 4.2,). Also, based on field evidence, the impermeable units may likewise be quartzite intercalations, as seen at the exposed weathered-profile at Itaagbe, adjacent to the well (Plate 4.3C). Additionally, it may just be that the wells terminated on fresh amphibolite, since the average regolith thickness in areas underlain by amphibolite is 18.06m, compared to the average well depth of 27.47m for wells

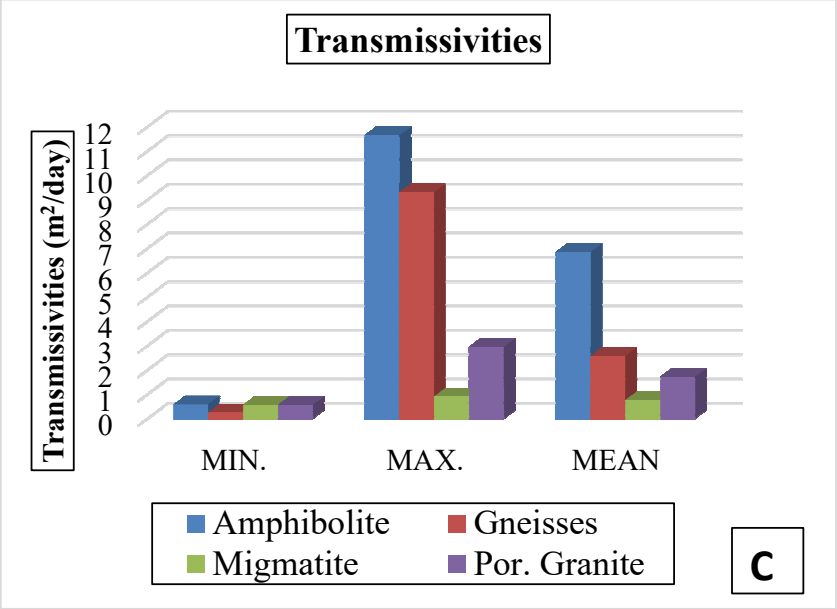

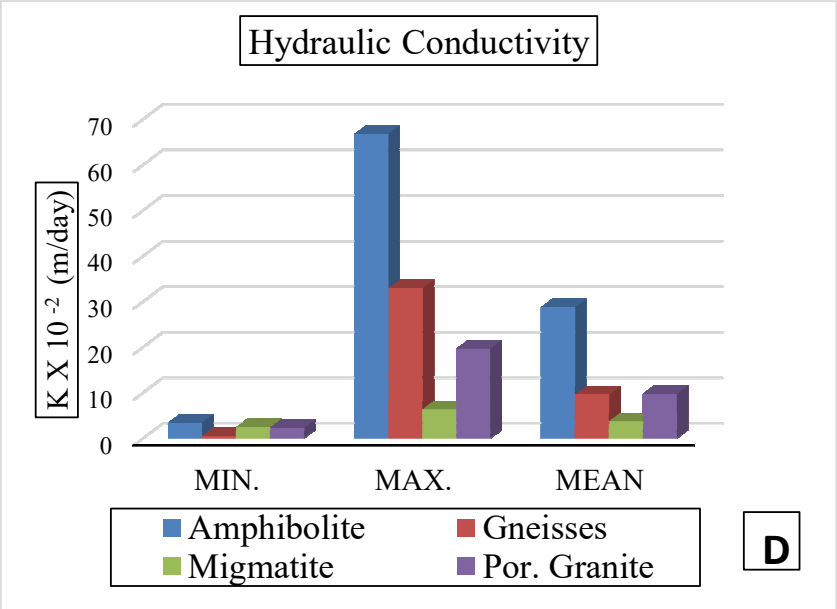

Figure 4.27 cont.: Histogram illustrations of hydraulic properties by bedrock

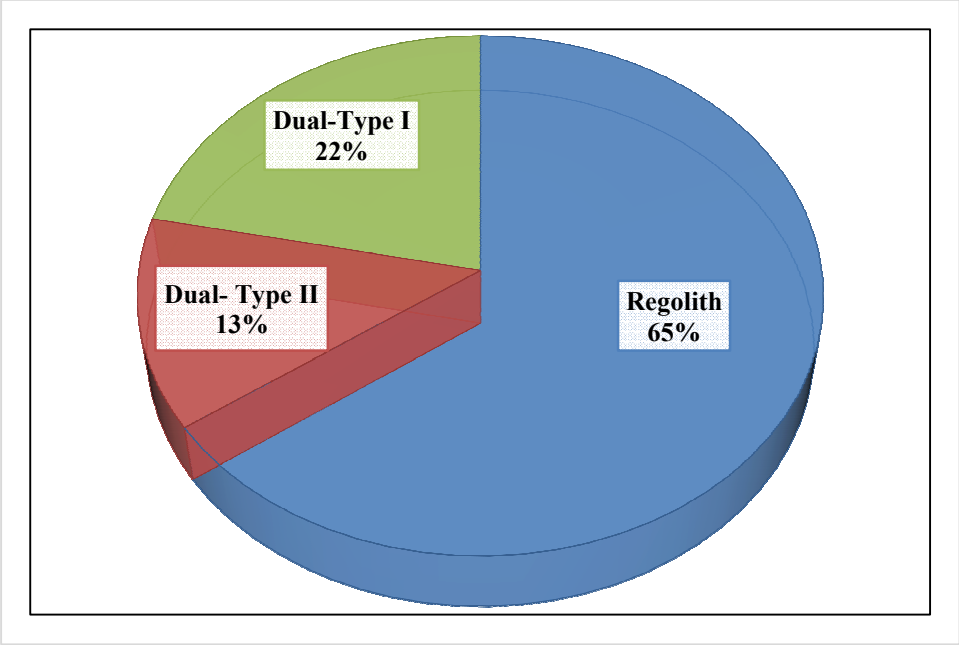

Figure 4.28a: Percentage Occurrences by aquifer systems

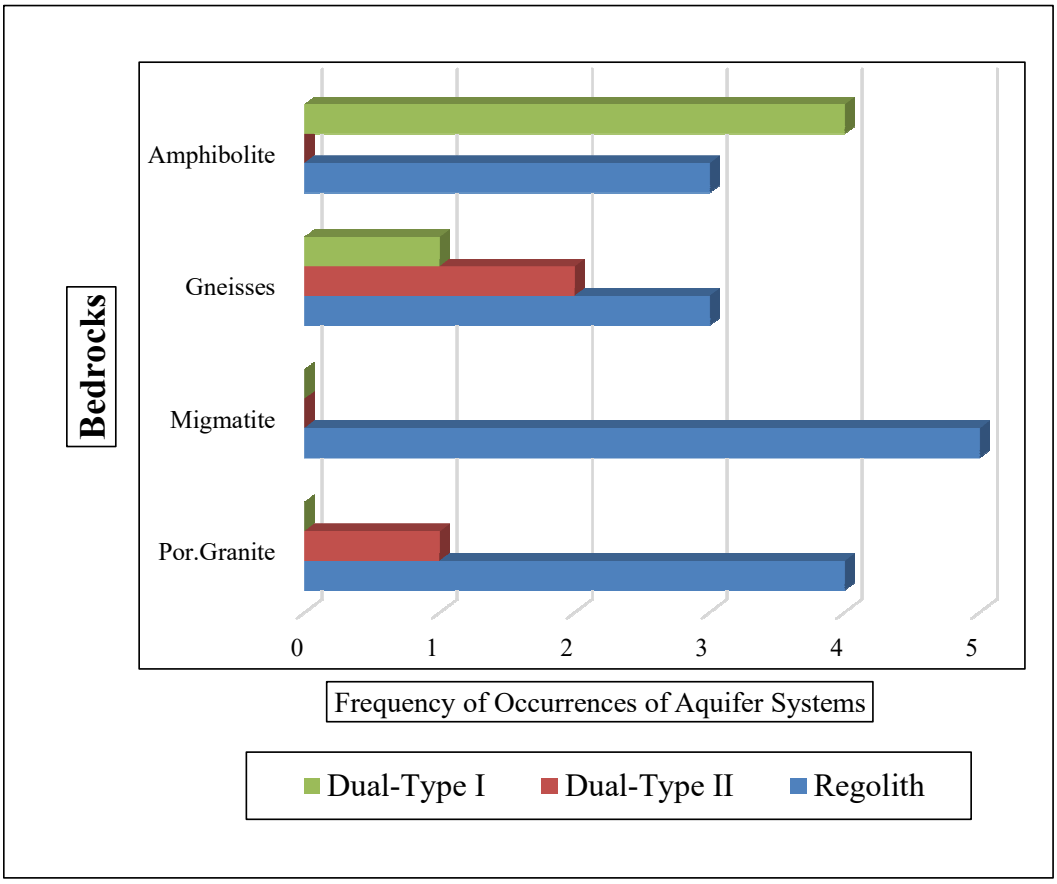

Figure 4.28b: Frequencies of occurrences of Aquifer Systems by bedrock

within amphibolite bedrock (Tables 4.2 and 4.10). Hence, if the well does not penetrate fractured or weathered bedrock, then the only water-bearing zones will be the regolith. This may be the reason why boreholes at Onilado, Sagaun and Itaagbe were the only ones that did not penetrate water-bearing bedrock zones. Also, these three wells were on the same axis (and are neighbouring wells) along the amphibolite and quartzite intercalations axis. The transmissivities of these three wells were less than 1.30 m^2/day, compared to the other four that were grouped under dual aquifer systems with transmissivities range of 11.65 to 10.34 m^2/day (Tables 4.4A & 4.4B).These four wells located at Ajegunle, Pako, and Igboole I and II are regarded as being prolific and groundwater yield is sustainable. This is as a result of good water transmission capacity, characterised by large pumping time without water cessation because of attainment of dynamic equilibrium water level during pumping. Sustainable groundwater supply in these four wells was facilitated by the fact that the wells penetrated fractured zones, and fractured zones are more numerous within amphibolite terrains than other bedrocks within the study area (Table 4.9, Figures 4.25 & 4.26). Additionally, the fine grained matrix component is able to provide a set of confining units for the productive fractured bedrocks, leading to generation of artesian wells (a situation where the groundwater pressure is greater than the atmospheric pressure and the enclosed groundwater in the aquifer rises to the surface and flows freely).

More so, wells tested within terrains underlain by amphibolite have the largest transmissivity of 0.58 to 11.65 m2/day with mean value of 6.85 m^2/day and much larger hydraulic conductivity (av. 28.76 X 10^{-2} m/day), compared to those within other bedrocks terrains (Table 4.10). Additionally, aside the fact that most wells tested in this terrain were found prolific, the wells with the largest transmissivity of 11.65 m^2/day at Ajegunle and the other three wells whose transmissivities are greater than 10.00 m^2/day are found within locations underlain by amphibolite. Hence this bedrock can therefore be regarded as the bedrock that has the highest potential for provision of prolific wells. This observation was also buttressed by both the geophysical and hydro-geomophologic studies presented earlier in this work.

A total number of six (6) wells were tested within areas underlain by gneisses. The two wells located at Alaagba and the one tested at Lamperu were bounded by fresh gneissic bedrocks, with transmissivities ranging from 0.25 to 0.65 m^2/day (Table 4.4B). Those tested at Abola, Apata and Agbede were characterised by dual aquifer systems.

Though, those at Abola and Apata were characterised by less prolific water-bearing bedrock with transmissivities of 2.13 and 1.54 m^2/day respectively. The well at Agbede, is characterised by high-yielding bedrock with transmissivity of 7.23 m^2/day (Table 4.4A). These prolific bedrocks are permeable boundaries.

Drawdowns in dual water- bearing aquifer systems attain dynamic equilibrium water levels at corresponding depths of 10.03m, 14.82m and 22.38m at Agbede, Abola and Apata (Appendix XII). The total transmissivities of these aquifers were 9.30, 2.68 and 2.02 m^2/day respectively. The well at Agbede was not only prolific, but adjudged to be the most productive well tested within gneissic terrains with transmissivity of 9.30 m^2/day and comparatively exceedingly large hydraulic conductivity of 33.00 m/day. Generally, the mean transmissivity and hydraulic conductivity of wells in gneissic terrains were 2.57 m^2/day and 9.61 X 10^{-2} m/day respectively. These values were comparatively lower than the corresponding average values of 6.85m^2/day and 28.76 X 10^{-2} m/day estimated for wells within amphibolite terrains (Table 4.10). The water bearing zones within gneisses bedrock are the most diversify in respect of variations in aquifer system and the dynamic equilibrium water level in these wells were deeper than those in amphibolite terrains in which the equilibrium water level was < 9m except at Igboole II.

Water-bearing zones tested in migmatite bedrock are identical in respect of consistency in aquifer system. All the five boreholes tested within this bedrock were bounded by fresh granitic bedrocks. These wells were associated with fairly large discharge and large change in drawdowns during pumping with average values of 68.27m^3/day and 17.69m respectively (Table 4.10). The large drawdown signifies low groundwater yield. Among other bedrocks that underlain the study area, the water bearing zones in migmatite terrain have the lowest transmission capacity with transmissivities range of 0.56 - 0.91 m^2/day (av. 0.76 m^2/day) and average hydraulic conductivity of 3.73m/day (Table 4.10). Though, in respect of groundwater occurrence potentials, migmatitic terrains were adjudged to have moderate potentials (Figures 4.7 and 4.15).

Contrastingly, in respect of bedrock fractures, 39% of migmatite bedrocks were fractured, second only to amphibolite (Figure 4.26). Hence, wells tested within this terrains are expected to be at least fairly prolific! This conflict is as a result of well locations, which are not sited within migmatite terrains where bedrock fractures are

common. There exists a localised region in SE where there is high frequency of bedrock fractures (Figure 4.25). Generally, the localised fractured bedrock within migmatite terrains were found to cluster within the south-east region and these fractured zones were arranged in a NW-SE trend (Figure 4.25). This prominent bedrock fracture zone on migmatite was within uninhabited region where there are no wells to be tested, except at Sekere village. Even, the well tested at Sekere cannot be said to be prolific though it has the second largest transmissivity and hydraulic conductivity of 0.88 m^2/day and 3.99 m/day among wells tested in migmatite terrains (Table 4.4B). The low yielding attribute of the well at Sekere, despite being sited within fractured zone could either be that the fractured bedrock is narrowly missed or the fractures are dry at Sekere village. This observation is buttressed by the groundwater indication map (Figure 4.4), that showed sparse vegetal response for migmatite terrains. This corroborates the observation within migmatite terrains. Hence, regolith within migmatite terrains either terminate on fresh bedrocks (especially at the NE region characterised by scanty bedrock-fractures) or dry fractured zones at SE locations around Sekere. (Figure 4.25). Other locations with close, but less clustered bedrock fractures were found on gneisses terrain at northwest region.

The granitic bedrocks are largely unfractured and non-weathered, and the weathered overburden terminates on fresh basement, or on a network of unconnected (or dry) fractures. Notably, in granitic bedrock, weathering and bedrock fracturing are least developed (Figures 4.12, 4.13 and 4.25). This is enunciated by the fact that out of the five wells tested within granitic terrains, four terminated on fresh granitic bedrock units. These wells were mostly affected by well-bore storage (stagnant water in the borehole being measured as if representative of water from the aquifer). These wells were also characterized by small recharge.

Well-bore storage affected all pumping tests and are more dominant in the two wells tested at Idere. These wells were characterised by large discharges that were only sustainable over very short period of time between two and five minutes (Table 4.4B). It should also be noted that the weathering products are coarser and are more of sandy units along the N-S geo-electric section (Figure 4.14C). This sandy regolith may facilitate good water transmission but as a result of paucity of bedrock fractures, groundwater discharge is not sustainable.

Notwithstanding, there was one prolific well on granitic terrain at Ayete I. This well penetrated fractured bedrock. Though, the yield of the well is low, the water flows for hours and throughout pumping phase. The transmissivity of the upper regolith aquifer was 2.00 m/day, while that of the permeable bedrock is 0.95 m^2/day. This is because Ayete I is sited in valley incision of the granitic ridges. The low elevation attribute creates lower hydraulic or pressure head that guarantees water influx from higher grounds. The coarse (sandy) regolith unit associated with granitic terrains aids good water transmission in the area.

The widespread occurrences of regolith aquifers is an indication of rarity and localized nature of dual aquifers that are the sustainable water-bearing zones. This is as a result of infrequency of bedrock fractures across the study area (Figure 4.25). Type I-Dual aquifers is the second largest group with 22% occurrence and are mainly associated with amphibolite terrains. Four out of a total of five occurrences of Type I aquifers are within the amphibolite terrains. The remaining one located at Agbede is sited on gneisses bedrock terrain. On the other hand, two out of the three wells that penetrated Dual aquifer –Type II, penetrated gneissic bedrock; while the only one at Ayete I is found within porphyritic granite terrain and this well (Ayete I) is the only sustainable well within granitic terrains and it is characterised by the largest transmissivity value of 2.95 m^2/day. Percentage occurrence of Dual-type II aquifer system is just 13% and the least occurring aquifer system (Figure 4.28a).

Dynamic water level developed in a total number of eight wells during pumping phase. Out of which four were within amphibolite terrains, namely wells at Ajegunle, Pako, Igboole I and II; three were located in gneissic terrains at Apata, Abola, Agbede, and the last one at Ayete I on porphyritic granite bedrock terrains. The locations of these wells were within vicinity marked by deep saprolite layer (Figures 4.12b, 4.14a-c) that terminate on either weathered or fractured basement (Figure 4.25). These zones are marked by moderate to high groundwater potentials (Figure 4.29). Basically, in respect of aquifer sustainability, the only sustainable wells tested on granitic terrain was Ayete I, though it has similar transmissivity compared to those at Idere, there is continuous discharge throughout the length of the pumping period. Wells located at Idere with transmissivities of 2.94 and 1.19 m^2/day for Idere I and II respectively, are not sustainable for large pumping time as Ayete I (Appendix XII). The rates of pumping rapidly decline during pumping at Idere.

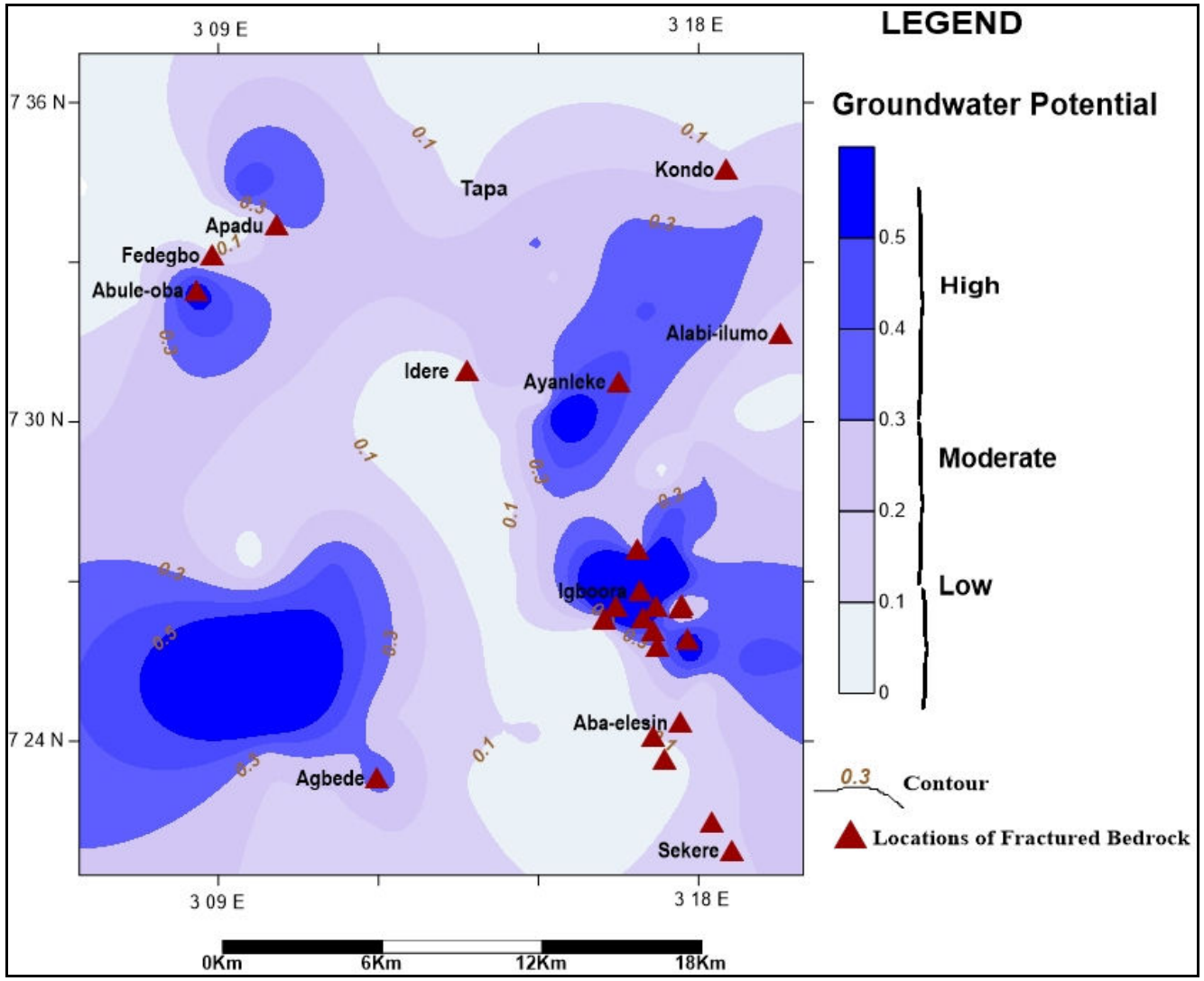

Figure 4.29: Locations of fractured bedrocks on groundwater potential map

Dual aquifer systems are characterised by two distinct time-drawdown curves representing two individual flow regimes or water-bearing zones separated by a transition zone. The upper aquifer system is the thick regolith cover known to have developed upon areas underlain by these bedrocks. The second aquifer zone is a lower permeable zone which represents the dominance water flow from the underneath fractured basement over the thick regolith cover. The second water bearing zones could also be another confined regolith layer disconnected from the upper one by fine grained matrix. In most of the dual- aquifer system, the top aquifers were succeeded by more prolific permeable zone with notable increase in both transmissivity and hydraulic conductivity (Table 4.4A).

Notably, fractured bedrocks are mostly sandwiched within zones interpreted as having high longitudinal conductance due to development of thick fine grained regolith units (Figure 4.29). These zones were located within terrains underlain by amphibolite and gneisses bedrocks, and in locations close to rock contacts. The hydraulic results showed that almost all the wells that developed dynamic water level during pumping and that were adjudged as prolific were found within these zones. This is due to favourable hydrogeological framework discussed earlier. This also showed the important of fractured bedrocks to groundwater sustainability.

Another reason for occurrences of more successful boreholes in amphibolite and gneisses was the hydro-geomorphic situations, whereby waters are drained from the high-lying areas mainly underlain by migmatite and porphyritic granite to low - moderately high-lying regions of amphibolite and gneisses terrains. Hence, migmatite and granitic terrains are more of run-off zones, whereas most terrains underlain by amphibolite and gneisses bedrocks are low-lying to moderately high-lying recharge zones (Figures 4.2). This is buttressed by the good water indication seen within bedrock contacts at Idere in central and at the south-west area.

4.5.2.3 Influence of Hydrological Parameters on Hydraulic Parameters by Bedrocks

The measured and estimated hydraulic parameters included the drawdowns in the well, the water discharge, transmissivity, hydraulic conductivity and specific capacity. However, the discharge and drawdown were directly measured from the pumping test, while other properties were estimated using appropriate analytical models and formula.

Notwithstanding, the transmissivity of aquifer incorporated both the discharge and drawdown in the wells which were measured directly from the field. Hence, the relationships between the aquifer transmissivities and hydrological parameters will also include other hydraulic properties, since other hydraulic properties were ultimately included in or estimated from the aquifer transmissivity. The plots of the transmissivities against hydrological parameters and the type and significance of the relationships in each bedrock (denoted by R) are illustrated and presented in Figures 4.30.

Relationships between the aquifer transmissivities and well elevation are positive in amphibolite and granite, but negative in migmatite and gneisses. The significance of this association is high only in gneisses, moderate in migmatite, low in granite and insignificant in amphibolite (Figure 4.30A). This suggests that the relief of the borehole has no relevant to the aquifer transmissivities in amphibolite, whereas it does in other bedrocks, particularly in gneisses where R = -0.62. This also suggests that the topography of borehole does not significantly influence both the drawdown and groundwater yield within amphibolite bedrock with R = 0.08; but in migmatite these hydraulic properties are moderately influenced by borehole relief with R = - 048, and weak relationships in porphyritic granite with R = 0.27, and strong influences in gneisses bedrocks, where R = -0.62 (Figure 4.30A). The strong and moderate indirect relationships between transmissivities and borehole elevations correspondingly obtained for gneisses and migmatite, (R = - 0.62 and - 0.48) may indicate that wells situated at low-lying areas will be characterised by fairly large transmissivity within these bedrocks, whereas in porphyritic granite where the relationship is low but direct (R = 0.27); high-lying wells may be more prolific. This is corroborated in Idere area on higher relief of >200m where the two tested wells were characterised by large discharge and higher transmissivity of 2.95 and 1.19 m^2/day. Although, these wells were not grouped along with prolific wells since the large discharge falls drastically as pumping continues, and the regolith unit terminate on fresh basement, where there is no water inputs.

Figure 4.30B illustrated the relationships between aquifer transmissivities and borehole depths. The relationships are indirect in gneisses, migmatite and porphyritic granite, while it is positive and moderate in amphibolite. The indirect relationships are low for

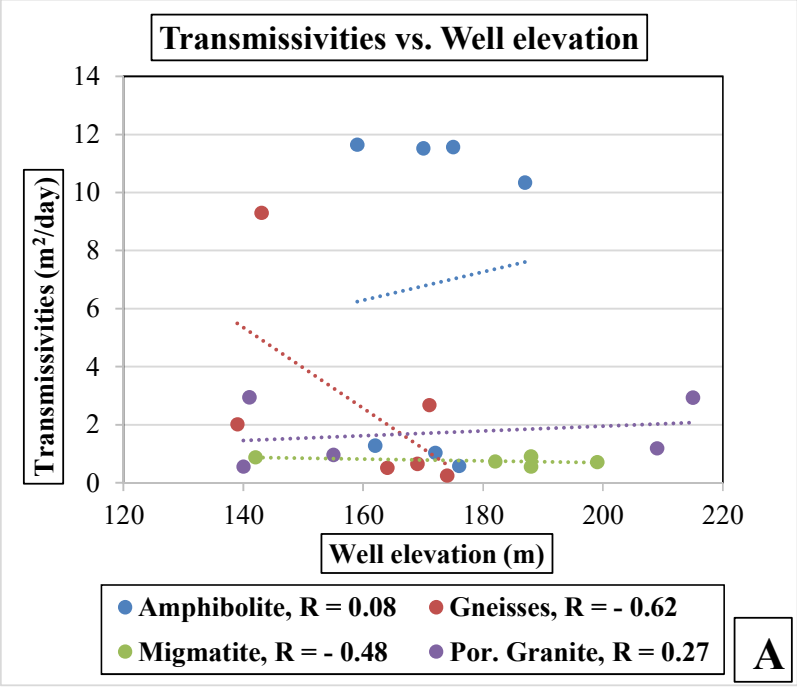

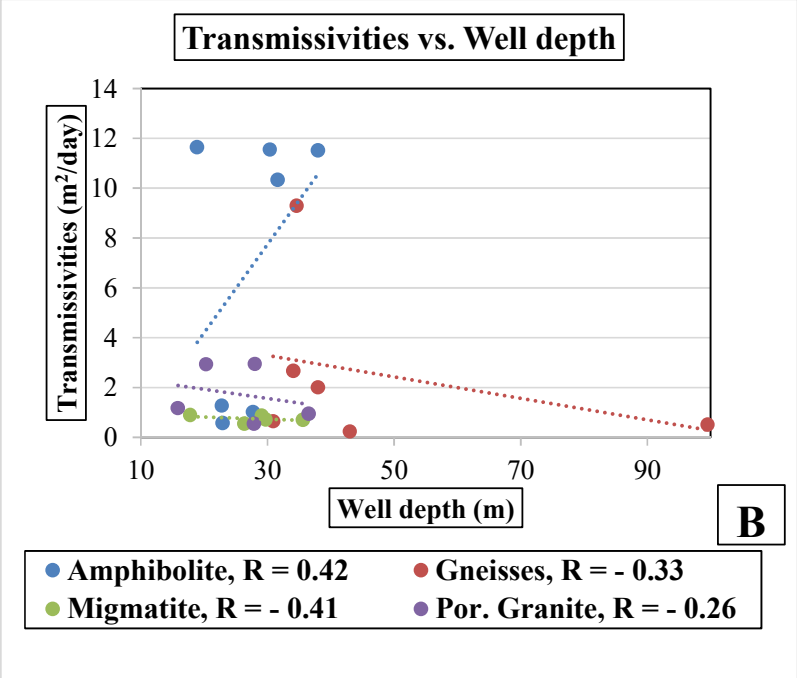

Figure 4.30: Linear relationships between transmissivities of aquifers and hydrological parameters

gneisses with R= - 0.33, and porphyritic granite with R = - 0.26, and moderate for migmatite bedrock with R = - 0.41. This implies that deep wells may not improve hydraulic properties in gneisses, and in por. granite, and to a larger extent in migmatite bedrocks. However, the positive moderate relationships in amphibolite with R = 0.42, indicate that deep boreholes may be more prolific in amphibolite bedrock; This is supported by the fact that amphibolite terrains have more fracture zones occurrences than other bedrocks, apart from the fact that terrains within amphibolite bedrocks are found to be characterised by good weathering development. Also, the prominent occurrences of dual aquifer systems within amphibolite terrains justify this claim. However, a well sited shallow wells may also be prolific. A good example of this insinuation is the well at Ajegunle, which though is the shallowest well (with depth of 18.9m) across the study area (Tables 4.5 & 4.10), but it is regarded as the most prolific well, having the largest transmissivity of 11.65 m^2/day and third largest sustainable discharge of 93.58 m^3/day.

For gneissic terrains, the relationships between the transmissivity and well depth is indirect and the significances is between low to moderate. Normally, terrains underlain by gneisses were notably characterised by deeper boreholes with depth range of 30.90 to 99.50m and an average depth of 46.68m (Table 4.10). The relatively deeper wells associated with gneissic bedrock may be due to rich regolith development associated with gneissic terrain in the study area which encourages deep drilling into the matrix block to increase the saturated column of the boreholes. The linear relationship occurring between the transmissivities of wells in gneissic terrain against the wells' depths is weak and indirect R = - 0.33. This suggested that deep wells in gneissic bedrock terrains may not give large water transmission. This is also strengthened by the fact that gneissic bedrocks gneissic has just a frequency of 26% bedrock fractures as against 44% bedrock fractures in amphibolite (Table 4.9). Hence, it can be said that the development of fractures has greater influence on the transmissivities (or groundwater transmission) of the boreholes than the weathering or regolith development. Additionally, the deepest boreholes at the study area were found at Alaagba on gneissic bedrocks terrain with a mean depth of 71.25m. However, these depths did not improve the water transmission capacity, since the transmissivities of Alaagba I and II were correspondingly 0.25 and 0.55 m^2/day. These values were among the lowest obtained for gneissic bedrocks. Well depths at Alaagba seems to

have exceeded the range of 16.6m to 27.3m (av. 22.5m) for the fracture zones obtainable in gneissic bedrocks (Table 4.9). Comparatively, the range of the well depth of the three prolific wells located at Apata, Abola and Agbede on gneisses terrains was 34m to 36m depth, and these wells were bounded by recharge boundary units that are most likely to be the fracture zones. Hence, there is no guarantee of striking a fracture zone at depth beyond this range on gneissic terrains.

For migmatite bedrock terrains, although these areas have fairly developed fractured zone of 39% (Table 4.9) the relationship is also indirect with R = - 0.41 (Figure 4.30B). Wells available for pumping test in migmatised terrains did not fall within zones marked as having high potential in respect of frequency of basement fractures. Nonetheless, this R value obtained for wells located outside the fractured bedrock zones, is also an indication of the large influence of fractures development on the capacity of an aquifer to transmit water. Fractured zones occurred at an average of 13.7m in migmatite bedrocks (Table 4.9) and borehole depths were between 17.80 to 35.60m at an average of 27.72m (Table 4.10).

Wells tested in granitic bedrock terrains penetrated an average depth of 25.7m, which is shallower compared to 27.47m, 46.68m and 27.72m average borehole depths correspondingly for wells within amphibolite, gneisses and migmatite bedrocks (Table 4.10). First and foremost, the relatively shallower boreholes are are indications of less weathering development and infrequent occurrences of bedrock fractures in porphyritic granite terrains by which most wells terminate on fresh basement. The R relationship between transmissivity and well depths is indirect though it is low (R = - 0.26; Figure 4.30B). This means that transmissivities will decline with increasing well depths to some extent in granitic terrains. This also implies that drawdown will decline and rates of pumping will fall rapidly during discharge as well depth increases. This insinuation was buttressed at Idere where there is sharp drop in discharge and the eventual water cessation in the well as pumping time increases and drawdown in the drops drastically. It should also be noted that only one location has fracture zone development in granitic terrain (Table 4.9 and Figure 4.25) and it is located at a very shallow depth of 5.8m.

The only significant relationship existing between the aquifer transmissivities and the groundwater table in Figure 4.30C is within the amphibolite terrains with R = - 0.52.

This relationship is indirect, and it connotes that groundwater table do influences the yield and the drawdown in boreholes in wells tested within amphibolite bedrock. This means that when the groundwater table is shallow, the transmissivity will be high. Shallow groundwater table is an indication of high aquifer pressure, which is most likely in amphibolite, whereby the regolith units are largely fine grained, and are acting as aquiclude over the fractured bedrock horizon. This creates a confined aquifer system in amphibolite bedrock terrains. Hence, the groundwater system is under hydrostatic pressure and the water is able to rise up above the top of the aquifer, leading to occurrences of artesian aquifers in areas underlain by amphibolite bedrock. There are little significance in relationships between transmissivities and groundwater table for other bedrocks.

In Figure 4.30D, the relationship between the transmissivities of the aquifer and the apparent aquifer thicknesses are negative for migmatite, gneisses and granite, it is however positive and strong for amphibolite with R = 0.68. The level of significance of negative/indirect relationship is however higher and strong in migmatite with R = - 0.63, and lower and weak in porphyritic granite and gneisses bedrocks with R = - 0.20 and – 0 .32 respectively. The contrast in type of and similarity in level of significance of relationships between amphibolite and migmatite can be explained by the aquifer systems occurrences within the two bedrocks. For amphibolite, the degree and extent of occurrences of both the bedrock-fractures and weathering are high, hence there are prominence of dual aquifer system within amphibolite bedrock, whereas all aquifer systems within migmatite are regolith-types. The negative but strong relationship in migmatite (i.e. R = - 0.63) indicated that regolith units alone do not really facilitate favourable hydraulic properties, since these aquifers are characterised by large drawdowns, and eventual water cessation as pumping continues. However, in amphibolite where fractured zones are most abundant and are more clustered, the penetrated wells are characterised by large transmissivities, small drawdowns and attainment of steady-state water level, which ensures large pumping time. The strong and direct association between amphibolite aquifer transmissivities and the apparent aquifer thickness, with R = 0.68 supported this insinuation. This relationship further confirms that fracture bedrocks have more positive influences on the transmissivities of aquifer than mere regolith, and that wells that penetrate fracture zones are more prolific than those within regolith alone.

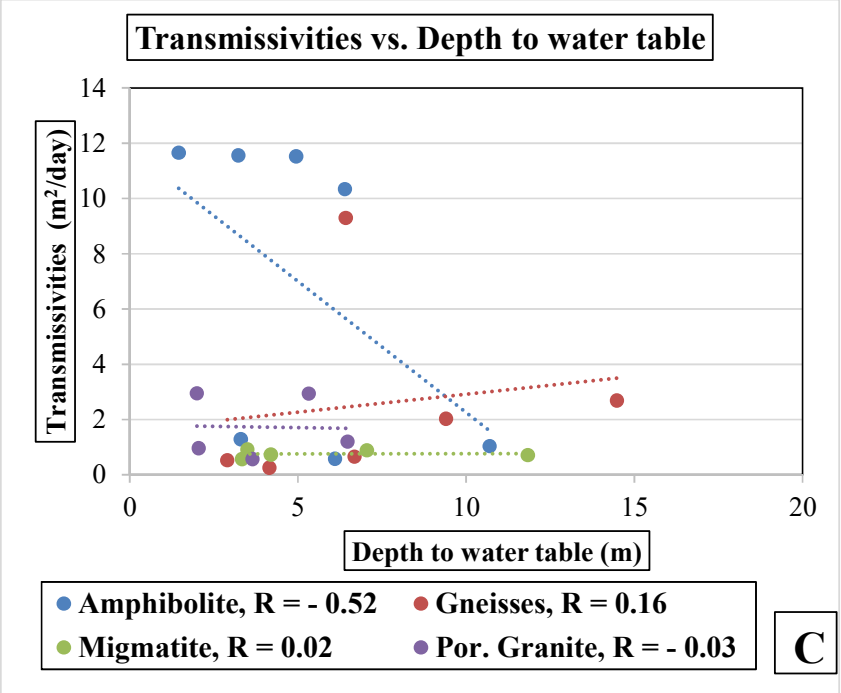

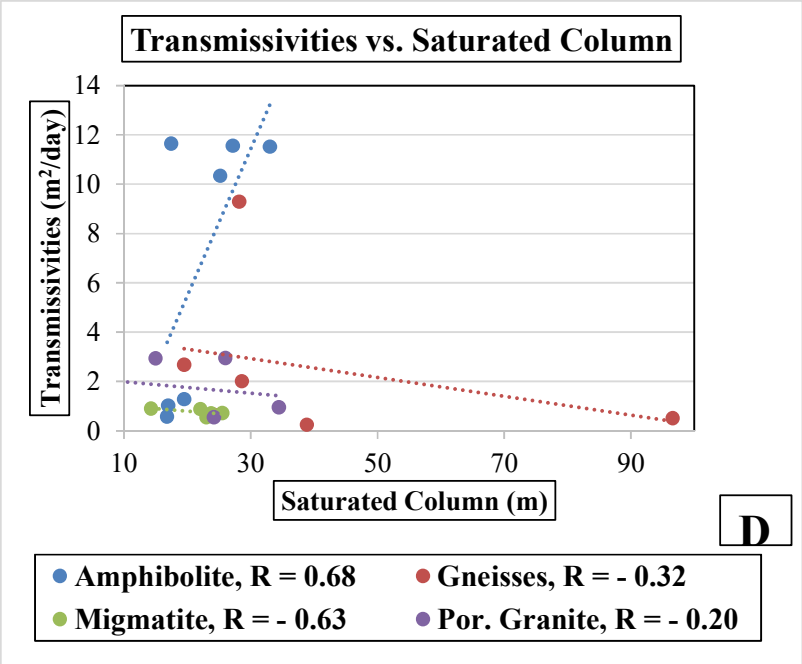

Figure 4.30 cont.: Linear relationships between transmissivities of aquifers and hydrological parameters

Out of all the tested wells, a total number of eight (8) wells at Ajegunle, Igboole II, Igboole I, Pako, Agbede, Ayete I, Abola and Apata with transmissivities of 2.02 – 11.65 (av. 7.75) m2/day (Table 4.4A) are regarded as prolific and sustainable. This is as a result of long pumping time, small drawdown, and development of steady-state water level during pumping period. Each of these wells terminate on recharge boundary that is either fractured or weathered-bedrock. The aforementioned wells are grouped in decreasing values of transmissivities. The first four with the largest corresponding transmissivities values- 11.65, 11.56, 11.52, 10.34 and 9.30m^2/day, were within amphibolite terrains. Wells tested at Agbede, Abola and Apata are sited on gneissic bedrock, while Ayete I is the only prolific well tested on porphyritic granite terrains.

The depths of these prolific wells were mostly within the range of 30 to 38m, except the one at Ajegunle that has a depth of 18.9m. The average depth for these prolific wells is 31.7m. These wells are mainly found in amphibolitic and gneissic bedrocks terrains. However, the depths of wells that terminated on regolith zones were mostly below 30m (Table 4.4B).

From the values of standard deviation (S.D) of transmissivity of water-bearing zones by bedrocks (Table 4.10), the more diverse in aquifer systems within a bedrock, the larger the standard variation (S.D). Hence, S.D values of 5.53 was obtained for amphibolite, since the bedrock has more widespread aquifer system than others. For gneisses and porphyritic granite that were characterised by two types of aquifer systems, i.e regolith and dual–Type II, the S.D were 3.43 and 1.14 respectively. However, migmatite that is characterised by a single aquifer system also has the lowest variation from the mean with S.D. of 0.14. In other word, the S.D of transmissivities of water bearing zones in amphibolite where all the four boundary conditions were represented was the largest whereas, the transmissivities of water bearing zones in migmatite where just one aquifer system (i.e. regolith) was represented (Figure 4.28b) has the least S.D of 0.14. Moreover, the aquifer transmissivities are similar and are much lower in migmatite with av. 0.76 m^2/day, compared to other bedrocks where average transmissivities all exceeded 1.0 m^2/day (Table 4.10).

Additionally, the range of S.D by aquifer categories was 1.03 – 0.48 (Table 4.5), while by bedrocks, S.D spread was 5.53 to 0.14 (Table 4.10). This indicated that variations

from the mean or S.D is lower when the aquifers are grouped by hydraulic affiliation rather than by geological (or rock-type) associations.

Hence, it can be concluded that the degrees of disparities in hydraulic properties are as a result of the level of heterogeneities in respect of rock types, weathering and bedrock-fracturing, as well as variations in hydro-geomorphological units such as the relief, landforms and surface water drainage network across the study area. Also, the aquifer systems are more associated by hydraulic (and hydrogeological) similarities than by mere geological affinity. Although, the geological and geomorphological factors clearly determines the hydrogeological conditions of the water-bearing zones that developed within the basement area of Ibarapa region.

4.5.2.4 Groundwater Recovery and Sustainability

Statistics of the rates of groundwater recharge extracted from Table 4.6 is presented in Table 4.11 and Figure 4.31 is the bar chart illustrating the average rates of recovery for the first two 15 minutes and fro the entire recovery period by bedrocks. It is clearly seen from Figure 4.31 that the rates of groundwater recharge were not uniform from one bedrock to another.

For the entire recovery phase, the rates of groundwater recovery in litre/minute were between 0.62 and 3.68 (av. 1.84), 0.62 and 7.14 (av. 2.63), 1.15 and 3.35 (av. 1.89) and 0.55 and 3.22 (av. 1.72) on amphibolite, gneisses, migmatite and porphyritic granite terrains respectively (Table 4.11). The recovery rates for the entire period was not as wide-ranging as recoveries within the first and second 15minutes, where, there is significant changes in the rates of recharge. Comparatively, the average rates of recharge in litre/minutes for the first 15 minutes and the second 15 minutes by bedrocks were 3.53 and 0.81 in amphibolite, 3.89 and 1.53 in gneisses, 5.59 and 1.73 in migmatite and lastly in porphyritic granite 4.64 and 1.44. This correspondingly represents 435%, 253%, 323% and 322% reduction in recharge rates as recovery time increases from 15 to 30 minutes over these terrains.

Locations with maximum groundwater recharges on each bedrocks were found at Itaagbe, Agbede, Alabi-Oja and Tapa. With the exception of the tested well at Agbede, the wells in other three locations were earlier categorized as being bounded by impermeable geological units and were not expected to have large groundwater

Table 4.11: General statistics for the phases of groundwater recovery and water discharge in the wells for various bedrocks

Bedrock Units	1st recovery phase	2nd recovery phase	Entire recovery phase	Entire discharge
	litre/min	litre/min	litre/min	litre/min
Amphibolite				
min	1.84	0.25	0.62	30.25
max	5.92	1.85	3.68	68.14
mean	3.53	0.81	1.84	50.03
std.dev.	1.67	0.65	1.01	13.39
Gneisses				
min	1.57	-	0.62	22.76
max	5.42	2.89	7.14	54.81
mean	3.89	1.53	2.63	37.12
std.dev.	1.26	1.07	2.28	13.87
Migmatite				
min	2.64	0.57	1.15	29.11
max	9.11	2.70	3.35	69.30
mean	5.59	1.73	1.89	47.41
std.dev.	2.55	0.85	0.87	15.51
Porphyritic granite				
min	1.62	0.15	0.55	31.68
max	8.39	2.43	3.22	63.20
mean	4.64	1.44	1.72	44.66
std.dev.	2.75	1.11	1.01	12.02

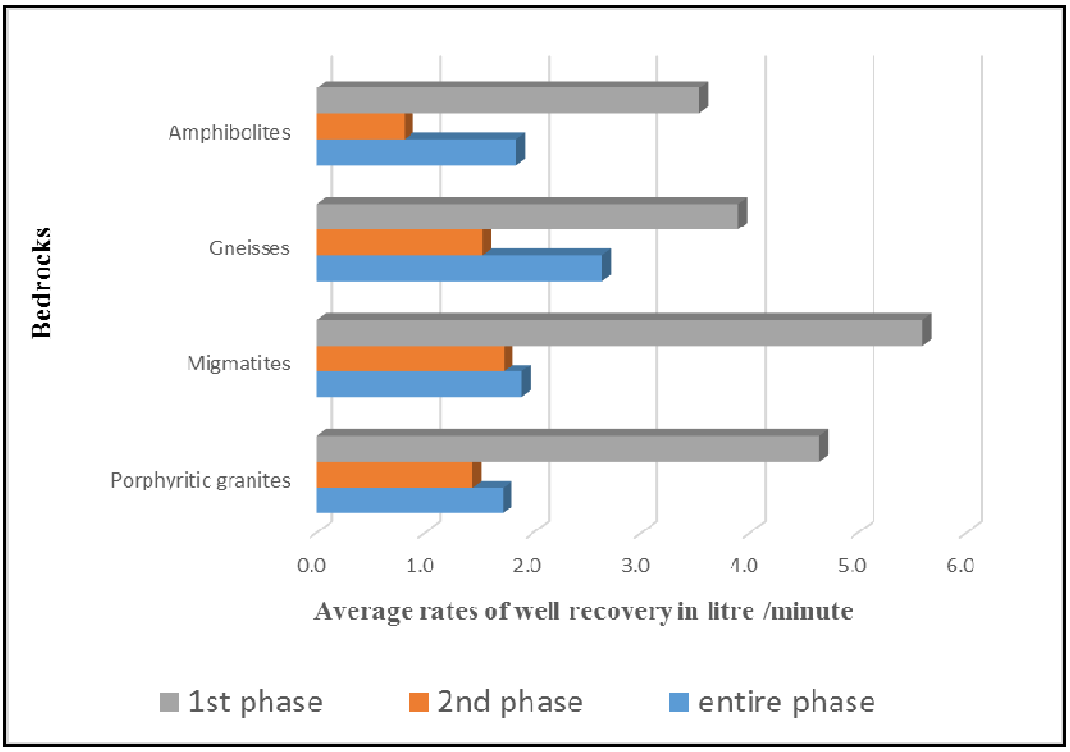

Figure 4.31: Average rates of groundwater recharge at different phases of recovery

recharge. This phenomenon is due to rapid water input from the matrix/weathered units which are known to have high storativity (Chilton and Foster 1995, Singhal and Gupta 1999 and Holland, 2011), but this is not sustainable over long period. So, as recovery progresses, the rates of groundwater recharge decline in most of the wells.

Additionally, eight wells representing, 35% of all tested wells exhibited dynamic water level, whereby the drawdown stabilized during pumping operation (Appendix XII). These wells were regarded as being sustainable (Figure 4.32) and they included all the eight wells that penetrated dual aquifer systems (Table 4.4A). These prolific wells were mainly those that were tested within amphibolite and gneisses terrains.

Only Ayete I is on granitic terrain. Contrastingly, these wells were associated with zones with high total longitudinal conductance (S) characterised by thick fine grained regolith. Notwithstanding, wells at Ayete and Abola were found to lie within terrains classified with moderate groundwater potentials (Figure 4.32). Consequently, the yield and transmissivity values of wells tested at Abola and Apata were correspondingly small, though, it is still sustainable.

On the other hand, all the wells marked as unsustainable (Figure 4.32), were characterised by reducing pumping rates, whereby discharge is not sustainable, which led to water cessation during pumping operations. Notably, these wells included all those categorized under regolith aquifers, which are known to be mostly characterised by transmissivities of <1.0 m^2/day (Table 4.5). Although, many of these wells were characterised by large water discharge at the early pumping time. Groundwater discharge drastically falls as pumping operation continues, which is a clear case of well-bore storage effect, whereby water storage in the well lead to initial good yield that decline with time. Early time-drawdown data does not represent input from the aquifer (Kruseman and de Ridder, 2000). This is also supported by the fact that the rates of discharge are several times higher than the rates of recharge, even in wells that developed dynamic water level during pump operation. The effect of well bore storage was largely reduced in prolific wells that were characterised by longer pumping time in estimating the transmissivity of the well.

Additionally, comparison of recharge with discharge without drawdown input is inappropriate. Hence, it is more appropriate to relate the groundwater recharge to the

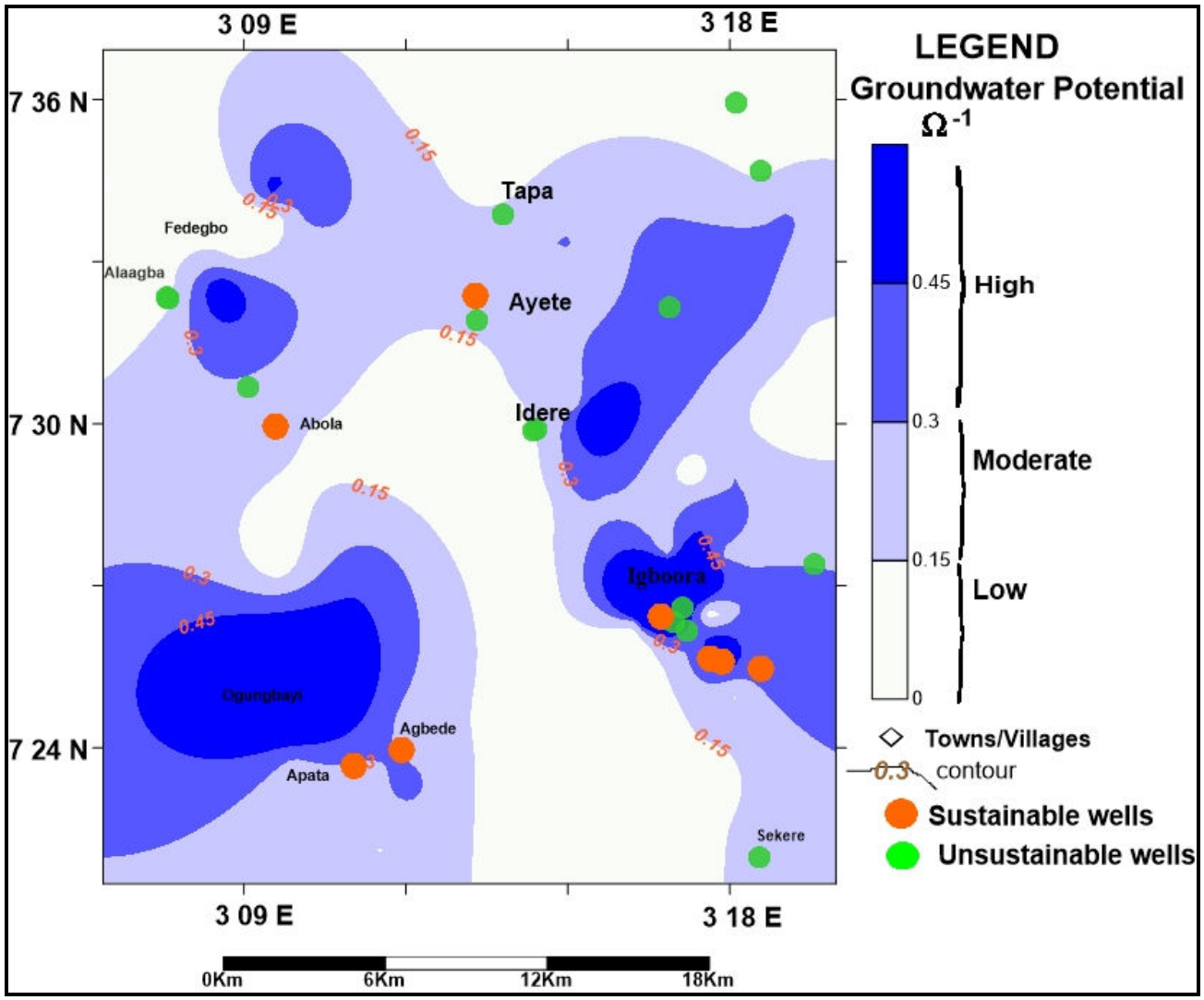

Figure 4.32: Locations of sustainable and unsustainable wells on groundwater potential map

transmissivity of the water-bearing zones which incorporate both the rates of discharge and changes in drawdown during pumping, instead of relating it to discharge alone.

Aside the well bore storage effect, the large deficit in groundwater recharge, compared to discharge (Table 4.11) could also be adjudged to loss of water to the matrix component that surround the well during recovery, since the matrix components that contribute water during discharge also receives water during recovery. The deficit can also be due to the influence of skin during pumping operations. The decline in rates of groundwater recharge during recovery phase as recharge time increases buttressed the fact that water is lost to the matrix components during recovery of wells. Additionally, the occurrence of double porosity water bearing zones where there is abrupt change in water transmission confirms this insinuation. Also, the moderate positive relation existing between transmissivities and discharge for regolith aquifers (Figure 4.21A) depicts that aside the factor of well discharge, there are other factors (mentioned above) that are influencing the rates of discharge and recharge during pumping and recovery operations. Hence, as water rises in the well, recharge rate reduces owing to loss of water to the vadose or matrix zones, which are mostly unconfined and unsaturated.

Generally, most of the water bearing zones in the study area can be described as low transmitting geological units, which may not be able to sustain a continuous water discharge, even by using a low capacity pump of 0.5HP as was the case for the current study. Nonetheless, 35% of the encountered wells were adjudged to be prolific, and based on the locations of these wells, they obviously penetrated fractured bedrocks mostly within amphibolite and gneisses terrains. Other wells that penetrated mere regolith aquifers, were more numerous and are found within all bedrocks terrains. These regolith aquifers, in which about 65% of all tested wells penetrated can best be described as aquitards. The dominant water input is mainly from the regolith. Notwithstanding, these poor water-bearing zones are also being tapped daily to meet water need by the people, despite the fact that groundwater yield is poor within these overburden units, there are no cases of sand-pumping during pumping operations. Lastly, bedrock-fractures are the facilitators of development of dynamic water level that ensures good water transmission over long pumping time.

4.5.2.5 Groundwater Recharge Potential and Hydraulic Parameters

From the hydraulic characterisation, most areas underlain by amphibolite and gneisses were within terrains of moderate to high groundwater potential. This is as a result thick overburden units. Also, the landforms are low-lying landform and are characterised by sustainable wells that have good yield in most cases. However, previous works (Oladapo, and Akintorinwa, 2007; Jayeoba and Oladunjoye, 2013) ascribed high longitudinal conductance to zones with poor potential for groundwater as a result of coarseness of regolith units alone without recourse to the bedrock resistivity. This phenomenon could be explained from the formula for estimating the total longitudinal conductance (S) from which the recharge potentials are derived. Total longitudinal conductance presented in Appendix IX is derived from the summation of the ratios of respective layer's thickness and its corresponding resistivity in a geo-electric sequence. The bedrock resistivity being the infinity layer has unquantifiable thickness, hence it is not among the factors that define the longitudinal conductance from which the recharge potential of each VES point is described. . For the present work, areas with thick clayey overburden units and high S values are those characterised by more fractured bedrocks (Figure 4.29) that prominently influence the sustainability of groundwater. The hydraulic characterisation also revealed that fractured bedrocks are dominant transmitting medium for groundwater. They are more determinant factor of groundwater sustainability than the overlying regolith units in basement areas of Ibarapa region. This studies also indicated that basement crusts that are characterised by thick clayey-silty regolith units are more likely to terminate on fractured bedrocks.

This present work also revealed that the overburden units may not be the main or dominant passage for groundwater recharge. Rock contacts are also paramount channel of water infiltration within the basement terrains of Ibarapa region. This is corroborated by good groundwater indication expressions from the geomorphological studies (Figure 4.7). It is also possible to have subsurface fractures pathways within the overburden units in amphibolite and gneisses through which water seeps or recharges the bedrocks when they are fractured or weathered. In amphibolite terrains these subsurface groundwater fractures pathways possibly inter-connect with those from the neighbouring high-lying run-off zones at the NE migmatite bedrock terrains characterised by good lineament features and coarser regolith overburden units

(Figures 4.2, 4.4, 4.5, 4.7 and Table 4.1) that aid vadose water transmission. More so, the fine grained regolith may also be involved in the process of groundwater recharge. This is evidenced by the occurrences of dual porous aquifer system within amphibolite and gneisses terrains, which indicated that there is active water transmission within the regolith units as well. It is also an indication of the importance of the occurrences of fractured bedrocks for safeguarding sustainable groundwater supply in basement areas. On the other hand; for gneissic terrains at the western axis, there are evidences of water seepage into the subsurface along the channel of the major River (Ofiki) that drains those locations, and this River runs through the rock contact between gneisses and porphyritic granite at the central axis of the study area (Figure 1.4). More so, the regolith at the NE region on gneisses terrains are sandy and coarser than other regions within this bedrock units, and the longitudinal conductance is low (typifying high recharge potential (Figure 4.15), hence; the conspicuous groundwater occurrence along the main lineament (NNW trending) in this area (Figure 4.7) is an indication of the importance of porous overburden in groundwater development in basement area as well. Lastly, areas with thick fine grained regolith units are associated with clustered or diverse groundwater occurrences. These zones included portions along rock boundaries at Idere at the central region, Igboora at the SE region, and gneissic terrains at the SSW location of the study area.

4.5.2.6 Conceptual Model for the Hydrogeological Settings of Water-Bearing Zones across the Study Area

The overall theoretical model of the hydrogeological situations of water-bearing zones within the study area can be categorized into four major groups as illustrated in Figure 4.33. Water-bearing zones in groups A and B are regolith aquifers, and their hydrogeological settings cannot sustain their respective discharges over long pumping period. However, in group B, the seven wells were characterised by large groundwater discharge greater than $70m^3$/day and the yield is sustainable for not more than eight (8) minutes. The transmissivities of the wells are mostly greater than $1.0m^2$/day. However, the initial large discharge from group B aquifers fell as pumping continues. Contrastingly, the transmissivities of wells in group A aquifers were mainly below $1.0m^2$/day with associated lower groundwater yields of less than $60m^3$/day. However, group A aquifers are characterised by longer pumping periods that ranges between 9 to

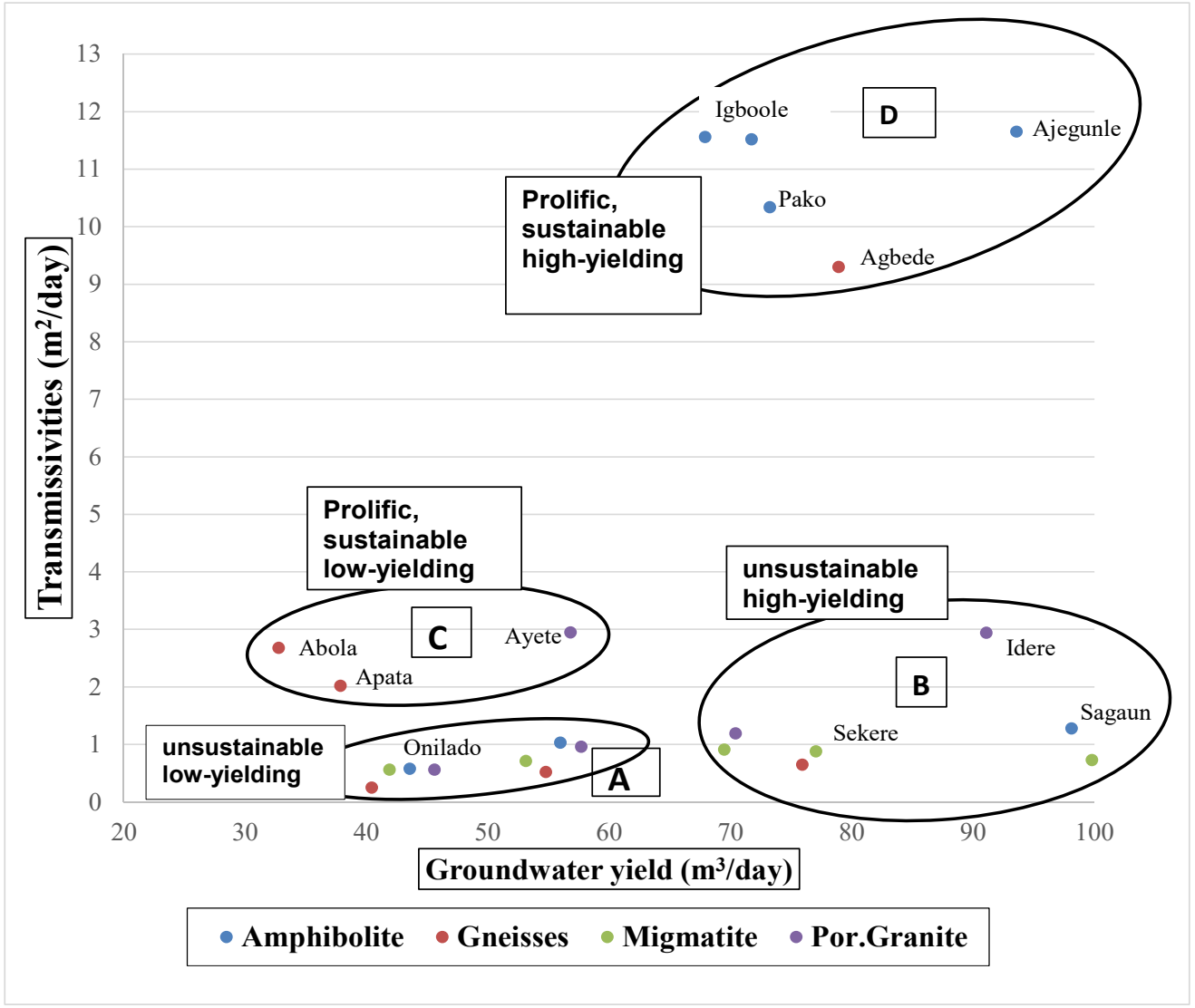

Figure 4.33: Major conceptual hydrogeological models with variations in water-bearing attributes across the various bedrock terrains in the study area

20 minutes before water cessation. Regolith aquifer systems are more widespread across all the bedrock settings, though they are mostly associated with terrains underlain by migmatite and porphyritic granite.

The hydrogeological settings of eight aquifers in groups C and D sustained continuous groundwater yield for hours of pumping. However, three out of these eight aquifers in group C (Figure 4.33) were characterised by an average groundwater yield of 42.49m^3/day and mean transmissivity of 2.55m^2/day (Table 4.5). Though the groundwater yields in these three wells (that were tested at Abola, Apata and Ayete I) were sustainable, the yields are lower, compared to those in group D. Group D aquifers were characterised by larger transmissivities with an average value of 10.87m^2/day and relatively larger yields greater than 67m^3/day.

The hydrogeological attributes of the four aquifer models (Figure 4.33) can be represented under four hydrogeological settings illustrated in Figure 4.34 with four representative Wells labelled as A, B, C, and D. Typically, the hydrogeological settings of Well A and B are mainly regolith (or weathered-overburden unit) that terminated on un-fractured and fresh bedrocks. This hydrogeological setting is attributed to group A and B models in Figure 4.33. Nonetheless, in Well B (Figure 4.34), the regolith aquifer terminate on fairly weathered bedrock (or saprock) with little water input. This stands for regolith wells that are characterised by either larger or lower yields that are still unsustainable. This is typical of aquifers in models A and B (Figure 4.33).

Conversely, Wells C and D were those that penetrate dual aquifer systems, characterised by two distinct aquifer zones. These aquifer zones are the overburden layer (i.e. the regolith units), succeeded by water – bearing bedrock units. The latter aquifer i.e. the bedrock can either be weathered as in Well B; and/or fractured as in Wells C and D. However, in well C, the bedrock fractures are less dense, compared to Well D that is characterised by denser and more prolific bedrock fractures. Conclusively; in the study area, Wells A and B are representatives of wells that mostly penetrated migmatite and granitic bedrocks, with water bearing regolith units, whose yields are not sustainable either when large or low. These aquifers can only sustain short pumping period, which may be lengthened when the bedrock is slightly

weathered, whereas Wells C and D are mostly typical of wells that penetrated fractured amphibolitic and gneissic bedrocks, with varying degrees of water – bearing capacities depending on the density and interconnectivity of bedrock fractures.

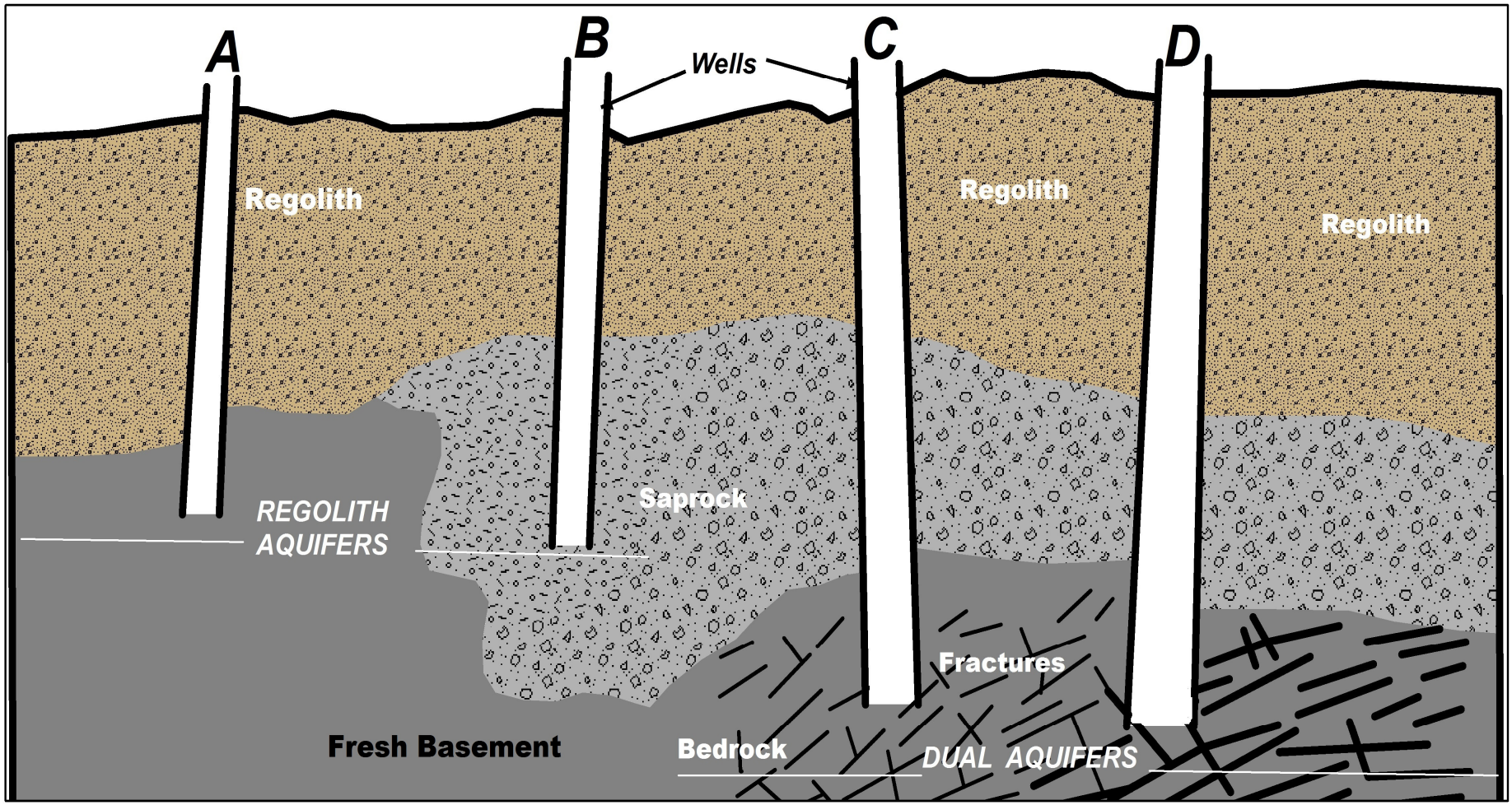

Figure 4.34: Major hydrogeological settings across the study area

CHAPTER 5

5.0 CONCLUSIONS AND RECOMMENDATIONS

5.1 Conclusions

The hydrogeology of the crystalline basement aquifers of part of Ibarapa area of SW-Nigeria has been characterised using four methods. These methods included geological, geomorphological, geophysical and hydraulic investigations.

The entire Ibarapa region is underlain by crystalline basement rocks of Precambrian age. Notably, the main bedrocks mapped in the study area included, the migmatite-gneiss complex and the Older Granite series. The migmatite-gneiss complex comprises biotite gneisses, the massive and schistose amphibolite, migmatite, and augen gneiss. Also, included are the Older Granite series that is made up of the porphyritic granite and the medium grained biotite granite.

Potentials for groundwater occurrence are diverse across the study area as a result of heterogeneity in underlying bedrock, structural complexity and topographical variations. Terrains underlain by porphyritic granite that were associated with lots of short-length fractures have low groundwater potential. This is due to associated elevated landforms of ridges and inselbergs with related adjacent valley. Also, the granitic highlands were characterised by mainly less persistent fractures with variable fracture orientations that aided high surface water run-off and low water seepage. Major towns underlain by porphyritic granite are Tapa and Ayete. Nonetheless, zones of bedrocks contacts at Idere showed a fairly high potential for groundwater occurrence. However, the orientation of water-bearing fractures is not uniform. For areas underlain by gneisses, fractures with groundwater are aligned along the strike of the bedrock foliation at the north-west region, while the south-west gneissic terrain is characterised by scanty but more penetrative fractures. Migmatite bedrock terrain at the north-east part has the second largest fracture development in the area (after

porphyritic granite terrains). However, the fractures are not productive as noted in granitic terrains. The poor occurrences of groundwater in migmatite and porphyritic granite terrains, despite high fracture density is related to associated elevated landforms of these terrains, characterised by high run-off and low water infiltration as a result of steep slope. However, there are evidences of water-bearing fractures within terrains underlain by amphibolite that underlie most parts of Igboora town and areas underlain by gneissic rocks.

The fair representation of water-containing fractures on amphibolite and gneisses terrains is not due to associated low elevation landform alone. It is also as a result of thicker occurrences of regolith units within these terrains. Regolith units are similarly thick on terrains underlain by amphibolite and gneisses and the corresponding average regolith thicknesses were 18.23m and 18.49m. On the other hand, weathering is comparatively less pronounced within terrains underlain by porphyritic granite and migmatite with corresponding average regolith thickness values of 12.77m and 11.29m. Nevertheless, the degree of weathering can be said to be generally fairly high across the study area. The average regolith thickness is greater than 15m and accordingly, the saprolite units can be exploited for groundwater.

Bedrock-fractures are much less evenly distributed across the study area. Basement fractures occurred in just twenty-four (24) locations, which is just about twenty-eight (28) percent of all the geo-electric soundings conducted across the areas. About sixty-seven (67) percent of bedrock-fractures were found localised at the south-east region underlain by amphibolite, and near zones of bedrock contacts within migmatite terrains. Bedrock-fractures occurred at an average depth of about 18m across the study area. On amphibolite and gneisses terrains, bedrock-fractures occurred at deeper zones with corresponding average depths of 18.3m and 22.5m. Bedrock-fractures are almost completely absent in granitic terrain.

The relevance of bedrock-fractures and rock decomposition to generation of sustainable groundwater yield in basement crust were largely demonstrated by the results of hydraulic characterisations of the aquifer systems. Groundwater table occurred at an average depth of 5.64m below the ground surface and the aquifers supplied an average of 64.69 m^3 of water per day. The average total drawdown in the wells was 16.23m. The average transmissivity and hydraulic conductivity were

correspondingly 3.29m^2/day and 14.34 X 10^{-2} m/day. Thirty-five percent (eight wells) out of all the tested wells developed dynamic equilibrium water level during pumping operation at various drawdowns ranging from 5 to 22.4m (av. 12.68m). The aquifer systems of these eight (8) wells were regarded as sustainable due to higher yield, attainment of dynamic equilibrium level, low drawdown during pumping and continuous groundwater flow without water cessation for hours of pumping. These viable aquifer systems were mainly dual aquifers characterised by two distinct water-bearing zones that included an upper regolith unit and an underlying fractured or weathered bedrock. These prolific wells were mainly found in zones adjudged to have high to moderate potentials for groundwater as a result of occurrences of thick overburden units overlying fractured or weathered bedrocks. These dual productive aquifers were mainly localised within terrains underlain by amphibolite and gneisses bedrocks.

The occurrences of eight dual aquifer in the study area reflected the relevance of the weathered layer in groundwater storage and transmission in basement terrains. Most of the very high-yielding dual aquifers were found in amphibolite terrains with transmissivities greater than 10m^2/day, while the low-yielding prolific aquifers with an average transmissivity of 2.55m^2/day were associated with gneissic bedrock. Groundwater yield was over 77m^3/day in high-yielding aquifers, whereas it was less than 50m^3/day in low-yielding aquifers. The water-bearing zones tested within migmatite and porphyritic granite terrains were mainly regolith aquifers that terminated on fresh basement and the yields are not sustainable over long period of pumping. Additionally, rate of water recovery was fastest in gneissic aquifers with 2.63litre/minute and least in granite with 1.72 litre/minute.

The sustainability of groundwater is aided by bedrock-fractures and this limits groundwater prospect as a result of localised occurrences of fractured bedrocks across the study area. Notwithstanding, weathering development is more spatially distributed, and the regolith unit can provide an alternative to groundwater supply, even where bedrock-fractures are absent. Nevertheless, successful groundwater prospect of the weathered layer will depend on recurrent and adequate meteoric recharge during rainy season between the months of March and October in the study area.

The hydrogeological conditions are not totally consistent (even in same bedrock terrains); though, to some extent bedrock has influence on the hydrological and hydraulic parameters. However, this research has shown that there is more similarity in hydraulic attributes of same hydrogeological settings than there is in aquifer systems of similar bedrock. This is as a result of heterogeneities in weathering characteristics, fracture attributes and landform situations. Therefore, the complexities in geology and structural settings of Basement Complex also have bearing effects on the hydrogeological situations of the study area.

In conclusion, variance in weathering and discrepancies in bedrock-fracture as well as the physiography of the land surface are the prominent factors that influence groundwater occurrences across the study area of Ibarapa region in south-western Nigeria. These factors control the hydrogeological settings of the aquifer system, though the underlying bedrocks also regulate the heterogeneities of rock weathering and basement fractures.

5.2 Recommendations

Based on the study of the hydrogeological characterisation of the crystalline basement aquifer systems of Ibarapa region, the following recommendations are made.

1. Hundreds of boreholes have been sited within the study area. Igboora and its adjoining settlements alone have probably over two hundred boreholes. These individual wells, particularly the prolific ones that penetrated fractured bedrocks can be connected to provide town water supply for the entire Ibarapa region. This will ensure even distribution and judicious utilisation of groundwater system for the entire Ibarapa region, including areas characterised by poor groundwater potential like Ayete and Tapa.

2. Alternatively, since the average regolith thickness across the study area is >15m, groundwater may also be exploited from the overburden units (through hand dug wells) in areas with poor groundwater potential. Although, water yield may be low, there will be fair provision of water supply in low yielding aquifers if discharge is controlled. The yield will improve from meteoric recharge during the recurrent rainy season.

3. More so, the fact that aquifer zones are largely semi-confined, the enclosed groundwater is vulnerable to contamination from the surface environment. Hence; the need for groundwater quality assessment in the area. This is not just important for domestic utilisation of groundwater, it is also necessary when the water is employed for agricultural purposes. Therefore, biological and physico-chemical analyses, as well as studies of the sodium adsorption ratio (SAR) and other water quality related investigations should be carried out to know the worth of the groundwater for each utilisation.

4. Lastly, the recording and documentation of pre-drilling and drilling data particularly borehole logs are helpful in maintaining the existing groundwater facilities and in developing future groundwater development. These data are also essential for academic purposes like the present work. Unfortunately, these data, which are to be supportive materials for the present study were not available- not even in the archives of the government agencies saddled with this responsibility. Therefore, there should be enforcement of the collation, reporting and documentation of every borehole data by the appropriate agencies. Hydrogeologists or experienced geologists should be employed for this duty.

REFERENCES

Abimbola, A.F., Tijani, M.N. and Nurudeen, S.I. 1999. Some aspects of groundwater quality in Abeokuta and its environs, southwestern Nigeria. *Water resources- Journal of NAH* 10: 6-11.

Abiola, O., Enikanselu, P. A. and Oladapo, M. I. 2009. Groundwater potential and aquifer protective capacity of overburden units in Ado-Ekiti, southwestern Nigeria. *International Journal of Physical Sciences* 4.3: 120-132. Retrieved May 18, 2011, from http://www.academicjournals.org/IJPS.

Acworth, R. I. 1987. The development of crystalline basement aquifers in a tropical environment. *Quarterly Journal of Engineering Geology* 20: 265-272.

Akanbi, O. A. 2016. Use of vertical electrical geophysical method for spatial characterisation of groundwater potential of crystalline crust of Igboora area, southwestern Nigeria. *International Journal of Scientific and Research Publications* 6.3: 399-406.

Ako, B. D., Adeniyi, F. I. and Adepoju, J. F. 1990. Statistical tests and chemical quality of shallow groundwater from a metamorphic terrain, Ile-ife/Modakeke, SW. Nigeria. *Journal African Earth Sciences* 10.4: 603-613.

Alley, W. M., Reilly, T. E and Franke, O. L. 1999. Sustainability of groundwater resources. U.S Geological Survey Circular 1186.

Alile, O. M., Amadasun, C. V. O. and Evbuomwan, A. I. 2008. Application of vertical electrical sounding method to decipher the existing subsurface stratification and groundwater occurrence status in a location in Edo North of Nigeria. *International Journal of Physical Sciences*. 3.10: 245-249. Retrieved May 18, 2011, from http://www.academicjournals.org/IJPS.

Aweto K.E. 2011. Aquifer vulnerability assessment at Oke-Ila area, southwestern Nigeria. *International Journal of the Physical Sciences* 6.33: 7574-7583. Retrieved Jan. 17, 2012, from http://www.academicjournals.org/IJPS.

Banks, D., Solbjorg, M. L., and Rohr-Torp, E. 1992. Permeability of fracture zones in a Precambrian granite. Q. J. Eng. Geol. 25. 377-88.

Barker, J. A.1988. A generalized Radial flow model for hydraulic tests in fractured rock. *Water resources Res*., 24 .10: 1796-1804.

Bhattacharya, P. K. and Patra, H. P., 1968. Direct current geo-electric sounding principles and interpretation, Elsevier, Amsterdam.

Bobba, A. G., Bukata, R. P. and Jerome J. H., 1992. Digitally processed satellite data as a tool in detecting potential groundwater flow system. *Journal of hydrology*, 131:25-62.

Carlsson, L., and Carlstedt, A. 1977. Estimation of transmissivity and permeability in Swedish bedrock. Nordic Hydrology, 8, 103-16.

Carvalho, J. M., 1993. Mineral and thermal water resources development in the Portuguese Hercynian Massif in Mem. 24th congress of IAH, Oslo, pp.548-61.

Chilton, P. J. and Smith- Carington, A. K. 1984. Characteristics of the weathered basement aquifer in Malawi in relation to rural water supplies. Symposium on Challenges in African hydrology and water resources. IAH Series Publ., 144:15-23.

Chilton, P. J. and Foster, S. S. D. 1995. Hydrological characterization and water supply potential of basement aquifers in tropical Africa. *Hydrogeology*, 3:36-49.

Cook, P. G., 2003. A guide to regional groundwater flow in fractured rock aquifers. Seaview Press, Adelaide, Australia.

Cooper, H. H. and Jacob, C. E.1946. A generalized graphical method for evaluating formation constants and summarising well field history. American Geophysical Union Transactions, 27: 526-534.

Dada, S. S., 1998. Crust-forming ages and proterozoic evolution in Nigeria: a reappraisal of current interpretations. *Precamb. Res*.87: 65- 74.

Daly, M., Faniran, A. and Areola, A. 1981. The Ibarapa planning atlas- Problems of rural development in Ibarapa division, Oyo state, Nigeria. Tech. Rpt. No. 1. Department of Geography, University of Ibadan.

Danskin, W. R. 1998. Evaluation of hydrologic system and selected water management alternatives in the Owens valley, California: USGS water-supply paper 2370, 175p.

Daubree, A. 1887. Les eaux souterraines, aux epoques anciennes et a l'epoque actuelle. Paris, Dunod, 3 vols.

David, L. M. 1988. Geo-electric study of shallow hydrogeological parameters in the area around Idere, south-western Nigeria. PhD thesis. Dept. Of Geology. University of Ibadan. Xvi + 279pp.

Davis, S. N. and DeWeist, R. J. M. 1966. *Hydrogeology*. John Wiley and Sons: New York.

De Wiest, R. J. M., 1964. Educational facilities in groundwater hydrology and geology. Groundwater, 2:18-24.

Driscoll, F. G. (1986) Groundwater and Wells, 2nd edn, Johnson Division, St Paul, Minnesota.

Dustan, W. R. 1910a. Southern Nigeria. Report on the results of the Mineral survey, 1905-6. Colonial Reports- Misc., No. 67.

Dustan, W. R. 1911. Southern Nigeria. Report on the results of the Mineral survey, 1907-8. Colonial Reports- Misc., No. 76.

Edet, A. E., Okereke, C. S., Teme, S. C., Esu, E. O. 1998. Application of remote-sensing data to groundwater exploration: a case study of the Cross River State, southeastern Nigeria. Hydrogeology Journal 6, pp. 394–404.

Edmunds, W. M., and Smedley, P. L. 2005. Fluoride in natural waters essentials of medical geology. Alloway, B.J., and Selinus O. eds. Elsevier 301-329.

Egboka, B. C. E. 1987. Water resources problem of Enugu area, Anambra state, Nigeria. I.AH.S. 153: 119- 125.

Ellyett, C. D. and Pratt, D. A. 1975. A review of the potential applications of remote sensing techniques to hydrogeological studies in Australia, AWRC, Tech Paper No.13, 147pp.

Fashae O. A., Tijani M. N., Talabi A. O., and Adedeji O. I. 2014. Delineation of groundwater potential zones in the crystalline basement terrain of SW-Nigeria: an integrated GIS and remote sensing approach. Appl Water Sci. 4: 19-38.

Fetter, C. W. 2007. Applied hydrogeology. Second edition. Merrill Publishing Company, USA.

Freeze, R. A. and Cherry, J. A. (1979). Groundwater, Prentice Hall, Englewood Cliffs, New Jersey.

Gonthier, G. J., 2009. Conceptual model of groundwater flow in fractured crystalline rock- a case study based on constant discharge tests at a U.S. Air force plant 6, Marietta. *Proceedings of the Georgia Water Resources Conference*. 27-29th April, 2009.

Granados-Olivas, A. and Corral Diaz, R. 2003. Fracture trace and alignment analysis for groundwater characterization. *Hydrology of Mediterranean and Semiarid regions*. IAHS Publ. 278 (Montpellier Symposium), pp. 24–28.

Gringarten, A.C. and Ramey, H.J. 1974. Un-steady state pressure distribution created by a well with single horizontal fracture, partially penetrating or restricted entry. Trans. Am. Inst. Min. Eng. 257:413-426.

Gustafson, G. and Krasny, J. 1994. Crystalline rock aquifers: Their occurrence, use and importance. *Applied hydrogeology*, 2:64-75.

Hamil L. and Bell, F. G.1986. Groundwater Resources Development, Britain Library Cataloguing in Publication. Data London. pp. 151 – 158.

Hantush, M. S., 1964. Hydraulics of wells. In: V.T. Chow (editor). Advances in hydroscience. 1: 281-432. Academic press.

Hazell, J. R. T., Cratchley, C. R. and Jones, C. R. C. 1992. The hydrogeology of crystalline aquifers in northern Nigeria and geophysical techniques used in their

exploration. E. P. Wright and W. G. E. Burgess (eds) Hydrogeology of crystalline basement aquifers in Africa. Geological Society Special Publ. No. 66, pp 155–82.

Healy, R. W., Winter, T. C., LaBaugh, J.W. and Franke, O.L. 2007. Water Budgets-Foundation for effective water resources and environmental Management; USGS Circular 1308:90p.

Heilman, J. L. and Moore D. G. 1981. Ground water applications of the heat capacity mapping mission. Satellite hydrology. *Proceedings of the 5th Annual William T. Pecora Memorial Symposium on Remote Sensing*. 10 – 15th June 1979. Sioux Falls, South Dakota. 446–49.

Heath, R. C. 1983. Basic groundwater hydrology. USGS water supply paper 2220:84p. Denver, C.O.

Holland, Martin 2011. Hydrogeological characterisation of crystalline basement aquifers within the Limpopo Province, South Africa. PhD Thesis. Department of Geology, University of Pretoria. Xiv + 163p.

Houston, J.F.T. and Lewis, R.T.1988. The Victoria province drought relief project, II. Borehole yield relationship. *Ground Water* 26.4: 418- 426.

Jayeoba A., and Oladunjoye, M. A. 2013. Hydro-geophysical evaluation of groundwater potential in hard rock terrain of southwestern Nigeria. RMZ- Materials and Geo-environment 60:271-284.

Jones, M.J. 1985. The weathering zone aquifers of the Basement Complex areas of Africa. *Quarterly Journal of engineering Geology* 18: 35-46.

Jones, H. A. and Hockey, R. D. 1964. The geology of part of south-western Nigeria. Bull. Geol. Surv. Nigeria, No.31.

Koefoed, O. 1979. *Geosounding principles I: Resistivity sounding measurements*. Amsterdam: Elsevier Scientific publ.

Kruseman, G. P. and de Ridder, N. A. 2000. *Analysis and evaluation of pumping test data*. 2nd edition. Wageningen: International institute for land reclamation and improvement.

Lattman, L. H. 1958. Technique of mapping geological fracture traces and lineaments on aerial photographs. *Photogrammetric Engineering* 24: 568–76.

Lattman, L. H. and Parizek, R. R. 1964. Relationship between fracture traces and the occurrence of groundwater in carbonate rocks. *Journal of Hydrology* 2: 73–91.

Leblanc, M, Leduc, C., Razack, M., Lemoalle, J., Dagorne, D.and Mofor, L. 2003. Applications of remote sensing and GIS for groundwater modelling of large semiarid areas; example of Lake Chad Basin, Africa. *Proceedings International symposium on Hydrology of the Mediterranean and Semiarid Regions*, *2003*. Montpellier: IAHS Publ. (Red Book) No.278. 186 – 92.

Maillet, R., 1947. The fundamental equation of electrical prospecting. *Geophysics* 2: 529-556.

Morris, D. A. and Johnson, A. I., 1967. Summary of hydrogeological and physical properties of rocks and soil materials as analysed by the hydrogeologic laboratory of the U.S. Geologic survey 1948 – 1960. U.S Geol. Survey. Water supply paper, 1839-Dp. 42.

Orellana, E. and Mooney, H. M., 1966. Master Tables and curves for vertical electrical sounding over layered structures: Madrid Interciecia, *Geophysics* 28: 99-110.

Oyawoye, M. O., 1972. The Basement Complex of Nigeria. In: Dessauvagie, T.F.J., Whiteman, A.J. (Eds.), African Geology, Ibadan University Press, Ibadan, Nigeria. pp. 66-102.

MacDonald, A., Davies, J., Calow, R. and Chilton, J. 2005. Developing groundwater: A guide for rural water supply. ITDG Publ. UK 358p.

Malomo, S., Okufarasin, V. A., Olorunniwo, M. A. and Omode, A. A. 1991. Groundwater chemistry of weathered zone aquifers of an area underlain by basement complex rocks. *Journal African Earth sciences* 11: 357 -371.

Marechal, J. C., Dewandel, B. and Subrahmanyam, K. 2004. Contribution of hydraulic tests at different scales to characterise fracture network properties in the weathered-fissured layer of a hard-rock aquifer. *Water resources research* 40: W11508.

Marechal, J. C., Dewandel, B. and Subrahmanyam, K. 2007. Characterization of fracture properties in hard aquifer system. Groundwater, resource evaluation, augmentation, contamination, restoration, modelling and management. M. Thangarajan Ed. Springer, New York.

Meijerink, A. M. J. 2007. *Remote sensing applications to groundwater*. Paris: UNESCO.

Mulder, P. J. M. 1983. Rapportage putproef Hoogezand. Dienst Grondwaterverkenning TNO Delft, OS.83-24,7p.

Munaserei, D. 1979. A comparative analysis of the streamflow for instrumented basins of rivers Ogun and Ofiki. B.sc. Project. Department of Geography. University of Ibadan.

Munch, Z. and Conrad, J. 2007. Remote sensing and GIS based determination of groundwater dependent ecosystems in the Western Cape, South Africa. *Hydrogeology Journal* 15.1: 9–28.

Murali, S. and Patangay, N. S. 2006. *Principles and applications of groundwater geophysics*. B. Shireesha Ed. 3rd edition. Hyderabad: Association of Exploration Geophysicists. 371pp.

Neuman, S. P. 1972. Theory of flow in unconfined aquifers considering delayed response of the water. *Water resources* 8.4: 1031 -1045.

NGSA, 2006. *Geological and mineral resources map of Oyo State, Nigeria*. Abuja:NGSA

NGSA, 2009. *Geological and mineral resources map of south-western zone, Nigeria*. Abuja:NGSA.

Offodile, M. E. 2002. *Ground water study and development in Nigeria*. 2nd edition. Jos: Mecon geology and engineering services limited.

Ojo O., Gbuyiro, S. O., and Okoloye, C. U. 2004. Implications of climatic variability and change for water resources availability and management in West Africa. GeoJournal 61: 111-119.

Oladapo, M. I. and Akintorinwa, O. J. 2007. Hydrogeophysical study of Ogbese southwestern Nigeria. *Global journal of pure and applied sciences* 13.1: 55-61

Olayinka, A. I and Mbachi,C. N. C. 1992. A technique for the interpretation of electrical soundings from crystalline basement areas of Nigeria. *Journal of Mining and Geology,* 28.2: 273-281.

Olayinka, A. I. and Olayiwola, M. A. 2001. Integrated use of geo-electrical imaging and hydrochemical methods in delineating limits of polluted surface and ground-water at landfill site in Ibadan areas, soutwestern Nigeria. *Journal of Mining and Geology,* 37.1: 55-68.

Olorunfemi, M. O. and Okhue, E. T. 1992. Hydrogeologic and geologic significance of a geo-electric survey at Ile-Ife, Nigeria. *Journal of Mining and Geology,* 28.2: 221-229.

Olorunfemi, M. O. and Olorunniwo, M. A. 1985. Geo-electric parameters and aquifer characteristics of some parts of southwestern Nigeria. *Geologia Applicata E. Idrogeologia*, 20: 99-109.

Olorunfemi, M. O. and Olorunniwo, M. A. 1990. The determination of the geo-electric parameters of some Nigerian residual and detrital clays. *Journal of Mining and Geology,* 26.1: 81-85.

Oseji, J. O., Atakpo, E. A., Okolie, E. C. 2005. Geo-electric investigation of the aquifer characteristics and groundwater potential in Kwale, Delta state, Nigeria. *Journal of appl. Sci. Environ. Mgt.,* 9.1: 157 – 160. Retrieved May 18, 2011, from www.bioline.org.br/ja.

Papadopulos, I. S. and Cooper, H. H. 1967. Drawdown in a well of large diameter. *Water resources research* 3.1: 241- 244.

Pekeris, C. L. 1940. Direct method of interpretation in resistivity prospecting. *Geophysics* 5: 31- 46.

Phillippe, R., Damian, G. and Miguel M. 2008. Understanding diagnostic plots for well-test interpretation. *Hydrogeology Journal* 17: 589-600.

Philip G. and Singhal B. B. G. 1992. Importance of geomorphology for hydrogeological study in hard rocks terrain, an example from Bilhar Plateau through remote sensing. *Ind. J. Earth Science*, 19(4). 177-188.

Price, M. (1996) Introducing Groundwater, 2nd edn, Chapman and Hall, London.Gemand, J. D. and Heidtman, J. P., 1997. Detailed pumping test to characterise a fractured bedrock aquifer. *Ground Water*, 35.4: 632-637.

Rahaman, M. A. 1976. A review of the basement geology of southwestern Nigeria. Geology of Nigeria. C.A. Kogbe Ed. Lagos: Elizabethan Publ. 41-58.

Robinson, C. A., Werwer, A., El-Baz, F., El-Shazly, M., Fritch, T. and Kusky, T. 2007. The Nubian aquifer in south-west Egypt. *Hydrogeology Journal*, Vol. 15(1), pp. 33–45.

Rushton, K. R., and Singh, V. S. 1983. Drawdown in large-diameter wells due to decreasing abstraction rates. *Groundwater*, 21:671-677.

Rushton, K. R. and Weller, J. 1985. Response to pumping of a weathered-fractured granite aquifer. *Journal of hydrology*, 80: 299-309.

Sander, P. 2007. Lineaments in groundwater exploration: a review of applications and limitations. *Hydrogeology Journal* 15.1: 71–74.

Sekhar, M., Mohan Kumar, M. S. and Sridbaran, K. 1994. A leaky aquifer model for hard rock aquifers. *Applied hydrogeology* 3: 32-39.

Shaban A., Khawlie M. and Abdalla C. 2006. Use of GIS and remote sensing to determine recharge potential zones; the case of occidental Linanon. *Hydrogeology Journal* 14.4: 433–43.

Sheppard, T. 1917. William Smith, his maps and memoirs: Proceeding Yorkshire Geol. Society, 19: 75-253.

Sidle, W. C. and Lee, P. Y. 1995. Estimating local groundwater flow conditions in a granitoid: Preliminary assessments in the Waldoboro Pluton Complex, Maine Ground Water, 33(2), 291-303.

Siebert, S. 2010. Groundwater use for irrigation- A global inventory. Hydrol. Earth Syst. Sci 14: 1863-1880.

Singhal, B. B. S. and Gupta, R. P. 1999. Applied hydrogeology of fractured rocks. Dordrecht, The Netherlands: Kluwer Academic Publishers.

Slichter, C. S. 1899. Theoretical investigation of the motion of ground waters. U. S. Geological Survey 19th annual report, part 2: 295-384.

Sreedevi, P. D., Subrahmanyam, K. and Ahmed, S. 2005. Integrated approach for delineating potential zones to explore for groundwater in the Paguru River Basin, Cuddapah District, A.P., India. *Hydrogeology Journal* 13.3: 534–43.

Talabi O. A. and Tijani, M. N. 2011. Integrated remote sensing and GIS approach to groundwater potential assessment in the basement terrain of Ekiti area south-western Nigeria. *RMZ- materials and geoenvironment* 58.3: 303-328.

Taylor, R. and Howard, K. 2000. A tectono-geomorphic model of the hydrogeology of deeply weathered crystalline rock: Evidence from Uganda. *Hydrogeology Journal* 8.3: 279- 294.

Teme, S. C. and Oni, S. F. 1991. Detection of groundwater flow in fractured media through remote sensing techniques- Some Nigerian cases. *Journal of African Earth Science* 12.3:461–66.

Theis, C. V. 1935. The relation between the lowering of the piezometric surface and the rate and duration of discharge of a well using ground-water storage. American Geophysical Union Transactions, 14: 519-524.

Thiem, G. 1906. Hydrologische Methoden. Gebhardt, Leipzig, 56 pp.

Tijani M.N. and Abimbola, A.F. 2003. Groundwater chemistry and isotope studies of weathered basement aquifer: a case study of Oke-Ogun area, S.W.-Nigeria. Africa Geoscience Review, 10.4: 373-387.

Tijani, M. N., Oyewumi, Y. and Akanbi, O. A. 2006. Heavy metals contamination of stream waters and bottom sediments of urban drainage systems in Abeokuta area,

southwestern Nigeria. - *Journal of African water resources and environment- Vol. 1, No. 1, pp. 1-15.*

Tijani, M. N. 2016. Groundwater: the Buried Vulnerable Treasure. Inaugural lecture. University of Ibadan, Ibadan-Nigeria.

Todd, D. K. (1980). Groundwater hydrology, 2nd edn, John Wiley, New York.

UNESCO, 1972. Ground water studies (eds R. H. Brown, A.A. Konoplyantsev, J. Ineson and V.S. Kovalevsky), UNESCO, Paris.

UNESCO, 1975. Analytical and investigation techniques for fissured and fractured rocks, in Ground Water studies (eds. R.H. Brown *et al*). Studies and Reports in Hydrology (Chapter 14), Supplement 2. UNESCO, Paris.

UNESCO, 1984a. Groundwater in hard rocks. *Studies and reports in hydrology 33*. Paris: UNESCO.

Van Tonder, G. Bardenhagen, I. Riemann, K. Van Bosch, J., Dzanga, P and Xu, Y. 2002. Manual on pumping test analysis in fractured rock aquifers. WRC Report No. 1116/1/02.Water Research Commission Pretoria.

Waters, P., Greenbaum D., Smart P. L. and Osmaston H. 1990. Applications of remote sensing to groundwater hydrology. Harwood Academic Publishers GmbH, Remote Sensing Reviews 4.2: 223–64.

Weerawarnakula, S. 1986. Petrology and geochemistry of Precambrian rocks in Igboora area, southwestern Nigeria. M.Phil. Thesis. Department of Geology. University of Ibadan. xxiii+280pp.

Wilson, R. C. 1922. The geology of the western railway. Bull. Geol. Surv. Nigeria, No.2.

Wright, E. P.1992. The hydrogeology of crystalline basement aquifers in Africa. Hydrogeology of crystalline basement aquifers in Africa. E.P. Wright and W.G. Burgess. Eds. Geological society special publication No. 66. Geological society, London.

Wright, E. P. and Burgess, W. G. 1992. The hydrogeology of crystalline Basement aquifers in Africa. Geol. Soc. Special Publ. No. 66. The Geological Society, London, p. 264.

Yakubovsky, U. V.1973. *Electrical prospecting*. Moscow:Nedra.

EXPLANATION ON APPENDIX IA

A: Prominent mineral assemblage in porphyritic granite, showing the conspicuous large grains of K-feldspars at Idere.

B: Cylindrical feldspathic grains of coarse biotite porphyritic granite at Tapa

C. Porphyritic Granite with the phenocrysts aligned in north-east trend at Okedere-Idere

D. Uniformly aligned feldspathic porphyries mainly in north-west trend at Tapa

E Inconsistent porphyries orientation at Tapa

F. Homogeneous medium grained granite occurring as intrusion within augen gneiss at Sekere off Igboora-Abeokuta express way

G. Disjointed small size and low-lying outcrop of amphibolite at Pako-Igboora

H Outcrop of amphibolite with hammer resting on the foliation plane dipping btw $38\text{-}42^0$ at Akede-Igboora.

I Exposed weathered ampibolite with resistant quartzite intercalations at Itaagbe-Igboora

J Amphibolite with an inclusion of quartz vein at Apata-giri Igboora

K. Schistose foliated amphibolite at Pako-Igboora

L Banded biotite gneiss with garnet grains inclusions at Apata

M Perpendicularly dipping gneiss, hammer resting on the foliation plane at Alaagba

N Quartz boulder in migmatite at Apata-Faju-along Igboora-Iseyin road

O Reverse fault at Abola near Idere

P Rock boundary exposure between gneisses with the hammer end resting on banded gneiss at Alagbede.

Q An outcrop of porphyroblastic gneiss showing sheared porphyroblast at Alagbede area.

R Diorite sill intrusion in banded gneiss at Alaagba

APPENDIX IA
FIELD EXPOSURES OF ROCKS AND STRUCTURES

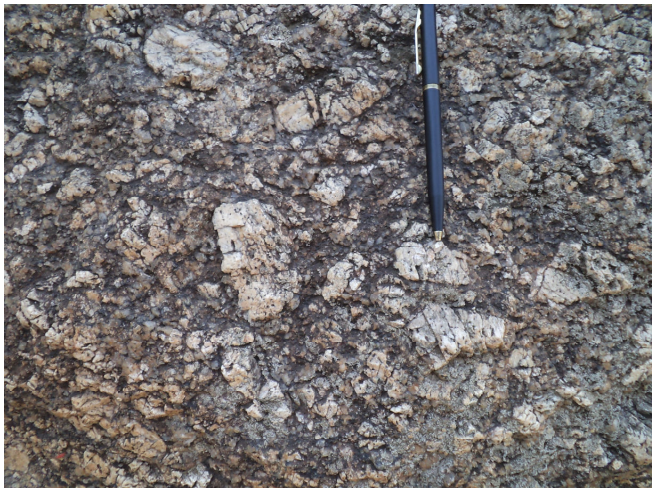

A

B

C.

D

E

F

G

H

I

J

K

L

M

N

O

P

Q

R

EXPLANATION ON APPENDIX IB

A-B: Pumping test equipment, including water meters, submersible pump, water-level indicator and power generating set.

C-E: Pumping test exercise at Agbede, Ayete and Igboora

F-G Pumping test crew enroute Alabi-Oja. G: Crew on site at Lamperu village

H: Installation of submersible pump and the PVC pipes

I-L: Various water infiltration controls. **I** shows water directly being discharged into concrete drainage network at Igboole. **K** shows a long water flowline at Onilado-Igboora. **L** shows long flowline discharging water into the concrete drainage at Isale-Ajegunle. **L1** shows discharged water being collected in large containers at Ayete. **L2** shows discharge water being scooped out at Alaagba I. **L3** shows the indigenes queuing up to collect the discharge water from the flowline pipe at Alaagba II.

M-N: Water meter readings to 0.0001 M^3 (or 0.1 litre) accuracy at Ayete.

O: Shows residual drawdown measurement in the well during recovery test at Apata-Faju

P: Shows the water level indicator set-up for taken recovery test data immediately after pumping test at Alabi-Oja.

APPENDIX IB

PHOTOGRAPHS ON HYDRAULIC TESTS OPERATIONS

A

B

C

D

E

F

G

H

I

J

K

L1

L2

L3

M

N

O

P

EXPLANATION ON APPENDIX II
PHOTOMICROGRAPHS

A-D Photomicrographs of sections through amphibolites, showing the brown and green varieties of hornblende (H), plagioclase feldspars (PL), and biotite (B) under cross polarised light and X40 magnification at A: Akede, B: Apata-Giri, C: Pako and D: Onilado. Location:Igboora.

E-F Photomicrographs through amphibolites revealing the cleavages crossing of hornblende mineral crystals at about 60^0 and 120^0 under plane and cross polarised light at X40 magnification at E: Akede and F: Apata-Giri. Location: Igboora.

G-I Photomicrographs of the sections through gneiss, showing hornblende (H) and biotite (B) as the major mafic minerals in the biotite-hornblende gneiss under plane polarised light and X40 magnification. Location: Abola.

J-K Photomicrographs of sections through the fine grained melanocratic rock that intruded into the banded biotite gneiss, showing biotite (B) and plagioclase feldspars (PL) as prominent minerals under plane and cross polarised light and at X100 magnification respectively. Location: Alaagba.

L Photomicrograph of section through fine grained leucocratic granitic rock that intruded into the porphyritic granite, showing microcline feldspars (M) as abundant minerals. Location: Idere.

M Photomicrographs of section through biotite-garnet gneiss, showing garnet grain (G) with feldspar inclusions under cross polarised light and X40 magnification. Location: Apata.

APPENDIX II: PHOTOMICROGRAPH

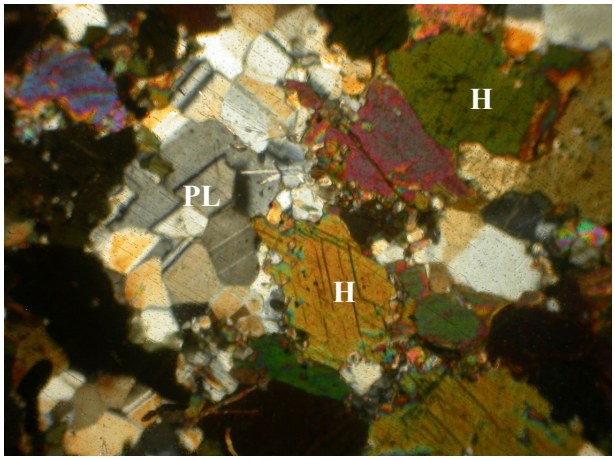

A

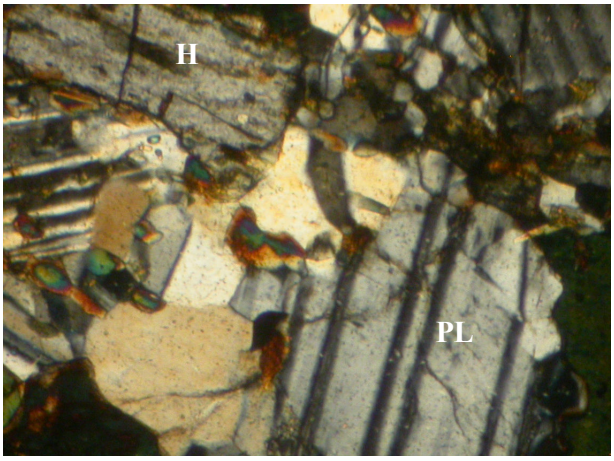

B

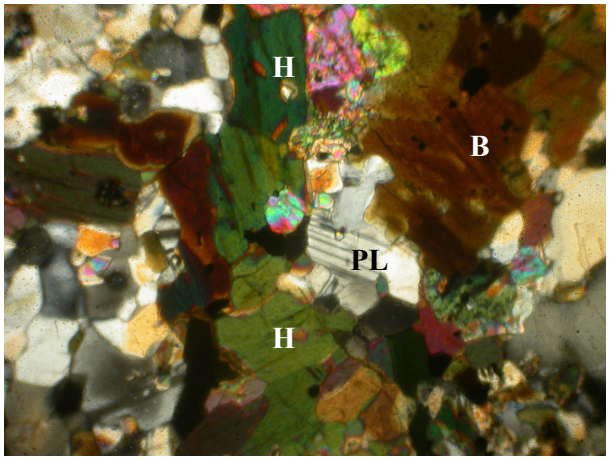

C

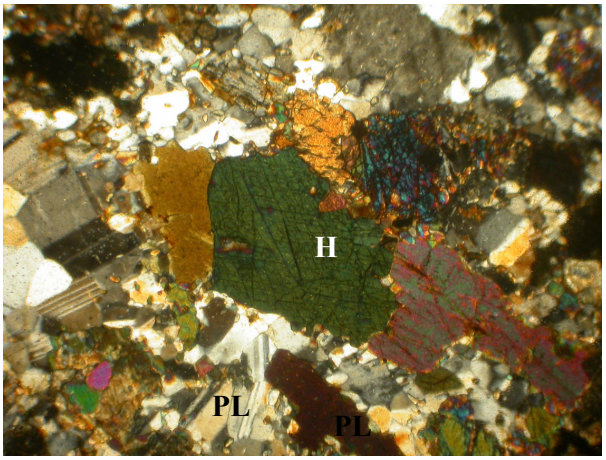

D

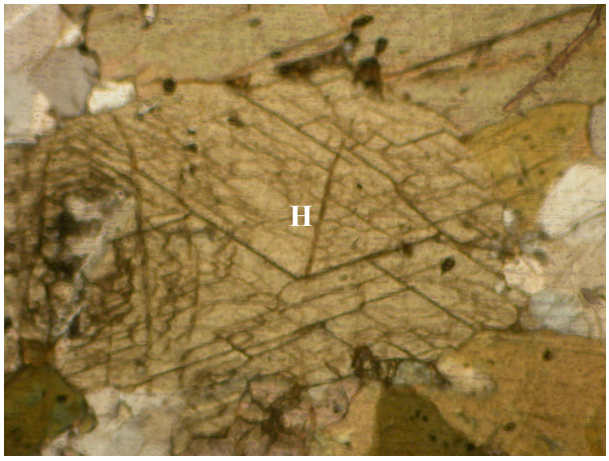

E

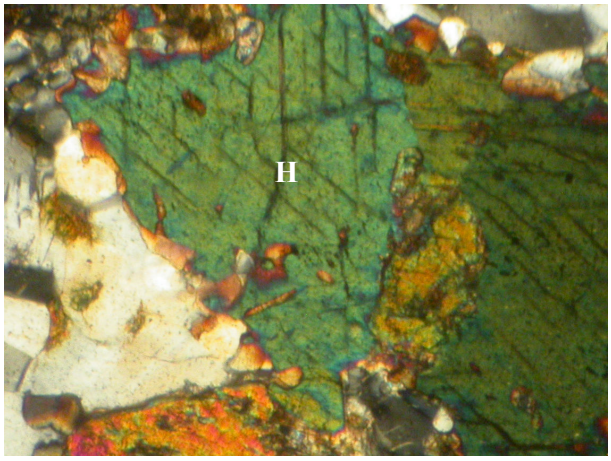

F

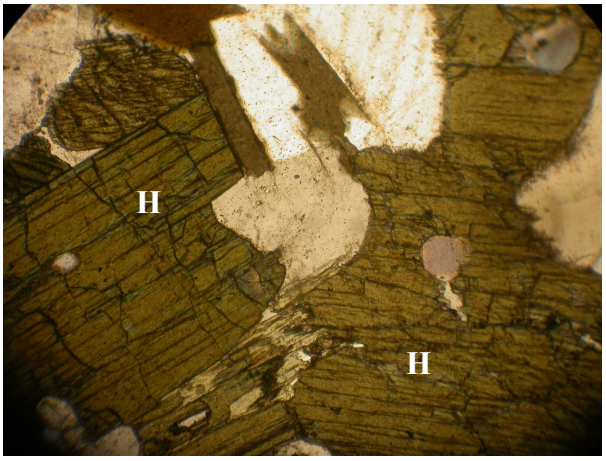

G

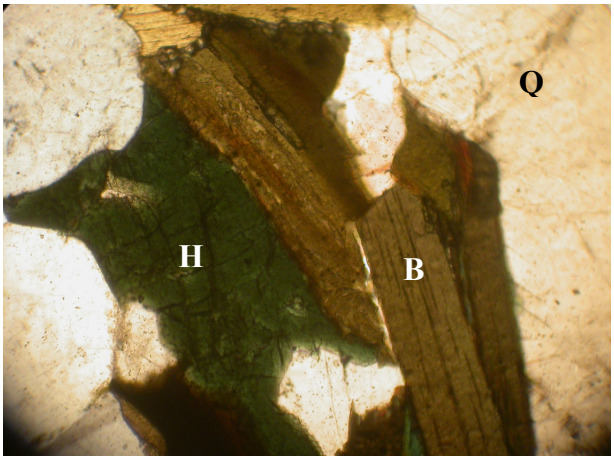

H

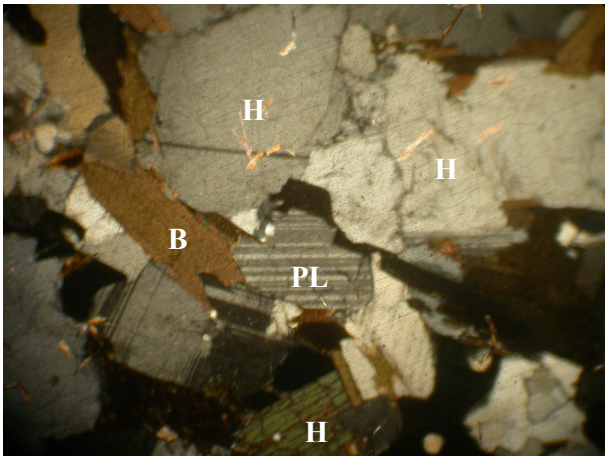

I

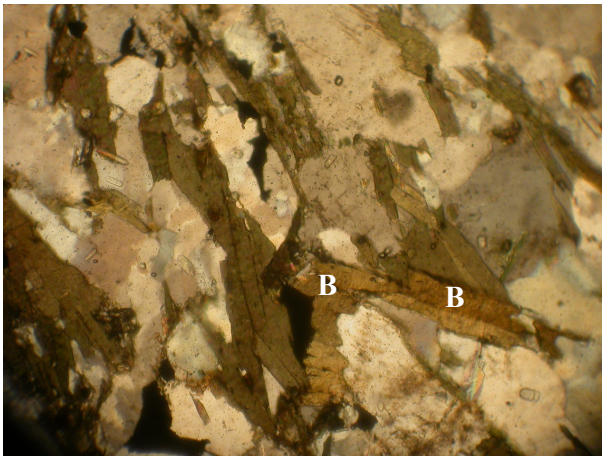

J

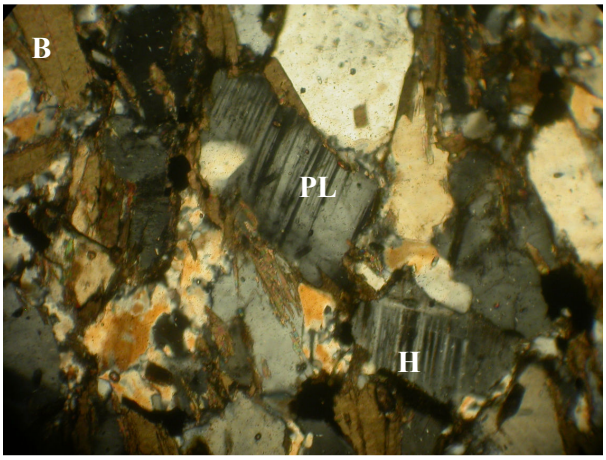

K

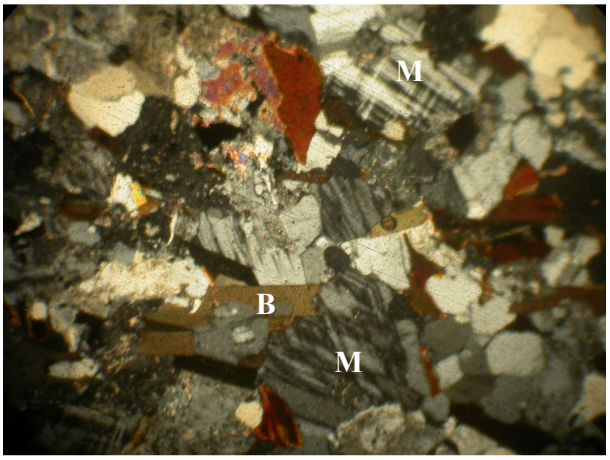

L

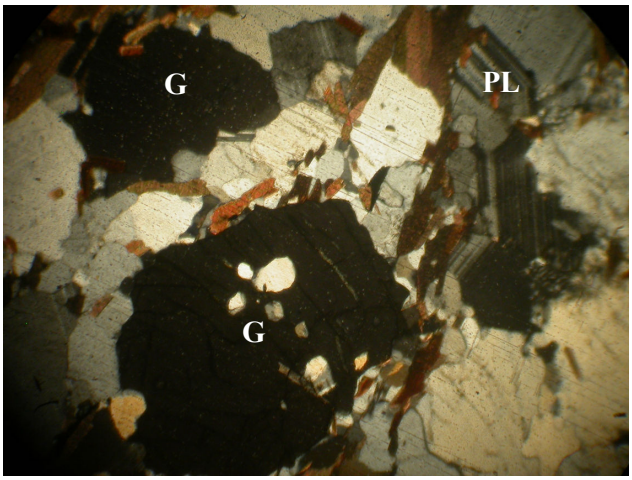

M

APPENDIX III

CHARACTERISTICS OF THE APPLICABLE SATELLITE IMAGERIES

1. RADAR

The radar satellites images are readily applicable for interpretation of many significant parameters of hydrogeological important such as terrain analysis, lineament mapping, geologic interpretation, ground penetration. The Shuttle Radar Terrain Model (SRTM) owned by NASA is a name given to the C and X radar bands, having an approximate of 3-10 GHz frequency with a resolution of 25-90m. The SRTM used the so called single or simultaneous pass interferometry, because the two receiving antennas were mounted on a long mast. The simultaneous recording eliminates effects of changes (moisture, vegetation) of the land objects, which do occur when radar images of different times (orbits) are used.

Digital Elevation Model (DEM): The SRTM is a digital elevation Model (DEM) aspect of radar which has strong application to the land surface relief and can give a 3D elevation impression of the study area.

Using a download of a Shuttle Radar Terrain Model (SRTM), planimetric visualization of the DEM contents can be achieved by way of contours, by shadow effect (known as hill-shading) or by both, using GIS functionalities.

Before the availability of the SRTM data, DEMs were created by digitizing contours on a topographic map, followed by interpolation to obtain a DEM, usually in raster format. There are some problems using this method, such as low accuracy due to deformation of the paper of the topographic map – and contours are anyway cartographic generalizations. Interpolation across drainage divides or small valleys gives inaccuracies; relief features between two contours are ignored; pits or artificial steps may appear in gently sloping or flat terrain. Mitigation of some of the problems is possible, depending on the interpolation method used and by adding topographic information.

The absolute height accuracy of SRTM DEM is 16 m and the relative accuracy is <10 m. DEMs from active radar systems, including the widely used SRTM data, have been used for various groundwater studies most especially in developed nations (e.g. Leblanc et al., 2003; Munch and Conrad, 2007; Robinson et al., 2007).

SRTM data in the form of DEMs are available globally between 60ºN and 58ºS. The SRTM data has to be imported into a GIS, for visualization of hill shading, contours, and 3D display, and for preparing derivatives such as slope maps or automated drainage network generation.

For a comprehensive hydrogeological evaluation the associations between lithology, geomorphology, soils and land cover need to be evaluated. A SRTM radar image is helpful in taking cognizance or mapping such associations, which are termed 'terrain units'. Combining the SRTM elevation map with other satellites images such as NDVI, colour composite, and Thermal band of Landsat, structural map of the study area was produced.

2. LANDSAT THEMATIC MAPPER (TM)

Landsat TM is an advanced multispectral scanner used in Landsat 4 and 5 missions. It has seven ranges of wavelengths specifications. Bands of Blue, Green, Red and Thermal-InfraRed (TIR) were processed and employed for specific hydrogeological investigations in the present work. The Blue, Green and Red (RGB) Landsat bands have ground resolution of 30m, while the TIR has 120m resolution. The use of TIR has a wide application to studying the hydro-geomorhic features, such as for identifying lineaments (Shaban et al., 2006; Granados-Olivas and Corral-Diaz, 2003), information on surface water flow and groundwater recharge (Leblanc et al., 2003), and shallowness of groundwater (Heilman and Moore, 1981; Bobba et al., 1992). The original downloaded imagery form NASA is in figure below.

For structural characterisation of crystalline rocks, the TIR Landsat band is quite influential in delineation structural features such as folds, faults, foliation, layering etc.

These topographic features are distinguished due to spatial differences in thermal (heating) characters of the rocks. Lineaments that act as conduit for water will produce a linear features, due to contrasting heat variations along the region of groundwater

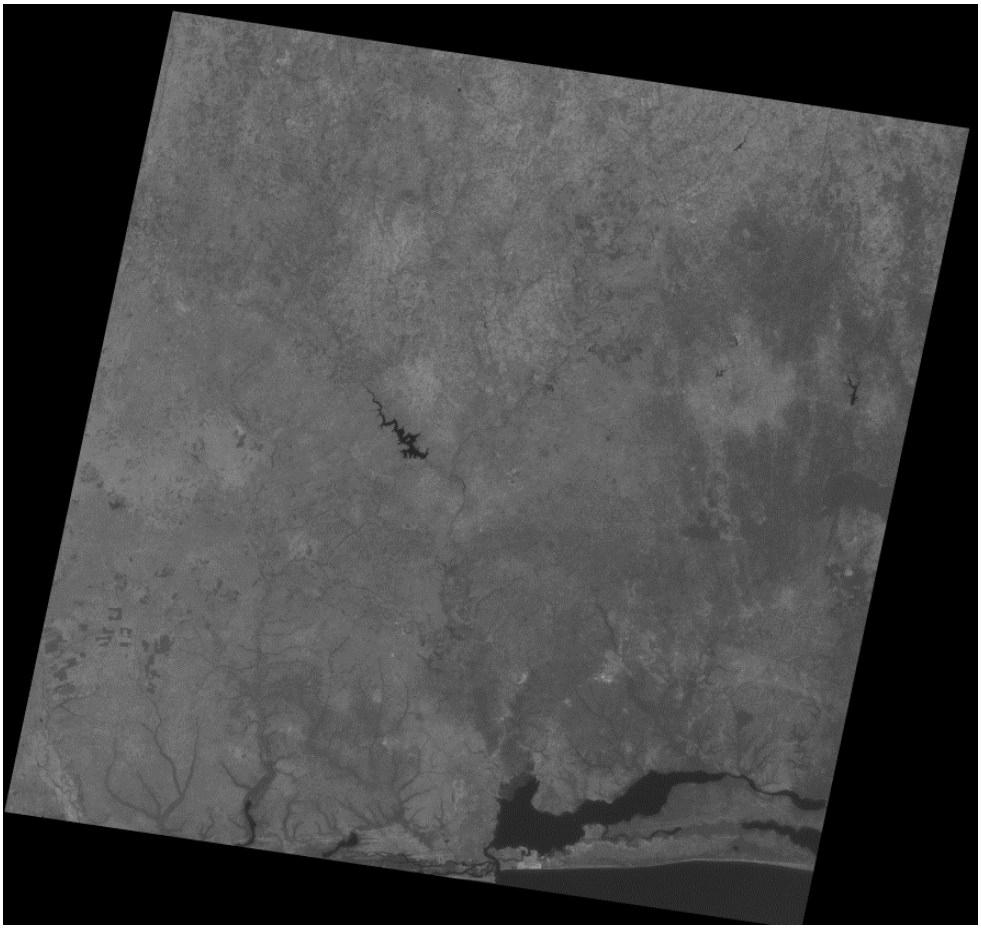

Figure: Showing the original downloaded picture from NASA.

flow. These linear features are mappable (or traceable) on the processed images with the aid of ArcGIS and Edas Imagine softwares .

Also, by applying appropriate filters and image processes, the vegetation index can also be generated. The NDVI transform in primary colour composites can provide an indirect information on groundwater occurrence and these images are essential for hydrogeological interpretation.

A. The NDVI Transform: Vegetation Index: Green vegetation reflects much light in the near infrared (NIR) band but not much in the red band (RED). Therefore, the simplest vegetation index is the difference between the two bands (i.e, NIR–RED) because that difference has a positive and large value much more so than would be obtained for the other land covers. Since the NIR domain is invisible to the human eye, the higher reflectance in the green band make the visualization of vegetation as green.

The low reflectance and transmittance in the visible range is caused by the strong absorption of chlorophyll pigment. Absorbing effects are less strong in the near infra-red (0.7 -1.30 μm) but reflectance and transmittance are higher. Type of pigment, leaf water content, cell-structure, thickness of the leaves and their orientation in the sun-sensor path influence the details of the spectral signature.

The difference in reflection (expressed by DNs) of the NIR and RED bands is much greater for green vegetation than the difference for bare soils, outcrops water, dried out vegetation, and so on. An image containing pixel values of the difference is termed a vegetation index image. The 'Normalized Difference Vegetation Index (NDVI)' is widely used, where normalization is given by dividing the difference by the sum, in order to bring the range of NDVI values to -1 and 1.

$$NDVI = (NIR- Red) / (NIR + Red)$$

Pixels with lush vegetation on a NDVI image will appear as whitish tones (if such tones are assigned to high values, as is customary) and pixels with no or poor vegetation in dark grey to black tones. Hence, the NDVI transform is applicable for detecting fractures and faults bearing water. The soil moisture attributes of an area can also be inferred from the vegetation response to groundwater localised in fractures.

Hydrogeological interpretation using vegetation index assumes that areas with lushness are characterised by fractures having water, since vegetation response to presence of water. It is also an attribute of groundwater recharge point and an indication for the wetness of the soil moisture.

B. Colour Composite image: This images transform assigns specific colour to some satellites images spectral band range. In Landsat ETM, the three primary colours, namely Blue, Green and Red are assigned to 0.45-0.52, 0.52-0.60, and 0.63-0.69 μm spectral bands respectively. The combination of these bands is applicable to distinguishing geomorphologic features, such as vegetation, landform and land-use pattern, soil moisture, drainage, etc. It is then easier to interpret the geologic and hydrogeologic characteristics of the area, and their variations from place to place. The colour composites images has an edge over the transform NDVI, since interpretation in the latter is by considering the tones of uses light and dark shades for distinguishing features. The high tone spots in NDVI are now seen as green colour spots on the colour composite image, which represent locations with lush vegetation.

APPENDIX IV

CONCEPTS, FIELD PROCEDURES AND INTERPRETATION OF ELECTRICAL RESISTIVITY GEOPHYSICAL METHOD

Electrical resistivity method is the most widely used geophysical methods which give a good indication of the occurrence of fracture horizons, groundwater and its quality. It is based on the principle of that electrical resistivity of a geological formation is dependent upon the material as well as upon the bulk porosity and water content in the formation.

The theoretical basis for electrical resistivity method is demonstrated that when an Electromotive force (EMF) is applied to a resistance R in a circuit, then the current I in the circuit is given by Ohm's law as;

$$I = E/R$$

As regards the substance which offers the resistance, the numerical value of resistance R can be related to the dimensions L and a specific property of the medium known as resistivity and denoted by ρ as;

$R = \rho.L/A$, where A is the sectional area of the substance.

It is conventional to express the resistance in ohm for a unit cube of Im side, and resistivity in terms of ohm.m.

CONCEPT OF GROUND PENETRATION

Electric current is introduced into the earth through two current electrodes. The resulting electric potential drop depends upon the resistance of the earth material and the amount of current flow. Two potential electrodes positioned within the field of the current electrodes give potential data. The current flow and potential drop are converted into resistivity values. The field resistivity values obtained are apparent rather than true.

Generally, the depth of investigation of a resistivity survey is directly proportional to the electrode separation and increases with increasing electrode separation

(Bhattacharya and Patra, 1968; Koefoed, 1979). Though, at first approximation the depth of investigation due to current penetration may be taken as roughly equal to the spacing between the current electrodes, it is an arbitrary value which could increase or decrease depending upon the acceptable value of current density. More so the concept takes into account only homogeneous earth and in any inhomogeneous or layered earth the depth of current will be comparatively much less. Hence, Murali and Patangay, 2006 emphasized that one may have to use an electrode spacing many times larger than the depth to be investigated under practical circumstances in order to obtain reasonable degree of signals from bodies at depth.

The value of apparent resistivity ρ_a measured over a layered earth is dependent upon the resistivity ρ and thickness h, of the subsurface layers as well as the current electrodes A and B separation.

i.e $\rho_a = f(\rho_1, \rho_2, \rho_3 \ldots\ldots\ldots h_1, h_2, h_3 \ldots\ldots\ldots, AB/2)$

It follows that over a geo-electric section where ρ_1, ρ_2, ρ_3 and h_1, h_2, h_3 are known, the ρ_a value changes with the separation. When AB/2 is very small the ρ_a value approximate the the value ρ_1 and when AB/2 is very large the ρ_a tends toward the ρ_n. The manner of variation of ρ_a for different values of AB/2 represents what is called vertical electrical sounding (VES) curve. Since, the VES curve is dependent upon layer parameters; it should be possible to determine the layer parameters from the curve. However as this is theoretically true, the relationship becomes extremely complicated as the number of layers increases. Reliable determination of layer parameters is possible only when the subsurface consists of a maximum of 4 layers or less.

ELECTRODE CONFIGURATIONS AND SEPARATION

In VES, the distances between electrodes are increased so that so that the electric current penetrates deeper levels, which allows resistivity measurements of a deeper and larger volume of the earth. The electrodes are normally linear, aligned parallel to the trend of rock discontinuity, which may be deciphered from other surveys or rock outcrops. For geophysical groundwater exploration, the most commonly used electrode configurations are the Wenner and Schlumberger arrays. In wenner the electrodes spacing *a,* is equal, while in schlumberger, the distance *L* between the current electrodes is varied and the distance *l* between the potential electrodes are kept

constant for a while over a set of AB separation. For these configurations, the ρa which is a measure of the effects of all the layers between the maximum depth of penetration and the surface is calculated as follows.

$\rho_a = 2\pi aR$ ------ Wenner array

$\rho_a = \pi (L^2/2l)R$------- Schlumberger array;where,

R is the measured resistance (in voltage/current) and *a, L* and *l* are as defined above. The electrode separations, L and l determines the depth of investigation.

CONCEPT OF DAR ZARROUK PARAMETERS

The concepts of longitudinal unit conductance and transverse unit resistance which are known as the Dar Zarrouk parameters were first introduced by Maillet, 1947 and now emphasized by more recent research works (Oladapo and Akintorinwa, 2007; Abiola et. al., 2009; Aweto; 2011) and literature (Sabnavis and Patangay, 2006). Sabnavis and Patangay, 2006, highlighted the use of these parameters to quantify water transmission through the porous regolith overburden. These Dar Zarrouk parameters are derivatives of the primary geo-electric parameters which are the layer thicknesses and their corresponding true resistivities.

The background concept for Dar Zarrouk parameters assumes that the earth is parallel with n layer and the flow of current through such sequence is controlled by individual layer resistivities and their respective thicknesses.

The longitudinal conductance S: is the parameter that influences current flow when the current flow is parallel to the geo-electric boundaries and when the current flow normal the geo-electric boundaries the significant parameter is the transverse resistance T. When a no of layers are involved in a geo-electric section, their total longitudinal conductance S and total transverse resistance T are:

$S= S_1 +S_2 + S_3 +....$, where $S_1 = h1/\rho1$, $S_2 = h2/\rho2$ etc, and

$T= T_1+ T_2 + T_3 +....$where $T1 = h1.\rho1$, $T_2 = h2.\rho2$ etc. where;

h1 and ρ1 are the layer's thickness and resistivity

The Dar Zarrouk parameters liken the passage of current parallel to and across the geo-electric boundaries to water passage through subsurface layers. These parameters are quantifiable using the primary geo-electric parameters. Hence, the water recharge potential of the regolith unit developed upon the various bedrock settings was inferred from the Dar Zarrouk variables particularly from the longitudinal conductance.

Coefficient of electrical anisotropy, λ

The Coefficient of electrical anisotropy, λ is computed from the square root of the ratio of average transverse resistance ρt and average longitudinal resistivity ρl i.e;

$$\lambda = \sqrt{\rho t/\rho l}$$

The average transverse resistance, ρt = T/H, where H is the total thickness of the layers in the geo-electric section. The average longitudinal resistivity, ρl = H/S.

FIELD PROCEDURES FOR CARRYING OUT VES SURVEY

The field procedures of Murali and Patangay, 2006 were considered for VES survey using Schlumberger configuration. The measuring instrument is placed at an observation station which is suitable for spreading the cable in either direction. The electrodes that measure the potential difference are placed on either side of a chosen center near to the measuring instrument.

Two current electrodes are driven into the ground 10-15 cm deep each on either side of the center. These current electrodes ate connected to instrument by PVC covered cable.

The electrical connections and separations of electrodes are checked before each measurement. The apparent resistivity value is determined by sending current (I) into the earth and measuring the potential drop ΔU or ΔU/I ratio multiplied by configuration constant K. The electrode (AB) spacing is then increased and the corresponding ρa value measured.

The operation is repeated again and again while the current electrodes are expanded away from the center, keeping the potential electrodes stationary. The distance between the potential electrodes should be increased by 3-4 times compared to the previous distance when the potential difference (ΔU) values become very small. After

this increase, the apparent resistivities can be measured for increasing current electrode separations using the larger potential electrode separation.

The current electrode separations are chosen in such a manner that when plotted on log-log graph the distances between neighbouring points are approximately equal. This is achieved by increasing the current electrode separations by a factor of about 1.5. The observations are plotted on a log-log graph paper of 62.5mm modulus with apparent resistivity on one axis and half the current electrode, separations (AB/2) on the other. Whenever the potential electrodes are changed, two apparent resistivity values will be obtained, one for the smaller potential electrode distance and another for the larger potential setup. Depending upon the conditions near the contacts of potential electrodes, the two apparent resistivity values might differ by a small percentage instead of being equal.

Further, it is better to plot the measured values on the graph immediately after measurement since any departure from the normal trend of values can be checked in the field for authenticity. Often, errors in the distances of electrodes on either side of the center cause such departures. Another common reason could be due to lateral inhomogeneities very near to the surface.

The precautions to be observed during VES investigation are:

a) The electrodes on either side of the center should be placed at equal distances from the center since the symmetric configuration is being used.
b) All the four electrodes should lie in a straight line.
c) The location should be away from industrial areas and should not be near high tension wires
d) The electrodes should be expanded parallel to topographic contours.

METHODS OF QUANTITATIVE INTERPRETATION OF VES

This approach assigns values to the geo-electric parameters of the respective geo-electric sequence. This can be done by either curve matching or computer techniques using the field data.

- **Curve matching techniques**

These methods ascribe geo-electrical parameters to field data by comparing the shape of the field curve with that of a theoretically computed curve for a known geo-electric section. This can be done either by complete or partial curve matching.

In complete curve matching, interpretation of the two layer curve is quite simple as only a few theoretical curves are to be compared with the field curve and they are available in a single sheet (after Yakubovsky, 1973). There is complexity of curve matching when there is more than two layers, since theoretical (master) curves has to be prepared for various values of ρ2 and ρ3 as well as for various values of h2/h1. Hence, comparison of three layer curve requires that the curve type is first identified before the interpretation could be done.

However, in partial curve matching technique, a three-layer field curve can be interpreted with a good degree of accuracy using only a two layer master curve set, with the help of some auxiliary curve charts of Orellana-Mooney, 1966. Though, the process carries along with it an increasing amount of error and ambiguity if the section consists of more than four layers.

- **Computer techniques**

With the application of computer techniques of direct inversion or iterative method, it is possible to interpret multi-layered VES curve rapidly and more exactly.

The direct inversion method is dependent on the recurrence formula developed by Pekeris (1940) which can be used for reducing apparent resistivity values observed on any plane surface to a lower boundary plane. Thus, the response due to an 'n' layer medium can be reduced to that of 'n-1' layer medium, after removing the influence of the top layer. Proceeding in this manner till all the layers are exhausted, the parameters of the geo-electric section can be obtained.

The automatic iterative techniques are more popular as existing information can be used in the interpretation of VES data. The procedure as outlined by Murali and Patangay, 2006) are outlined below.

- From the VES data a model is either guessed or derived from the less exact method such as curve matching method.

- From the initial model a VES curve is generated which is compared with the original field curve.

- If the discrepancy typified by RMS error between the two is very large than the desired accuracy of match, the model parameters are changed either manually or automatically based on the type of software employed.

This method of interpretation is very rapid and can give satisfactory results depending on the model given initially.

In order to arrive at precise conclusions from the VES surveys, the present research employs the partial curve matching techniques to generate the model parameters (since all the generated VES curves exceed two-layer sequence) and apply automatic iterative computer method to establish the sequence layering and true resistivities of respective layers.

Primary geo-electric and Dar Zarrouk parameters

The primary geo-electric parameters are the layer thickness in metre and the layer resistivity ρ in ohm.meter.

The secondary resistivity parameters known as Dar Zarrouk parameters was introduced by Maillet (1947) and are significant in understanding the subsurface lithology and the permeability of the regolith unit for groundwater recharge.

The Dar Zarrouk parameters include transverse resistance T, longitudinal conductance S and coefficient of anisotropy λ.

METHODS OF QUALITATIVE APPROACH

The qualitative interpretation approach involved constructing maps and sections to visualise changes in vertical section which is the weathering development pattern at a location and spatial distribution of the vertical section. This is better coupled with prior knowledge of the environmental and geological conditions of the area. Some examples of qualitative maps are discussed below.

- **Curve type**

The changes in VES curve over an area of investigation are an indication of changes in geo-electrical characteristics of the area. This may indicate lithological variations, increase or decrease in the number of layers in the subsurface etc. If there are frequent changes in VES curve type over the region of investigation, then a VES curve map could be drawn; on which the curve type is inserted on the point of the map, corresponding to its location on the ground.

- **Basement topography map**

The basement topography involves contouring by which points (areas) that are having similar high resistivity values (typifying degree of impermeable zones) are connected together. Hence, information about the variation of the highly resistive subsurface zones is given. This provides prior knowledge of the groundwater potential of the area.

- **Apparent resistivity pseudo-section**

By constructing apparent resistivity pseudo-section along a profile with a large number of stations where VES data is available is a convenient way of graphically representing the electrical resistivity distribution in that particular subsurface depth. At each VES location, the AB/2 separations (depth) of interest are traced upward to the corresponding apparent resistivity. As a result one obtains a chart of consisting of number of ρ_a values which can be contoured by drawing iso-apparent resistivity lines for any depth of interest. When the subsurface structures are similar, the contour lines will be exhibiting a similarity. These lines are nearly horizontal when the layering has a low or zero dip and the resistivities are not varying much. The contour lines are found to become nearly vertical in the presence of faults, contacts etc. It should also be noted that when the basement has very high resistivity then the contour lines of resistivity at deepest depths reflect the shape of the basement (Murali and Patangay, 2006).

- **Vertical profile section: Vertical expression of weathering Development**

The resistivities of the derived layered sequence are pointers of the grain size dominating in that horizon. The layer lithology is inferred from the characteristic

resistivity value of the layer sequence interpreted from the field VES data. The lithologic interpretation and the thicknesses of the geo-electric layers of a particular VES survey indicate the degree and the extent of decomposition of the fresh basement. By the quantitative and lithologic descriptions, even the nature of the infinite layer can be detected whether fractured or fresh.

The thickness, area extent and physical characteristics of the weathered layer vary from one region to another depending on climate, topography, lithology and vegetative cover. Since all the locations in the study area lie within the same climatic region, emphasis is placed on the last three factors above. The weathering profile development in a crystalline rocks terrain is a paramount decisive factor in any groundwater exploration scheme in the area. The fractured zones and the weathered layers are targets for water occurrence in basement terrain.

- **Geo-electric section over a profile: Spatial distribution of weathering development**

The geo-electric sections show the variations of vertical sections (in terms of lithology and thickness) of geo-electric layering sequence over a particular azimuthally profile. The profiles of choice will constitute several VES stations and by this, the topography of any lithology (such as topsoil, weathered layers, and basement) could be traced along any traverse in the study area. This will give the overview of the variation of the degree of weathering and the correlation of any lithology over the study areas.

- **Recharge potential**

Groundwater investigations in any area should not just be about finding promising water bearing zones in the subsurface, also; of great concern is the sustainable water yield over period of pumping. Groundwater recharge potentials were also estimated using secondary geo-electric parameters known as the Dar Zarrouk parameters.

- **Aquifer prospect- Isoresistivity map**

The aquifer prospect of the weathered (saprolite) layer and the basement can be understood by plotting the points of equal resistivity known as iso-resistivity maps. The true layer resistivity interpreted from the VES survey do reflect the textural character of the matrix component; as well as the state of the underlying bedrock, whether it is fresh, fractured, or partially weathered.

Preliminary aquifer prospect of the weathered layer and that of the basement can be deducted from the layer resistivity and by integrating other geo-electric parameters such as the layer thickness, spatial weathering development and the Dar Zarrouk parameters. These parameters can further enhance the evaluation of groundwater potential of the weathered-fractured components.

The above parameters were evaluated from the 85 VES surveys conducted over the study area, and the potential occurrence and water transmission of the various underlying bedrocks were characterised.

APPENDIX VA

PRINCIPLES AND PROCEDURES FOR HYDRAULIC CHARACTERISATION OF AQUIFER SYSTEM OF IBARAPA REGION

The transmission of groundwater in any geological formation is a function of the hydraulic properties of the water-bearing geological material. Consequently, for the management and protection of groundwater resources reliable estimates of aquifer parameters are necessary. This is more important in crystalline terrain, where the complexity of geo-hydrological properties of rocks, is greater and more unpredictable.

SELECTION OF SUITABLE PUMPING TESTS AND THE STATE OF THE TESTED WELLS

The sole purpose of pumping test is to characterize the hydraulic parameters of the water bearing zone in the subsurface environment by substituting the discharge and the drawdown measurements in the well (or/and piezometers) into an appropriate well-flow equation and calculating the hydraulic characteristics of the aquifer. Typical pumping tests include the multiple discharges or step-drawdown test, a constant discharge test, a recovery tests and single-well tests which could be constant or variable discharge.

The choice of a particular test depends on the prevailing hydrogeological conditions, and economic factors. On the strength of these conditions, single-well pumping tests with constant discharge along with the corresponding recovery tests were considered appropriate for hydraulic characterisation of basement aquifers of Ibarapa areas. Single-well pumping tests require no piezometer or observation wells, and the constant discharge entails maintaining a uniform pumping rate throughout the period of pumping. This was ensured in the field by using a 0.5HP sigma submersible pump, powered by a 2.75KVA generator for all the pumping tests conducted.

The fact that essential aquifer properties such as transmissivity can be reliably estimated from single-well test and that there is no need for observation wells, makes it the most appropriate pumping test for the present study, since it is less cumbersome

and less expensive to conduct compared to others. More so, considering that the lithological and structural complexities often associated with basement areas such as Ibarapa region (Jones and Hockey, 1964) could bear effects on the water-bearing attributes of the aquifer system, the appropriate pumping tests should be able to provide immediate hydraulic conditions of aquifer system being tested from point to point, even within the same bedrock terrain. Hence, due to the expected localised nature of the hydraulic conditions of the bedrock aquifers of the study area, and the fact that single-well test can provide essential aquifer properties such as transmissivity of the immediate water-bearing zones, its choice is considered most suitable for the present research. Additionally, many methods of analysis of single well pumping tests data based on aquifer type encountered in the field have been designed. For example, the analytical methods of Papadopulos and Cooper (1967), and Rushton and Singh (1983) were designed for analysis of confined aquifers, while Hantush (1964) and Jacob's straight line (of Cooper and Jacob, 1946) methods are appropriate for analysing pumping test data not just from confined but also leaky aquifers.

PRINCIPLE OF SINGLE WELL PUMPING TEST

A single-well test is a test in which no piezometer is used. The changes in water-level during pumping or recovery period are measured in the well itself. In the hydraulics of well flow, the well is generally regarded as a line source or line sink, i.e. the well is assumed to have an infinitesimal radius so that the well-bore storage can be neglected. In reality, any well has a finite radius and thus a certain storage capacity. Hence, the drawdown in a pumped well could be influenced by well losses and well-bore storage. Therefore, in a single-well test, well-bore storage must be considered when analyzing the drawdown data.

Papadopulos and Cooper (1967) observed that the influence of well-bore storage on the drawdown in a well decreases with time and becomes negligible at $t > 25r_c^2/T$, where r_c is the radius of the unscreened part of the well, where the water level is changing and T is the transmissivity.

To determine whether the early-time drawdown data are dominated by well-bore storage, a log-log plot of drawdown s, versus pumping time t should be made. If the

early-time drawdowns plot as a unit-slope straight line, we can conclude that wellbore storage effects exist.

RECOVERY TEST

A recovery test is very useful if the pumping test is performed without the use of piezometers (Kruseman and de Ridder, 2000) as was the case in the present work.

When the pump is shut down after a pumping test, the water levels in the well and the piezometers will start to rise. This rise in water levels is known as residual drawdown denoted as **'s'.** It is expressed as the difference between the original water level before the start of pumping and the water level measured at a time t' after the cessation of pumping (figure AIII.1).

It is always a good practice to measure the residual drawdowns during the recovery period. Recovery-test measurements allow the transmissivity of the aquifer to be calculated, thereby providing an independent check on the results of the pumping test, although costing very little in comparison with the pumping test. Residual drawdown data are more reliable than pumping test data because recovery occurs at a constant rate, whereas a constant discharge during pumping is often difficult to achieve in the field.

CRITERIA CONSIDERED BEFORE CONDUCTING PUMPING TESTS

For conducting pumping tests in basement complex terrain of Ibarapa areas, there are four fundamental facts that are of crucial importance prior to the selection of the appropriate type and the conduct of the test, these are;

1. **The geologic and hydrogeologic settings of the area:** The emphasis is on the following:
   a. The bedrock setting of the locality of the borehole to be tested ;
   b. The subsurface lithological and structural features that may influence the flow of groundwater such as the nature of regolith and bedrock fracturing as interpreted from the geophysical surveys;
   c. Any surface water occurrence nearby that may influence the pumping tests

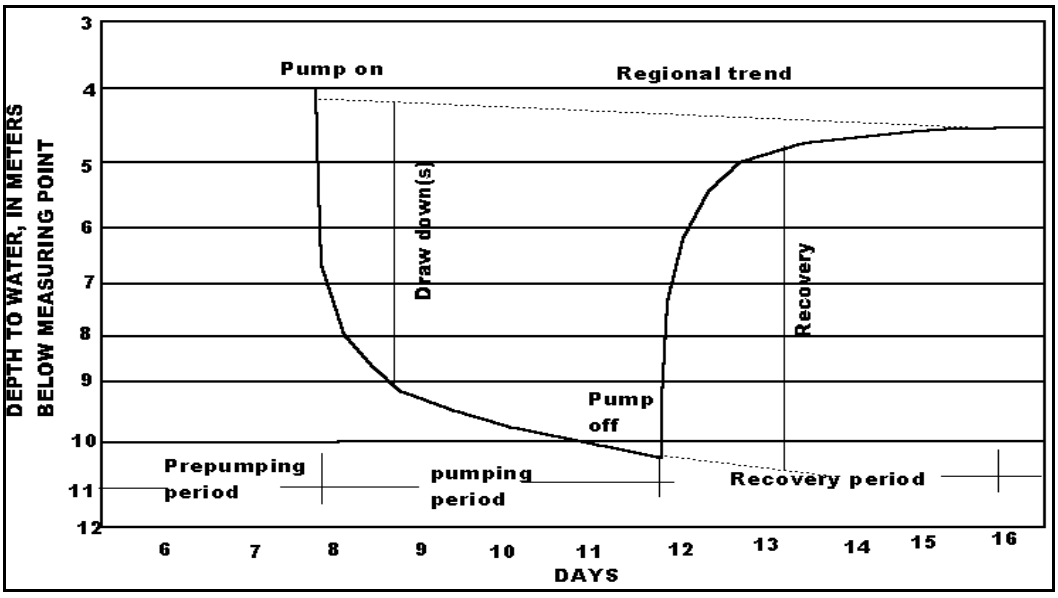

Figure AIII.1: Time drawdown and residual drawdown for pumping and recovery phases

2. Economic factors and feasibility studies considerations: This factor is crucial in making appropriate choices in the following considerations:

a. Choosing of appropriate and cost effective pumping test method; and ensuring proper execution and monitoring of pumping test.

b. Providing and maintaining a portable and uninterrupted electrical power supply during the pumping test operations.

c. Ensuring non-failure of pumping test instruments and facilities; such as the submersible pump, water-level indictors and flow meter.

d. Maintaining constant discharge rates; and uniform power supply;

e. For recovery tests, the water level measurements have to be carried out till the level returns almost to the pre-pumping state.

3. State of the tested wells: Many of the existing wells tested were out of use, due to mechanical faults. According to Kruseman and de Ridder (2000) existing wells may also be used for pumping test to reduce the cost of the fieldwork. The conditions of the existing boreholes tested were suitable for the conduct of pumping tests due to long period of non-pumping as a result of mechanical failure of wells' installations. This

ensures the pre-pumping water level is similar to the regional static water level for that area.

Five of these existing boreholes were operative and functioning wells, but had to be used because they are the only available ones for testing for that bedrock terrain. Two boreholes are new but not yet installed and remained unused till the time of testing.

To ensure their appropriateness for testing; those at Agbede and Apata villages were not in use possibly hours prior to testing, while those at Abola, Ajegunle and Itaagbe were first of all uninstalled and left to recharge for hours before they were tested. Additionally, it took about an average of 2hrs to remove the manual installations and to prepare each borehole for testing during which time the water level in the wells would have returned to the pre-pumping level.

This has been discussed above.

4. Human factors: Pumping tests exercise requires a dedicated, knowledgeable working team. A local team consisting of an experienced Plumber, and three technicians were hired for the whole exercise. This team already had the experience of installation of manually operated hand pump well and were also educated prior to the commencement of the pumping test exercise. Also, a pick-up van was hired to convey both human and materials to sites.

FIELD PROCEDURES OF CONDUCTING SINGLE WELL PUMPING AND RECOVERY TESTS

The field procedures involved the installation of the pump and riser pipes, and field measurements.

1. **Installation of Pump and Pipes**

The installation structure of the hand pump facility is illustrated in Figure 3.2b. The surface steel lever, the 2.5 inch PVC riser pipes, and the stem rods were first uninstalled prior to testing.

The depth of installation of the pump has to be in respect to the borehole depth. There must be a distance of not less than 1.5m for appropriate water intake by the pump. The pump can pick up fines when it is installed either too close to bottom or at the bottom

of the well. This can clog the intake and the rotor/motor part of the pump, leading to the damaging of the submersible pump. Pumping out sands or fines is similar to mining which is destructive to the water bearing formation.

The submersible pump is connected to the 1'' riser pipe and lowered into the well inside the inner casing. Most boreholes tested in the area have four layers structure (fig.3.2b). The inner diameter of the inner casing is 4'' in diameter and it is designed to host the 4'' submersible pump. The depth of the well and the depth of installation of the pump were noted for each well tested. It must however, be noted that the depth of pump installation has a direct influence on the pumping rate or the pressure at which the water is discharged. The discharge of the sigma submersible pump used for this exercise is at the lowest rate of 24litre/min (or 0.024m^3/min) when installed at 31m (102ft) depth and the highest water discharge rate of 90 litre/minute (0.09m^3/min) for shallow depth installation of 12m (39.6ft).

The depth of installation is a critical factor that controls the pumping rate during aquifer tests. If there is a change in the depth of installation, the water discharge rate will change even for a repeated test conducted in the same borehole using a constant discharge pumping test method.

2. Control of the discharged water

To rid the test of backflow of discharged water into the well or nearby immediate surrounding area in the vicinity of the pumped wells, precaution were taken; such as extending the end of the riser pipes for about 24 feet away from the vicinity of the well or discharging the released water into the surface concrete drainage network where available (see Plates 3.2). But in most cases, the discharged water was collected by the local people living around the vicinity.

PROCEDURES AND ANALYSES OF PUMPING AND RECOVERY TESTS DATA

PROCEDURES FOR ANALYSIS OF TIME-DRAWDOWN PLOTS

A single analytical method for the analysis of the single-well pumping tests with constant discharge conducted in the boreholes that penetrated the various bedrocks in Ibarapa areas is not feasible. This is because it is possible that the water bearing zones

may exhibit differing flow regimes. More so, inclusion of recovery tests along with the pumping phase for tests conducted in more low permeable water bearing zones require a different approach of analysis. Hence; each water-bearing zone contributing to the system has to be identified, isolated and the hydraulic parameters separately estimated where possible. In the light of this, the procedures itemised below was designed for the analysis of single well pumping tests conducted in basement terrain of Ibarapa region of Nigeria:

- An understanding of the continuity of the water discharge during the period of pumping.
- Measurements of the drawdown at specific time intervals and corresponding residual drawdowns after pump cessation.
- Create the diagnostic plots by plotting the Time- Drawdown on both semi-log and log-log scales
- Define the various and the dominant flow regime(s) from the drawdown plots
- Determine the aquifer and well parameters using appropriate analytical method. If different flow regimes can be identified during a test, each section can be separately evaluated.
- For drawdown curves that show undefined flow regime, residual drawdown obtained from the recovery tests are incorporated for an accurate description of the flow regime in the aquifer system; and hydraulic properties estimation. Recovery tests are quite essential for pumping test analysis, especially in single-well constant discharge tests carried out in the study area. Although, recovery tests could be weak in defining the flow regime, they are not affected by well-storage, well 2.losses and partial well penetration. Recovery phase includes the measurements of the residual drawdowns against time.

Time-drawdown plots: The drawdown behaviour of the aquifer system is influenced by the type of aquifer, and the boundary conditions. These factors dominate at different times during the pumping test. So, to identify an aquifer system, one must compare its drawdown behaviour with that of the various theoretical models. The model that

compares best with the real system is then selected for the calculation of the hydraulic characteristics. Aquifer system identification includes the construction of diagnostic plots and specialized time-drawdown plots. The time-drawdown curves could be on log-log or semi-log scale.

Semi-log Scale: In semi-log scale, the time is plotted on the log scale while the drawdowns are on arithmetic scale. The significant of a time-drawdown graph on semi-log scale is that it shows different slope typifying the drawdown response to pumping at each stage (fig.3.3). Semi-log plots of time-drawdown data are specialized plots, specific to a given flow regime. There are four segments that could be recognized from the semi-log plot of time-drawdown curve.

- The earliest time response is usually due to well-bore storage as most water at this stage comes from the well itself.
- Skin effect stage; the curve is influenced by the contact between the well and the aquifer. This is known as the skin effect. It is the transition zone between the influence from the well-bore water and aquifer.
- The later stage when the aquifer type and its hydraulic characteristics influence the rate of drawdown.
- The final stage, which is controlled by the influence of the boundary conditions. The direction of the change of the slope at the final segment is a diagnostic parameter that could be used to decipher the type of boundary condition. An upward kick of the curve away from the earlier trend is an indication of recharge boundary, while a downward kick, typifies an impermeable boundary.

Log-log scale, diagnostic plots: Time-Drawdown data plotted on log-log scale are otherwise called diagnostic plots. A diagnostic plot allows the dominating flow regimes to be identified; hence it is used to know the type of aquifer. The characteristic shapes of the curves can also help in selecting the appropriate model.

It is recommended that both plots are produced, since each has its significant.

MODELS FOR INTERPRETATION OF PUMPING TESTS DATA

Models for the interpretation of pumping test data were initiated by Thiem (1906) under constant pumping test rate and steady-state conditions for confined and unconfined aquifers. Since then, different methods have been designed for pumping test analysis. The regular analytical methods of pumping test are discussed below:

1. Theis (1935) - Curve fitting method

The Theis equations below, describes transient (non-equilibrium) flow towards a fully penetrating well in a confined aquifer, forming the bases for all pumping test analysis. Using theses equation, the transmissivity and storage coefficients can be calculated from drawdowns without the need of stabilization of pump water levels as in the case of steady state methods. In addition, only one observation well (piezometer) or only the pumping well may be needed to calculate the hydrogeologic parameters of the aquifer as opposed to steady state observations that require at least two observation wells.

The non-equilibrium equation proposed by Theis (1935) for the ideal aquifer is

$$s = Q/4\pi T\, W(u) \ldots\ldots \text{ confined aquifer} \qquad 1$$

$$s' = s - (s^2/2b) \ldots\ldots \text{ unconfined aquifer} \qquad 2$$

$$u = r^2S/4Tt$$

Where:

s = drawdown at a point in the vicinity of a well pumped at a constant rate (m)

s' = pseudo-drawdown, i.e. if no dewatering had occurred.

Q = discharge of the well (m^3/s)

T =Transmissibility (m^2/s)

r = distance from pumped well to the observation well (m)

S = coefficient of storage of aquifer

t = time of the well pumped (min)

W (u) = well function of u

Because of the complications in solving equations (1) and (2), the best alternative is by graphical methods, which gives values for T and S using type curves (fig. AIII.2).

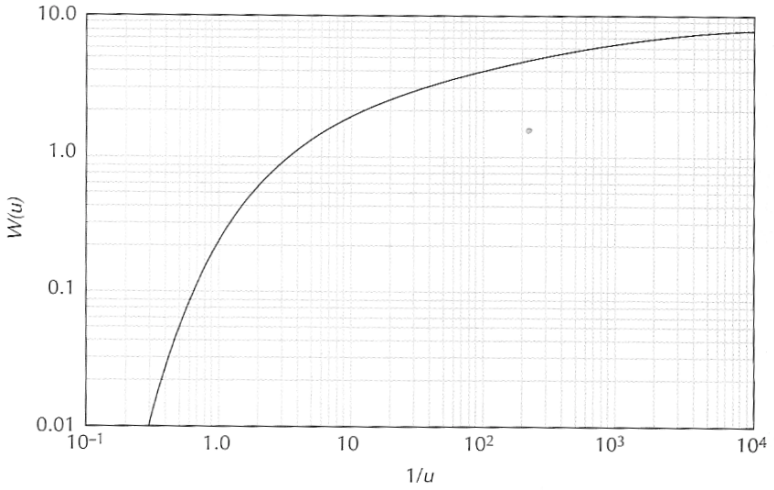

Figure AII1.2: showing the relationship between well function W (u) and 1/u.

The Theis (1935) type curve consists of plotting the values of W (u) and versus 1/u on a log-log paper. Calculated drawdowns of observation well (s) are plotted versus time (t) making sure that both curves have the identical logarithmic scales and cycles. The field curve is superimposed on the type curve, keeping coordinates axis of both curves parallel. A match point is selected on the overlapping graphs, defined by four coordinates; W (u) and 1/u on the Theis curve, drawdown s and time t on the field graph. Substitute the values of W(u), s, and Q into Equation 1 and solve for T. Calculate S by substituting the values of T, t/r2, and u into Equation 2.

2. Cooper –Jacob method (1946)

This is a modification of the Theis (non-equilibrium) equation. It considers the fact that the parameter *u* becomes very small for large values of *t* and small values of *r* (i.e. when an observation well is close to the pumping well). When *u* is equal or less than 0.05, the well function is considered in practice and assumes steady-shape conditions of the cone of depression of the pumping well.

$$W(u) = \ln 2.25Tt/r^2 S$$

This brings the Theis equation 1 to:

$$s = Q/4\pi T \ln 2.25Tt/r^2S$$

If the discharge rate (Q) is kept constant, and assuming that the transmissivity (T) and storage coefficient (S) remain the same (implying that u u ≤ 0.05), the time t_c at which steady-shape conditions would develop is given by:

$$t_c = 7.20r^2S/T$$

If a steady-state condition were satisfied, the semi-log graph of drawdowns (vertical/arithmetic axis) versus time (horizontal/logarithmic axis) would fall on a straight line when plotted on a semi-logarithmic paper.

From the graph, the transmissivity and storage coefficient are given as:

$$T = 2.3Q/4\pi\Delta s, \ldots\ldots\ldots 3, \quad \text{and}$$

$$S = 2.25Tt_0/r^2 \ldots\ldots\ldots\ldots 4$$

Where,

Q = pumping rate, proportional to the slope of the straight line.

Δs = drawdown across one log cycle

t_0 = point of intersection of the straight line to the zero drawdown line

r = distance of the observation well to pumping well

The Cooper-Jacob method is quite useful in identifying the heterogeneity of an aquifer. In the analysis of multiple wells, the transmissivity or storage coefficient can be calculated from the time drawdown graph of any of the wells, since the results would be the same, if the aquifer were homogeneous and isotropic. Before the achievement of a steady-shape condition, the drawdowns plot below the extension of the straight line. A deviation from the straight line at the beginning of pumping indicates that *u* is still greater than 0.05 and the distance *r* is quite large, requiring more time for the observation well to achieve a steady state.

3. Analytical methods for interpreting Single-well test

Kruseman and de Ridder (2000) presented many methods for the analysis of single-well constant-discharge tests. In the present work, two methods were found applicable based on the sustainability of water discharge during the pumping period and are discussed below:

- The Jacob's straight-line method which does not require any corrections for nonlinear well losses and applicable for confined or leaky aquifers, applicable for wells with continuous water flow during the pumping tests.
- Theis-recovery straight-line method, applicable for very low permeable formation, in which there is possible cessation of water during pumping. Data from both the pumping and recovery phases are used. Also, drawdown data from pumping tests conducted in boreholes that are largely affected by skin effect are also corrected by employing the residual drawdown data.

A. Jacob's straight-line method for analysis of confined and leaky aquifers

Jacob's straight-line method is applicable to analyzing the aquifer transmissivity from the drawdown data obtained in single-well constant discharge pumping tests. However, not all the assumptions underlying the Jacob method are met if data from single-well tests are used. Therefore, the following additional conditions should also be satisfied:

- For single-well tests in confined aquifers, Jacob's straight-line method is applicable when, $t > 25r^2_c/T$, where r_c is the radius of the well casing. If this time condition is met, the effect of well-bore storage can be neglected; while,
- For single-well tests in leaky aquifers, the method is applicable when $25r_c^2/T < t < cS/20$, where c is in days and S is the storativity of the aquifer. As long as $t < cS/20$ the influence of leakage is negligible. According to Mulder (1983), the values of c and S can be estimated at c=1000 days and $S = 4 \text{ X } 10^{-4}$. Hence at t < 1728seconds, the drawdown in the well is not influenced by leakage.

- To obtain the second condition entails that, the estimated T has to be checked and the straight line must connect drawdowns points that lie between $t > 25r^2_c/T$ and $t < cS/20$ (1728 seconds).

The transmissivity and the storativity of the aquifer can then be estimated using equations 3 and 4 of the Cooper-Jacob (1946) straight line method as described above. However, for single well tests, only the transmissivity can be reliably estimated, since the estimation of the storativity will require the use of at least one observation well.

Limitation

The main constraint is the need for an observation well for estimating the storativity of the aquifer. Also, the required time of pumping for the application of Jacob's method may not be attainable for aquifers with very low transmissivity, as in basement terrain areas, where there could be decrease in discharge rate or outright cessation of water during pumping test.

However, for this present work, this method may be the most suitable for estimating the hydraulic parameters of aquifers bounded by recharged boundary where there is continuous flow and enough sufficient pumping time.

Step

- On semi-log paper, plot the observed values of s, versus the corresponding time t (t on logarithmic scale) and draw a straight line through the plotted points;
- Determine the slope of the straight line, i.e. the drawdown difference Δs**,** per log cycle of time;
- Substitute the values of Q and Δs_w, into $T = 2.30Q/4\pi\Delta s_w$, and calculate T.

B. Theis-Recovery method for analysis of wells penetrating low permeable zones

Recovery data are more reliable than the drawdown data because the water-table recovers at a constant rate, which is impractical to achieve during the pumping phase in constant discharge tests. The rate of water discharge is not just a function of using the same pump capacity throughout the testing period, but it also govern by the depth of pump installation and the pressure head or the water column. The distance between the water level measured during the recovery tests and the pre-pumping level is called the residual drawdown (fig.A1.1). The time interval schedule for recovery measurements could be the same as that used during the pumping test; although, the time schedule may vary depending on the rate of recharge. If the recovery is slow, longer time intervals could be used, but when it is rapid, it is advisable to use shorter time intervals at initial stage of recovery which may not correspond to that used during the pumping phase. This was the case of the well tested at Ibarapa region, where the recharge rate varies from one borehole to another due to prevailing changing hydrogeological conditions from well to well.

The analysis of a recovery test is based on the principle of superposition. In applying this principle, it is assumed that after the pump has been shut down, the well continues to be pumped at the same discharge as before, and that an imaginary recharge, equal to the discharge, is injected into the well. The recharge and the discharge thus cancel each other, resulting in an idle well as is required for the recovery period.

The methods for analyzing residual drawdown data in recovery tests are straight-line methods. The transmissivity of the aquifer is calculated from the slope of a semi-log straight-line, i.e. from differences in residual drawdown. Those influences on the residual drawdown that become constant with time, i.e. well losses, partial penetration, do not affect the calculation of the transmissivity.

The Theis recovery method is widely used for the analysis of recovery tests and it is valid for confined, leaky and unconfined aquifers in well that is pumped at a constant rate.

A. Recovery tests after constant-discharge tests

For confined aquifers, Theis's recovery method is applicable. According to Theis (1935), the residual drawdown after a pumping test with a constant discharge is

$$s' = Q/4\pi T \ (W(u) - W(u')) \qquad 5$$

where, $u = r^2S/4KDt'$ and $u' = r^2S/4KDt'$

When u and u' are sufficiently small, equation 6.1 can be approximated by

$$s' = Q/4\pi T \ (\ln 4KDt/r^2S - \ln 4KDt'/r^2S'), \qquad 6$$

where;

s'= residual drawdown in m

r= distance in m from well to piezometer

T = transmissivity of the aquifer in m^2/d

S'= storativity during recovery, dimensionless

S= storativity during pumping, dimensionless

t= time in days since the start of pumping

t'= time in days since the cessation of pumping

Q= rate of recharge = rate of discharge in m^3/d

When S and S‘are constants and equal and T is constant, Equation 6 can also be written as

$$s' = \frac{2.30Q}{4\pi T} \log t/t' \qquad 7$$

A plot of s’ versus t/t’ on semi-log paper (t/t’ on logarithmic scale) will yield a straight line. The slope of the line is

$$\Delta s' = \frac{2.30Q}{4\pi T} \qquad 8$$

Where Δs**’** is the residual drawdown difference per log cycle of t/t’. If Δs and Q are known then the transmissivity is:

$$T = \frac{2.30Q}{4\pi \Delta s}$$

The Theis recovery method is applicable if the following assumptions and conditions are met:

- The flow to the well is in an unsteady state;
- $u < 0.01$, i.e. pumping time $tp > (25\ r_c^2 S)/T$
- $u' < 0.01$, i.e. $t' > (25\ r_c^2 S)/T$,

The Theis recovery method is also applicable to data from single-well recovery tests conducted in confined, leaky or unconfined aquifers. The following conditions are added:

A. For leaky aquifers, the sum of the pumping and recovery times should be
   $tp + t' < L^2S/20T$ or $tp + t' < cS/20$.
B. For unconfined aquifers only late-time recovery data can be used. The flow to the well is in an unsteady state;
   - $u < 0.01$, i.e. $tp > 25\ r^2 wS/T$;
   - $u' < 0.01$, i.e. $t' > 25\ r^2 wS/T$.

Step

- For each observed value of s’, calculate the corresponding value of t/t’
- Plot s’ versus t/t’ on semi-log paper (t/t’ on the logarithmic scale);
- Fit a straight line through the plotted points;
- Determine the slope of the straight line, i.e. the residual drawdown difference ‘Δs’ per log cycle of t/t’,
- Substitute the known values of Q and Δs’ into Equation 8 (i.e Δs’ = 2.30Q/4nT), and calculate T.

It is however, clear that it is difficult to stick to one analytical model for weathered-fractured dual crystalline aquifers, due to the intrinsic complexity of the groundwater flow pattern because of the notoriously heterogeneity nature of weathering pattern development and geological discontinuities in the subsurface. Cook (2003) gave a practical guide of the advantages and limitations of each approach and the principles that guide the choice of modeling approach. Therefore; for the present work, the following conditions were considered before considering a method appropriate for the analysis of the pumping test data.

- Well influences, such as well-bore storage, well-losses (skin effect) and boundary conditions;
- The volume of hydraulic properties that can be estimated from such method;
- The precision of estimation of hydraulic properties, eg Papadopulos and Cooper (1967) was preferred to Ruston-Singh method, because the estimation of storativity value is discrete and cumbersome in the latter, whereas in the former absolute values of hydraulic properties can be estimated;
- The simplicity of application of the interpretation technique. Preferable, it is better to use field data for analysis, since too much of conversion to other parameters may not represent the real field conditions.

Water transmission and storage abilities as well as other hydraulic characteristics of the water bearing zone in the subsurface can only be reliably estimated quantitatively by conducting appropriate pumping tests. The understanding of the response of aquifer to pumping through pumping tests is primary in determining the safe yield and characterizing the water bearing zones in the subsurface.

APPENDIX VB

ESTIMATION OF GROUNDWATER RECHARGE AND SPECIFIC CAPACITY

I GROUNDWATER RECHARGE

Groundwater recharge is calculated from the volume of a cylinder. The cylinder represent the inner casing through which water declines and rises during pumping and recovery tests operations from the water bearing zones.

Volume of a cylinder = $\prod r^2h$

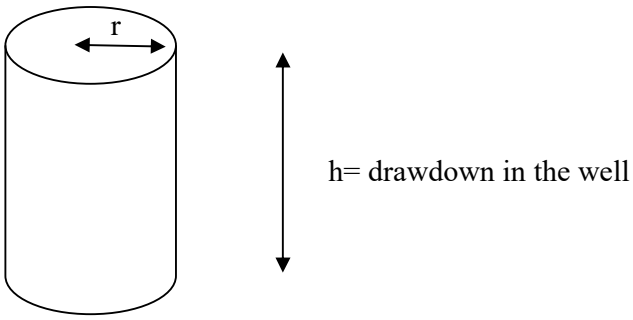

$\prod$ = constant = 3.14

r = radius of the cylinder, which otherwise represents the 4'' diameter inner casing in each well = 0.0508m

h = the residual drawdown at that particularly time during recovery phase.

Δsi = change in residual drawdown between two measured time intervals.

Note

Water discharge was obtained in the field and it is the average pumping rate per unit time

A1, A2, A3= initial residual drawdowns in 1st, 2nd and third phases of recovery corresponding to the first 15 minutes, second 15 minutes and entire recovery period respectively. (see Appendix VII).

B1, B2, B3 = final residual drawdowns after 1st, 2nd and entire phases of recovery.

C1, C2, C3 = Change in residual drawdowns ie. Δsi at the end of1st, 2nd and entire phases, equivalent to:

C1= A1-B1, C2= A2-B2, and C3= A3-B3. All in meter.

II SPECIFIC CAPACITY

The specific capacity of water bearing zones is used to estimate the efficiency of the well and it is simply the ratio of the average pumping rate or water discharge to the total drawdown in the well during the entire pumping period.

Specific capacity = discharge/total drawdown

Conversion Notation

1 meter = 39.370 inches

1 cubic meter (m^3) = 1000 liters = 264 gallon

CHANGES IN RESIDUAL DRAWDOWNS

sn	location	A1 m	A2 m	A3 m	B1 m	B2 m	B3 m	C1= A1-B1 Δsi m	C2= A2-B2 Δsi m	C3= A3-B3 Δsi m	Total recovery time minutes
1	Onilado	12.96	8.80	12.96	8.80	5.37	0.20	4.16	3.43	12.76	60
2	Sagaun	15.36	10.70	15.36	10.70	7.71	1.51	4.66	2.99	13.85	60
3	Pako	7.90	2.46	7.90	2.46	1.15	0.25	5.44	1.31	7.65	60
4	Igboole I	5.20	1.80	5.20	1.80	1.34	0.60	3.40	0.46	4.60	60
5	Igboole II	13.51	2.55	13.51	2.55	1.47	1.14	10.96	1.08	12.37	40
6	Ajegunle	8.50	2.14	8.50	2.14	1.65	1.48	6.36	0.49	7.02	40
7	Itaagbe	11.49	0.79	11.49	0.79	0.00	0.15	10.70	0.79	11.34	25
8	Alaagba I	31.90	29.00	31.90	29.00	28.00	18.85	2.90	1.00	13.05	171
9	Alaagba II	33.50	26.00	33.50	26.00	23.00	10.62	7.50	3.00	22.88	100
10	Lamperu	19.32	11.27	19.32	11.27	5.92	1.52	8.05	5.35	17.80	80
11	Abola	14.82	7.42	14.82	7.42	3.70	2.27	7.40	3.72	12.55	50
12	Apata	22.38	15.04	22.38	15.04	11.13	7.85	7.34	3.91	14.53	50
13	Agbede	6.26	0.00	6.26	0.00	0.00	1.22	10.03	0.00	8.81	10
14	Sekere	18.70	11.80	18.70	11.80	7.40	1.60	6.90	4.40	17.10	120
15	Tobalogbo	11.49	6.60	11.49	6.60	3.51	0.92	4.89	3.09	10.57	60
16	Kondo	18.40	7.97	18.40	7.97	5.53	3.63	10.43	2.44	14.77	60
17	Alabi-Oja	18.63	1.76	18.63	1.76	0.70	0.46	16.87	1.06	18.17	44
18	Apata-Faju	21.23	8.60	21.23	8.60	3.60	0.18	12.63	5.00	21.05	110
19	Idere I	9.27	6.28	9.27	6.28	5.66	1.18	2.99	0.62	8.09	120
20	Idere II	7.00	0.52	7.00	0.52	0.25	0.17	6.48	0.27	6.83	50
21	Ayete I	19.70	7.65	19.70	7.65	4.10	2.70	12.05	3.55	17.00	76
22	Ayete II	19.91	14.02	19.91	14.02	9.65	5.86	5.89	4.37	14.05	60
23	Tapa	22.04	6.50	22.04	6.50	2.00	0.16	15.54	4.50	21.88	55

RATES OF RECOVERY FOR THE PHASES AND OTHER PARAMETERS FOR AQUIFER SUSTAINABILITY

sn	location	Recovery 1st phase Liter/min.	Recovery 2nd phase Liter/min	Recovery for entire period Liter/min.	Discharge for entire pumping period Liter/min	Transmissivity Liter/min	Specific capacity
1	Onilado	2.25	1.85	1.72	30.25	0.40	3.36
2	Sagaun	2.52	1.62	1.87	68.14	0.89	6.39
3	Pako	2.94	0.71	1.03	50.86	5.38	9.27
4	Igboole I	1.84	0.25	0.62	49.95	0.77	13.83
5	Igboole II	5.92	0.58	2.51	47.17	3.39	5.03
6	Ajegunle	3.44	0.26	1.42	64.99	4.05	11.01
7	Itaagbe	5.78	0.43	3.68	38.87	0.72	4.87
8	Alaagba I	1.57	0.54	0.62	28.08	0.17	1.27
9	Alaagba II	4.05	1.62	1.85	38.05	0.36	1.64
10	Lamperu	4.35	2.89	1.80	52.72	0.45	3.93
11	Abola	4.00	2.01	2.03	22.76	0.38	2.21
12	Apata	3.97	2.11	2.35	26.30	0.35	1.69
13	Agbede	5.42	-	7.14	54.81	3.23	7.87
14	Sekere	3.73	2.38	1.15	53.50	0.61	4.12
15	Tobalogbo	2.64	1.67	1.43	48.25	0.63	6.05
16	Kondo	5.63	1.32	1.99	36.91	0.49	2.89
17	Alabi-Oja	9.11	0.57	3.35	29.10	0.39	2.25
18	Apata-Faju	6.82	2.70	1.55	69.30	0.51	4.70
19	Idere I	1.62	0.33	0.55	63.26	2.05	9.83
20	Idere II	3.50	0.15	1.11	48.90	0.83	10.06
21	Ayete I	6.51	1.92	1.81	39.45	0.78	2.88
22	Ayete II	3.18	2.36	1.90	31.68	0.39	2.29
23	Tapa	8.39	2.43	3.22	40.07	0.67	2.62

APPENDIX VI

APPARENT RESISTIVITIES AND VES COORDINATES

VES NO	1	2	3	4
AREA NAME	OYE IGANGAN	TAPA 1- IMOFIN	TAPA II-COM.HIGSCH	AIYETE-IMOFIN
LATITUDE	7 36 07.7	7 35 12.5	7 34 30.0	7 32 25.5
LONGITUDE	3 12 24.5	3 12 28.5	3 13 34.6	3 13 14.2
ELEVATION (m)	136	147	139	142

CE AB/2	PE MN/2	GF K	R1	KR1	R2	KR2	R3	KR3	R4	KR4
1.00	0.25	6.286	58.17	365.6566	138.6	871.2396	107.9	678.2594	15.87	99.75882
1.30	0.25	10.62334	26.42	280.6686	66.46	706.0272	99.95	1061.803	9.784	103.9388
1.80	0.25	20.36664	11.05	225.0514	23.97	488.1884	49.06	999.1874	4.761	96.96557
2.40	0.25	36.20736	5.113	185.1282	8.75	316.8144	24.78	897.2184	2.441	88.38217
3.20	0.25	64.36864	2.35	151.2663	2.551	164.2044	10.54	678.4455	1.125	72.41472
4.20	0.25	110.885	1.115	123.6368	0.8076	89.55076	4.068	451.0803	0.5826	64.60162
4.20	1.00	27.72126	5.505	152.6055	4.5	124.7457	21.24	588.7996	3.064	84.93794
5.50	1.00	47.53788	2.622	124.6443	1.587	75.44261	6.879	327.013	1.506	71.59204
7.50	1.00	88.39688	1.356	119.8662	0.7795	68.90536	1.818	160.7055	0.7233	63.93746
10.00	1.00	157.15	0.9091	142.8651	0.4751	74.66197	0.7866	123.6142	0.4138	65.02867
13.00	1.00	265.5835	0.67	177.9409	0.3285	87.24418	0.5023	133.4026	0.2571	68.28152
13.00	2.50	106.2334	1.758	186.7583	0.8508	90.38338	1.366	145.1148	0.6047	64.23934
18.00	2.50	203.6664	1.275	259.6747	0.5706	116.212	0.9302	189.4505	0.3475	70.77407
24.00	2.50	362.0736	0.9382	339.6975	0.4229	153.1209	0.6931	250.9532	0.239	86.53559
32.00	2.50	643.6864	0.6459	415.757	0.3154	203.0187	0.5284	340.1239	0.1798	115.7348
42.00	2.50	1108.85	0.4711	522.3794	0.2411	267.3438	0.4098	454.4069	0.1476	163.6663
55.00	2.50	1901.515	0.3355	637.9583	0.2059	391.5219	0.3204	609.2454	0.1205	229.1326
55.00	5.00	950.7575	0.7429	706.3177	0.442	420.2348	0.6429	611.242	0.2491	236.8337
75.00	5.00	1767.938	0.4289	758.2684	0.3737	660.6782	0.449	793.8039	0.2029	358.7145
100.00	5.00	3143	0.2913	915.5559	0.2441	767.2063	0.2652	833.5236		

VES NO	5	6	7	8	9
AREA NAME	IDERE-AIYETE	AIYETE-IDERE	IYANA-OBA-IDERE	IDERE MKT	AYELOG SCH IDERE
LATITUDE	7 30 57.5	7 30 50.0	7 31 03.4	7 30 23.9	7 30 10.3
LONGITUDE	3 13 39.5	7 12 33.4	3 13 59.9	3 15 06.6	3 15 23.4
ELEVATION (m)	111	93	123	189	169

CE AB/2	**PE MN/2**	**GF K**	**R5**	**KR5**	**R6**	**KR6**	**R7**	**KR7**	**R8**	**KR8**	**R9**	**KR9**
1.00	0.25	6.286	114.3	718.4898	159.8	1004.503	124.4	781.9784	222.5	1398.635	76.38	480.1247
1.30	0.25	10.62334	58.98	626.5646	79.92	849.0173	79.41	843.5994	108.2	1149.445	49.47	525.5366
1.80	0.25	20.36664	23	468.4327	28.42	578.8199	37.93	772.5067	51.19	1042.568	32.37	659.2681
2.40	0.25	36.20736	9.443	341.9061	9.754	353.1666	20.69	749.1303	15.77	570.9901	20.09	727.4059
3.20	0.25	64.36864	3.787	243.764	3.104	199.8003	10.04	646.2611	5.083	327.1858	11.15	717.7103
4.20	0.25	110.885	1.697	188.1719	1.115	123.6368	4.912	544.6673	1.486	164.7752	6.047	670.5218
4.20	1.00	27.72126	8.267	229.1717	5.394	149.5285	20.09	556.9201	8.428	233.6348	32.27	894.5651
5.50	1.00	47.53788	3.948	187.6795	2.632	125.1197	8.569	407.3521	2.39	113.6155	14.26	677.8901
7.50	1.00	88.39688	1.979	174.9374	1.617	142.9377	2.692	237.9644	0.7162	63.30984	4.56	403.0898
10.00	1.00	157.15	1.305	205.0808	1.084	170.3506	0.792	124.4628	0.3988	62.67142	1.135	178.3653
13.00	1.00	265.5835	0.9161	243.301	0.8087	214.7774	0.2893	76.83331	0.3204	85.09295	0.2421	64.29777
13.00	2.50	106.2334	2.481	263.5651	1.818	193.1323	0.8046	85.47539	0.7444	79.08014	0.7303	77.58225
18.00	2.50	203.6664	1.637	333.4019	1.265	257.638	0.2853	58.10602	0.5063	103.1163	0.1567	31.91452
24.00	2.50	362.0736	1.175	425.4365	0.8639	312.7954	0.1958	70.89401	0.3747	135.669	0.0877	31.75385
32.00	2.50	643.6864	0.668	429.9825	0.3907	251.4883	0.1547	99.57829	0.2973	191.368	0.07032	45.26403
42.00	2.50	1108.85	0.4611	511.2909	0.3045	337.6449	0.1155	128.0722	0.233	258.3621	0.0555	61.5412
55.00	2.50	1901.515	0.3445	655.0719	0.2109	401.0295	0.09413	178.9896	0.1888	359.006	0.05043	95.8934
55.00	5.00	950.7575	0.6409	609.3405	0.3596	341.8924	0.1878	178.5523	0.3465	329.4375	0.1637	155.639
75.00	5.00	1767.938	0.4309	761.8043	0.2491	440.3932	0.1456	257.4117	0.2431	429.7856	0.07604	134.434
100.00	5.00	3143	0.3064	963.0152	0.1818	571.3974	0.1064	334.4152	0.1405	441.5915	0.06128	192.603

VES NO			10		11		12		13		14	
AREA NAME			OKEDERE HIGH SCH		ISLAMIC SCH, IDERE		MET GRA SCH,IDERE		MISION sch, IDERE		DLINK HOTEL,IDERE	
LATITUDE			7 29 37.4		7 29 57.3		7 29 40.4		7 28 54.8		7 28 34.6	
LONGITUDE			3 14 06.4		3 14 12.5		3 14 52.3		3 15 16.6		3 15 43.4	
ELEVATION (m)			201		208		185		169		164	
CE AB/2	**PE MN/2**	**GF K**	**R10**	**KR10**	**R11**	**KR11**	**R12**	**KR12**	**R13**	**KR13**	**R14**	**KR14**
1.00	0.25	6.286	90.04	565.9914	32.47	204.1064	34.7	218.1242	234.7	1475.324	42.28	265.7721
1.30	0.25	10.62334	47.04	499.7219	16.47	174.9664	17.98	191.0077	133.5	1418.216	22.2	235.8381
1.80	0.25	20.36664	20.39	415.2758	6.278	127.8618	8.669	176.5584	66.87	1361.917	11.65	237.2714
2.40	0.25	36.20736	9.483	343.3544	2.642	95.65985	4.008	145.1191	31.86	1153.566	6.198	224.4132
3.20	0.25	64.36864	4.289	276.0771	1.064	68.48823	1.858	119.5969	14.26	917.8968	3.194	205.5934
4.20	0.25	110.885	1.958	217.1129	0.5525	61.26398	0.89	98.68769	3.777	418.8128	1.647	182.6277
4.20	1.00	27.72126	9.332	258.6948	2.26	62.65005	5.756	159.5636	20.49	568.0086	7.042	195.2131
5.50	1.00	47.53788	4.359	207.2176	1.275	60.61079	2.471	117.4661	8.448	401.6	3.194	151.836
7.50	1.00	88.39688	2.069	182.8931	0.7444	65.80263	0.9774	86.39911	1.537	135.866	1.105	97.67855
10.00	1.00	157.15	1.356	213.0954	0.4671	73.40477	0.4611	72.46187	0.3576	56.19684	0.3958	62.19997
13.00	1.00	265.5835	0.9995	265.4507	0.3254	86.42087	0.227	60.28745	0.1778	47.22075	0.1828	48.54866
13.00	2.50	106.2334	2.551	271.0014	0.8177	86.86705	0.6429	68.29745	0.5203	55.27324	0.4902	52.07561
18.00	2.50	203.6664	1.828	372.3022	0.5414	110.265	0.3154	64.23638	0.3274	66.68038	0.2531	51.54797
24.00	2.50	362.0736	1.336	483.7303	0.3938	142.5846	0.1989	72.01644	0.1727	62.53011	0.3706	134.1845
32.00	2.50	643.6864	0.9262	596.1823	0.3053	196.5175	0.1456	93.72074	0.1215	78.2079	0.3064	197.2255
42.00	2.50	1108.85	0.6339	702.9003	0.2431	269.5615	0.1175	130.2899	0.09292	103.0344	0.09744	108.0464
55.00	2.50	1901.515	0.4952	941.6302	0.1908	362.8091	0.09212	175.1676	0.06429	122.2484	0.06951	132.1743
55.00	5.00	950.7575	0.9372	891.0499	0.3767	358.1504	0.1928	183.306	0.1265	120.2708	0.1526	145.0856
75.00	5.00	1767.938	0.7584	1340.804	0.2792	493.6082	0.1436	253.8758	0.09975	176.3518	0.1255	221.8762
100.00	5.00	3143	0.5665	1780.51			0.1215	381.8745	0.08729	274.3525	0.09704	304.9967

VES NO			15		16		17		18		19	
AREA NAME			IGBOORA- OBA MKT		OKE-ODO		IDOFIN		OKE-AGOGO		HIGH SCH, IGBOLE	
LATITUDE			7 26 32.5		7 25 58.4		7 25 47.6		7 26 04.2		7 25 02.3	
LONGITUDE			3 16 26.6		3 16 29.9		3 17 13.1		3 17 08.5		3 18 04.1	
ELEVATION (m)			150		150		171		171		167	
CE AB/2	**PE MN/2**	**GF K**	**R15**	**KR15**	**R16**	**KR16**	**R17**	**KR17**	**R18**	**KR18**	**R19**	**KR19**
1.00	0.25	6.286	7.594	47.73588	32.47	204.1064	30.45	191.4087	127.4	800.8364	66.97	420.9734
1.30	0.25	10.62334	3.998	42.47211	16.47	174.9664	12.65	134.3853	59.79	635.1695	36.92	392.2137
1.80	0.25	20.36664	1.607	32.72919	8.699	177.1694	4.52	92.05721	25.19	513.0357	21.19	431.5691
2.40	0.25	36.20736	0.7494	27.1338	5.073	183.6799	1.858	67.27327	11.45	414.5743	12.05	436.2987
3.20	0.25	64.36864	0.3355	21.59568	3.033	195.2301	0.9523	61.29826	4.54	292.2336	6.067	390.5245
4.20	0.25	110.885	0.1567	17.37569	1.838	203.8067	0.5364	59.47874	1.868	207.1333	3.325	368.6928
4.20	1.00	27.72126	0.7564	20.96836	9.041	250.6279	2.692	74.62563	8.529	236.4346	17.27	478.7462
5.50	1.00	47.53788	0.3325	15.80634	4.671	222.0494	1.637	77.8195	3.345	159.0142	8.006	380.5882
7.50	1.00	88.39688	0.1316	11.63303	3.174	280.5717	0.9774	86.39911	1.084	95.82221	3.365	297.4555
10.00	1.00	157.15	0.06971	10.95493	1.818	285.6987	0.5886	92.49849	0.4721	74.19052	1.416	222.5244
13.00	1.00	265.5835	0.03938	10.45868	1.034	274.6133	0.3737	99.24855	0.2712	72.02625	0.6549	173.9306
13.00	2.50	106.2334	0.1052	11.17575	2.722	289.1673	0.9433	100.21	0.6831	72.56804	1.818	193.1323
18.00	2.50	203.6664	0.06788	13.82488	1.155	235.2347	0.5213	106.1713	0.3475	70.77407	0.9161	186.5788
24.00	2.50	362.0736	0.0434	15.71399	0.5354	193.8542	0.2913	105.472	0.1928	69.80779	0.5866	212.3924
32.00	2.50	643.6864	0.02873	18.49311	0.3023	194.5864	0.1567	100.8657	0.1175	75.63315	0.3897	250.8446
42.00	2.50	1108.85	0.02792	30.9591	0.1918	212.6775	0.09593	106.372	0.08338	92.45595	0.2802	310.6999
55.00	2.50	1901.515	0.01881	35.7675	0.1426	271.156	0.06529	124.1499	0.06077	115.5551	0.1979	376.3098
55.00	5.00	950.7575	0.03817	36.29041	0.2812	267.353	0.1285	122.1723	0.1245	118.3693	0.4199	399.2231
75.00	5.00	1767.938	0.03033	53.62154	0.1989	351.6428	0.08157	144.2107	0.08428	149.0018	0.3013	532.6796
100.00	5.00	3143	0.0235	73.8605	0.1376	432.4768	0.05756	180.9111	0.05665	178.051	0.2159	678.5737

VES NO	20	21	22	23	24
AREA NAME	AFRICA SCH, IGBOLE	OKE AYIN	PAKO	IGBOLE	ONILADO
LATITUDE	7 25 32.0	7 26 18.0	7 25 54.9	7 25 45.0	7 26 32.5
LONGITUDE	3 17 50.7	3 16 13.4	3 17 47.4	3 18 28.8	3 17 12.3
ELEVATION (m)	168	148	165	163	175

CE AB/2	PE MN/2	GF K	R20	KR20	R21	KR21	R22	KR22	R23	KR23	R24	KR24
1.00	0.25	6.286	71.12	447.0603	128.4	807.1224	68.39	429.8995	119.3	749.9198	25.31	159.0987
1.30	0.25	10.62334	36.01	382.5465	65.35	694.2353	28.32	300.853	60.39	641.5435	13.46	142.9902
1.80	0.25	20.36664	17.07	347.6585	31.36	638.6978	10.74	218.7377	26.22	534.0133	7.012	142.8109
2.40	0.25	36.20736	8.649	313.1575	15.77	570.9901	3.907	141.4622	11.95	432.678	3.706	134.1845
3.20	0.25	64.36864	3.626	233.4007	7.142	459.7208	1.185	76.27684	4.972	320.0409	1.647	106.0152
4.20	0.25	110.885	1.989	220.5503	3.365	373.1282	0.3877	42.99013	1.969	218.3326	0.5143	57.02818
4.20	1.00	27.72126	10.11	280.2619	17.37	481.5183	1.858	51.5061	10.14	281.0936	3.144	87.15564
5.50	1.00	47.53788	4.309	204.8407	6.459	307.0471	0.6821	32.42558	3.646	173.3231	1.697	80.67177
7.50	1.00	88.39688	1.506	133.1257	1.908	168.6612	0.2893	25.57322	1.044	92.28634	0.5645	49.90004
10.00	1.00	157.15	0.5233	82.2366	0.8669	136.2333	0.2089	32.82864	0.3767	59.19841	0.2411	37.88887
13.00	1.00	265.5835	0.2109	56.01156	0.4309	114.4399	0.3064	81.37478	0.1979	52.55897	0.1235	32.79956
13.00	2.50	106.2334	0.6459	68.61615	1.155	122.6996	0.2742	29.1292	0.5706	60.61678	0.3184	33.82471
18.00	2.50	203.6664	0.2571	52.36263	0.4832	98.4116	0.1476	30.06116	0.2953	60.14269	0.1737	35.37685
24.00	2.50	362.0736	0.1526	55.25243	0.3485	126.1826	0.1054	38.16256	0.1647	59.63352	0.1346	48.73511
32.00	2.50	643.6864	0.231	148.6916	0.2611	168.0665	0.07775	50.04662	0.1095	70.48366	0.07584	48.81718
42.00	2.50	1108.85	0.06539	72.50773	0.1838	203.8067	0.04812	53.35788	0.1034	114.6551	0.05043	55.91933
55.00	2.50	1901.515	0.04822	91.69105	0.1456	276.8606	0.03445	65.50719	0.07705	146.5117	0.03375	64.17613
55.00	5.00	950.7575	0.09895	94.07745	0.2832	269.2545	0.08508	80.89045	0.1275	121.2216	0.06881	65.42162
75.00	5.00	1767.938	0.06881	121.6518	0.1677	296.4831	0.05314	93.9482	0.1054	186.3406	0.04621	81.69639
100.00	5.00	3143	0.04972	156.27	0.1054	331.2722	0.03295	103.5619	0.0661	207.7523	0.03526	110.8222

VES NO	25	26	27	28	29
AREA NAME	ALAGBAGBA	OLOKODO	OKE-OYINBO	OKE-OYINBO II	IDI MANGORO
LATITUDE	7 27 06.6	7 26 49.5	7 26 30.2	7 26 32.8	7 26 54.6
LONGITUDE	3 17 23.7	3 16 53.6	3 17 39.7	3 17 41.2	3 18 40.0
ELEVATION (m)	168	198	179	175	145

CE AB/2	PE MN/2	GF K	R25	KR25	R26	KR26	R27	KR27	R28	KR28	R29	KR29
1.00	0.25	6.286	10.84	68.14024	20.13	126.5372	43.3	272.1838	31.86	200.272	146.6	921.5276
1.30	0.25	10.62334	6.318	67.11826	86.9	923.1682	24.91	264.6274	17.9	190.1578	87.1	925.2929
1.80	0.25	20.36664	2.622	53.40133	33.18	675.7651	12.05	245.418	8.032	163.5849	38.74	789.0036
2.40	0.25	36.20736	1.436	51.99377	13.16	476.4889	6.63	240.0548	4.128	149.464	20.09	727.4059
3.20	0.25	64.36864	0.5987	38.5375	4.4	283.222	3.596	231.4696	2.451	157.7675	7.645	492.0983
4.20	0.25	110.885	0.2461	27.28881	1.496	165.884	2.421	268.4527	1.567	173.7569	2.21	245.0559
4.20	1.00	27.72126	1.054	29.21821	8.358	231.6943	11.65	322.9527	6.539	181.2693	12.55	347.9018
5.50	1.00	47.53788	0.454	21.5822	2.009	95.50359	7.434	353.3966	4.169	198.1854	3.988	189.581
7.50	1.00	88.39688	0.1727	15.26614	0.5404	47.76967	4.872	430.6696	2.4	212.1525	0.7142	63.13305
10.00	1.00	157.15	0.08448	13.27603	0.236	37.0874	3.415	536.6673	1.446	227.2389	0.2481	38.98892
13.00	1.00	265.5835	0.05213	13.84487	0.1456	38.66896	2.441	648.2893	0.8408	223.3026	0.1557	41.35135
13.00	2.50	106.2334	0.1396	14.83018	0.3867	41.08046	6.992	742.7839	2.22	235.8381	0.4279	45.45727
18.00	2.50	203.6664	0.08137	16.57233	0.232	47.2506	4.068	828.5149	1.074	218.7377	5.615	1143.587
24.00	2.50	362.0736	0.05875	21.27182	0.1547	56.01279	2.501	905.5461	0.5726	207.3233	0.1778	64.37669
32.00	2.50	643.6864	0.03917	25.2132	0.1135	73.05841	1.446	930.7705	0.3064	197.2255	0.1275	82.07002
42.00	2.50	1108.85	0.02983	33.07701	0.08328	92.34506	0.8187	907.8158	0.1778	197.1536	0.08026	88.99633
55.00	2.50	1901.515	0.0238	45.25606	0.05816	110.5921	0.3847	731.5128	0.09644	183.3821	0.08277	157.3884
55.00	5.00	950.7575	0.04982	47.36674	0.1074	102.1114	0.7182	682.834	0.223	212.0189	0.1406	133.6765
75.00	5.00	1767.938	0.03948	69.79817	0.07082	125.2053	0.3365	594.911	0.1386	245.0361	0.1366	241.5003
100.00	5.00	3143	0.03214	101.016	0.05153	161.9588	0.1788	561.9684	0.0881	276.8983	0.1175	369.3025

VES NO	30	31	32	33
AREA NAME	ITA-AGBE	IDOFIN	JAGUNODE I	JAGUNODE II
LATITUDE	7 26 19.4	7 25 17.5	7 24 39.4	7 23 13.3
LONGITUDE	3 16 57.4	3 16 24.7	3 15 22.3	3 13 53.9
ELEVATION (m)	136	151	158	150

CE AB/2	PE MN/2	GF K	R30	KR30	GF K	R31	KR31	R32	KR32	R33	KR33
1.00	0.25	6.286	12.34	77.56924	6.286	25.29	158.97	177.00	1112.62	236.70	1487.90
1.30	0.25	10.62334	5.033	53.46727	10.62334	11.53	122.49	82.35	874.83	137.50	1460.71
1.80	0.25	20.36664	1.788	36.41555	20.36664	4.41	89.82	27.82	566.60	65.25	1328.92
2.40	0.25	36.20736	0.9101	32.95232	36.20736	1.94	70.17	11.35	410.95	30.45	1102.51
3.20	0.25	64.36864	0.4651	29.93785	64.36864	1.03	66.56	4.73	304.53	12.35	794.95
4.20	0.25	110.885	0.3043	33.74232	110.885	0.64	70.84	1.86	206.02	4.68	519.05
4.20	1.00	27.72126	1.557	43.162	27.72126	3.03	84.08	9.74	270.12	21.39	592.96
5.50	1.00	47.53788	0.9865	46.89611	47.53788	1.99	94.55	3.58	170.00	7.43	353.40
7.50	1.00	88.39688	0.5424	47.94647	88.39688	1.35	118.98	1.33	117.21	2.43	214.89
10.00	1.00	157.15	0.3435	53.98103	157.15	0.90	141.91	0.69	108.43	1.16	181.51
13.00	1.00	265.5835	0.2139	56.80831	265.5835	0.77	204.63	0.50	132.58	0.70	186.76
13.00	2.50	106.2334	0.5766	61.25418	106.2334	1.97	209.17	1.46	154.68	1.89	200.57
18.00	2.50	203.6664	0.235	47.8616	203.6664	1.54	313.04	1.03	210.59	1.10	223.01
24.00	2.50	362.0736	0.1165	42.18157	362.0736	1.30	468.89	0.77	279.34	0.70	252.76
32.00	2.50	643.6864	0.06509	41.89755	643.6864	1.06	684.88	0.60	385.38	0.51	329.76
42.00	2.50	1108.85	0.04771	52.90325	1108.85	0.83	916.69	0.46	513.51	0.40	444.43
55.00	2.50	1901.515	0.03365	63.98598	1901.515	0.62	1188.07	0.33	628.45	0.30	561.52
55.00	5.00	950.7575	0.06881	65.42162	950.7575	1.29	1221.72	0.72	687.68	0.57	542.50
75.00	5.00	1767.938	0.05133	90.74823	1767.938	0.91	1616.07	0.30	530.91	0.33	578.82
100.00	5.00	3143			3143	0.62	1954.32	0.18	571.40	0.20	628.29

VES NO	34	35	36	37	38
AREA NAME	IGBO-OLORIN			ABOLA	ARAROMI
LATITUDE	7 22 33.4	7 24 18.2	7 23 55.4	7 30 05.0	7 29 20.4
LONGITUDE	3 12 20.2	3 10 34.3	3 09 47.1	3 09 58.0	3 08 23.0
ELEVATION (m)	121	150M		154	161

CE AB/2	PE MN/2	GF K	R34	KR34	R35	KR35	R36	KR36	R37	KR37	R38	KR38
1.00	0.25	6.286	2.50	15.70	1.01	6.35	1.35	8.45	173.00	1087.48	228.60	1436.98
1.30	0.25	10.62334	1.34	14.19	2.91	30.95	5.23	55.59	98.53	1046.72	131.50	1396.97
1.80	0.25	20.36664	5.09	103.73	3.16	64.28	1.84	37.43	44.00	896.13	61.81	1258.86
2.40	0.25	36.20736	7.91	286.26	3.32	120.14	4.21	152.40	17.90	648.11	27.01	977.96
3.20	0.25	64.36864	9.01	580.03	3.49	224.65	2.74	176.43	5.89	378.87	9.48	610.15
4.20	0.25	110.885	12.35	1369.43	1.95	216.00	2.10	232.75	1.83	202.70	2.77	307.37
4.20	1.00	27.72126	11.45	317.41	1.77	49.01	2.05	56.80	10.34	286.64	14.36	398.08
5.50	1.00	47.53788	10.44	496.30	1.98	94.08	2.90	138.00	3.84	182.40	3.82	181.45
7.50	1.00	88.39688	7.08	626.03	0.76	67.39	4.60	406.71	1.72	151.78	0.95	83.83
10.00	1.00	157.15	2.10	329.86	2.14	336.14	13.45	2113.67	0.97	151.87	0.44	69.77
13.00	1.00	265.5835	2.58	685.47	0.95	253.45	2.74	727.96	0.56	149.66	0.29	77.10
13.00	2.50	106.2334	2.56	272.06	0.83	88.14	2.57	273.13	1.39	147.24	0.70	74.70
18.00	2.50	203.6664	0.79	161.63	1.34	272.10	0.22	45.62	0.76	154.66	0.40	82.44
24.00	2.50	362.0736	0.57	205.48	2.20	796.56	7.46	2702.52	0.46	167.31	0.58	210.22
32.00	2.50	643.6864	1.65	1060.15	4.39	2825.78	12.65	8142.63	0.26	168.07	0.20	126.03
42.00	2.50	1108.85	4.19	4643.87	6.92	7674.35	5.35	5936.79	0.18	197.15	0.78	867.68
55.00	2.50	1901.515	2.01	3820.14	4.83	9188.12	2.97	5655.11	0.14	259.75	0.10	190.06
55.00	5.00	950.7575	3.18	3027.21	4.88	4636.84	1.54	1461.31	0.27	257.85	0.19	178.55
75.00	5.00	1767.938	0.88	1560.56	10.73	18969.97	3.85	6801.26	0.24	417.23	0.14	255.64
100.00	5.00	3143	2.25	7071.75	16.08	50539.44			0.12	378.73	0.20	633.00
133.00	5.00	5559.653							0.08	418.31		
133.00	10.00	2779.826							0.16	443.94		

VES NO	39	40	41	42
AREA NAME	ABULE-OBA	FEDEGBO	ABOKOLAIYA	BADA
LATITUDE	7 32 28.6	7 33 08.2	7 34 27.4	7 33 57.9
LONGITUDE	3 08 34.8	3 08 53.3	3 08 18.7	3 09 06.6
ELEVATION (m)	174	179	169	199

CE AB/2	PE MN/2	GF K	R39	KR39	GF K	R40	KR40	R41	KR41	R42	KR42
1.00	0.25	6.286	85.89	539.90	6.286	164.90	1036.56	530.20	3332.84	274.10	1722.99
1.30	0.25	10.62334	46.74	496.53	10.62334	71.72	761.91	290.60	3087.14	140.60	1493.64
1.80	0.25	20.36664	20.09	409.17	20.36664	26.01	529.74	122.40	2492.88	65.65	1337.07
2.40	0.25	36.20736	9.30	336.80	36.20736	10.64	385.25	56.75	2054.77	29.13	1054.72
3.20	0.25	64.36864	3.87	248.91	64.36864	4.92	316.82	26.10	1680.02	10.00	643.69
4.20	0.25	110.885	1.65	182.63	110.885	2.06	228.31	12.34	1368.32	3.32	367.58
4.20	1.00	27.72126	7.07	196.04	27.72126	12.75	353.45	58.88	1632.23	16.97	470.43
5.50	1.00	47.53788	2.48	117.94	47.53788	5.69	270.30	25.69	1221.25	5.98	284.13
7.50	1.00	88.39688	0.83	73.79	88.39688	2.48	219.31	11.12	982.97	2.78	245.92
10.00	1.00	157.15	0.36	55.88	157.15	1.35	211.52	5.72	898.27	1.52	238.24
13.00	1.00	265.5835	0.14	37.34	265.5835	0.63	168.27	3.30	875.89	0.99	261.73
13.00	2.50	106.2334	0.45	47.81	106.2334	1.97	209.17	9.76	1037.26	2.42	257.19
18.00	2.50	203.6664	0.22	44.60	203.6664	1.03	210.59	5.34	1088.39	1.38	280.24
24.00	2.50	362.0736	0.13	46.53	362.0736	0.67	241.87	4.97	1800.23	0.82	298.60
32.00	2.50	643.6864	0.09	58.07	643.6864	0.43	276.72	2.20	1416.11	0.50	322.62
42.00	2.50	1108.85	0.05	54.02	1108.85	0.40	447.75	1.41	1559.04	0.32	355.28
55.00	2.50	1901.515	0.04	78.87	1901.515	0.19	370.42	1.00	1894.86	0.22	412.44
55.00	5.00	950.7575	0.09	81.08	950.7575	0.40	375.93	1.90	1804.54	0.45	431.64
75.00	5.00	1767.938	0.05	93.90	1767.938	0.18	314.69	0.58	1017.62	0.27	474.16
100.00	5.00	3143	0.04	130.03	3143	0.16	489.68	0.29	915.56	0.20	632.37
133.00	5.00	5559.653	0.02	106.86	5559.653			0.16	882.32		
133.00	10.00	2779.826	0.08	227.78	2779.826			0.30	832.00		

VES NO			43		44		45		46		47	
AREA NAME			ALALADE						OKE-AYIN		EJEGUN	
LATITUDE			7 34 19.7		7 33 41.5		7 33 48.2		7 27 19.9		7 28 04.1	
LONGITUDE			3 09 28.7		3 10 05.0		3 09 34.2		3 14 56.2		3 14 25.8	
ELEVATION (m)			161		149		163		171		197	
CE AB/2	**PE MN/2**	**GF K**	**R43**	**KR43**	**R44**	**KR44**	**R45**	**KR45**	**R46**	**KR46**	**R47**	**KR47**
1.00	0.25	6.286	393.60	2474.17	75.67	475.66	228.60	1436.98	226.60	1424.41	418.10	2628.18
1.30	0.25	10.62334	188.10	1998.25	43.30	459.99	131.50	1396.97	145.60	1546.76	202.30	2149.10
1.80	0.25	20.36664	61.10	1244.40	17.68	360.08	66.36	1351.53	83.20	1694.50	98.03	1996.54
2.40	0.25	36.20736	22.50	814.67	7.54	273.15	37.93	1373.35	45.52	1648.16	43.50	1575.02
3.20	0.25	64.36864	7.21	464.29	2.45	157.77	17.07	1098.77	27.42	1764.99	15.47	995.78
4.20	0.25	110.885	2.50	277.32	0.95	105.04	6.62	734.06	15.37	1704.30	4.81	533.58
4.20	1.00	27.72126	15.47	428.85	5.72	158.45	31.56	874.88	115.30	3196.26	25.21	698.85
5.50	1.00	47.53788	4.27	202.94	1.91	90.70	9.80	466.06	60.39	2870.81	10.04	477.28
7.50	1.00	88.39688	0.82	72.55	0.88	77.52	3.13	277.04	20.39	1802.41	4.10	362.25
10.00	1.00	157.15	0.23	35.52	0.46	72.30	1.27	198.79	5.47	858.82	3.49	547.67
13.00	1.00	265.5835	0.10	27.46	0.27	72.56	0.72	192.10	1.13	299.05	1.28	338.62
13.00	2.50	106.2334	0.28	29.66	0.79	83.45	2.34	248.59	3.89	412.93	3.23	343.56
18.00	2.50	203.6664	0.16	32.12	0.51	102.91	1.27	257.64	0.65	133.38	1.63	331.37
24.00	2.50	362.0736	0.11	41.46	0.21	76.72	0.41	147.04	0.24	87.66	0.91	330.61
32.00	2.50	643.6864	0.04	23.15	0.13	86.00	0.67	429.98	0.15	99.58	0.58	375.66
42.00	2.50	1108.85	0.10	114.66	0.08	92.46	0.49	543.56	0.14	157.01	0.36	394.31
55.00	2.50	1901.515	0.06	107.72	0.05	102.95	0.42	790.84	0.11	217.72	0.24	446.86
55.00	5.00	950.7575	0.11	101.16	0.11	100.21	0.74	699.09	0.19	177.03	2.71	2578.45
75.00	5.00	1767.938	0.06	98.03	0.08	140.13	0.51	909.25	0.11	200.66	1.22	2148.04
100.00	5.00	3143	0.08	260.46	0.01	34.73	0.32	1010.16	0.09	270.93	1.01	3180.72

VES NO			48		49		50		51		52	
AREA NAME			GOBA		OFIKI		ALARABA				AGBEDE	
LATITUDE			7 26 31.6		7 27 15.7		7 27 21.0		7 24 29.4		7 23 18.2	
LONGITUDE			3 14 24.0		3 11 09.1		3 09 37.4		3 12 09.1		3 11 58.5	
ELEVATION (m)			195		112		133		144			
CE AB/2	**PE MN/2**	**GF K**	**R48**	**KR48**	**R49**	**KR49**	**R50**	**KR50**	**R51**	**KR51**	**R52**	**KR52**
1.00	0.25	6.286	576.10	3621.36	310.50	1951.80	579.70	3643.99	141.60	890.10	37.33	234.66
1.30	0.25	10.62334	343.60	3650.18	191.20	2031.18	387.40	4115.48	75.97	807.06	20.89	221.92
1.80	0.25	20.36664	163.80	3336.06	84.78	1726.68	192.20	3914.47	32.37	659.27	8.93	181.87
2.40	0.25	36.20736	66.06	2391.86	39.15	1417.52	91.55	3314.78	13.26	480.11	4.29	155.29
3.20	0.25	64.36864	27.22	1752.11	14.06	905.02	37.77	2431.20	4.56	293.52	1.89	121.53
4.20	0.25	110.885	11.35	1258.55	5.07	562.52	15.37	1704.30	1.53	169.21	0.89	98.91
4.20	1.00	27.72126	55.84	1547.96	24.51	679.45	62.72	1738.68	8.80	243.95	3.99	110.55
5.50	1.00	47.53788	19.79	940.77	6.40	304.19	21.39	1016.84	2.76	131.30	1.93	91.65
7.50	1.00	88.39688	9.34	825.80	1.10	96.79	4.93	435.97	0.78	69.17	0.85	74.85
10.00	1.00	157.15	2.11	331.43	0.26	40.87	1.20	187.79	0.39	60.77	0.43	67.40
13.00	1.00	265.5835	1.10	290.81	0.14	36.01	0.65	172.60	0.30	79.22	0.27	72.03
13.00	2.50	106.2334	2.69	285.98	0.35	37.02	1.63	173.16	0.75	79.93	0.76	80.78
18.00	2.50	203.6664	1.53	310.79	0.25	50.73	1.77	360.08	0.48	98.00	0.39	80.20
24.00	2.50	362.0736	0.92	334.19	0.16	59.63	1.35	487.35	0.33	118.18	0.22	80.74
32.00	2.50	643.6864	0.79	507.61	0.10	67.20	0.94	602.62	0.22	143.54	0.13	81.43
42.00	2.50	1108.85	0.56	622.62	0.06	68.62	0.89	991.31	0.15	170.43	0.09	103.70
55.00	2.50	1901.515	0.43	809.86	0.07	127.97	0.77	1468.92	0.11	212.02	0.07	128.16
55.00	5.00	950.7575	0.77	734.84	0.13	127.02	1.05	1002.10	0.24	232.08	0.11	106.96
75.00	5.00	1767.938	0.57	1005.07	0.09	163.39	0.65	1143.68	0.19	332.02	0.08	143.86
100.00	5.00	3143	0.41	1278.26	0.06	193.23	0.51	1603.87	0.15	476.48	0.05	167.02

VES NO			53		54		55		56		57	
AREA NAME			AYANLEKE		TOBALOGBO				AFEFU-AIYETE		IYALASE	
LATITUDE			7 30 45.4		7 32 09.2		7 32 10.5		7 32 45.7		7 33 46.0	
LONGITUDE			3 16 29.7		3 16 54.8		3 18 06.9		3 15 16.3		3 16 45.9	
ELEVATION (m)			191		180		168		223		196	
CE AB/2	PE MN/2	GF K	R53	KR53	R54	KR54	R55	KR55	R56	KR56	R57	KR57
1.00	0.25	6.286	116.3	731.06	337.50	2121.53	139.6	877.53	414	2602.40	106.2	667.57
1.30	0.25	10.62334	70.81	752.24	191.20	2031.18	72.43	769.45	221.5	2353.07	49.57	526.60
1.80	0.25	20.36664	35.91	731.37	78.91	1607.13	32.27	657.23	109.2	2224.04	17.27	351.73
2.40	0.25	36.20736	19.08	690.84	27.82	1007.29	11.35	410.95	58.88	2131.89	6.459	233.86
3.20	0.25	64.36864	9.161	589.68	10.14	652.70	3.74	240.74	27.92	1797.17	1.727	111.16
4.20	0.25	110.885	4.098	454.41	2.79	309.59	1.074	119.09	13.56	1503.60	0.506	56.11
4.20	1.00	27.72126	21.19	587.41	12.95	359.07	5.454	151.19	60.29	1671.31	2.31	64.04
5.50	1.00	47.53788	8.046	382.49	3.06	145.66	1.577	74.97	24.81	1179.41	0.785	37.32
7.50	1.00	88.39688	2.169	191.73	0.74	65.24	0.593	52.42	8.91	787.62	0.35	30.94
10.00	1.00	157.15	0.623	97.90	0.37	58.77	0.315	49.50	3.124	490.94	0.239	37.56
13.00	1.00	265.5835	0.214	56.83	0.22	57.87	0.205	54.44	0.937	248.85	0.143	37.98
13.00	2.50	106.2334	0.654	69.48	0.67	70.65	0.472	50.14	2.601	276.31	0.398	42.28
18.00	2.50	203.6664	0.209	42.57	0.28	57.64	0.268	54.58	0.717	146.03	0.267	54.38
24.00	2.50	362.0736	0.13	47.07	0.35	125.28	0.228	82.55	0.371	134.33	0.204	73.86
32.00	2.50	643.6864	0.0938	60.38	0.15	94.62	0.119	76.60	0.267	171.86	0.149	95.91
42.00	2.50	1108.85	0.0584	64.76	0.10	109.78	0.085	94.25	0.184	204.03	0.112	124.19
55.00	2.50	1901.515	0.04189	79.65	0.07	141.28	0.069	131.20	0.176	334.67	0.089	169.23
55.00	5.00	950.7575	0.09141	86.91	0.17	158.78	0.144	136.91	0.478	454.46	0.188	178.74
75.00	5.00	1767.938	0.0561	99.18	0.08	149.21	0.096	169.72	0.173	305.85	0.124	219.22
100.00	5.00	3143	0.03817	119.97	0.06	190.78	0.0656	206.18	0.135	424.31	0.0924	290.41

VES NO	58	59	60	61	62
AREA NAME	KONDO	ALABI-OJA	BALOGUN	ALABI-ILUMO	APARA
LATITUDE	7 34 44.9	7 35 43.3	7 33 50.7	7 31 40.3	7 30 11.8
LONGITUDE	3 18 31.5	3 18 11.5	3 19 04.4	3 19 32.1	3 18 54.5
ELEVATION (m)	194m	174m	188m	172m	153m

CE AB/2	**PE MN/2**	**GF K**	**R58**	**KR58**	**R59**	**KR59**	**R60**	**KR60**	**R61**	**KR61**	**R62**	**KR62**
1.00	0.25	6.286	92.77	583.15	314	1973.80	126.4	794.55	35.3	221.90	233.7	1469.04
1.30	0.25	10.62334	51.39	545.93	180	1912.20	62.92	668.42	19.18	203.76	129.4	1374.66
1.80	0.25	20.36664	22.56	459.47	88.01	1792.47	26.72	544.20	11.05	225.05	50.98	1038.29
2.40	0.25	36.20736	10.14	367.14	39.55	1432.00	10.95	396.47	6.519	236.04	16.87	610.82
3.20	0.25	64.36864	4.209	270.93	15.77	1015.09	4.38	281.93	3.676	236.62	5.786	372.44
4.20	0.25	110.885	1.707	189.28	6.84	758.45	1.697	188.17	1.858	206.02	1.888	209.35
4.20	1.00	27.72126	8.338	231.14	31.86	883.20	7.855	217.75	7.534	208.85	7.825	216.92
5.50	1.00	47.53788	3.204	152.31	13.66	649.37	2.491	118.42	3.546	168.57	3.064	145.66
7.50	1.00	88.39688	1.356	119.87	6.439	569.19	0.698	61.70	1.406	124.29	1.727	152.66
10.00	1.00	157.15	0.756	118.81	3.837	602.98	0.316	49.66	0.667	104.82	1.135	178.37
13.00	1.00	265.5835	0.459	121.90	2.481	658.91	0.2001	53.14	0.403	107.03	0.751	199.45
13.00	2.50	106.2334	1.185	125.89	6.439	684.04	0.482	51.20	1.034	109.85	2.169	230.42
18.00	2.50	203.6664	0.643	130.96	3.144	640.33	0.293	59.67	0.598	121.79	1.336	272.10
24.00	2.50	362.0736	0.407	147.36	1.888	683.59	0.212	76.76	0.396	143.38	0.896	324.42
32.00	2.50	643.6864	0.269	173.15	1.205	775.64	0.153	98.48	0.256	164.78	0.562	361.75
42.00	2.50	1108.85	0.182	201.81	0.747	828.31	0.12	133.06	0.172	190.72	0.406	450.19
55.00	2.50	1901.515	0.135	256.70	0.478	908.92	0.091	173.04	0.12	228.18	0.266	505.80
55.00	5.00	950.7575	0.289	274.77	1.024	973.58	0.156	148.32	0.252	239.59	0.559	531.47
75.00	5.00	1767.938	0.156	275.80	0.445	786.73	0.1064	188.11	0.147	259.89	0.404	714.25
100.00	5.00	3143	0.1004	315.56	0.288	905.18	0.08187	257.32	0.0856	269.04		

VES NO	63	64	65	66	67
AREA NAME		OLA-IROKO	GAA-BABAODE	OLOPOTO	OREMEJI
LATITUDE	7 30 35.2	7 29 04.8	7 29 03.3	7 27 36.5	7 27 13.4
LONGITUDE	3 18 52.6	3 18 04.1	3 17 19.4	3 16 50.9	3 16 48.3
ELEVATION (m)	154	183	213	169	176

CE AB/2	PE MN/2	GF K	R63	KR63	R64	KR64	R65	KR65	R66	KR66	R67	KR67
1.00	0.25	6.286	82.34	517.59	84.37	530.35	234.7	1475.32	295.4	1856.88	44.11	277.28
1.30	0.25	10.62334	45.42	482.51	37.43	397.63	123.4	1310.92	177	1880.33	28.83	306.27
1.80	0.25	20.36664	18.38	374.34	15.97	325.26	54.22	1104.28	66.77	1359.88	16.07	327.29
2.40	0.25	36.20736	7.886	285.53	8.639	312.80	20.89	756.37	24.88	900.84	10.14	367.14
3.20	0.25	64.36864	2.973	191.37	3.214	206.88	7.544	485.60	7.825	503.68	6.057	389.88
4.20	0.25	110.885	0.916	101.57	1.346	149.25	2.762	306.26	2.27	251.71	3.586	397.63
4.20	1.00	27.72126	4.761	131.98	6.027	167.08	14.86	411.94	9.634	267.07	15.37	426.08
5.50	1.00	47.53788	1.416	67.31	2.2	104.58	5.575	265.02	2.662	126.55	8.227	391.09
7.50	1.00	88.39688	0.621	54.89	0.786	69.48	2.421	214.01	0.795	70.28	3.586	316.99
10.00	1.00	157.15	0.448	70.40	0.375	58.93	1.426	224.10	0.398	62.55	1.426	224.10
13.00	1.00	265.5835	0.364	96.67	0.224	59.49	0.919	244.07	0.271	71.97	0.566	150.32
13.00	2.50	106.2334	0.96	101.98	0.576	61.19	2.32	246.46	0.7363	78.22	1.486	157.86
18.00	2.50	203.6664	0.717	146.03	0.332	67.62	1.416	288.39	0.457	93.08	0.394	80.24
24.00	2.50	362.0736	0.733	265.40	0.22	79.66	0.967	350.13	0.303	109.71	0.131	47.43
32.00	2.50	643.6864	0.481	309.61	0.16	102.99	0.657	422.90	0.195	125.52	0.065	41.84
42.00	2.50	1108.85	0.387	429.13	0.117	129.74	0.444	492.33	0.13	144.15	0.0389	43.13
55.00	2.50	1901.515	0.272	517.21	0.0923	175.51	0.317	602.78	0.0889	169.04	0.0263	50.01
55.00	5.00	950.7575	0.573	544.78	0.189	179.69	0.656	623.70	0.18	171.14	0.055	52.29
75.00	5.00	1767.938	0.353	624.08	0.125	220.99	0.384	678.89	0.108	190.94	0.0367	64.88
100.00	5.00	3143	0.267	839.18	0.096	301.73	0.26	817.18	0.08	251.44	0.0303	95.23

VES NO	68	69	70	71	72
AREA NAME	OKE-ONILADO		OLOROMBO	OKE-OYINBO III	ABA-ELESIN
LATITUDE	7 27 42.6	7 28 18.0	7 27 32.6	7 26 45.9	7 24 20.8
LONGITUDE	3 17 16.4	3 17 32.0	3 17 50.8	3 17 54.4	3 17 39.6
ELEVATION (m)	182	199	159	148	145

CE AB/2	PE MN/2	GF K	R68	KR68	R69	KR69	R70	KR70	R71	KR71	R72	KR72
1.00	0.25	6.286	19.72	123.96	84.17	529.09	85.89	539.90	684.2	4300.88	56.35	354.22
1.30	0.25	10.62334	9.935	105.54	39.05	414.84	32.27	342.82	329.3	3498.27	28.12	298.73
1.80	0.25	20.36664	4.098	83.46	13.86	282.28	8.087	164.71	148.7	3028.52	12.55	255.60
2.40	0.25	36.20736	1.878	68.00	5.244	189.87	1.768	64.01	65.98	2388.96	4.621	167.31
3.20	0.25	64.36864	0.974	62.70	1.828	117.67	0.422	27.16	62.32	4011.45	1.647	106.02
4.20	0.25	110.885	0.511	56.66	0.885	98.13	0.203	22.51	9.905	1098.32	0.593	65.75
4.20	1.00	27.72126	2.039	56.52	3.988	110.55	0.883	24.48	45.02	1248.01	2.64	73.18
5.50	1.00	47.53788	1.024	48.68	2.059	97.88	0.541	25.72	15.16	720.67	0.881	41.88
7.50	1.00	88.39688	0.461	40.75	1.074	94.94	0.32	28.29	4.128	364.90	0.417	36.86
10.00	1.00	157.15	0.235	36.93	0.594	93.35	0.233	36.62	1.135	178.37	0.42	66.00
13.00	1.00	265.5835	0.143	37.98	0.36	95.61	0.218	57.90	0.299	79.41	0.299	79.41
13.00	2.50	106.2334	0.366	38.88	1.004	106.66	0.395	41.96	0.934	99.22	0.412	43.77
18.00	2.50	203.6664	0.214	43.58	0.434	88.39	0.26	52.95	0.35	71.28	0.314	63.95
24.00	2.50	362.0736	0.141	51.05	0.224	81.10	0.291	105.36	0.287	103.92	0.251	90.88
32.00	2.50	643.6864	0.094	60.51	0.128	82.39	0.142	91.40	0.145	93.33	0.1958	126.03
42.00	2.50	1108.85	0.0679	75.29	0.0866	96.03	0.114	126.41	0.107	118.65	0.1406	155.90
55.00	2.50	1901.515	0.0501	95.27	0.0595	113.14	0.0911	173.23	0.102	193.95	0.1064	202.32
55.00	5.00	950.7575	0.0942	89.56	0.144	136.91	0.182	173.04	0.172	163.53	0.174	165.43
75.00	5.00	1767.938	0.0664	117.39	0.0904	159.82	0.136	240.44	0.129	228.06	0.128	226.30
100.00	5.00	3143	0.05123	161.02	0.0737	231.64	0.104	326.87	0.099	311.16	0.091	286.01

VES NO	73	74	75	76	77
AREA NAME			GAA-ESEPO	ABULE-OGUN	IGBO-OLORI
LATITUDE	7 23 39.5	7 24 05.8	7 24 08.4	7 21 28.9	7 22 07.5
LONGITUDE	3 17 21.6	3 17 09.4	3 14 54.5	3 11 46.9	3 11 34.3
ELEVATION (m)	120	156	165	95	129

CE AB/2	PE MN/2	GF K	R73	KR73	R74	KR74	R75	KR75	R76	KR76	R77	KR77
1.00	0.25	6.286	284.2	1786.48	95.5	600.31	217.5	1367.21	242.8	1526.24	321.2	2019.06
1.30	0.25	10.62334	168.9	1794.28	55.92	594.06	122.4	1300.30	123.4	1310.92	200.3	2127.86
1.80	0.25	20.36664	69.4	1413.44	25.11	511.41	62.62	1275.36	55.64	1133.20	85.98	1751.12
2.40	0.25	36.20736	37.53	1358.86	13.46	487.35	33.58	1215.84	22.05	798.37	40.67	1472.55
3.20	0.25	64.36864	20.13	1295.74	7.132	459.08	16.69	1074.31	8.318	535.42	16.87	1085.90
4.20	0.25	110.885	7.645	847.72	3.777	418.81	7.403	820.88	2.722	301.83	6.027	668.30
4.20	1.00	27.72126	31.16	863.79	16.87	467.66	33.48	928.11	12.95	358.99	28.52	790.61
5.50	1.00	47.53788	11.45	544.31	8.308	394.94	12.25	582.34	3.58	170.19	8.96	425.94
7.50	1.00	88.39688	3.646	322.30	3.626	320.53	4.108	363.13	0.883	78.05	1.94	171.49
10.00	1.00	157.15	2.28	358.30	1.557	244.68	1.205	189.37	0.391	61.45	0.642	100.89
13.00	1.00	265.5835	1.245	330.65	0.781	207.42	0.522	138.63	0.256	67.99	0.375	99.59
13.00	2.50	106.2334	2.903	308.40	1.938	205.88	1.436	152.55	0.774	82.22	0.883	93.80
18.00	2.50	203.6664	2.481	505.30	1.004	204.48	0.7002	142.61	0.385	78.41	0.529	107.74
24.00	2.50	362.0736	1.115	403.71	0.591	213.99	0.566	204.93	0.334	120.93	0.384	139.04
32.00	2.50	643.6864	0.836	538.12	0.377	242.67	0.41	263.91	0.192	123.59	0.293	188.60
42.00	2.50	1108.85	0.411	455.74	0.254	281.65	0.3104	344.19	0.154	170.76	0.229	253.93
55.00	2.50	1901.515	0.228	433.55	0.176	334.67	0.235	446.86	0.146	277.62	0.166	315.65
55.00	5.00	950.7575	0.397	377.45	0.314	298.54	0.444	422.14	0.234	222.48	0.336	319.45
75.00	5.00	1767.938	0.152	268.73	0.204	360.66	0.3164	559.38	0.162	286.41	0.22	388.95
100.00	5.00	3143	0.197	619.17	0.126	396.02	0.251	788.89	0.108	339.44	0.162	509.17

VES NO			78		79		80		81		82	
AREA NAME			IDISE II		ALAFOSE				OGUNGBAYI			
LATITUDE			7 23 18.0		7 23 39.8		7 25 00.2		7 25 45.5		7 22 28.1	
LONGITUDE			3 11 21.9		3 09 55.8		3 09 55.8		3 08 52.0		3 18 14.4	
ELEVATION (m)			126		108		99		81		160	
CE AB/2	**PE MN/2**	**GF K**	**R78**	**KR78**	**R79**	**KR79**	**R80**	**KR80**	**R81**	**KR81**	**R82**	**KR82**
1.00	0.25	6.286	149.7	941.01	135.6	852.38	138.6	871.24	140.6	883.81	324.2	2037.92
1.30	0.25	10.62334	86.13	914.99	71.02	754.47	77.79	826.39	69.09	733.97	184.1	1955.76
1.80	0.25	20.36664	43.6	887.99	31.26	636.66	34.09	694.30	23.4	476.58	83.46	1699.80
2.40	0.25	36.20736	19.79	716.54	12.65	458.02	12.95	468.89	10.14	367.14	39.35	1424.76
3.20	0.25	64.36864	7.434	478.52	4.259	274.15	4.41	283.87	3.757	241.83	13.96	898.59
4.20	0.25	110.885	2.702	299.61	1.145	126.96	1.205	133.62	1.188	131.73	5.023	556.98
4.20	1.00	27.72126	12.55	347.90	5.856	162.34	6.379	176.83	5.133	142.29	22.66	628.16
5.50	1.00	47.53788	3.55	168.76	1.577	74.97	1.727	82.10	1.617	76.87	6.519	309.90
7.50	1.00	88.39688	0.822	72.66	0.593	52.42	0.5334	47.15	0.366	32.35	1.446	127.82
10.00	1.00	157.15	0.357	56.10	0.354	55.63	0.284	44.63	0.139	21.84	0.5304	83.35
13.00	1.00	265.5835	0.237	62.94	0.243	64.54	0.181	48.07	0.087	23.11	0.345	91.63
13.00	2.50	106.2334	0.6	63.74	0.581	61.72	0.508	53.97	0.852	90.51	0.836	88.81
18.00	2.50	203.6664	0.382	77.80	0.343	69.86	0.282	57.43	0.133	27.09	0.587	119.55
24.00	2.50	362.0736	0.283	102.47	0.255	92.33	0.208	75.31	0.097	35.12	1.024	370.76
32.00	2.50	643.6864	0.189	121.66	0.191	122.94	0.1084	69.78	0.0735	47.31	0.1779	114.51
42.00	2.50	1108.85	0.147	163.00	0.146	161.89	0.0594	65.87	0.0558	61.87	0.113	125.30
55.00	2.50	1901.515	0.104	197.76	0.1034	196.62	0.03616	68.76	0.0417	79.29	0.0785	149.27
55.00	5.00	950.7575	0.219	208.22	0.208	197.76	0.0666	63.32	0.08127	77.27	0.149	141.66
75.00	5.00	1767.938	0.16	282.87	0.139	245.74	0.0447	79.03	0.0574	101.48	0.099	175.03
100.00	5.00	3143	0.1044	328.13	0.09	282.87	0.03264	102.59	0.0443	139.23	0.07213	226.70

VES NO	83	84	85
AREA NAME	SEKERE	IGBOORA	IGBOORA
LATITUDE	7 21 57.1	7 25 28.9	7 25 24.5
LONGITUDE	3 18 37.3	3 19 57.8	3 18 55.4
ELEVATION (m)	144	119	151

CE AB/2	PE MN/2	GF K	R83	KR83	R84	KR84	R85	KR85
1.00	0.25	6.286	166.9	1049.13	33.08	207.94	4.631	29.11
1.30	0.25	10.62334	79.01	839.35	14.56	154.68	2.019	21.45
1.80	0.25	20.36664	30.85	628.31	5.756	117.23	0.775	15.78
2.40	0.25	36.20736	12.15	439.92	2.943	106.56	0.384	13.90
3.20	0.25	64.36864	4.48	288.37	1.888	121.53	0.173	11.14
4.20	0.25	110.885	1.567	173.76	0.435	48.23	0.10036	11.13
4.20	1.00	27.72126	8.659	240.04	1.808	50.12	0.4774	13.23
5.50	1.00	47.53788	2.802	133.20	0.655	31.14	0.3275	15.57
7.50	1.00	88.39688	0.909	80.35	0.248	21.92	0.2247	19.86
10.00	1.00	157.15	0.431	67.73	0.154	24.20	0.1569	24.66
13.00	1.00	265.5835	0.267	70.91	0.125	33.20	0.097	25.76
13.00	2.50	106.2334	0.687	72.98	0.253	26.88	0.239	25.39
18.00	2.50	203.6664	0.407	82.89	0.1898	38.66	0.164	33.40
24.00	2.50	362.0736	0.276	99.93	0.155	56.12	0.1195	43.27
32.00	2.50	643.6864	0.2	128.74	0.123	79.17	0.09975	64.21
42.00	2.50	1108.85	0.129	143.04	0.08995	99.74	0.084	93.14
55.00	2.50	1901.515	0.0962	182.93	0.07112	135.24	0.069	131.20
55.00	5.00	950.7575	0.196	186.35	0.136	129.30	0.145	137.86
75.00	5.00	1767.938	0.1044	184.57	0.0988	174.67	0.114	201.54
100.00	5.00	3143	0.0696	218.75	0.08046	252.89	0.0858	269.67

APPENDIX VII
VES CURVES WITH OUANTITATIVE INTERPRETATIONS

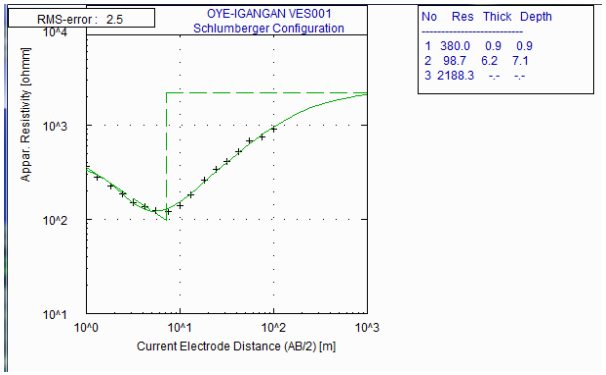

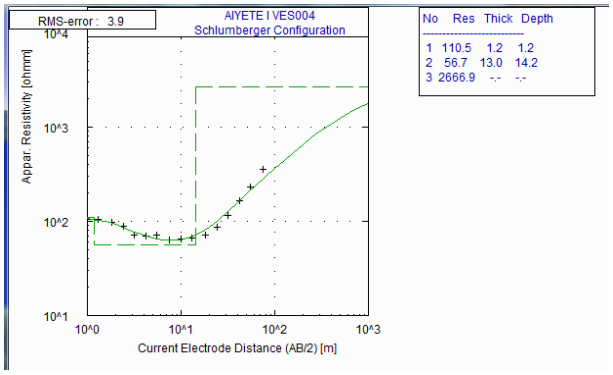

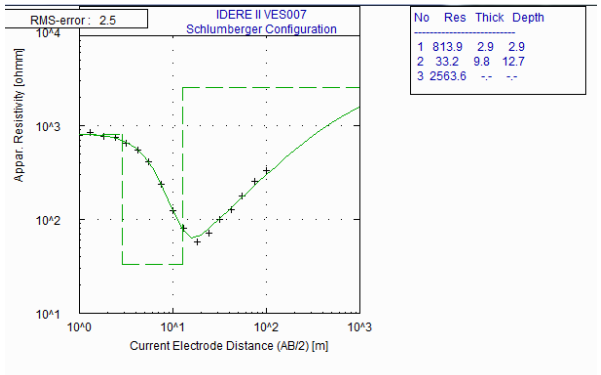

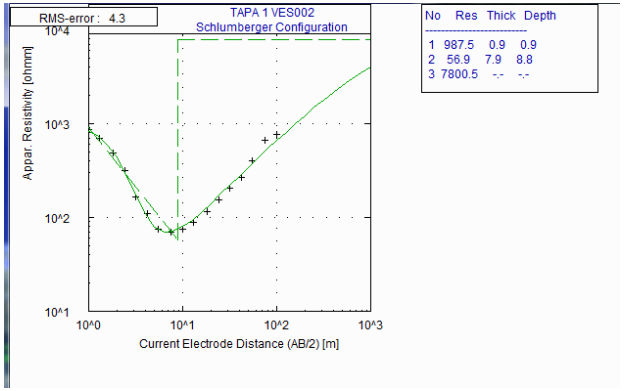

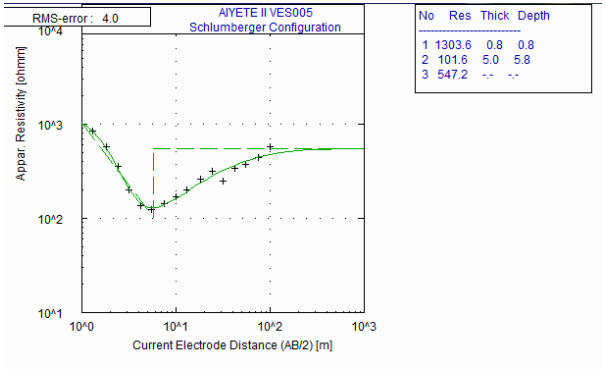

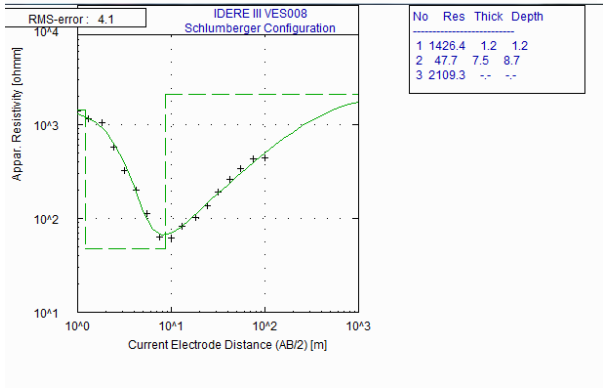

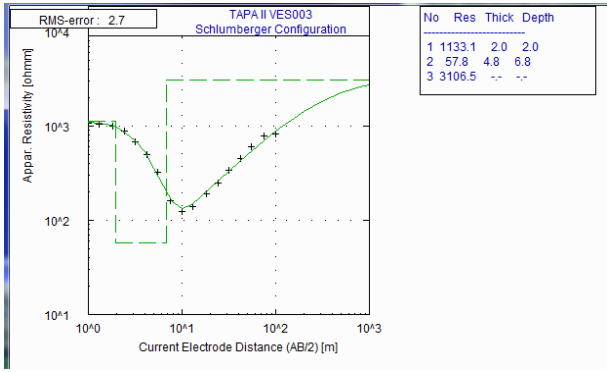

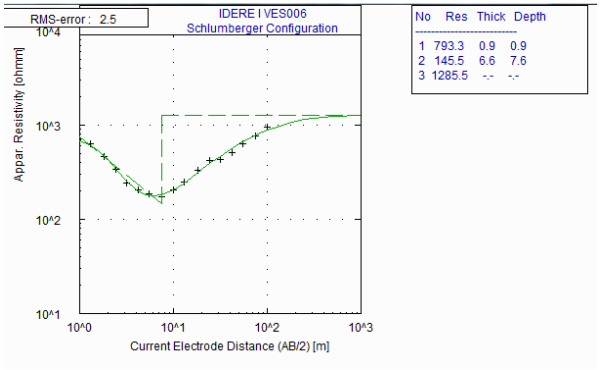

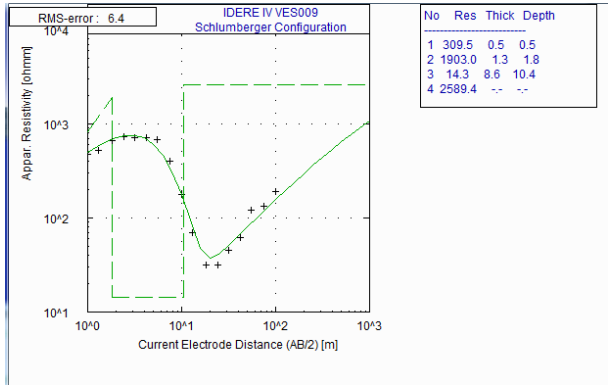

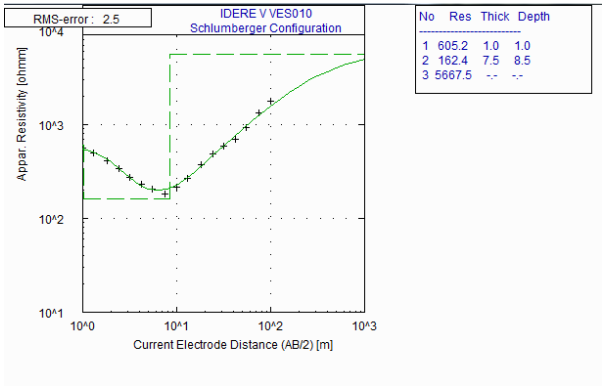
RMS-error : 2.5
IDERE V VES010
Schlumberger Configuration
Appar. Resistivity [ohmm]
Current Electrode Distance (AB/2) [m]
No Res Thick Depth
1 605.2 1.0 1.0
2 162.4 7.5 8.5
3 5667.5 -.- -.-

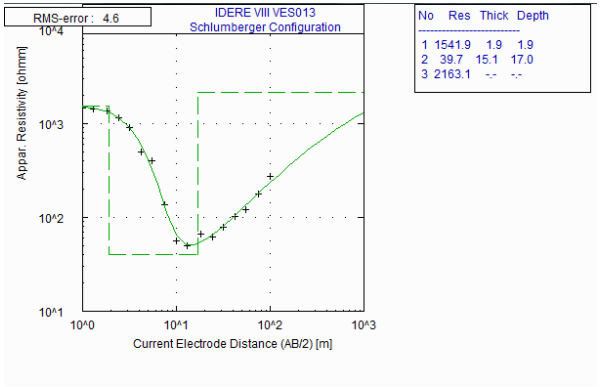
RMS-error : 4.6
IDERE VIII VES013
Schlumberger Configuration
Appar. Resistivity [ohmm]
Current Electrode Distance (AB/2) [m]
No Res Thick Depth
1 1541.9 1.9 1.9
2 39.7 15.1 17.0
3 2163.1 -.- -.-

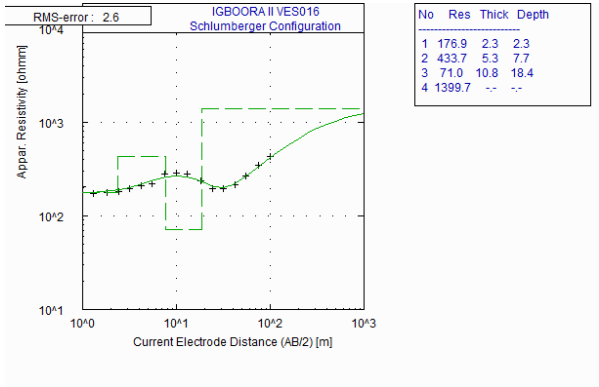
RMS-error : 2.6
IGBOORA II VES016
Schlumberger Configuration
Appar. Resistivity [ohmm]
Current Electrode Distance (AB/2) [m]
No Res Thick Depth
1 176.9 2.3 2.3
2 433.7 5.3 7.7
3 71.0 10.8 18.4
4 1399.7 -.- -.-

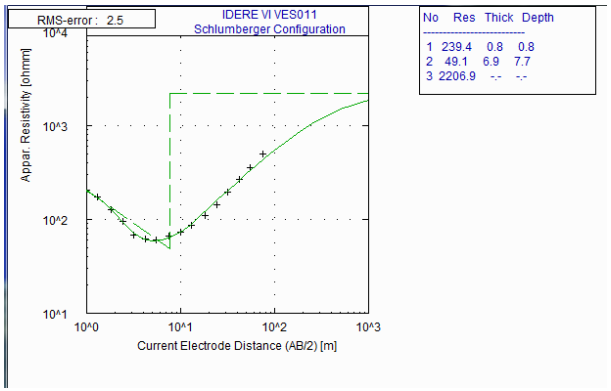
RMS-error : 2.5
IDERE VI VES011
Schlumberger Configuration
Appar. Resistivity [ohmm]
Current Electrode Distance (AB/2) [m]
No Res Thick Depth
1 239.4 0.8 0.8
2 49.1 6.9 7.7
3 2206.9 -.- -.-

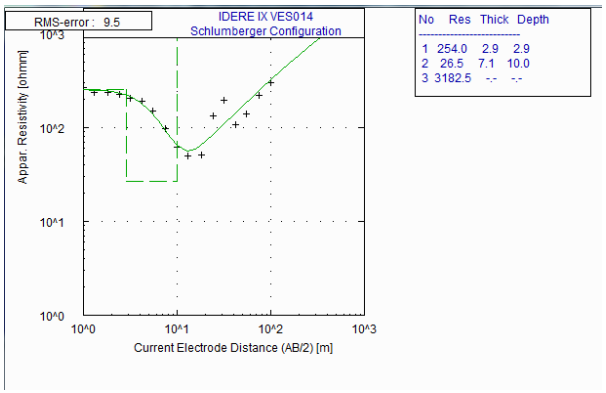
RMS-error : 9.5
IDERE IX VES014
Schlumberger Configuration
Appar. Resistivity [ohmm]
Current Electrode Distance (AB/2) [m]
No Res Thick Depth
1 254.0 2.9 2.9
2 26.5 7.1 10.0
3 3182.5 -.- -.-

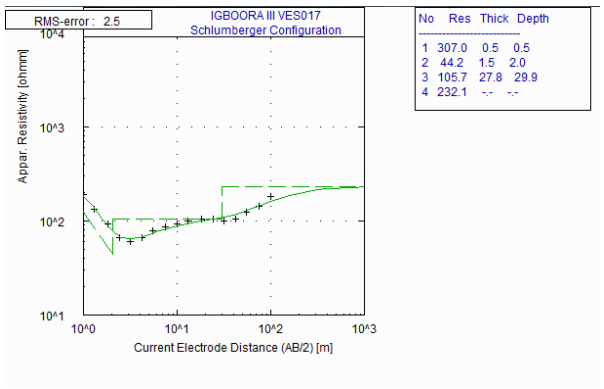
RMS-error : 2.5
IGBOORA III VES017
Schlumberger Configuration
Appar. Resistivity [ohmm]
Current Electrode Distance (AB/2) [m]
No Res Thick Depth
1 307.0 0.5 0.5
2 44.2 1.5 2.0
3 105.7 27.8 29.9
4 232.1 -.- -.-

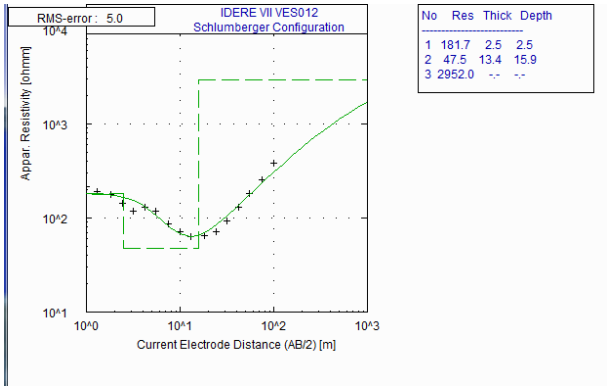
RMS-error : 5.0
IDERE VII VES012
Schlumberger Configuration
Appar. Resistivity [ohmm]
Current Electrode Distance (AB/2) [m]
No Res Thick Depth
1 181.7 2.5 2.5
2 47.5 13.4 15.9
3 2952.0 -.- -.-

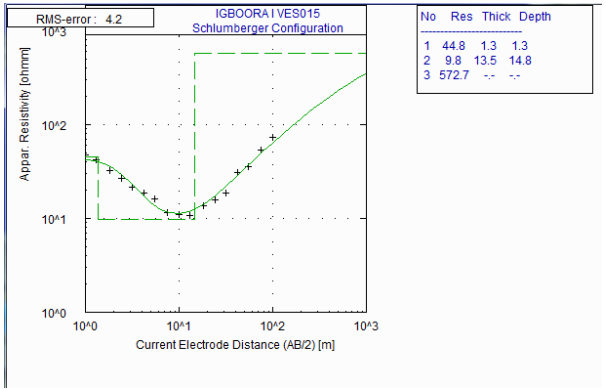
RMS-error : 4.2
IGBOORA I VES015
Schlumberger Configuration
Appar. Resistivity [ohmm]
Current Electrode Distance (AB/2) [m]
No Res Thick Depth
1 44.8 1.3 1.3
2 9.8 13.5 14.8
3 572.7 -.- -.-

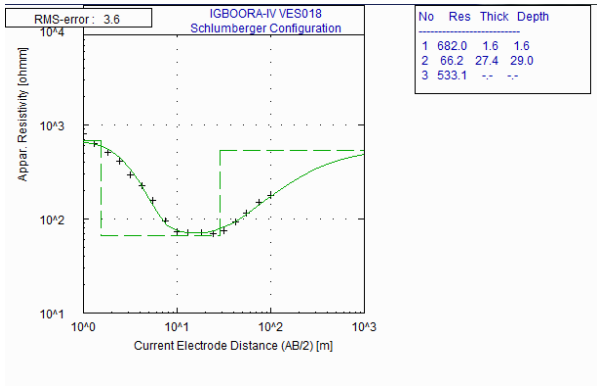
RMS-error : 3.6
IGBOORA-IV VES018
Schlumberger Configuration
Appar. Resistivity [ohmm]
Current Electrode Distance (AB/2) [m]
No Res Thick Depth
1 682.0 1.6 1.6
2 66.2 27.4 29.0
3 533.1 -.- -.-

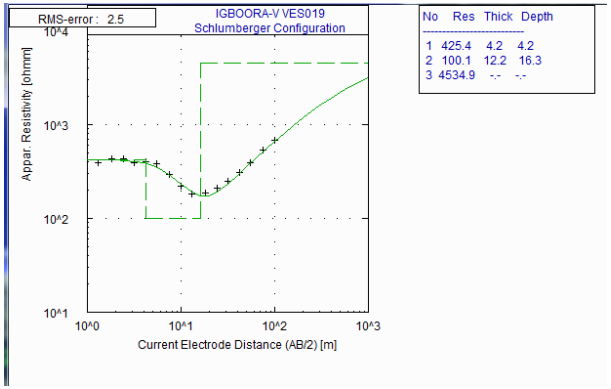
RMS-error : 2.5
IGBOORA-V VES019
Schlumberger Configuration
Appar. Resistivity [ohmm]
Current Electrode Distance (AB/2) [m]
No Res Thick Depth
1 425.4 4.2 4.2
2 100.1 12.2 16.3
3 4534.9 -.- -.-

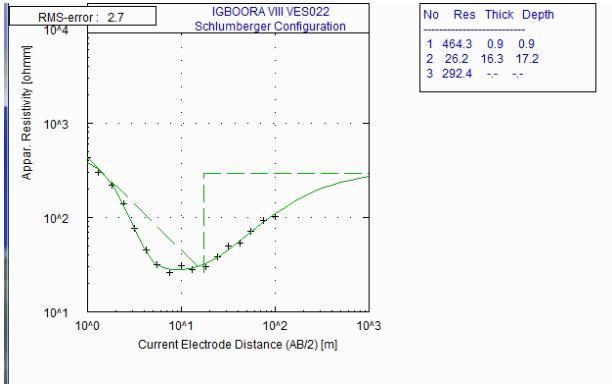
RMS-error : 2.7
IGBOORA VIII VES022
Schlumberger Configuration
Appar. Resistivity [ohmm]
Current Electrode Distance (AB/2) [m]
No Res Thick Depth
1 464.3 0.9 0.9
2 26.2 16.3 17.2
3 292.4 -.- -.-

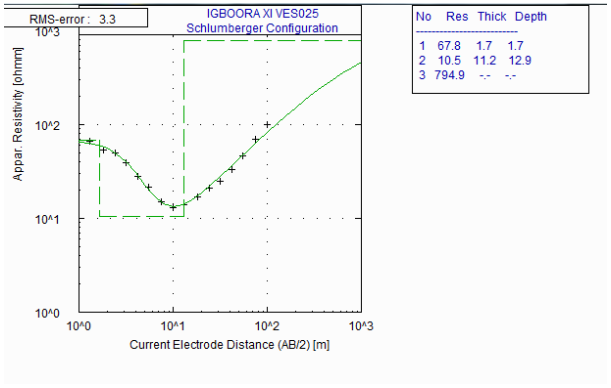
RMS-error : 3.3
IGBOORA XI VES025
Schlumberger Configuration
Appar. Resistivity [ohmm]
Current Electrode Distance (AB/2) [m]
No Res Thick Depth
1 67.8 1.7 1.7
2 10.5 11.2 12.9
3 794.9 -.- -.-

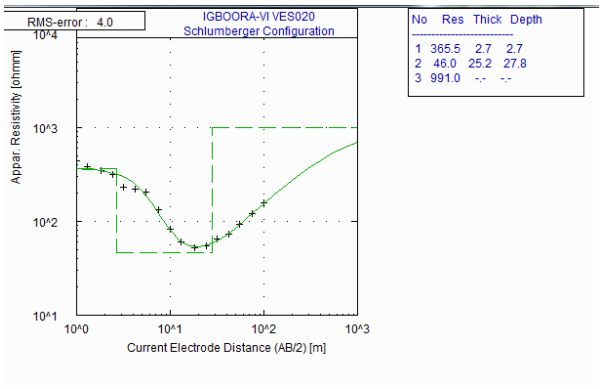
RMS-error : 4.0
IGBOORA-VI VES020
Schlumberger Configuration
Appar. Resistivity [ohmm]
Current Electrode Distance (AB/2) [m]
No Res Thick Depth
1 365.5 2.7 2.7
2 46.0 25.2 27.8
3 991.0 -.- -.-

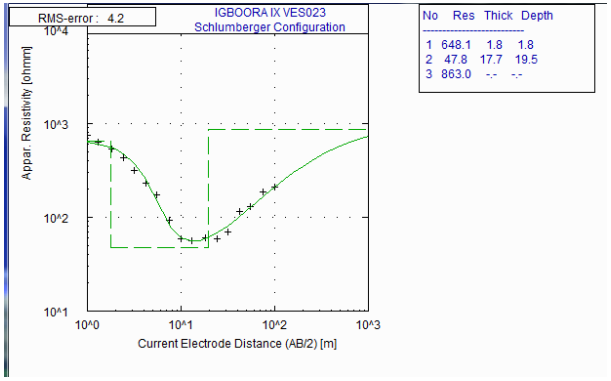
RMS-error : 4.2
IGBOORA IX VES023
Schlumberger Configuration
Appar. Resistivity [ohmm]
Current Electrode Distance (AB/2) [m]
No Res Thick Depth
1 648.1 1.8 1.8
2 47.8 17.7 19.5
3 863.0 -.- -.-

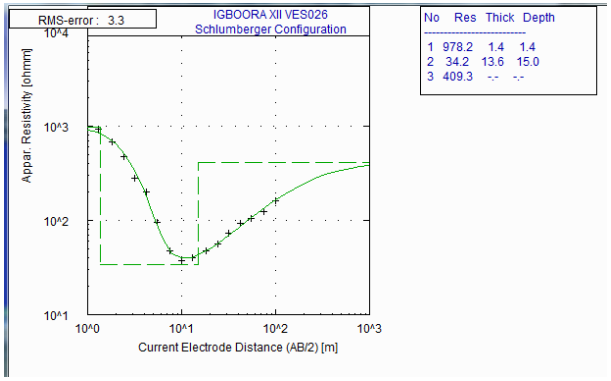
RMS-error : 3.3
IGBOORA XII VES026
Schlumberger Configuration
Appar. Resistivity [ohmm]
Current Electrode Distance (AB/2) [m]
No Res Thick Depth
1 978.2 1.4 1.4
2 34.2 13.6 15.0
3 409.3 -.- -.-

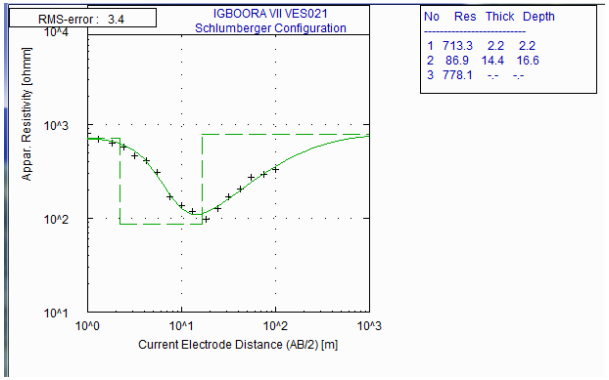
RMS-error : 3.4
IGBOORA VII VES021
Schlumberger Configuration
Appar. Resistivity [ohmm]
Current Electrode Distance (AB/2) [m]
No Res Thick Depth
1 713.3 2.2 2.2
2 86.9 14.4 16.6
3 778.1 -.- -.-

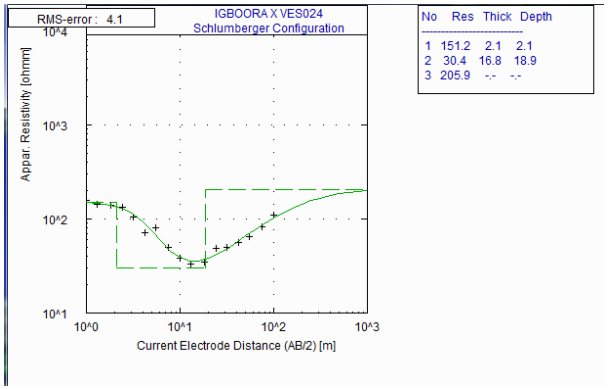
RMS-error : 4.1
IGBOORA X VES024
Schlumberger Configuration
Appar. Resistivity [ohmm]
Current Electrode Distance (AB/2) [m]
No Res Thick Depth
1 151.2 2.1 2.1
2 30.4 16.8 18.9
3 205.9 -.- -.-

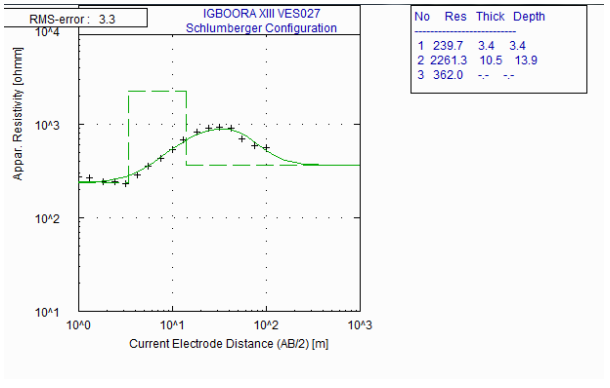
RMS-error : 3.3
IGBOORA XIII VES027
Schlumberger Configuration
Appar. Resistivity [ohmm]
Current Electrode Distance (AB/2) [m]
No Res Thick Depth
1 239.7 3.4 3.4
2 2261.3 10.5 13.9
3 362.0 -.- -.-

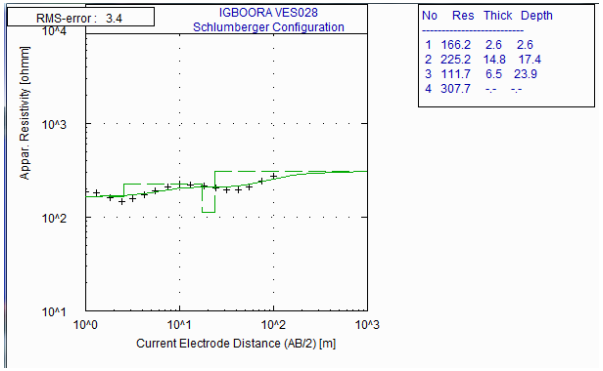
RMS-error : 3.4
IGBOORA VES028
Schlumberger Configuration
No Res Thick Depth
1 166.2 2.6 2.6
2 225.2 14.8 17.4
3 111.7 6.5 23.9
4 307.7 -.- -.-
Appar. Resistivity [ohmm]
Current Electrode Distance (AB/2) [m]

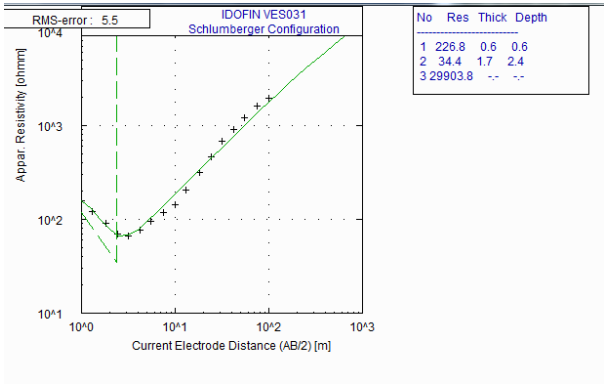
RMS-error : 5.5
IDOFIN VES031
Schlumberger Configuration
No Res Thick Depth
1 226.8 0.6 0.6
2 34.4 1.7 2.4
3 29903.8 -.- -.-
Appar. Resistivity [ohmm]
Current Electrode Distance (AB/2) [m]

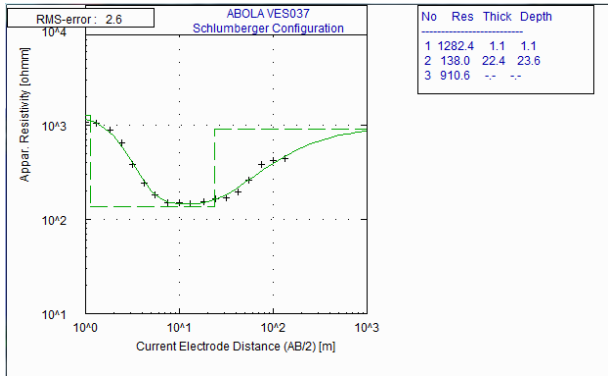
RMS-error : 2.6
ABOLA VES037
Schlumberger Configuration
No Res Thick Depth
1 1282.4 1.1 1.1
2 138.0 22.4 23.6
3 910.6 -.- -.-
Appar. Resistivity [ohmm]
Current Electrode Distance (AB/2) [m]

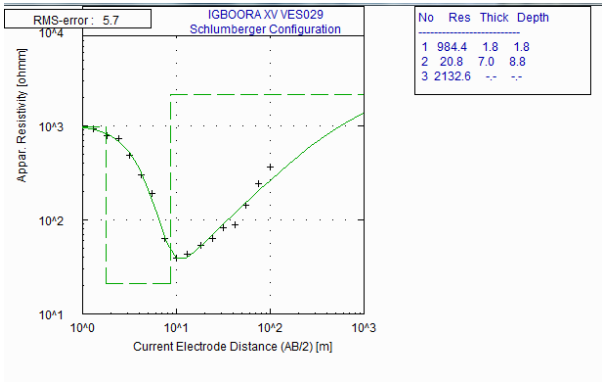
RMS-error : 5.7
IGBOORA XV VES029
Schlumberger Configuration
No Res Thick Depth
1 984.4 1.8 1.8
2 20.8 7.0 8.8
3 2132.6 -.- -.-
Appar. Resistivity [ohmm]
Current Electrode Distance (AB/2) [m]

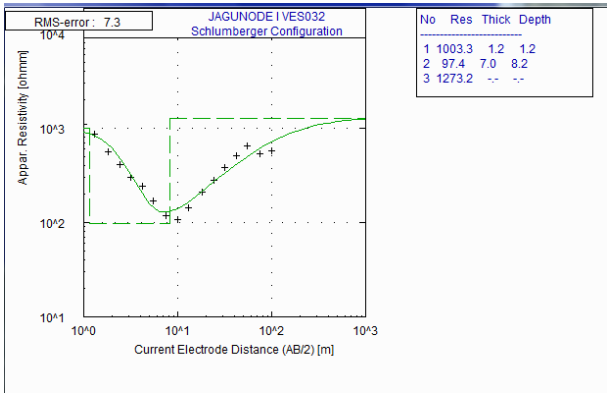
RMS-error : 7.3
JAGUNODE I VES032
Schlumberger Configuration
No Res Thick Depth
1 1003.3 1.2 1.2
2 97.4 7.0 8.2
3 1273.2 -.- -.-
Appar. Resistivity [ohmm]
Current Electrode Distance (AB/2) [m]

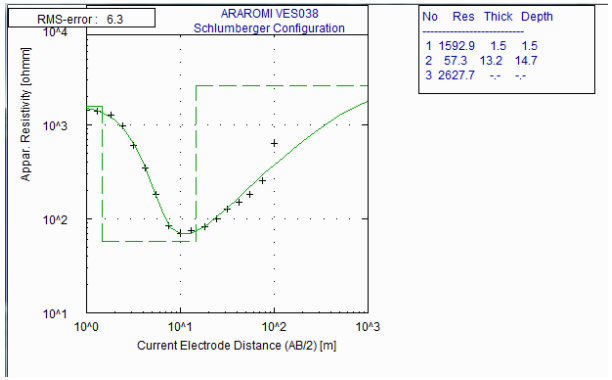
RMS-error : 6.3
ARAROMI VES038
Schlumberger Configuration
No Res Thick Depth
1 1592.9 1.5 1.5
2 57.3 13.2 14.7
3 2627.7 -.- -.-
Appar. Resistivity [ohmm]
Current Electrode Distance (AB/2) [m]

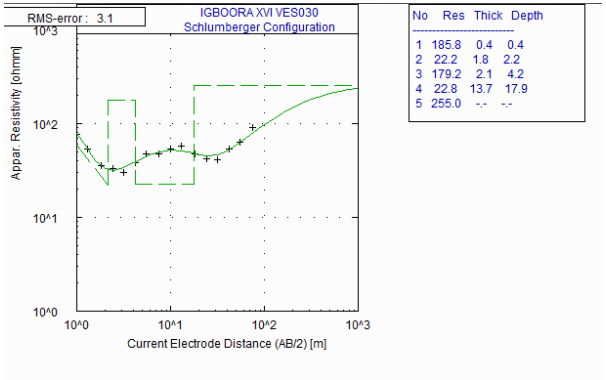
RMS-error : 3.1
IGBOORA XVI VES030
Schlumberger Configuration
No Res Thick Depth
1 185.8 0.4 0.4
2 22.2 1.8 2.2
3 179.2 2.1 4.2
4 22.8 13.7 17.9
5 255.0 -.- -.-
Appar. Resistivity [ohmm]
Current Electrode Distance (AB/2) [m]

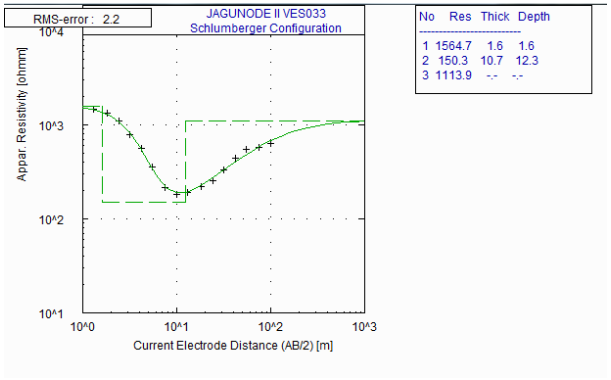
RMS-error : 2.2
JAGUNODE II VES033
Schlumberger Configuration
No Res Thick Depth
1 1564.7 1.6 1.6
2 150.3 10.7 12.3
3 1113.9 -.- -.-
Appar. Resistivity [ohmm]
Current Electrode Distance (AB/2) [m]

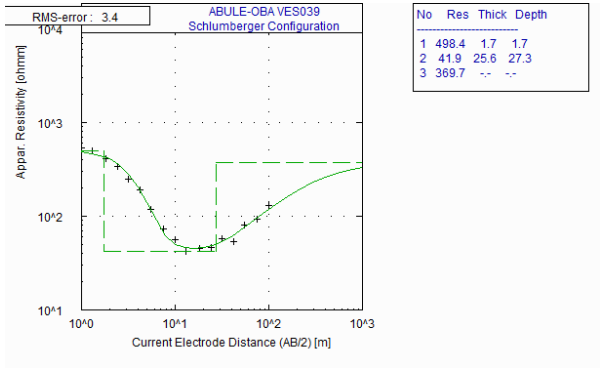
RMS-error : 3.4
ABULE-OBA VES039
Schlumberger Configuration
No Res Thick Depth
1 498.4 1.7 1.7
2 41.9 25.6 27.3
3 369.7 -.- -.-
Appar. Resistivity [ohmm]
Current Electrode Distance (AB/2) [m]

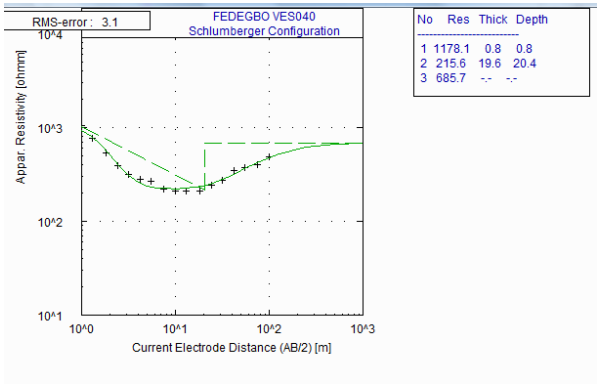
RMS-error : 3.1
FEDEGBO VES040
Schlumberger Configuration
No Res Thick Depth
1 1178.1 0.8 0.8
2 215.6 19.6 20.4
3 685.7 -.- -.-
Appar. Resistivity [ohmm]
Current Electrode Distance (AB/2) [m]

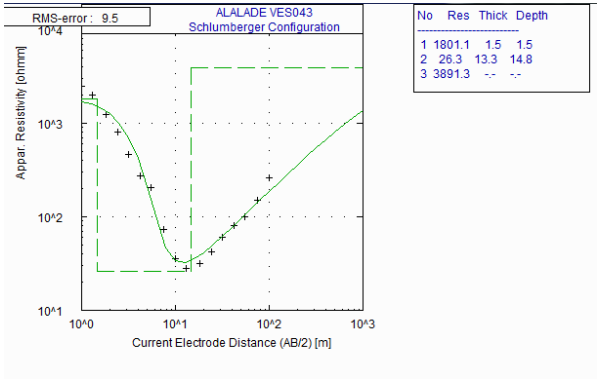
RMS-error : 9.5
ALALADE VES043
Schlumberger Configuration
No Res Thick Depth
1 1801.1 1.5 1.5
2 26.3 13.3 14.8
3 3891.3 -.- -.-
Appar. Resistivity [ohmm]
Current Electrode Distance (AB/2) [m]

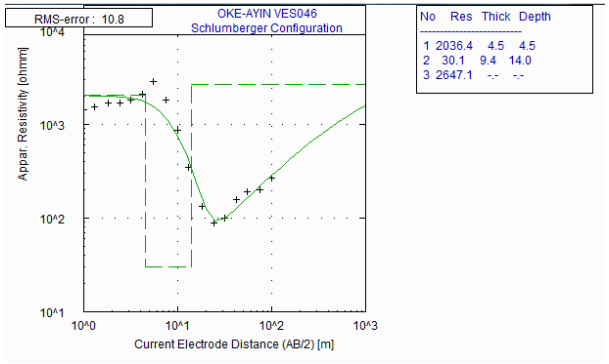
RMS-error : 10.8
OKE-AYIN VES046
Schlumberger Configuration
No Res Thick Depth
1 2036.4 4.5 4.5
2 30.1 9.4 14.0
3 2647.1 -.- -.-
Appar. Resistivity [ohmm]
Current Electrode Distance (AB/2) [m]

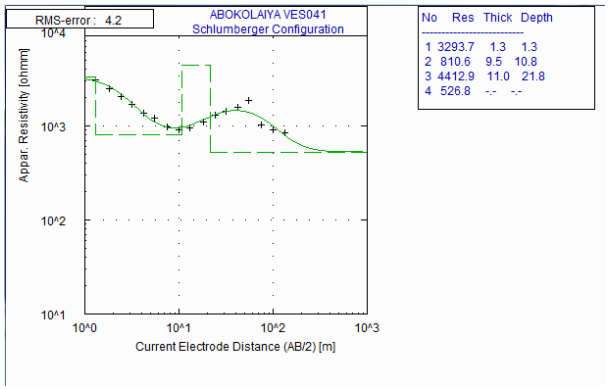
RMS-error : 4.2
ABOKOLAIYA VES041
Schlumberger Configuration
No Res Thick Depth
1 3293.7 1.3 1.3
2 810.6 9.5 10.8
3 4412.9 11.0 21.8
4 526.8 -.- -.-
Appar. Resistivity [ohmm]
Current Electrode Distance (AB/2) [m]

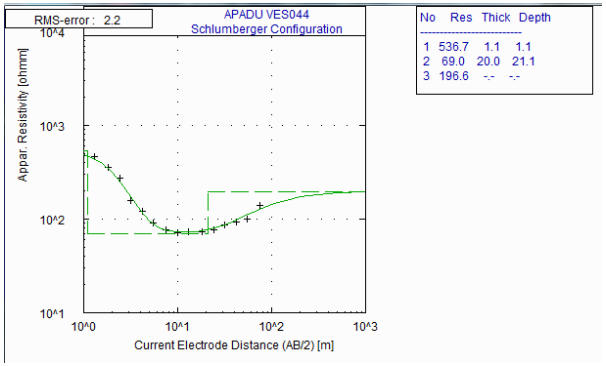
RMS-error : 2.2
APADU VES044
Schlumberger Configuration
No Res Thick Depth
1 536.7 1.1 1.1
2 69.0 20.0 21.1
3 196.6 -.- -.-
Appar. Resistivity [ohmm]
Current Electrode Distance (AB/2) [m]

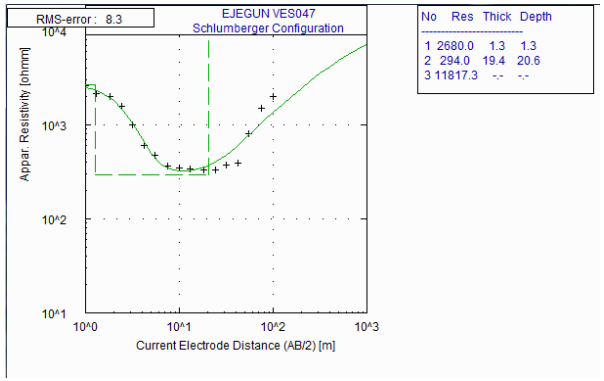
RMS-error : 8.3
EJEGUN VES047
Schlumberger Configuration
No Res Thick Depth
1 2680.0 1.3 1.3
2 294.0 19.4 20.6
3 11817.3 -.- -.-
Appar. Resistivity [ohmm]
Current Electrode Distance (AB/2) [m]

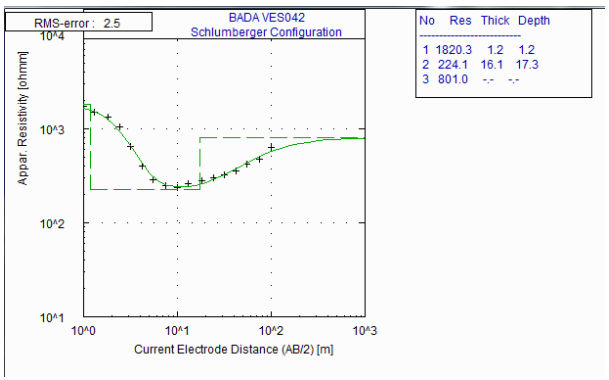
RMS-error : 2.5
BADA VES042
Schlumberger Configuration
No Res Thick Depth
1 1820.3 1.2 1.2
2 224.1 16.1 17.3
3 801.0 -.- -.-
Appar. Resistivity [ohmm]
Current Electrode Distance (AB/2) [m]

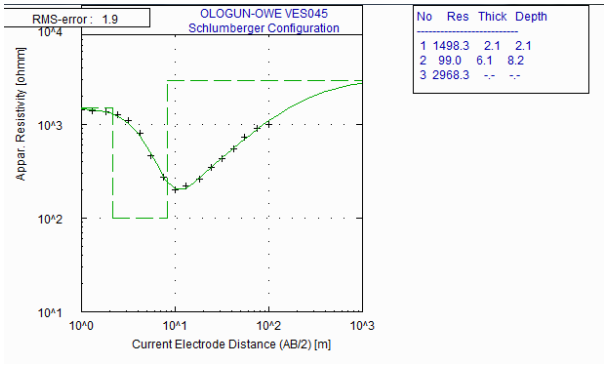
RMS-error : 1.9
OLOGUN-OWE VES045
Schlumberger Configuration
No Res Thick Depth
1 1498.3 2.1 2.1
2 99.0 6.1 8.2
3 2968.3 -.- -.-
Appar. Resistivity [ohmm]
Current Electrode Distance (AB/2) [m]

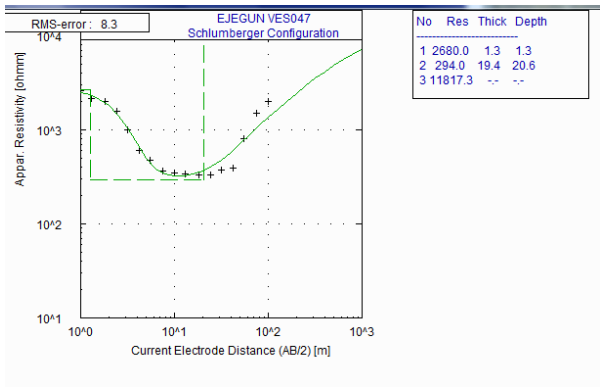
RMS-error : 8.3
EJEGUN VES047
Schlumberger Configuration
No Res Thick Depth
1 2680.0 1.3 1.3
2 294.0 19.4 20.6
3 11817.3 -.- -.-
Appar. Resistivity [ohmm]
Current Electrode Distance (AB/2) [m]

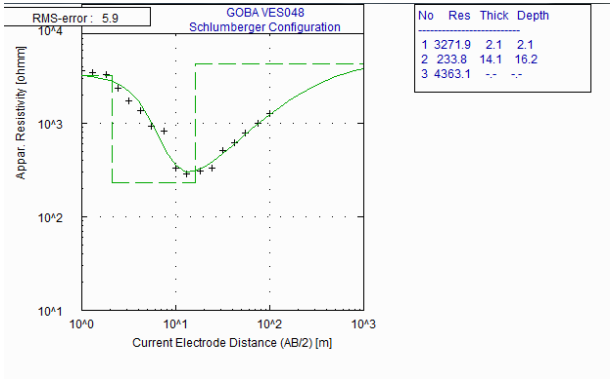
RMS-error : 5.9
GOBA VES048
Schlumberger Configuration
No Res Thick Depth
1 3271.9 2.1 2.1
2 233.8 14.1 16.2
3 4363.1 -.- -.-
Appar. Resistivity [ohmm]
Current Electrode Distance (AB/2) [m]

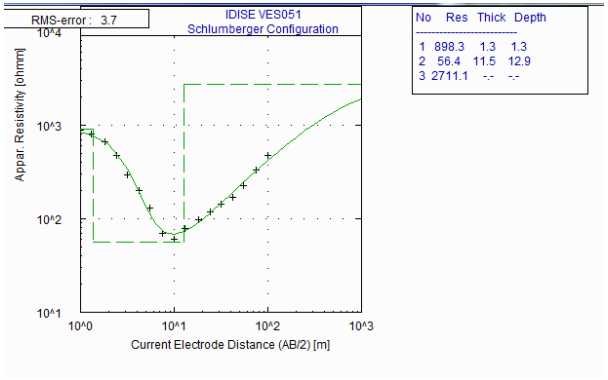
RMS-error : 3.7
IDISE VES051
Schlumberger Configuration
No Res Thick Depth
1 898.3 1.3 1.3
2 56.4 11.5 12.9
3 2711.1 -.- -.-
Appar. Resistivity [ohmm]
Current Electrode Distance (AB/2) [m]

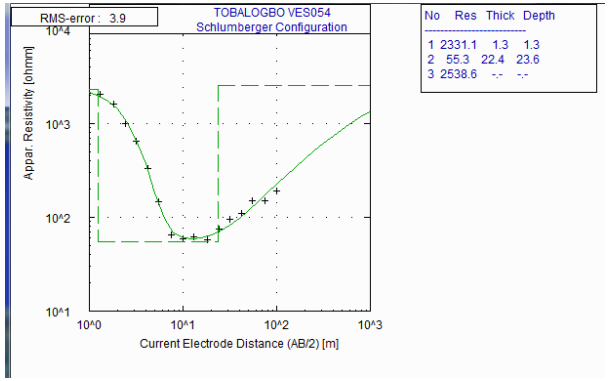
RMS-error : 3.9
TOBALOGBO VES054
Schlumberger Configuration
No Res Thick Depth
1 2331.1 1.3 1.3
2 55.3 22.4 23.6
3 2538.6 -.- -.-
Appar. Resistivity [ohmm]
Current Electrode Distance (AB/2) [m]

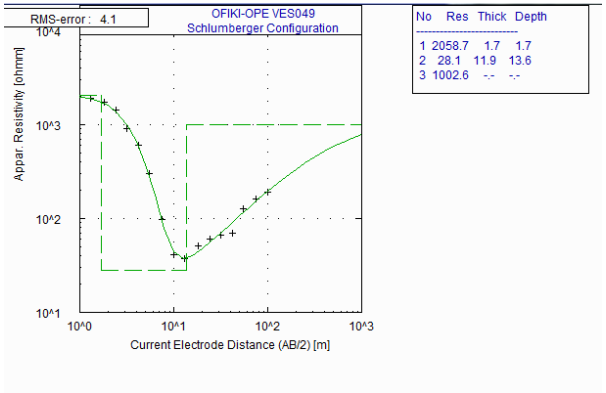
RMS-error : 4.1
OFIKI-OPE VES049
Schlumberger Configuration
No Res Thick Depth
1 2058.7 1.7 1.7
2 28.1 11.9 13.6
3 1002.6 -.- -.-
Appar. Resistivity [ohmm]
Current Electrode Distance (AB/2) [m]

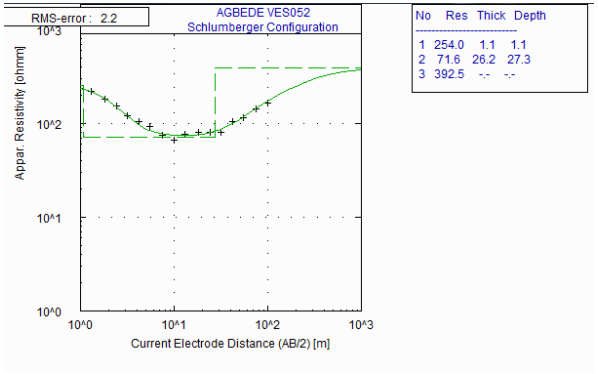
RMS-error : 2.2
AGBEDE VES052
Schlumberger Configuration
No Res Thick Depth
1 254.0 1.1 1.1
2 71.6 26.2 27.3
3 392.5 -.- -.-
Appar. Resistivity [ohmm]
Current Electrode Distance (AB/2) [m]

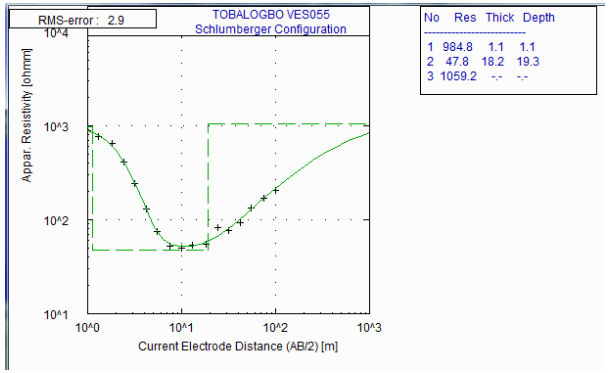
RMS-error : 2.9
TOBALOGBO VES055
Schlumberger Configuration
No Res Thick Depth
1 984.8 1.1 1.1
2 47.8 18.2 19.3
3 1059.2 -.- -.-
Appar. Resistivity [ohmm]
Current Electrode Distance (AB/2) [m]

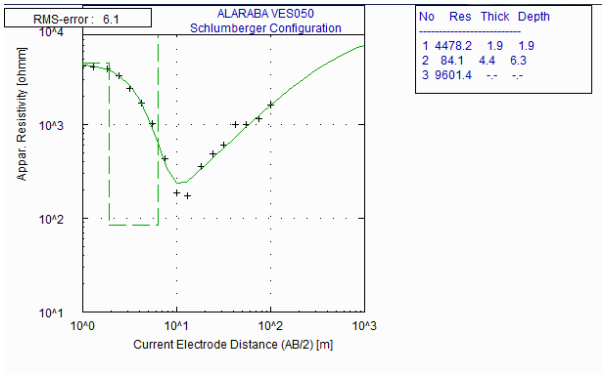
RMS-error : 6.1
ALARABA VES050
Schlumberger Configuration
No Res Thick Depth
1 4478.2 1.9 1.9
2 84.1 4.4 6.3
3 9601.4 -.- -.-
Appar. Resistivity [ohmm]
Current Electrode Distance (AB/2) [m]

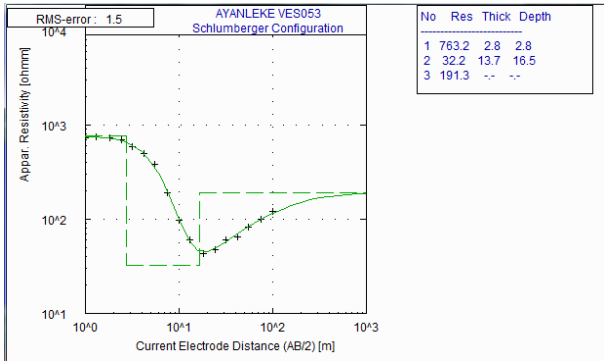
RMS-error : 1.5
AYANLEKE VES053
Schlumberger Configuration
No Res Thick Depth
1 763.2 2.8 2.8
2 32.2 13.7 16.5
3 191.3 -.- -.-
Appar. Resistivity [ohmm]
Current Electrode Distance (AB/2) [m]

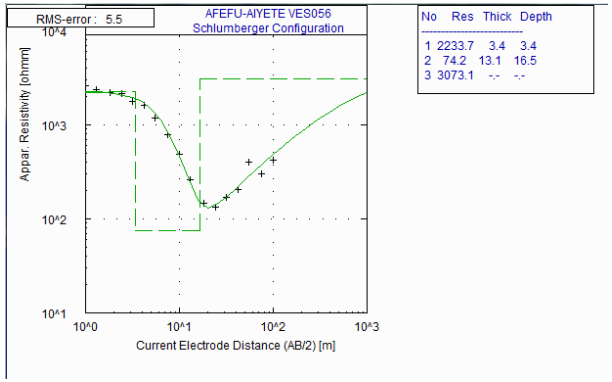
RMS-error : 5.5
AFEFU-AIYETE VES056
Schlumberger Configuration
No Res Thick Depth
1 2233.7 3.4 3.4
2 74.2 13.1 16.5
3 3073.1 -.- -.-
Appar. Resistivity [ohmm]
Current Electrode Distance (AB/2) [m]

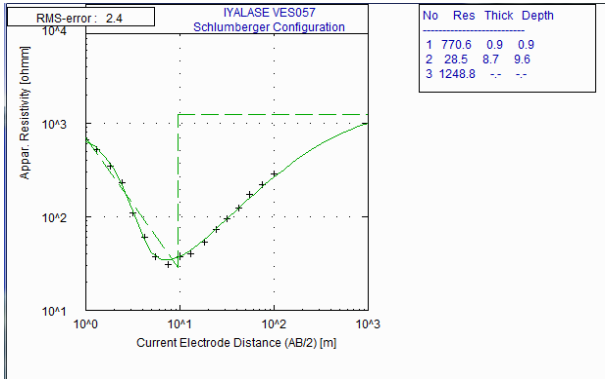
RMS-error : 2.4
IYALASE VES057
Schlumberger Configuration
No Res Thick Depth
1 770.6 0.9 0.9
2 28.5 8.7 9.6
3 1248.8 -.- -.-
Appar. Resistivity [ohmm]
Current Electrode Distance (AB/2) [m]

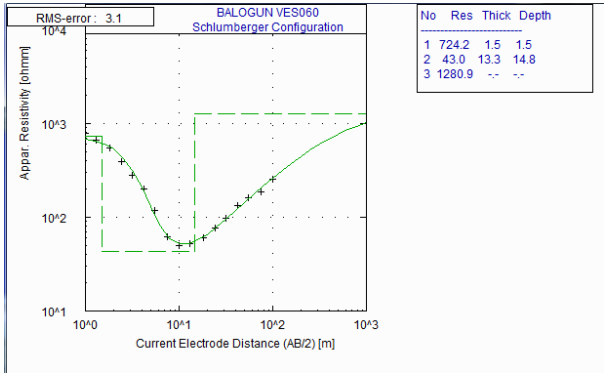
RMS-error : 3.1
BALOGUN VES060
Schlumberger Configuration
No Res Thick Depth
1 724.2 1.5 1.5
2 43.0 13.3 14.8
3 1280.9 -.- -.-
Appar. Resistivity [ohmm]
Current Electrode Distance (AB/2) [m]

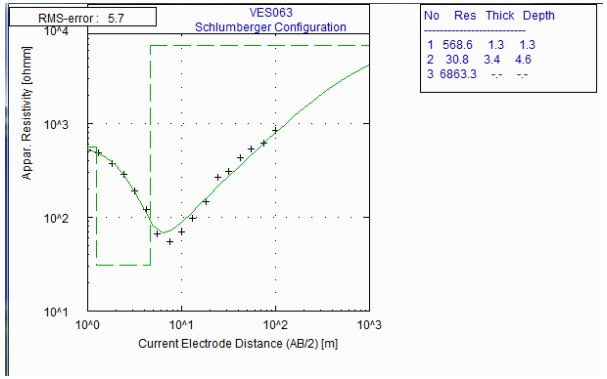
RMS-error : 5.7
VES063
Schlumberger Configuration
No Res Thick Depth
1 568.6 1.3 1.3
2 30.8 3.4 4.6
3 6863.3 -.- -.-
Appar. Resistivity [ohmm]
Current Electrode Distance (AB/2) [m]

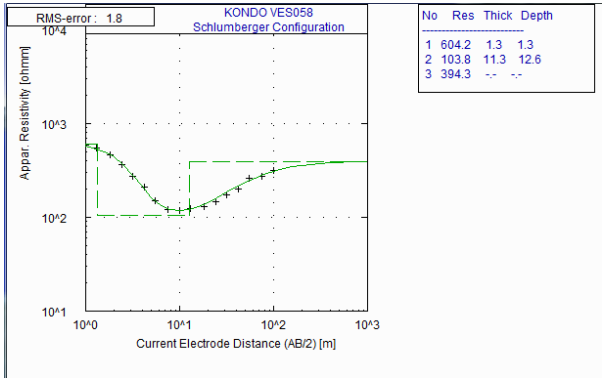
RMS-error : 1.8
KONDO VES058
Schlumberger Configuration
No Res Thick Depth
1 604.2 1.3 1.3
2 103.8 11.3 12.6
3 394.3 -.- -.-
Appar. Resistivity [ohmm]
Current Electrode Distance (AB/2) [m]

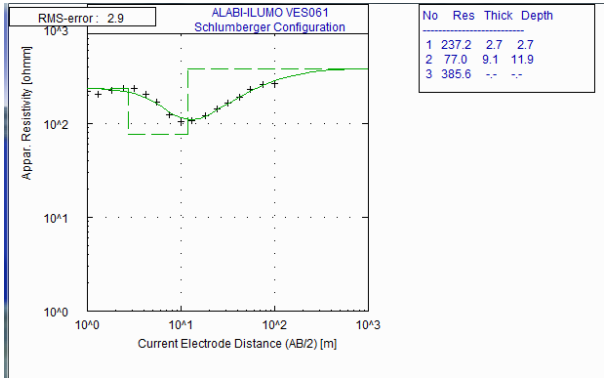
RMS-error : 2.9
ALABI-ILUMO VES061
Schlumberger Configuration
No Res Thick Depth
1 237.2 2.7 2.7
2 77.0 9.1 11.9
3 385.6 -.- -.-
Appar. Resistivity [ohmm]
Current Electrode Distance (AB/2) [m]

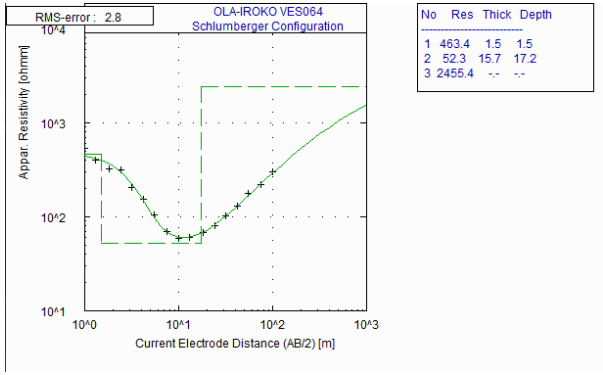
RMS-error : 2.8
OLA-IROKO VES064
Schlumberger Configuration
No Res Thick Depth
1 463.4 1.5 1.5
2 52.3 15.7 17.2
3 2455.4 -.- -.-
Appar. Resistivity [ohmm]
Current Electrode Distance (AB/2) [m]

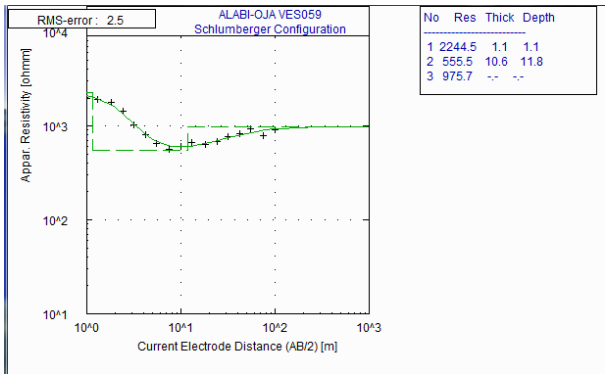
RMS-error : 2.5
ALABI-OJA VES059
Schlumberger Configuration
No Res Thick Depth
1 2244.5 1.1 1.1
2 555.5 10.6 11.8
3 975.7 -.- -.-
Appar. Resistivity [ohmm]
Current Electrode Distance (AB/2) [m]

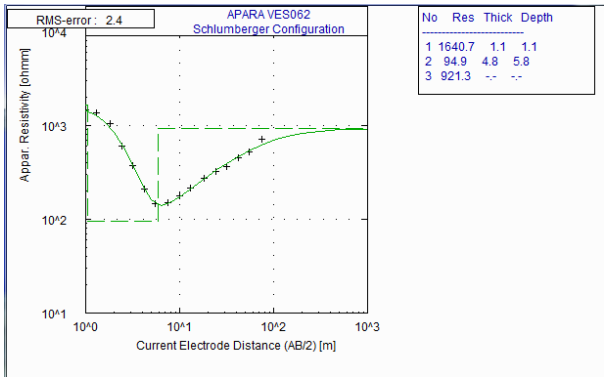
RMS-error : 2.4
APARA VES062
Schlumberger Configuration
No Res Thick Depth
1 1640.7 1.1 1.1
2 94.9 4.8 5.8
3 921.3 -.- -.-
Appar. Resistivity [ohmm]
Current Electrode Distance (AB/2) [m]

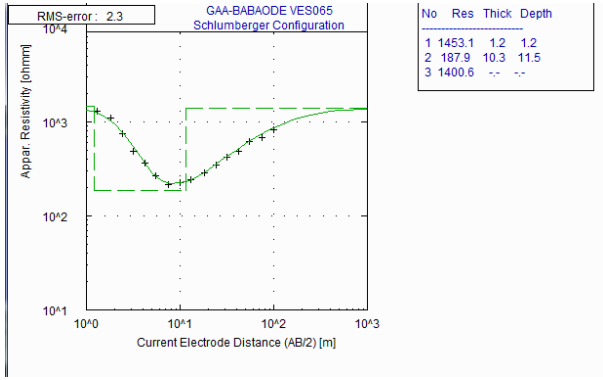
RMS-error : 2.3
GAA-BABAODE VES065
Schlumberger Configuration
No Res Thick Depth
1 1453.1 1.2 1.2
2 187.9 10.3 11.5
3 1400.6 -.- -.-
Appar. Resistivity [ohmm]
Current Electrode Distance (AB/2) [m]

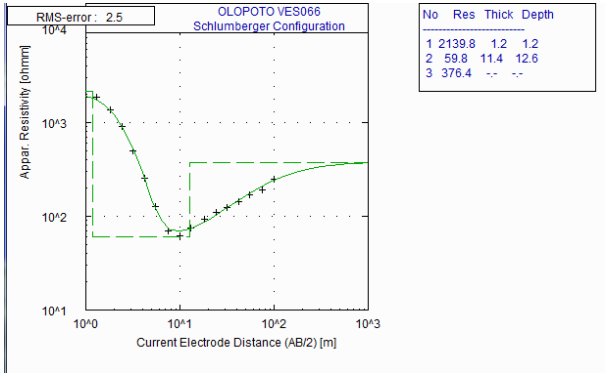
RMS-error : 2.5
OLOPOTO VES066
Schlumberger Configuration
Appar. Resistivity [ohmm]
Current Electrode Distance (AB/2) [m]
No Res Thick Depth
1 2139.8 1.2 1.2
2 59.8 11.4 12.6
3 376.4 -.- -.-

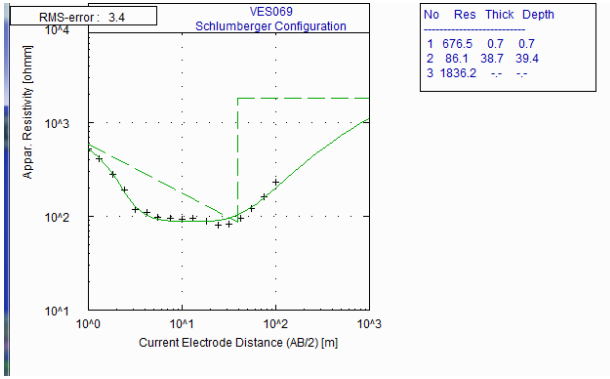
RMS-error : 3.4
VES069
Schlumberger Configuration
Appar. Resistivity [ohmm]
Current Electrode Distance (AB/2) [m]
No Res Thick Depth
1 676.5 0.7 0.7
2 86.1 38.7 39.4
3 1836.2 -.- -.-

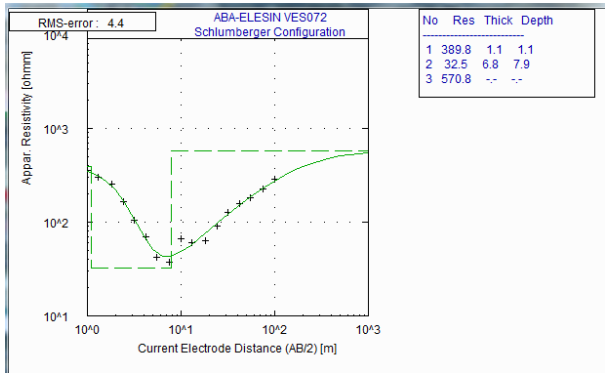
RMS-error : 4.4
ABA-ELESIN VES072
Schlumberger Configuration
Appar. Resistivity [ohmm]
Current Electrode Distance (AB/2) [m]
No Res Thick Depth
1 389.8 1.1 1.1
2 32.5 6.8 7.9
3 570.8 -.- -.-

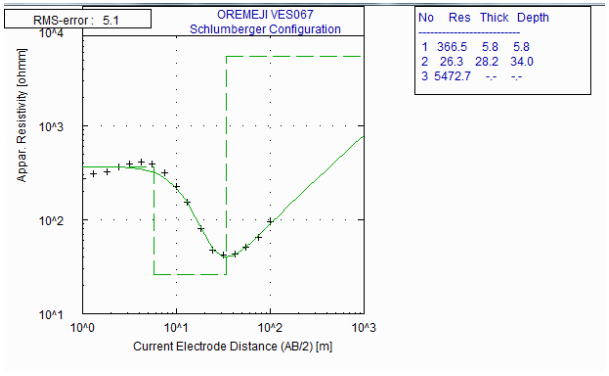
RMS-error : 5.1
OREMEJI VES067
Schlumberger Configuration
Appar. Resistivity [ohmm]
Current Electrode Distance (AB/2) [m]
No Res Thick Depth
1 366.5 5.8 5.8
2 26.3 28.2 34.0
3 5472.7 -.- -.-

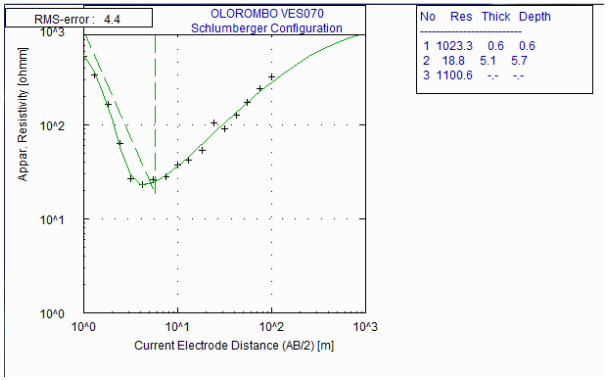
RMS-error : 4.4
OLOROMBO VES070
Schlumberger Configuration
Appar. Resistivity [ohmm]
Current Electrode Distance (AB/2) [m]
No Res Thick Depth
1 1023.3 0.6 0.6
2 18.8 5.1 5.7
3 1100.6 -.- -.-

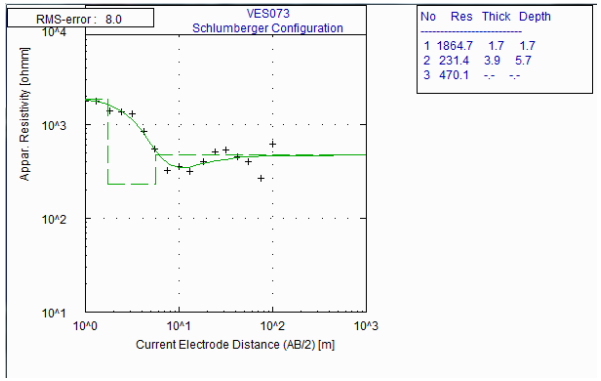
RMS-error : 8.0
VES073
Schlumberger Configuration
Appar. Resistivity [ohmm]
Current Electrode Distance (AB/2) [m]
No Res Thick Depth
1 1864.7 1.7 1.7
2 231.4 3.9 5.7
3 470.1 -.- -.-

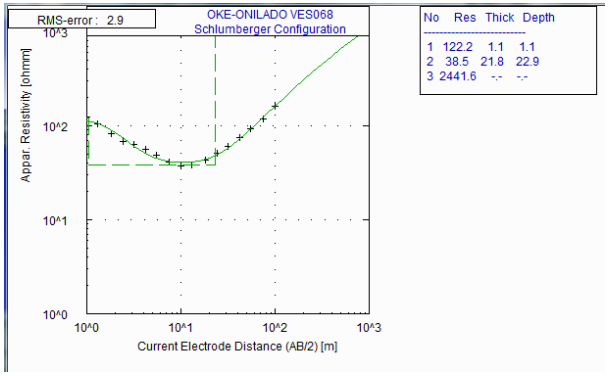
RMS-error : 2.9
OKE-ONILADO VES068
Schlumberger Configuration
Appar. Resistivity [ohmm]
Current Electrode Distance (AB/2) [m]
No Res Thick Depth
1 122.2 1.1 1.1
2 38.5 21.8 22.9
3 2441.6 -.- -.-

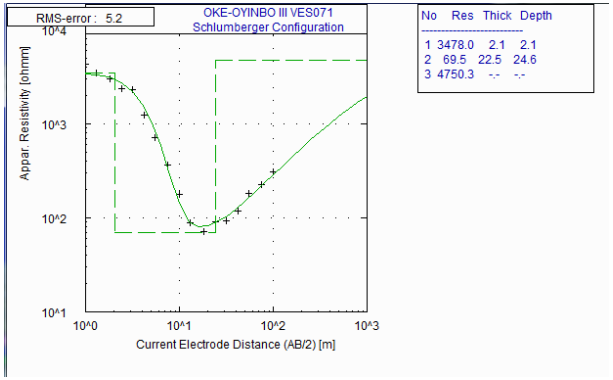
RMS-error : 5.2
OKE-OYINBO III VES071
Schlumberger Configuration
Appar. Resistivity [ohmm]
Current Electrode Distance (AB/2) [m]
No Res Thick Depth
1 3478.0 2.1 2.1
2 69.5 22.5 24.6
3 4750.3 -.- -.-

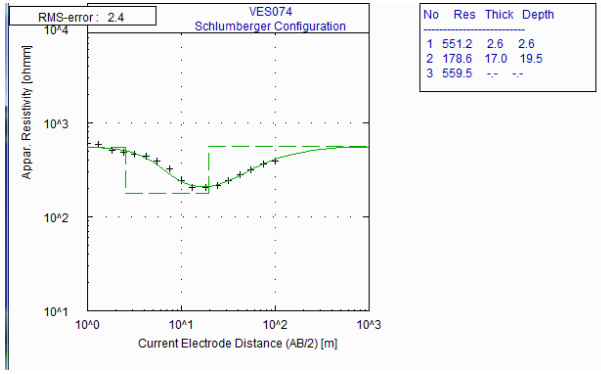
RMS-error : 2.4
VES074
Schlumberger Configuration
Appar. Resistivity [ohmm]
Current Electrode Distance (AB/2) [m]
No Res Thick Depth
1 551.2 2.6 2.6
2 178.6 17.0 19.5
3 559.5 -.- -.-

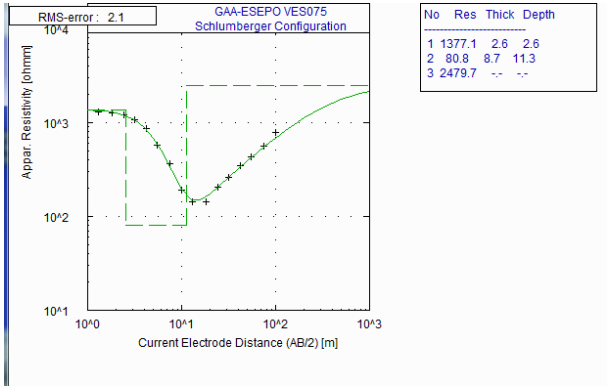
RMS-error : 2.1
GAA-ESEPO VES075
Schlumberger Configuration
Appar. Resistivity [ohmm]
Current Electrode Distance (AB/2) [m]
No Res Thick Depth
1 1377.1 2.6 2.6
2 80.8 8.7 11.3
3 2479.7 -.- -.-

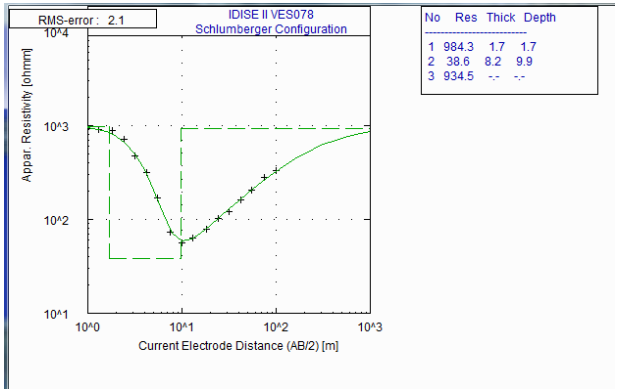
RMS-error : 2.1
IDISE II VES078
Schlumberger Configuration
Appar. Resistivity [ohmm]
Current Electrode Distance (AB/2) [m]
No Res Thick Depth
1 984.3 1.7 1.7
2 38.6 8.2 9.9
3 934.5 -.- -.-

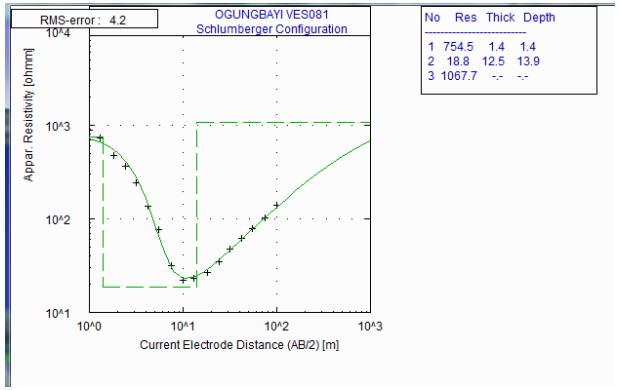
RMS-error : 4.2
OGUNGBAYI VES081
Schlumberger Configuration
Appar. Resistivity [ohmm]
Current Electrode Distance (AB/2) [m]
No Res Thick Depth
1 754.5 1.4 1.4
2 18.8 12.5 13.9
3 1067.7 -.- -.-

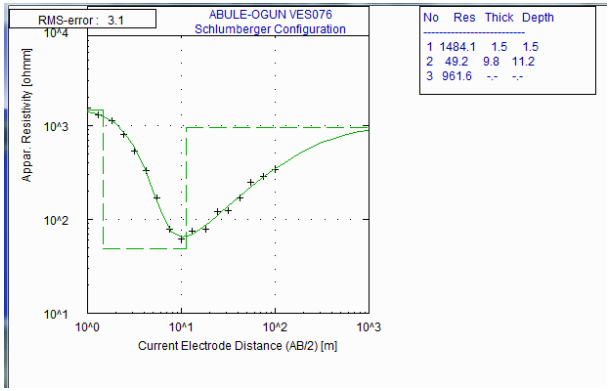
RMS-error : 3.1
ABULE-OGUN VES076
Schlumberger Configuration
Appar. Resistivity [ohmm]
Current Electrode Distance (AB/2) [m]
No Res Thick Depth
1 1484.1 1.5 1.5
2 49.2 9.8 11.2
3 961.6 -.- -.-

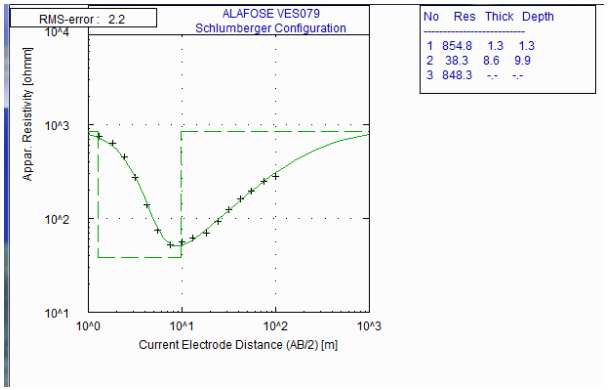
RMS-error : 2.2
ALAFOSE VES079
Schlumberger Configuration
Appar. Resistivity [ohmm]
Current Electrode Distance (AB/2) [m]
No Res Thick Depth
1 854.8 1.3 1.3
2 38.3 8.6 9.9
3 848.3 -.- -.-

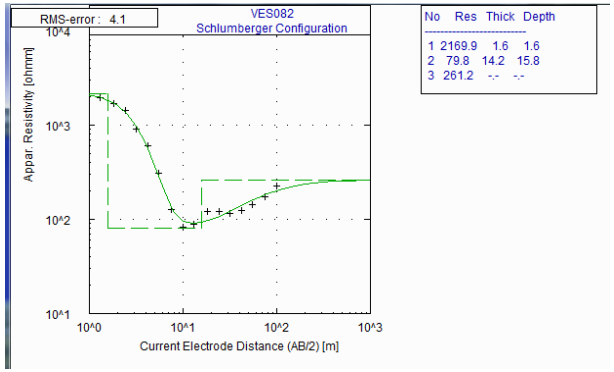
RMS-error : 4.1
VES082
Schlumberger Configuration
Appar. Resistivity [ohmm]
Current Electrode Distance (AB/2) [m]
No Res Thick Depth
1 2169.9 1.6 1.6
2 79.8 14.2 15.8
3 261.2 -.- -.-

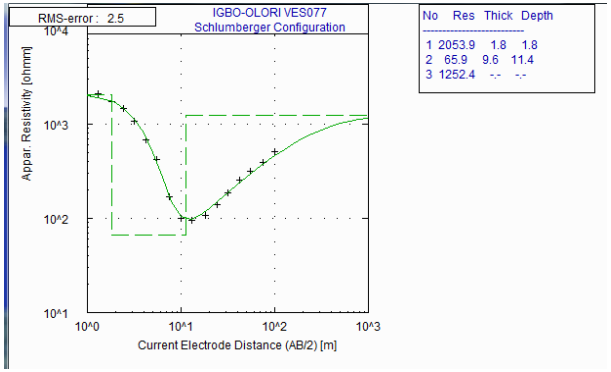
RMS-error : 2.5
IGBO-OLORI VES077
Schlumberger Configuration
Appar. Resistivity [ohmm]
Current Electrode Distance (AB/2) [m]
No Res Thick Depth
1 2053.9 1.8 1.8
2 65.9 9.6 11.4
3 1252.4 -.- -.-

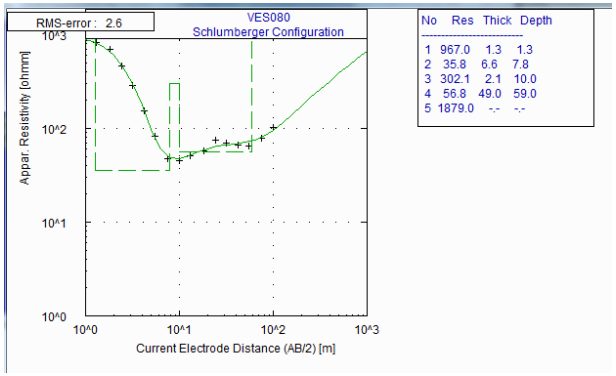
RMS-error : 2.6
VES080
Schlumberger Configuration
Appar. Resistivity [ohmm]
Current Electrode Distance (AB/2) [m]
No Res Thick Depth
1 967.0 1.3 1.3
2 35.8 6.6 7.8
3 302.1 2.1 10.0
4 56.8 49.0 59.0
5 1879.0 -.- -.-

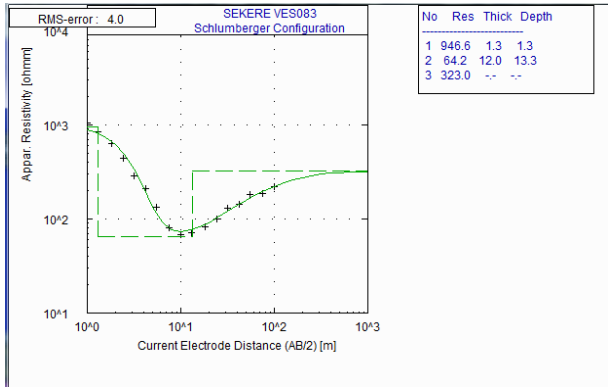
RMS-error : 4.0
SEKERE VES083
Schlumberger Configuration
Appar. Resistivity [ohmm]
Current Electrode Distance (AB/2) [m]
No Res Thick Depth
1 946.6 1.3 1.3
2 64.2 12.0 13.3
3 323.0 -.- -.-

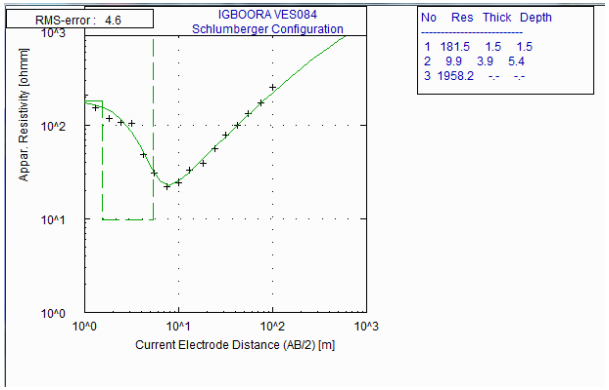
RMS-error : 4.6
IGBOORA VES084
Schlumberger Configuration
No Res Thick Depth
1 181.5 1.5 1.5
2 9.9 3.9 5.4
3 1958.2 -.- -.-
Appar. Resistivity [ohmm]
10^3
10^2
10^1
10^0
10^0 10^1 10^2 10^3
Current Electrode Distance (AB/2) [m]

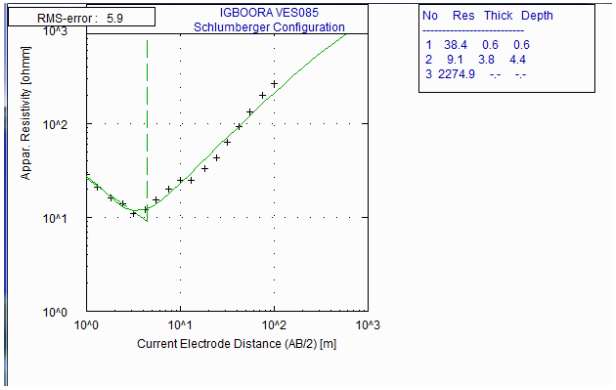
RMS-error : 5.9
IGBOORA VES085
Schlumberger Configuration
No Res Thick Depth
1 38.4 0.6 0.6
2 9.1 3.8 4.4
3 2274.9 -.- -.-
Appar. Resistivity [ohmm]
10^3
10^2
10^1
10^0
10^0 10^1 10^2 10^3
Current Electrode Distance (AB/2) [m]

APPENDIX VIII

QUANTITATIVE GEOELECTRIC PARAMETERS INTERPRETED FROM FIELD RESISTIVITY DATA

AMPHIBOLITES

			LAYER RESISTIVITY ohm.m					LAYER THICKNESS m					
s/n	VES stations	Elev.(m)	ρ1	ρ2	ρ3	ρ4	ρ5	h1	h2	h3	h4	TR m	Curve Type
1	15	150	44.8	9.8	572.7			1.3	13.6			14.8	H
2	17	171	307	44.2	105.7	232.1		0.5	1.5	27.8		29.9	HA
3	18	171	682	66.2	533.1	-	-	1.6	27.4			29	H
4	19	167	425.4	100.1	4534.9			4.2	12.2			16.3	H
5	20	168	365.5	46	991	-	-	2.7	25.2			27.9	H
6	22	165	464.3	26.2	292.4	-		0.9	16.3			17.2	H
7	23	163	648.1	47.8	863			1.8	17.7			19.5	H
8	24	175	151.2	30.4	205.9			2.1	16.8			18.9	H
9	25	168	67.8	10.5	794.9			1.7	11.2			12.9	H
10	26	198	978.2	34.2	409.3			1.4	13.6			15	H
11	27	179	239.7	2261.3	362			3.4	10.5			13.9	K
12	28	175	166.2	225.2	111.7	307.7		2.6	14.8	6.5		23.9	KH
13	29	145	984.4	20.8	2132.6			1.8	7			8.8	H
14	30	136	185.8	22.2	179.2	22.8	255	0.4	1.8	2.1	13.7	17.9	HKH
15	64	183	463.4	52.3	2455.4			1.5	15.7			17.2	H
16	65	213	1453.1	187.9	1400.6			1.2	10.3			11.5	H
17	66	169	2139.8	59.8	376.4			1.2	11.4			12.6	H
18	67	176	366.5	26.3	5472.7			5.8	28.2			34.0	H
19	68	182	122.2	38.5	2441.6			1.1	21.8			22.9	H
20	69	199	676.5	86.1	1836.2			0.7	38.7			39.4	H
21	70	159	1023.3	18.8	1100.6			0.6	5.1			5.7	H
22	71	148	3478	69.5	4760.3			2.1	22.5			24.5	H
23	72	145	389.8	32.5	570.8			1.1	6.8			7.9	H
24	84	119	181.5	9.9	1958.2			1.5	3.9			5.4	H
25	85	151	38.4	9.1	2274.9			0.6	3.8			4.4	H
	Min	119.00	38.40	9.10	105.70			0.40	1.50			4.40	
	Max	213.00	3478.00	2261.30	5472.70			5.80	38.70			39.40	
	Mean	167.00	641.72	141.42	1469.44			1.75	14.31			18.06	
	Median	168.00	389.80	38.50	863.00			1.45	13.60			17.20	
	Std dev.	20.61	767.34	444.71	1516.68			1.24	9.16			9.12	

TR: TOTAL REGOLITH THICKNESS

GNEISSES

			LAYER RESISTIVITY ohm.m				LAYER THICKNESS m				
s/n	**VES stations**	**Elev.(m)**	**ρ1**	**ρ2**	**ρ3**	**ρ4**	**h1**	**h2**	**h3**	**TR m**	**Curve Type**
1	16	150	176.9	433.7	71	1399.7	2.3	5.3	10.8	18.4	KH
2	21	148	713.3	86.9	778.1		2.2	14.4		16.6	H
3	37	154	1282.4	138	910.6		1.1	22.4		23.6	H
4	39	174	498.4	41.9	369.7		1.7	25.6		27.3	H
5	40	179	1178.1	215.6	685.7		0.8	19.6		20.4	H
6	41	169	3293.7	810.6	4412.9	536.8	1.3	9.5	11	21.8	HK
7	42	199	1820.3	224.1	801		1.2	16.1		17.3	H
8	43	161	1801.1	26.3	3891.3		1.5	13.3		14.8	H
9	44	149	536.7	69	196.6		1.1	20		21.1	H
10	45	163	1498.3	99	2966.3		2.1	6.1		8.2	H
11	50	133	4478.2	84.1	9601.4		1.9	4.4		6.3	H
12	51	144	898.3	56.4	2711.1		1.3	11.5		12.9	H
13	52	138	254	71.6	392.5		1.1	26.2		27.3	H
14	76	95	1484.1	49.2	961.6		1.5	9.8		11.2	H
15	77	129	2053.9	65.9	1252.4		1.8	9.6		11.4	H
16	78	126	984.3	38.6	934.5		1.7	8.2		9.9	H
17	79	108	854.8	38.3	848.3		1.3	8.6		9.9	H
18	80	99	1030.3	53	1039.4		1.2	46.4		47.5	H
19	81	81	754.5	18.8	1067.7		1.4	12.5		13.9	H
	Min	81.00	176.90	18.80	71		0.80	4.40		6.30	
	Max	199.00	4478.20	810.60	9601.40		2.30	46.40		47.50	
	Mean	141.61	1346.93	138.00	1783.80		1.50	15.20		17.88	
	Median	146.00	1030.30	69.00	934.50		1.40	12.50		16.60	
	Std dev.	31.49	1053.22	190.35	2256.87		0.40	10.00		9.47	

TR: TOTAL REGOLITH THICKNESS

MIGMATITES

			LAYER RESISTIVITY ohm.m				LAYER THICKNESS m				
s/n	**VES stations**	**Elev.(m)**	**ρ1**	**ρ2**	**ρ3**	**ρ4**	**h1**	**h2**	**h3**	**TR m**	**Curve Type**
1	3	139	1133.1	57.8	3106.4		2	4.8		6.8	H
2	9	169	309.5	1903	14.3	2589.4	0.5	1.3	8.6	10.4	KH
3	29	145	984.4	20.8	2132.6		1.8	7		8.8	H
4	38	161	1592.9	57.3	2627.7		1.5	13.2		14.7	H
5	49	112	2058.7	28.1	1002.6		1.7	11.9		13.6	H
6	53	191	763.2	32.2	191.3		2.8	13.7		16.5	H
7	54	180	2331.1	55.3	2538.6		1.3	22.4		23.6	H
8	55	168	984.8	47.8	1059.2		1.1	18.2		19.3	H
9	57	196	770.6	28.5	1248.8		0.9	8.7		9.6	H
10	58	194	604.2	103.8	394.3		1.3	11.3		12.6	H
11	59	174	2244.5	565.5	975.7		1.1	11.8		11.4	H
12	60	188	724.2	43	1280.9		1.5	13.3		14.8	H
13	61	172	237.2	77	385.6		2.7	9.1		11.9	H
14	62	153	1640.7	94.9	921.3		1.1	4.8		5.8	H
15	63	154	568.6	30.8	6863.3		1.3	3.4		4.6	H
16	73	120	1864.7	231.4	470.11		1.7	3.9		5.7	H
17	74	156	551.2	178.6	559.5		2.6	17		19.5	H
18	82	160	2169.9	79.8	251.2		1.6	14.2		15.8	H
19	83	144	946.6	64.2	323		1.3	12		13.3	H
	Min	112.00	237.20	20.8	14.30		0.50	1.30		4.60	
	Max	196.00	2331.10	1903.00	6863.30		2.80	22.40		23.60	
	Mean	161.89	1183.16	194.73	1386.65		1.57	10.63		12.56	
	Median	161.00	984.40	57.80	975.70		1.50	11.80		12.60	
	Std dev.	23.50	686.82	432.06	1603.63		0.61	5.52		5.12	

TR: TOTAL REGOLITH THICKNESS

PORPHYRITIC GRANITES

			LAYER RESISTIVITY ohm.m			LAYER THICKNESS m			
s/n	VES stations	Elev.(m)	ρ1	ρ2	ρ3	h1	h2	TR m	Curve Type
1	1	136	380	98.7	2188.3	0.9	6.2	7.1	H
2	2	147	987.5	56.9	7800.5	0.9	7.9	8.8	H
3	4	142	110.5	56.7	2686.9	1.2	13	14.2	H
4	5	111	1303.6	101.6	547.2	0.8	5	5.8	H
5	6	93	793.3	145.5	1285.5	0.9	6.6	7.6	H
6	7	123	813.9	33.2	2563.6	2.9	9.8	12.7	H
7	8	189	1426.4	47.7	2109.3	1.2	7.5	8.7	H
8	10	201	605.2	162.4	5667.5	1	7.5	8.5	H
9	11	208	239.4	49.1	2206.9	0.8	6.9	7.7	H
10	12	185	181.7	47.5	2952	2.5	13.4	15.9	H
11	13	169	1541.9	39.7	2163.1	1.9	15.1	17	H
12	14	164	254	26.5	3182.5	2.9	7.1	10	H
13	31	151	226.8	34.4	29903.8	0.6	1.8	2.4	H
14	32	158	1003.3	97.4	1273.2	1.2	7	8.2	H
15	33	150	1564.7	150.3	1113.9	1.6	10.7	12.3	H
16	46	171	2036.4	30.1	2647.1	4.5	9.5	14	H
17	47	197	2680	294	11817.3	1.3	19.4	20.8	H
18	48	195	3271.9	233.8	4363.1	2.1	14.1	16.2	H
19	56	168	2233.7	74.2	3073.1	3.4	13.1	16.5	H
20	75	165	1377.1	80.8	2479.7	2.6	8.7	11.3	H
	Min	93.00	110.50	26.50	547.20	0.60	1.80	2.40	
	Max	208.00	3271.90	294.00	29903.80	4.50	19.40	20.80	
	Mean	161.15	1151.57	93.03	4601.23	1.76	9.52	11.29	
	Median	164.50	995.40	65.55	2605.35	1.25	8.30	10.65	
	Std dev.	30.64	887.36	72.04	6494.13	1.06	4.11	4.59	

TR: TOTAL REGOLITH THICKNESS

APPENDIX IX
GEO-ELECTRIC PARAMETERS WITH CORRESPONDING ESTIMATED DAR-ZARROUK VARIABLES

AMPHIBOLITES

LAYER RESISTIVITY ohm.m LAYER THICKNESS m

s/n	VES STATIONS	elev.(m)	ρ1	ρ2	ρ3	ρ4	ρ5	h1	h2	h3	h4	H	S=∑hi/ρi	T=∑hi * ρi	ρl = H/S	ρt = T/H	ρt / ρl	λ= √ρt / ρl
1	15	150	44.8	9.8	572.7			1.3	13.6			14.8	1.42	191.52	10.45	12.94	1.24	1.11
2	17	171	307	44.2	105.7	232.1		0.5	1.5	27.8		29.9	0.30	3158.26	100.14	105.63	1.05	1.03
3	18	171	682	66.2	533.1	-	-	1.6	27.4			29	0.42	2905.08	69.67	100.18	1.44	1.20
4	19	167	425.4	100.1	4534.9			4.2	12.2			16.3	0.13	3007.90	123.72	184.53	1.49	1.22
5	20	168	365.5	46	991	-	-	2.7	25.2			27.9	0.56	2146.05	50.25	76.92	1.53	1.24
6	22	165	464.3	26.2	292.4	-		0.9	16.3			17.2	0.62	844.93	27.56	49.12	1.78	1.34
7	23	163	648.1	47.8	863			1.8	17.7			19.5	0.37	2012.64	52.27	103.21	1.97	1.41
8	24	175	151.2	30.4	205.9			2.1	16.8			18.9	0.57	828.24	33.36	43.82	1.31	1.15
9	25	**168**	67.8	10.5	794.9			1.7	11.2			12.9	1.09	232.86	11.82	18.05	1.53	1.24
10	26	198	978.2	34.2	409.3			1.4	13.6			15	0.40	1834.60	37.59	122.31	3.25	1.80
11	27	239	239.7	2261.3	362			3.4	10.5			13.9	0.02	24558.63	738.27	1766.81	2.39	1.55
12	28	175	166.2	225.2	111.7	307.7		2.6	14.8	6.5		23.9	0.10	4491.13	233.20	187.91	0.81	0.90
13	29	145	984.4	20.8	2132.6			1.8	7			8.8	0.34	1917.52	26.01	217.90	8.38	2.89
14	30	136	185.8	22.2	179.2	22.8	255	0.4	1.8	2.1	13.7	17.9	0.70	802.96	25.72	44.86	1.74	1.32
15	64	183	463.4	52.3	2455.4			1.5	15.7			17.2	0.30	1516.21	56.69	88.15	1.56	1.25
16	65	213	1453.1	187.9	1400.6			1.2	10.3			11.5	0.06	3679.09	206.68	319.92	1.55	1.24
17	66	169	2139.8	59.8	376.4			1.2	11.4			12.6	0.19	3249.48	65.90	257.90	3.91	1.98
18	67	176	366.5	26.3	5472.7			5.8	28.2			34	1.09	2867.36	31.25	84.33	2.70	1.64
19	68	182	122.2	38.5	2441.6			1.1	21.8			22.9	0.58	973.72	39.81	42.52	1.07	1.03
20	69	199	676.5	86.1	1836.2			0.7	38.7			39.4	0.45	3805.62	87.46	96.59	1.10	1.05
21	70	159	1023.3	18.8	1100.6			0.6	5.1			5.7	0.27	709.86	20.97	124.54	5.94	2.44
22	71	148	3478	69.5	4760.3			2.1	22.5			24.5	0.32	8867.55	75.54	361.94	4.79	2.19
23	72	145	389.8	32.5	570.8			1.1	6.8			7.9	0.21	649.78	37.25	82.25	2.21	1.49
24	84	119	181.5	9.9	1958.2			1.5	3.9			5.4	0.40	310.86	13.43	57.57	4.29	2.07
25	85	151	38.4	9.1	2274.9			0.6	3.8			4.4	0.43	57.62	10.16	13.10	1.29	1.14

GNEISSES

			LAYER RESISTIVITY ohm.m					LAYER THICKNESS m					DAR-ZARROUK VARIABLES				
s/n	VES STATIONS	elev.(m)	ρ1	ρ2	ρ3	ρ4	ρ5	h1	h2	h3	h4	H	S=∑hi/ρi	T=∑hi * ρi	ρl = H/S	ρt = T/H	ρt / ρl	λ= √ρt / ρl
1	16	150	176.9	433.7	71	1399.7		2.3	5.3	10.8		18.4	0.18	3472.28	103.76	188.71	1.82	1.35
2	21	148	713.3	86.9	778.1			2.2	14.4			16.6	0.17	2820.62	98.35	169.92	1.73	1.31
3	37	154	1282.4	138	910.6			1.1	22.4			23.6	0.16	4501.84	144.63	190.76	1.32	1.15
4	39	174	498.4	41.9	369.7			1.7	25.6			27.3	0.61	1919.92	44.43	70.33	1.58	1.26
5	40	179	1178.1	215.6	685.7			0.8	19.6			20.4	0.09	5168.24	222.74	253.35	1.14	1.07
6	41	169	3293.7	810.6	4412.9	526.8		1.3	9.5	11		21.8	0.01	60524.41	1492.43	2776.35	1.86	1.36
7	42	199	1820.3	224.1	801			1.2	16.1			17.3	0.07	5792.37	238.61	334.82	1.40	1.18
8	43	161	1801.1	26.3	3891.3			1.5	13.3			14.8	0.51	3051.44	29.22	206.18	7.06	2.66
9	44	149	536.7	69	196.6			1.1	20			21.1	0.29	1970.37	72.28	93.38	1.29	1.14
10	45	163	1498.3	99	2966.3			2.1	6.1			8.2	0.06	3750.33	130.12	457.36	3.51	1.87
11	50	133	4478.2	84.1	9601.4			1.9	4.4			6.3	0.05	8878.62	119.45	1409.30	11.80	3.43
12	51	144	898.3	56.4	2711.1			1.3	11.5			12.9	0.21	1816.39	62.82	140.81	2.24	1.50
13	52	138	254	71.6	392.5			1.1	26.2			27.3	0.37	2155.32	73.73	78.95	1.07	1.03
14	76	95	1484.1	49.2	961.6			1.5	9.8			11.2	0.20	2708.31	55.94	241.81	4.32	2.08
15	77	129	2053.9	65.9	1252.4			1.8	9.6			11.4	0.15	4329.66	77.79	379.79	4.88	2.21
16	78	126	984.3	38.6	934.5			1.7	8.2			9.9	0.21	1989.83	46.23	200.99	4.35	2.09
17	79	108	854.8	38.3	848.3			1.3	8.6			9.9	0.23	1440.62	43.79	145.52	3.32	1.82
18	80	99	967	35.8	302.1	56.8	1879	1.3	6.6	2.1	49	59	1.06	4910.99	55.91	83.24	1.49	1.22
19	81	81	754.5	18.8	1067.7			1.4	12.5			13.9	0.67	1291.30	20.85	92.90	4.46	2.11

MIGMATITES

LAYER RESISTIVITY ohm.m LAYER THICKNESS m DAR-ZARROUK VARIABLES

s/n	VES STATIONS	Elev. (m)	ρ1	ρ2	ρ3	ρ4	ρ5	h1	h2	h3	h4	H	S=∑hi/ρi	T=∑hi * ρi	ρl = H/S	ρt = T/H	ρt / ρl	λ= √ρt / ρl
1	3	139	1133.1	57.8	3106.4			2	4.8			6.8	0.08	2543.64	80.18	374.06	4.67	2.16
	9	169	309.5	1903	14.3	2589.4		0.5	1.3	8.6		10.4	0.60	2628.65	17.23	252.75	14.67	3.83
2	38	161	1592.9	57.3	2627.7			1.5	13.2			14.7	0.23	3145.71	63.55	213.99	3.37	1.84
3	49	112	2058.7	28.1	1002.6			1.7	11.9			13.6	0.42	3834.18	32.05	281.93	8.80	2.97
4	53	191	763.2	32.2	191.3			2.8	13.7			16.5	0.43	2578.10	38.45	156.25	4.06	2.02
5	54	180	2331.1	55.3	2538.6			1.3	22.4			23.6	0.41	4269.15	58.18	180.90	3.11	1.76
6	55	168	984.8	47.8	1059.2			1.1	18.2			19.3	0.38	1953.24	50.54	101.20	2.00	1.42
7	57	196	770.6	28.5	1248.8			0.9	8.7			9.6	0.31	941.49	31.33	98.07	3.13	1.77
8	58	194	604.2	103.8	394.3			1.3	11.3			12.6	0.11	1958.40	113.50	155.43	1.37	1.17
9	59	174	2244.5	565.5	975.7			1.1	11.8			11.4	0.02	9141.85	533.79	801.92	1.50	1.23
10	60	188	724.2	43	1280.9			1.5	13.3			14.8	0.31	1658.20	47.53	112.04	2.36	1.54
11	61	172	237.2	77	385.6			2.7	9.1			11.9	0.13	1341.14	91.85	112.70	1.23	1.11
12	62	153	1640.7	94.9	921.3			1.1	4.8			5.8	0.05	2260.29	113.17	389.71	3.44	1.86
13	63	154	568.6	30.8	6863.3			1.3	3.4			4.6	0.11	843.90	40.83	183.46	4.49	2.12
14	73	120	1864.7	231.4	470.11			1.7	3.9			5.7	0.02	4072.45	320.84	714.46	2.23	1.49
15	74	156	551.2	178.6	559.5			2.6	17			19.5	0.10	4469.32	195.19	229.20	1.17	1.08
16	82	160	2169.9	79.8	251.2			1.6	14.2			15.8	0.18	4605.00	88.43	291.46	3.30	1.82
17	83	144	946.6	64.2	323			1.3	12			13.3	0.19	2000.98	70.64	150.45	2.13	1.46
18																		

PORPHYRITIC GRANITE

			LAYER RESISTIVITY ohm.m					LAYER THICKNESS m				DAR-ZARROUK VARIABLES					
s/n	**VES STATIONS**	**Elev. (m)**	**ρ1**	**ρ2**	**ρ3**	**ρ4**	**ρ5**	**h1**	**h2**	**h3**	**h4**	**H**	**S=∑hi/ρi**	**T=∑hi * ρi**	**ρl = H/S**	**ρt = T/H**	**ρt / ρl**	**λ= √ρt / ρl**
1	1	136	380	98.7	2188.3			0.9	6.2			7.1	0.07	953.94	108.92	134.36	1.23	1.11
	2	147	987.5	56.9	7800.5			0.9	7.9			8.8	0.14	1338.26	62.97	152.08	2.42	1.55
2	4	142	110.5	56.7	2686.9			1.2	13			14.2	0.24	869.70	59.13	61.25	1.04	1.02
3	5	111	1303.6	101.6	547.2			0.8	5			5.8	0.05	1550.88	116.40	267.39	2.30	1.52
4	6	93	793.3	145.5	1285.5			0.9	6.6			7.6	0.05	1674.27	163.46	220.30	1.35	1.16
5	7	123	813.9	33.2	2563.6			2.9	9.8			12.7	0.30	2685.67	42.51	211.47	4.97	2.23
6	8	189	1426.4	47.7	2109.3			1.2	7.5			8.7	0.16	2069.43	55.04	237.87	4.32	2.08
7	10	201	605.2	162.4	5667.5			1	7.5			8.5	0.05	1823.20	177.70	214.49	1.21	1.10
8	11	208	239.4	49.1	2206.9			0.8	6.9			7.7	0.14	530.31	53.52	68.87	1.29	1.13
9	12	185	181.7	47.5	2952			2.5	13.4			15.9	0.30	1090.75	53.74	68.60	1.28	1.13
10	13	169	1541.9	39.7	2163.1			1.9	15.1			17	0.38	3529.08	44.55	207.59	4.66	2.16
11	14	164	254	26.5	3182.5			2.9	7.1			10	0.28	924.75	35.80	92.48	2.58	1.61
12	31	151	226.8	34.4	29903.8			0.6	1.8			2.4	0.05	198.00	43.66	82.50	1.89	1.37
13	32	158	1003.3	97.4	1273.2			1.2	7			8.2	0.07	1885.76	112.23	229.97	2.05	1.43
14	33	150	1564.7	150.3	1113.9			1.6	10.7			12.3	0.07	4111.73	170.33	334.29	1.96	1.40
15	46	171	2036.4	30.1	2647.1			4.5	9.5			14	0.32	9449.75	44.05	674.98	15.32	3.91
16	47	197	2680	294	11817.3			1.3	19.4			20.8	0.07	9187.60	312.92	441.71	1.41	1.19
17	48	195	3271.9	233.8	4363.1			2.1	14.1			16.2	0.06	10167.57	265.79	627.63	2.36	1.54
18	56	168	2233.7	74.2	3073.1			3.4	13.1			16.5	0.18	8566.60	92.66	519.19	5.60	2.37
19	75	165	1377.1	80.8	2479.7			2.6	8.7			11.3	0.11	4283.42	103.14	379.06	3.68	1.92
20																		

APPENDIX X

LITHOLOGIC INTERPRETATION OF THE RESISTIVITIES OF SAPROLITE LAYER

AMPHIBOLITES

s/n	VES station	thickness (m)	Layer resis. ρ2	Interpretation/lithology
1	15	13.6	9.8	clayey
2	17	1.5	44.2/105.7	clay/sandy clay
3	18	27.4	66.2	sandy clay
4	19	12.2	100.1	sandy clay
5	20	25.2	46	clayey
6	22	16.3	26.2	clayey
7	23	17.7	47.8	clayey
8	24	16.8	30.4	clayey
9	25	11.2	10.5	clay
10	26	13.6	34.2	clayey
11	27	10.5	2261.3	compacted lateritic clay
12	28	14.8/6.5	225.2/111.7	clayey sand/sandy clay
13	29	7	20.8	clay
14	30	1.8/4.2	22.2/179.2	clay/clayey sand
15	64	15.7	52.3	clayey
16	65	10.3	187.9	clayey sand
17	66	11.4	59.8	clayey
18	67	28.2	26.3	clayey
19	68	21.8	38.5	clayey
20	69	38.7	86.1	sandy clay
21	70	5.1	18.8	clayey
22	71	22.5	69.5	sandy clay
23	72	6.8	32.5	clayey
24	84	3.9	9.9	clayey
25	85	3.8	9.1	clayey

GNEISSES

s/n	VES station	Thickness m	layer resis. ρ2	Interpretation/lithology
1	16	5.3/10.8	433.7/71	compacted sand/sandy clay
2	21	14.4	86.9	sandy clay
3	37	22.4	138	sandy clay
4	39	25.6	41.9	clayey
5	40	19.6	215.6	clayey sand
6	41	9.5/11	810.6/4412.9	compacted lateritic clay
7	42	16.1	224.1	clayey sand
8	43	13.3	26.3	clayey
9	44	20	69	sandy clay
10	45	6.1	99	sandy clay
11	50	4.4	84.1	sandy clay
12	51	11.5	56.4	clayey
13	52	26.2	71.6	sandy clay
14	76	9.8	49.2	clayey
15	77	9.6	65.9	sandy clay
16	78	8.2	38.6	clayey
17	79	8.6	38.3	clayey
18	80	46.4	53	clayey
19	81	12.5	18.8	clayey

MIGMATITES

s/n	VES station	Thickness (m)	Layer resis. ρ2	Interpretation/lithology
1	3	4.8	57.8	clayey
2	9	1.3/8.6	1903/14.3	Compacted lateritic clay/clayey
3	38	13.2	57.3	clayey
4	49	11.9	28.1	clayey
5	53	13.7	32.2	clayey
6	54	22.4	55.3	clayey
7	55	18.2	47.8	clayey
8	57	8.7	28.5	clayey
9	58	11.3	103.8	sandy clay
10	59	11.8	565.5	sandy
11	60	13.3	43	clayey
12	61	9.1	77	sandy clay
13	62	4.8	94.9	sandy clay
14	63	3.4	30.8	clayey
15	73	3.9	231.4	clayey sand
16	74	17	178.6	clayey sand
17	82	14.2	79.8	sandy clay
18	83	12	64.2	sandy clay

PORPHYRITIC GRANITE

s/n	VES station	Thickness (m)	Layer resis. ρ2	Interpretation/lithology
1	1	6.2	98.7	sandy clay
2	2	7.9	56.9	clayey
3	4	13	56.7	clayey
4	5	5	101.6	sandy clay
5	6	6.6	145.5	sandy clay
6	7	9.8	33.2	clayey
7	8	7.5	47.7	clayey
8	10	7.5	162.4	clayey sand
9	11	6.9	49.1	clayey
10	12	13.4	47.5	clayey
11	13	15.1	39.7	clayey
12	14	7.1	26.5	clayey
13	31	1.8	34.4	clayey
14	32	7	97.4	sandy clay
15	33	10.7	150.3	sandy clay
16	46	9.5	30.1	clayey
17	47	19.4	294	sandy
18	48	14.1	233.8	clayey sand
19	56	13.1	74.2	sandy clay
20	75	8.7	80.8	sandy clay

APPENDIX XI

LITHOLOGIC INTERPRETATION OF THE BEDROCKS

AMPHIBOLITES

s/n	VES Points	Ωm	Depth (m)	Interpre.
1	15	572.7	14.8	FRB
2	17	232	29.9	FRB
3	18	533.1	29	FRB
4	19	4534.9	16.3	FB
5	20	991	27.9	WB
6	22	292.4	17.2	FRB
7	23	863	19.5	WB
8	24	205.9	18.9	FRB
9	25	794.9	12.9	WB
10	26	409.3	15	FRB
11	27	362	13.9	FRB
12	28	307.7	23.9	FRB
13	29	2132.6	8.8	FB
14	30	255	17.9	FRB
15	64	2455.4	17.2	FB
16	65	1400.6	11.5	FB
17	66	376.4	12.6	FRB
18	67	5472.7	34	FB
19	68	2441.6	22.9	FB
20	69	1836.2	39.4	FB
21	70	1100.6	5.7	FB
22	71	4760.3	24.5	FB
23	72	570.8	7.9	FRB
24	84	1958.2	5.4	FB
25	85	2274.9	4.4	FB

GNEISSES

s/n	VES Points	Ωm	Depth (m)	Interpre.
1	16	1400	18.4	WB
2	21	778.1	16.6	FRB
3	37	910.6	23.6	WB
4	39	369.7	27.3	FRB
5	40	685.7	20.4	FRB
6	41	4412.9	21.8	FB
7	42	801	17.3	WB
8	43	3891.3	14.8	FB
9	44	196.6	21.1	FRB
10	45	2966.3	8.2	FB
11	50	9601.4	6.3	FB
12	51	2711.1	12.9	FB
13	52	392.5	27.3	FRB
14	76	961.6	11.2	WB
15	77	1252.4	11.4	WB
16	78	934.5	9.9	WB
17	79	848.3	9.9	WB
18	80	1039.4	59	WB
19	81	1067.7	13.9	WB

MIGMATITES

s/n	VES Points	Ωm	Depth (m)	Interpret.
1	3	3106.4	6.8	FB
2	9	2589	10.4	FB
3	38	2627.7	14.7	FB
4	49	1002.6	13.6	WB
5	53	191.3	16.5	FRB
6	54	2538.6	23.6	FB
7	55	1059.2	19.3	WB
8	57	1248.8	9.6	WB
9	58	394.3	12.6	FRB
10	59	975.7	11.4	WB
11	60	1280.9	14.8	WB
12	61	385.6	11.9	FRB
13	62	921.3	5.8	WB
14	63	6863.3	4.6	FB
15	73	470.11	5.7	FRB
16	74	559.5	19.5	FRB
17	82	251.2	15.8	FRB
18	83	323	13.3	FRB

PORPHYRITIC GRANITE

s/n	VES Points	Ωm	Depth (m)	Interp.
1	1	2188.3	7.1	FB
2	2	7800.5	8.8	FB
3	4	2686.9	14.2	FB
4	5	547.2	5.8	FRB
5	6	1285.5	7.6	WB
6	7	2563.6	12.7	FB
7	8	2109.3	8.7	FB
8	10	5667.5	8.5	FB
9	11	2206.9	7.7	FB
10	12	2952	15.9	FB
11	13	2163.1	17	FB
12	14	3182.5	10	FB
13	31	29903.8	2.4	FB
14	32	1273.2	8.2	WB
15	33	1113.9	12.3	WB
16	46	2647.1	14	FB
17	47	11817.3	20.8	FB
18	48	4363.1	16.2	FB
19	56	3073.1	16.5	FB
20	75	2479.7	11.3	FB

FRB **Fractured bedrock**

WB **Weathered bedrock**

FB **Fresh bedrock**

APPENDIX XII

TIME-DRAWDOWN-RECOVERY DATA WITH RESPECTIVE SEMI-LOG PLOTS FROM SINGLE WELL PUMPING AND THE CORRESPONDING RECOVERY TESTS

BOREHOLE LOCATION 01: ONILADO-Igboora
LONGITUDE: 7 26 36.4
LATITUDE: 3 17 07.2
ELEVATION: 176m
PRE-TEST STATIC WATER LEVEL: 6.6m
DEPTH OF WELL: 22.9m/75.57FT.

t seconds	Drawdown (m)
0	0
30	1.05
60	2.14
90	3.32
120	4.27
180	5.95
240	7.74
300	9.46
420	11.35
540	11.97
720	12.96

t seconds	Recovery m
0	12.96
30	11.00
60	10.95
180	10.15
240	10.00
420	9.49
720	9.20
900	8.80
1200	7.30
1500	5.95
1800	5.37
2400	4.15
3000	3.47
3600	2.60
5400	1.40
7200	0.77
9000	0.49
10800	0.20

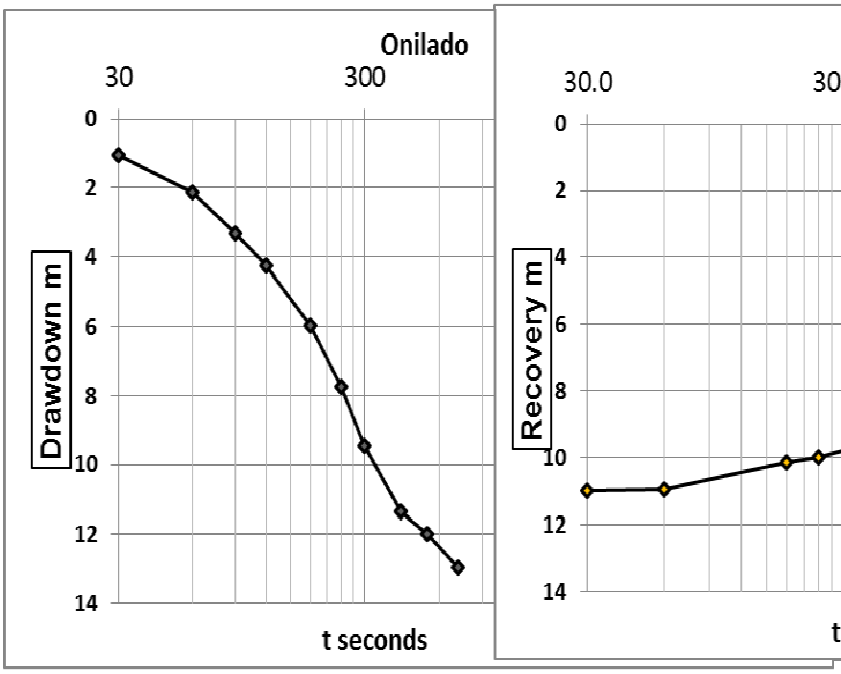

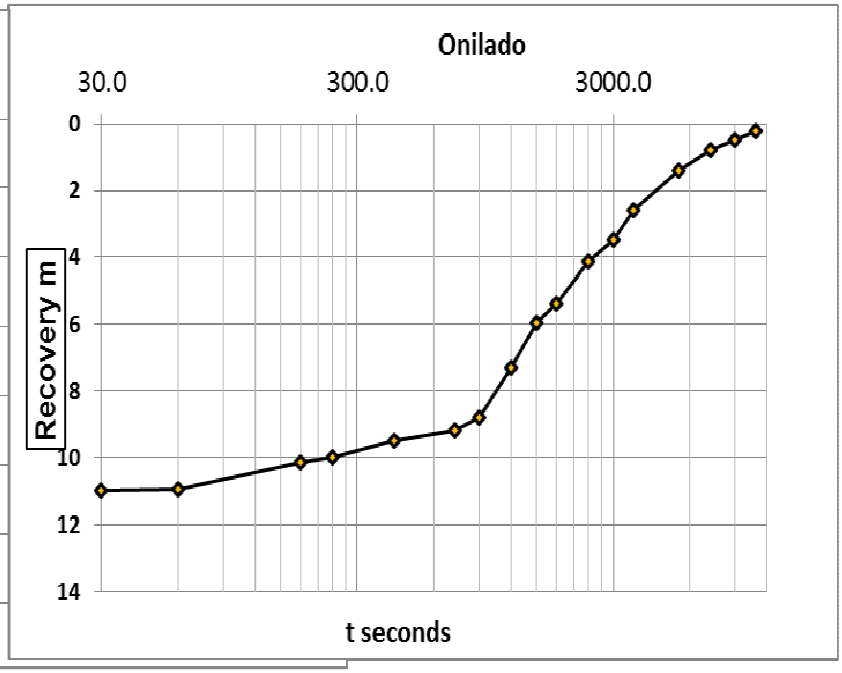

BOREHOLE LOCATION 02: SAGAUN-Igboora Old secretariat

LONGITUDE: 7 26 09.9
LATITUDE: 3 17 11.7
ELEVATION: 162m
PRE-TEST STATIC WATER LEVEL: 3.3m
DEPTH OF WELL: 22.8m/75.24FT.
DEPTH OF PUMP INSTALLATION: 18.18m/60FT

t seconds	Drawdown (m)	t seconds	Recovery (m)
0	0	0	15.36
30	1.50	30	15.14
60	3.40	60	15.22
90	5.08	90	15.01
120	6.69	120	14.83
150	8.31	180	14.49
180	12.01	240	14.14
240	14.05	360	13.29
300	15.36	480	12.74
		600	12.15
		900	10.70
		1200	9.08
		1800	7.71
		2400	6.40
		3600	4.45
		4800	3.31
		6000	2.25
		7200	1.51

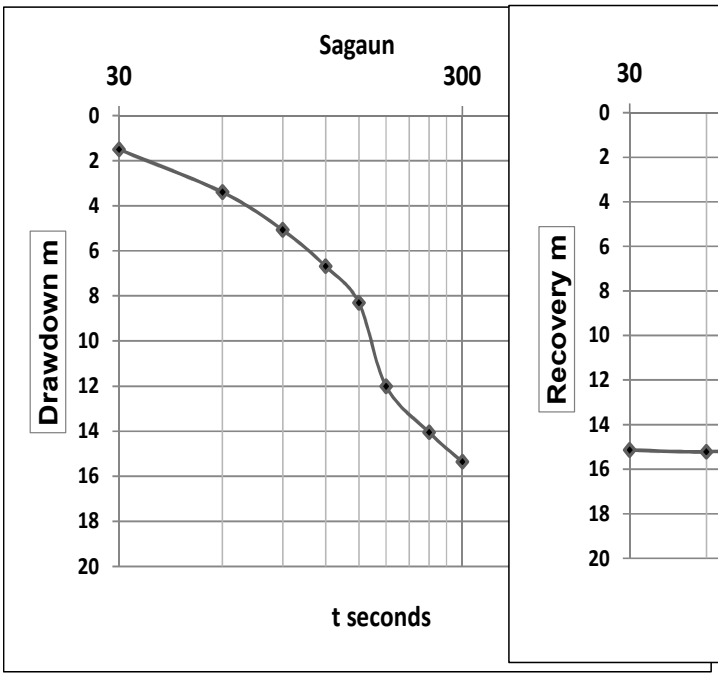

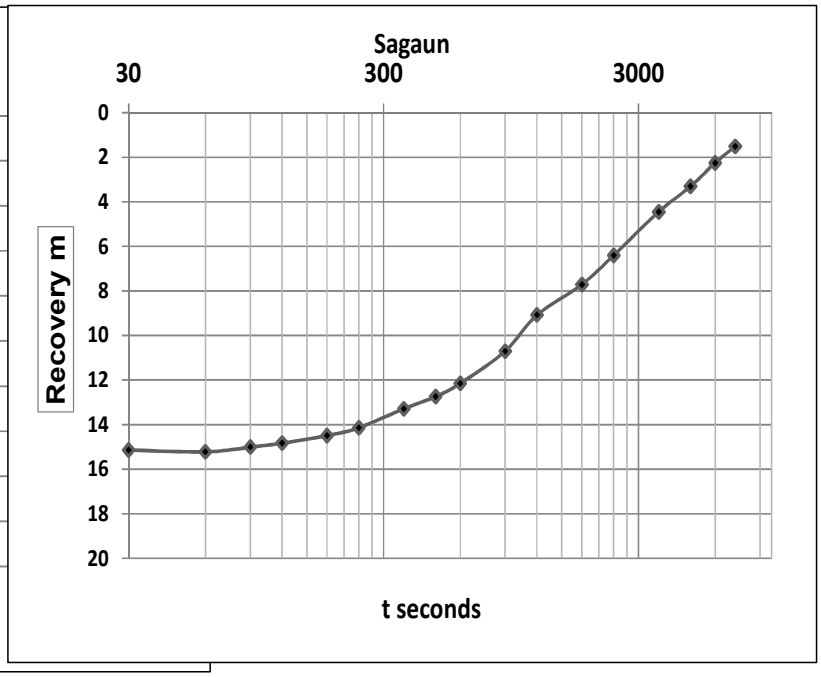

BOREHOLE LOCATION 03: PAKO-IGBOORA
LONGITUDE: 7 25 39.7
LATITUDE: 3 17 38.7
ELEVATION: 187m
PRE-TEST STATIC WATER LEVEL: 6.4m
DEPTH OF WELL: 31.55m/104.11
DEPTH OF PUMP INSTALLATION: 25.45m/80FT.

t seconds	drawdown (m)	t seconds	recovery m
0	0	0	7.90
30	1.71	30	5.92
60	2.69	60	5.30
90	3.08	90	5.17
120	3.51	120	4.93
150	3.90	180	4.41
180	4.05	240	4.12
240	4.29	360	3.84
300	4.40	480	3.35
360	4.58	600	2.99
420	4.76	900	2.46
540	4.87	1200	1.75
660	5.07	1800	1.15
780	5.30	2400	0.81
900	5.50	3600	0.45
1200	6.04	4800	0.30
1500	6.42	6000	0.25
1800	6.76		
2400	7.09		
3000	7.40		
3600	7.72		
5400	7.90		

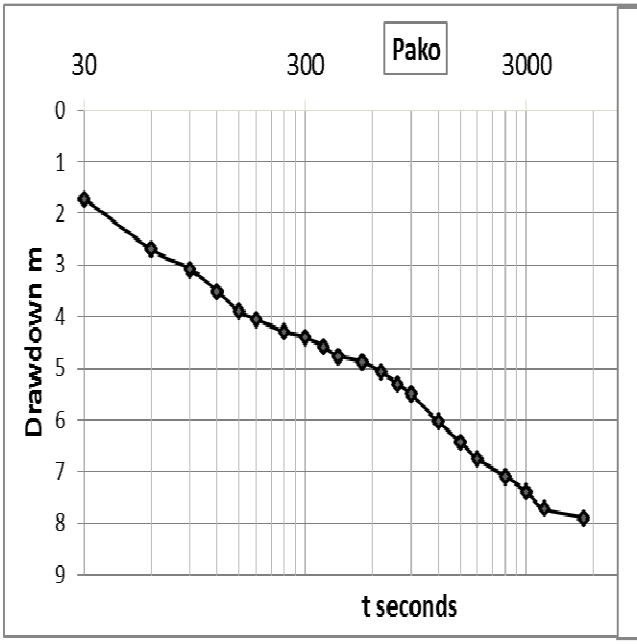

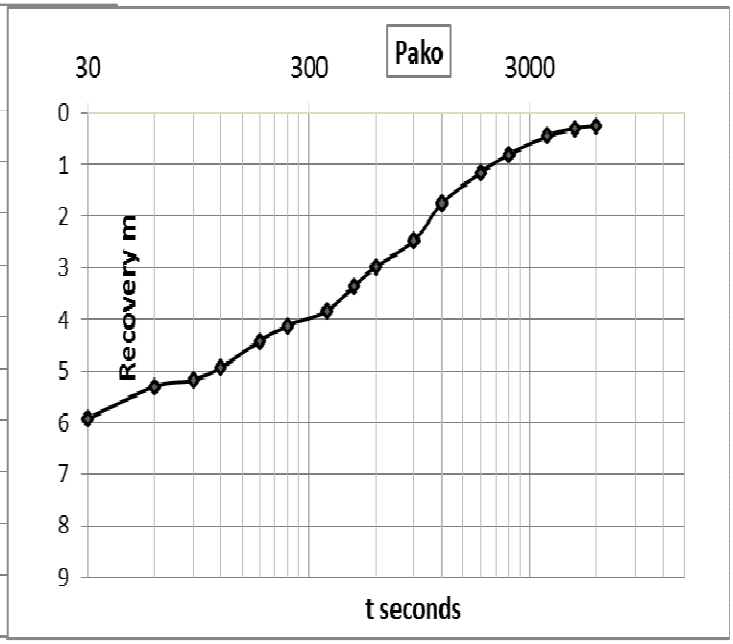

BOREHOLE LOCATION 04: Igboole I-Igboora Maternity centre
LONGITUDE: 7 25 35.9
LATITUDE: 3 17 51.5
ELEVATION: 170m
PRE-TEST STATIC WATER LEVEL: 4.95/4.9m
DEPTH OF WELL: 38m/125.4FT.
DEPTH OF PUMP INSTALLATION: 19.7m/65FT.

t seconds	Drawdown m	t/t1	Residual drawdown(m)	t seconds	Recovery m
0	0	361.00	4.00	0	5.2
30	1.37	181.00	3.79	30	4.00
60	1.90	121.00	3.58	60	3.79
90	2.57	91.00	3.33	90	3.58
120	4.08	73.00	3.12	120	3.33
150	4.93	61.00	3.05	150	3.12
180	5.40	46.00	2.89	180	3.05
240	3.00	30.83	2.63	240	2.89
300	3.61	23.25	2.45	360	2.63
360	3.78	18.70	2.25	480	2.45
420	4.07	12.60	1.80	600	2.25
540	4.05	9.55	1.63	900	1.80
660	3.87	6.43	1.34	1200	1.63
780	3.81	4.88	1.15	1800	1.34
900	3.66	3.33	0.85	2400	1.15
1200	3.66	2.56	0.70	3600	0.85
1500	3.89	2.10	0.60	4800	0.70
1800	4.00	2.00	0.52	6000	0.60
3600	4.50			7200	0.52
5400	4.70				
7200	5.03				
9000	5.15				
10800	5.20				

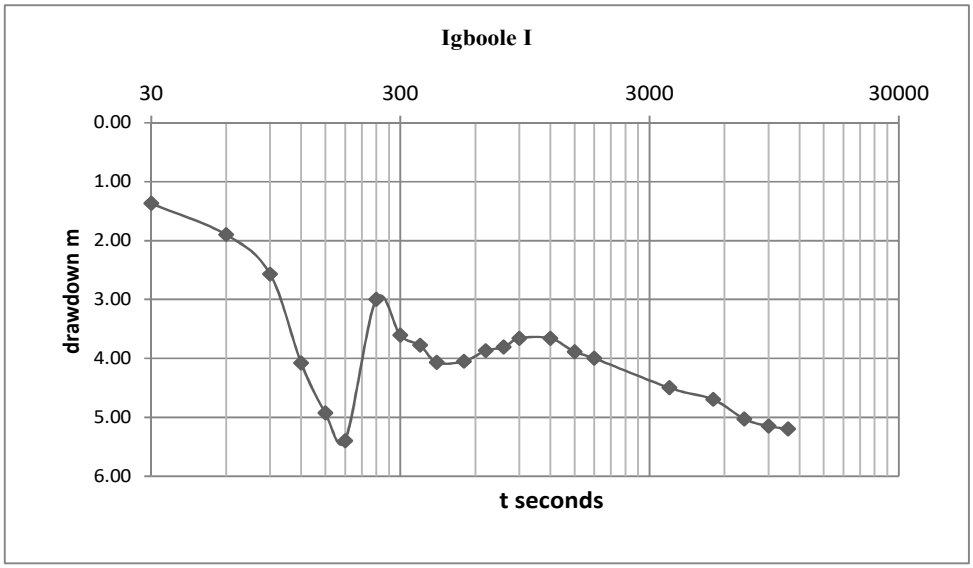
Igboole I
30
300
3000
30000
0.00
1.00
2.00
3.00
4.00
5.00
6.00
drawdown m
t seconds

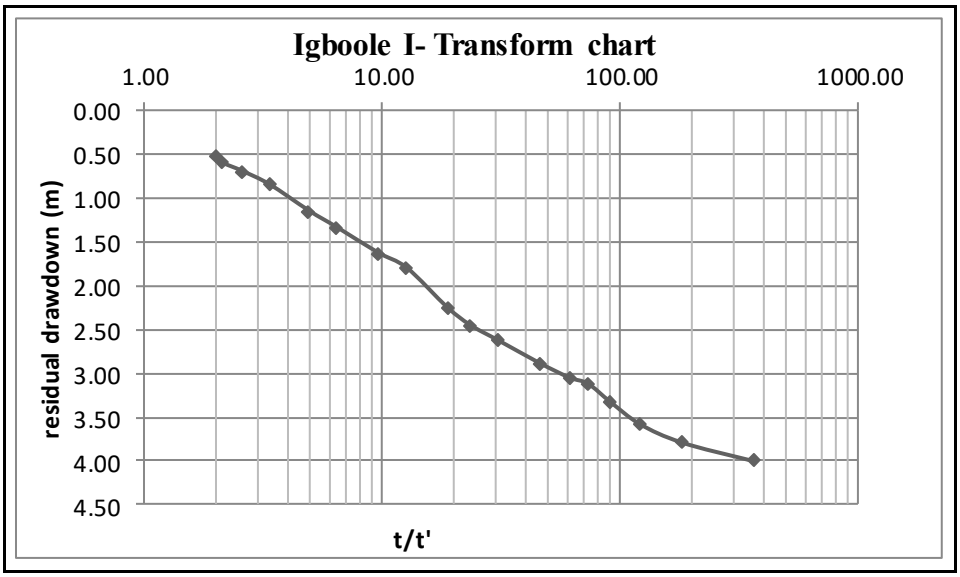
Igboole I- Transform chart
1.00
10.00
100.00
1000.00
0.00
0.50
1.00
1.50
2.00
2.50
3.00
3.50
4.00
4.50
residual drawdown (m)
t/t'

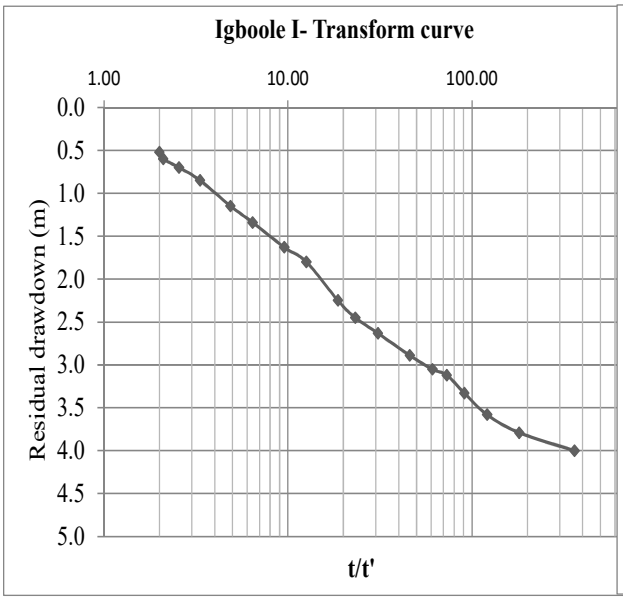
Igboole I- Transform curve
1.00
10.00
100.00
0.0
0.5
1.0
1.5
2.0
2.5
3.0
3.5
4.0
4.5
5.0
Residual drawdown (m)
t/t'

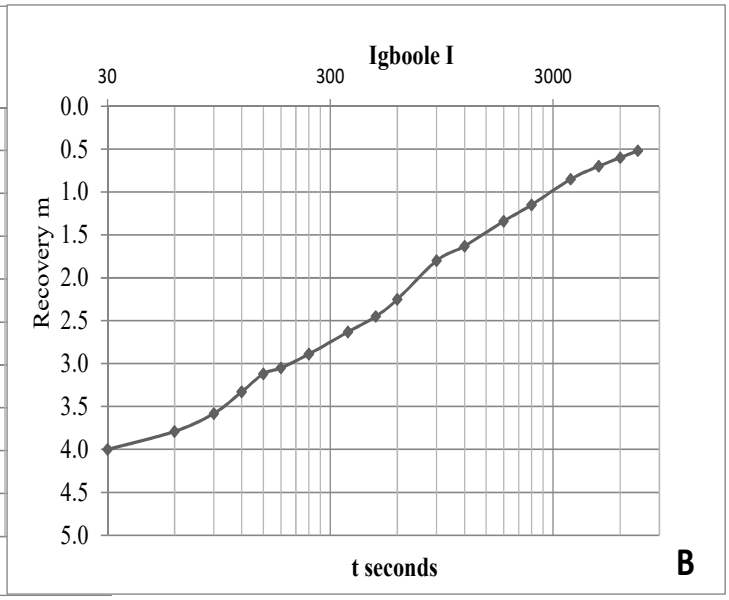
Igboole I
30
300
3000
0.0
0.5
1.0
1.5
2.0
2.5
3.0
3.5
4.0
4.5
5.0
Recovery m
t seconds
B

BOREHOLE LOCATION 05: Igboole II: Igboora express junction

LONGITUDE: 7 25 28.6
LATITUDE: 3 18 34.9
ELEVATION: 175m
PRE-TEST STATIC WATER LEVEL: 3.23/3.21m
DEPTH OF WELL: 30.4m/100.32ft.
DEPTH OF PUMP INSTALLATION: 25.45m/84FT.

t seconds	drawdown(m)	t seconds	Recovery m
0	0	0	13.51
30	1.8	30	13.11
60	2.97	60	12.33
90	3.46	90	10.56
120	5.39	120	9.79
150	6.51	180	8.46
180	7.19	240	7.51
240	8.56	360	6.04
300	9.65	480	4.88
360	10.53	600	3.74
420	11.25	900	2.55
540	12.32	1200	1.95
660	13.42	1500	1.70
780	13.9	1800	1.47
900	14.03	2400	1.14
1200	13.79		
1500	13.54		
1800	13.34		
2400	13.12		
3000	13.29		
3600	13.55		
5400	13.49		
7200	13.51		

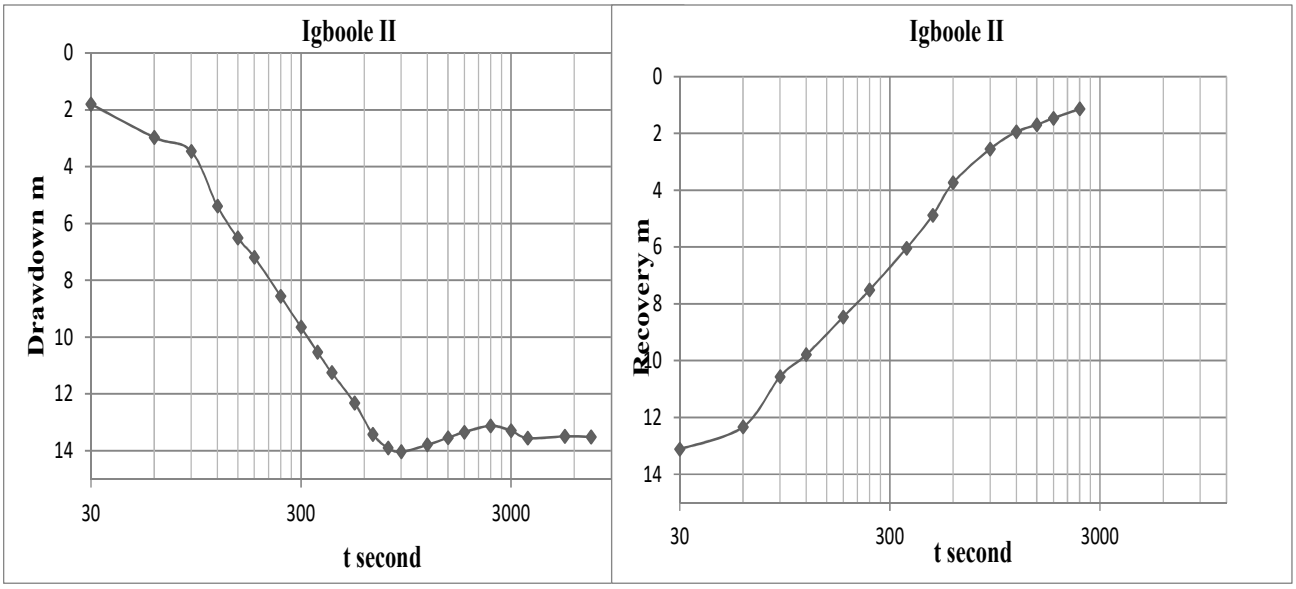

BOREHOLE LOCATION 06: ISALE AJEGUNLE –IGBOORA

LONGITUDE: 7 26 26.2
LATITUDE: 3 16 44.0
ELEVATION: 159m
PRE-TEST STATIC WATER LEVEL: 1.46/1.45m
DEPTH OF WELL: 18.85m/62.21ft.
DEPTH OF PUMP INSTALLATION: 14.55m/48FT.

t seconds	drawdown (m)	t seconds	recovery m
0	0	0	8.50
30	1.80	30	6.50
60	3.10	60	5.85
90	4.86	90	5.18
120	4.85	120	4.75
150	5.03	180	4.13
180	5.50	240	3.63
240	5.95	360	3.18
300	6.48	480	2.95
360	6.58	600	2.66
420	6.74	900	2.14
480	6.98	1200	1.97
600	7.30	1500	1.80
720	7.32	1800	1.65
900	6.70	2400	1.48
1200	6.76		
1500	6.99		
1800	7.18		
2400	7.53		
3000	7.73		
3600	7.95		
4200	8.05		
4800	8.21		
5400	8.28		
6600	8.35		
7800	8.50		

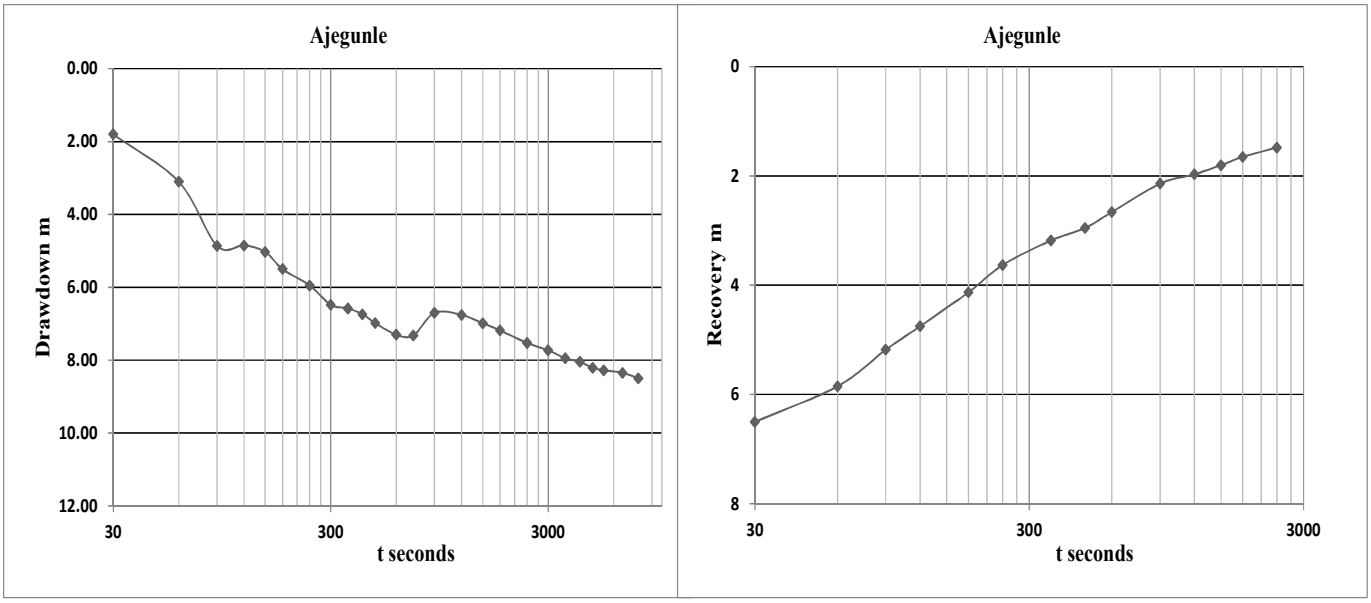
Ajegunle
Drawdown m
0.00
2.00
4.00
6.00
8.00
10.00
12.00
30
300
3000
t seconds
Ajegunle
Recovery m
0
2
4
6
8
30
300
3000
t seconds

BOREHOLE LOCATION 07: ITAAGBE -IGBOORA-

LONGITUDE: 7 26 19.2
LATITUDE: 3 16 57.4
ELEVATION: 172m
PRE-TEST STATIC WATER LEVEL: 10.5/10.45m
DEPTH OF WELL: 27.7m/91.4ft.
DEPTH OF PUMP INSTALLATION: 21.82m/72FT.

t second	drawdown (m)	t second	Recovery m
0	0	0	11.49
30	2.25	30	11.19
60	3.78	60	9.41
90	5.71	90	8.59
120	6.17	120	7.83
150	7.19	150	6.89
180	7.92	180	5.92
240	9.30	240	5.00
300	10.35	360	3.70
360	10.95	480	3.12
420	11.00	600	2.29
540	11.25	900	0.79
660	11.44	1200	0.31
780	11.45	1500	0.15
900	11.49		

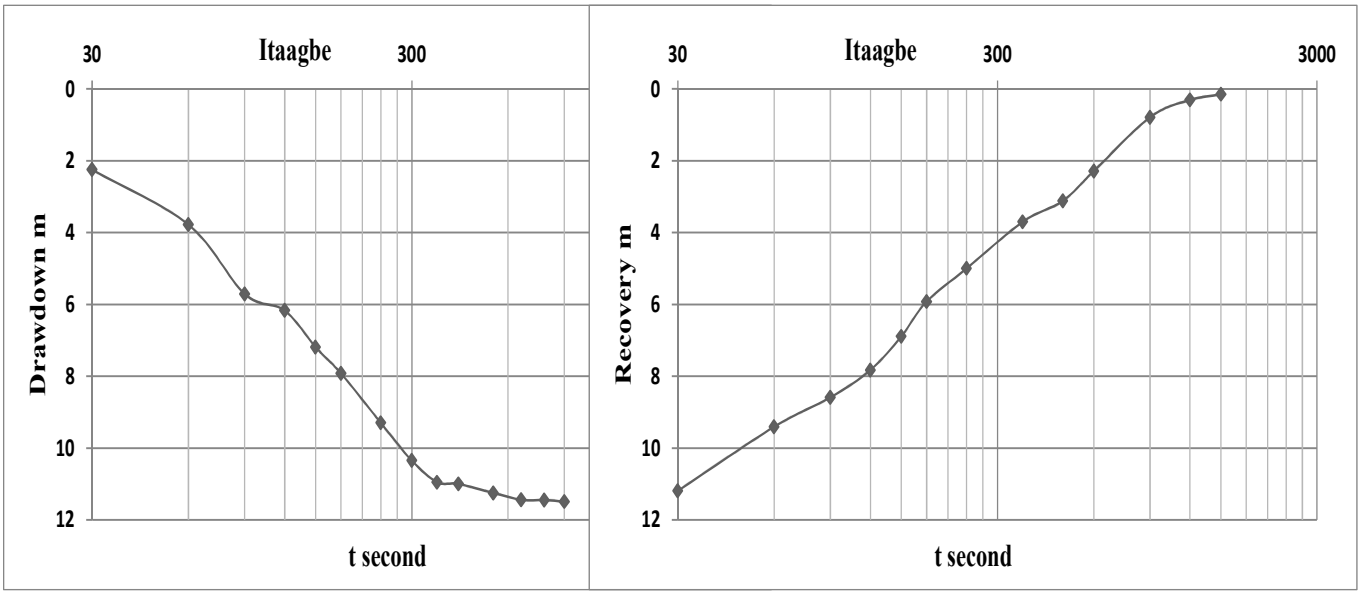

BOREHOLE LOCATION 08: ALAAGBA I

DATE: 16-11-2011
LONGITUDE: 7 32 18.4
LATITUDE: 3 07 35.7
ELEVATION: 174m
PRE-TEST STATIC WATER LEVEL: 5.3m/4.15m
DEPTH OF WELL: 43m/142ft.
DEPTH OF PUMP INSTALLATION: 37.9m/125FT.

t second	drawdown (m)	t second	Recovery m
0	0	0	31.90
30	2.0	30	29.93
60	5.0	60	29.86
90	6.3	360	29.5
120	7.8	660	29.13
150	9.9	1260	28.71
180	13.3	3060	27.41
240	16.3	4860	25.05
300	18.9	6660	22.76
360	21.6	8460	20.86
420	24.0	10260	19.4
540	25.7	10800	18.85
660	28.7		
780	28.7		
900	29.7		
1200	31.9		

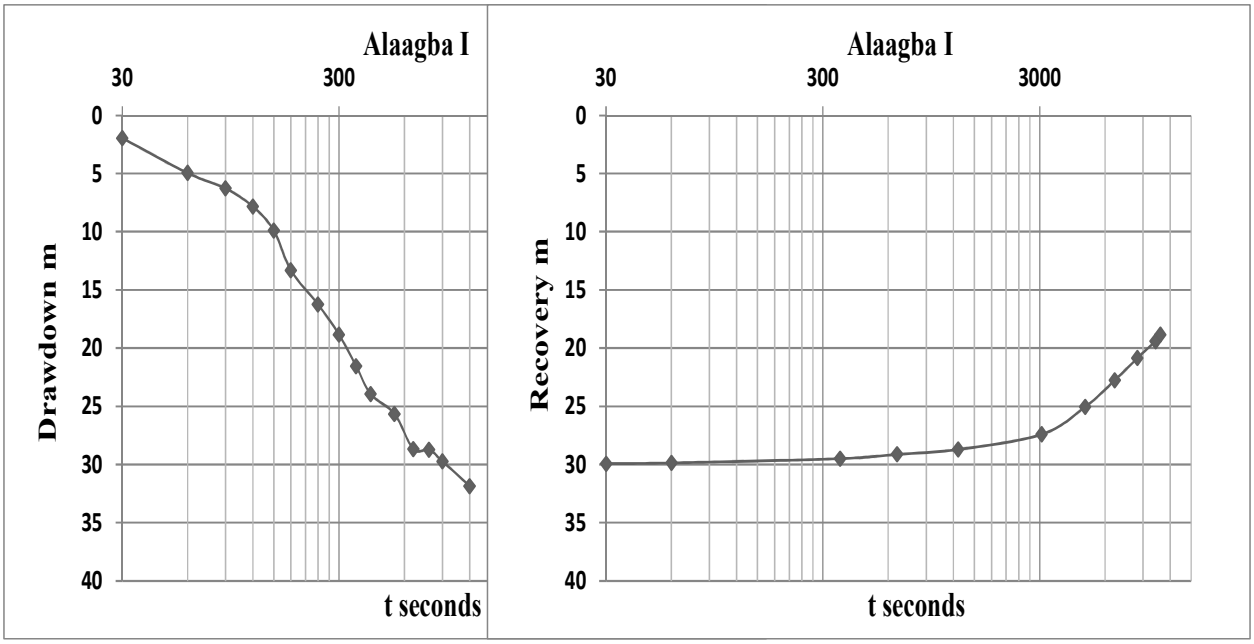

BOREHOLE LOCATION 09: ALAAGBA II

DATE: 16-11-2011
LONGITUDE: 7 32 20.2
LATITUDE: 3 07 35.1
ELEVATION: 164m
PRE-TEST STATIC WATER LEVEL: 2.9m
DEPTH OF WELL: 99.5m/328ft.
DEPTH OF PUMP INSTALLATION: 40m/132FT.

t seconds	drawdowns m	t seconds	Recovery m
0	0	0	33.50
30	1.56	30	27.66
60	3.4	1200	25.32
90	5.13	2400	21.4
120	6.47	3600	18.25
150	7.47	4800	14.95
180	8.19	6000	10.62
240	10.89		
300	13.14		
360	14.4		
420	15.44		
540	20.11		
660	21.7		
780	24.66		
900	27.66		
1200	33.5		

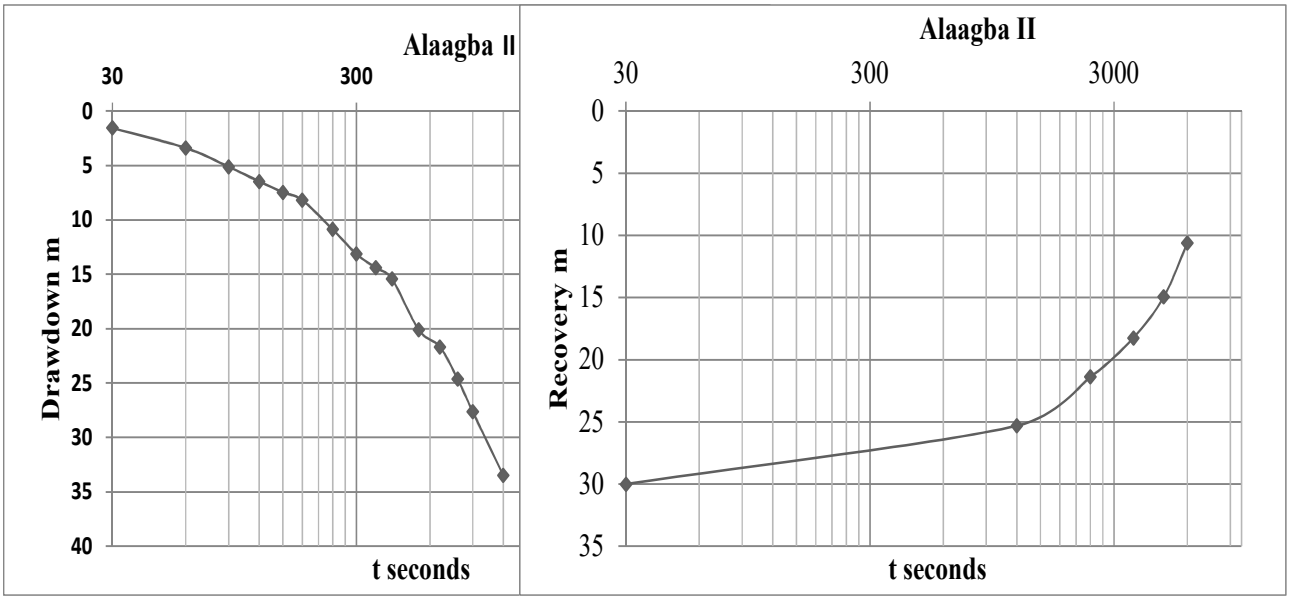

BOREHOLE LOCATION 10: LAMPERU VILLAGE

LONGITUDE: 7 30 40.8

LATITUDE: 3 09 05.4

ELEVATION: 169m

PRE-TEST STATIC WATER LEVEL: 6.68m/6.05m

DEPTH OF WELL: 30.85m/101.8ft.

DEPTH OF PUMP INSTALLATION: 25.5m/84FT.

t seconds	Drawdown (m)
0	0
30	1.81
60	3.96
90	5.84
120	7.35
150	9.08
180	10.55
240	13.05
300	15.22
360	17.51
420	19.32

t seconds	Recovery m
0	19.32
30	19.28
60	18.82
90	18.37
120	17.84
150	17.53
180	17.27
240	16.37
360	15.08
480	14.43
600	13.39
900	11.27
1200	8.91
1800	5.92
2400	4.43
3000	3.31
3600	2.35
4200	1.77
4800	1.52

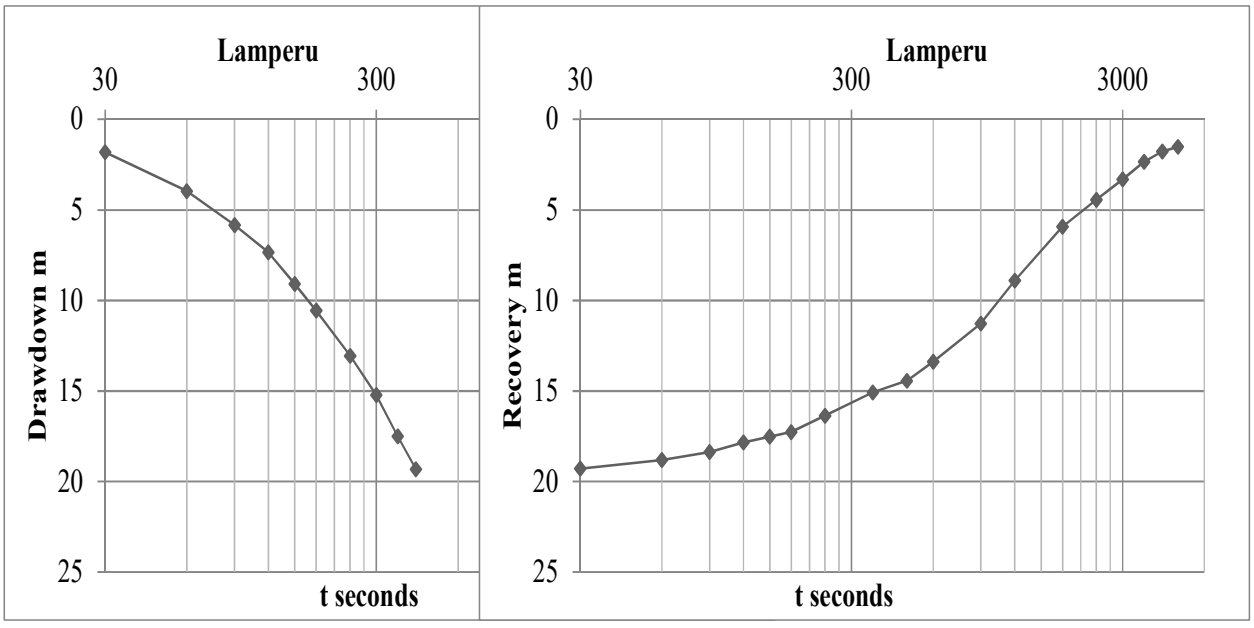

BOREHOLE LOCATION 11: ABOLA VILLAGE

LONGITUDE: 7 29 57.0
LATITUDE: 3 09 34.7
ELEVATION: 171m
PRE-TEST STATIC WATER LEVEL: 14.58m/14.47m
DEPTH OF WELL: 34.13m/112.6ft.
DEPTH OF PUMP INSTALLATION: 29.5m/97.4FT.

t seconds	drawdown m	t seconds	Recovery m
0	0	0	14.82
30	0.84	30	14.35
60	3.12	60	13.68
90	4.19	90	12.89
120	5.05	120	12.74
150	5.88	150	12.33
180	6.39	180	11.96
240	7.70	240	11.53
300	8.66	360	11.13
360	9.71	480	10.13
420	10.62	600	9.29
540	12.05	900	7.42
660	12.95	1200	5.62
780	13.76	1800	3.70
900	14.28	2400	2.78
1200	14.89	3000	2.27
1500	14.90		
1800	14.90		
2400	14.82		
3000	14.82		
3600	14.82		
4800	14.82		

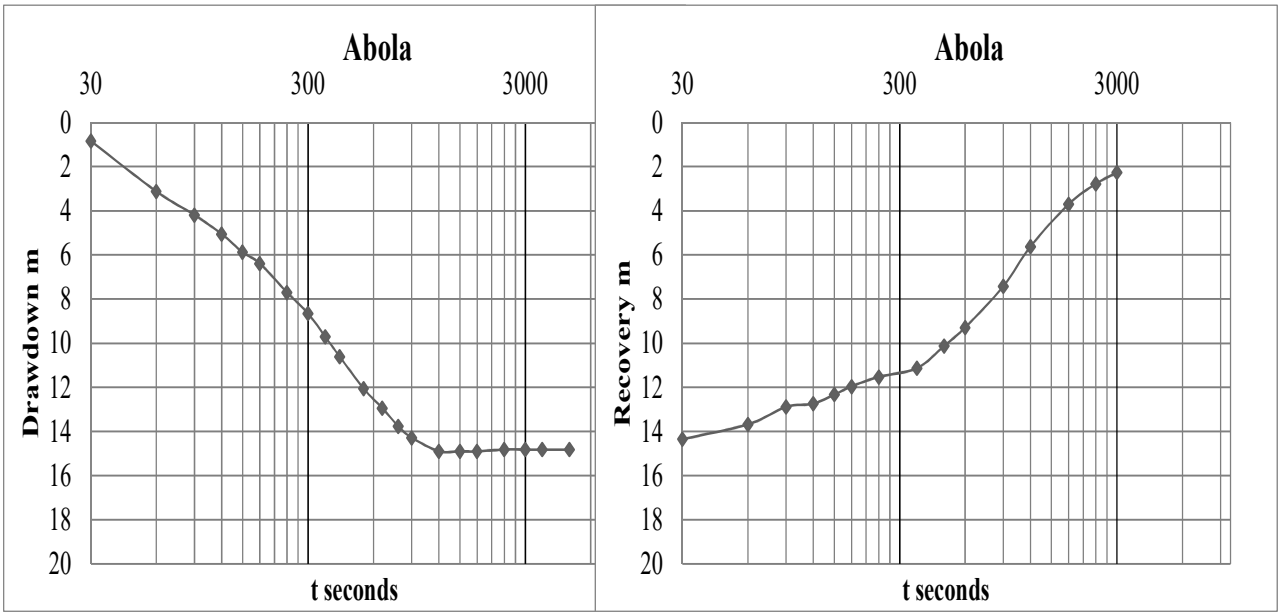

BOREHOLE LOCATION 12: APATA VILLAGE

LONGITUDE: 7 23 40.2
LATITUDE: 3 11 02.4
ELEVATION: 139m
PRE-TEST STATIC WATER LEVEL: 9.4m/8.55m
DEPTH OF WELL: 38m/125.4FT
DEPTH OF PUMP INSTALLATION: 31m/102FT.

t seconds	drawdowns m	t seconds	Recovery m
0	0	0	22.38
30	1.62	30	21.78
60	2.82	60	21.18
90	4.1	90	20.83
120	5.18	120	20.49
150	5.88	150	20.19
180	7.01	180	19.91
240	8.4	240	19.61
300	9.79	360	18.51
360	10.76	480	17.96
420	11.47	600	17.15
540	13.07	900	15.04
660	15.12	1200	13.3
780	15.15	1500	12.09
900	15.7	1800	11.13
1200	18.61	2400	9.4
1500	19.95	3000	7.85
1800	20.82		
2400	21.85		
3000	22.3		
3600	22.37		
4200	22.37		
4800	22.38		
5400	22.38		
6000	22.38		
6600	22.38		
7200	22.38		

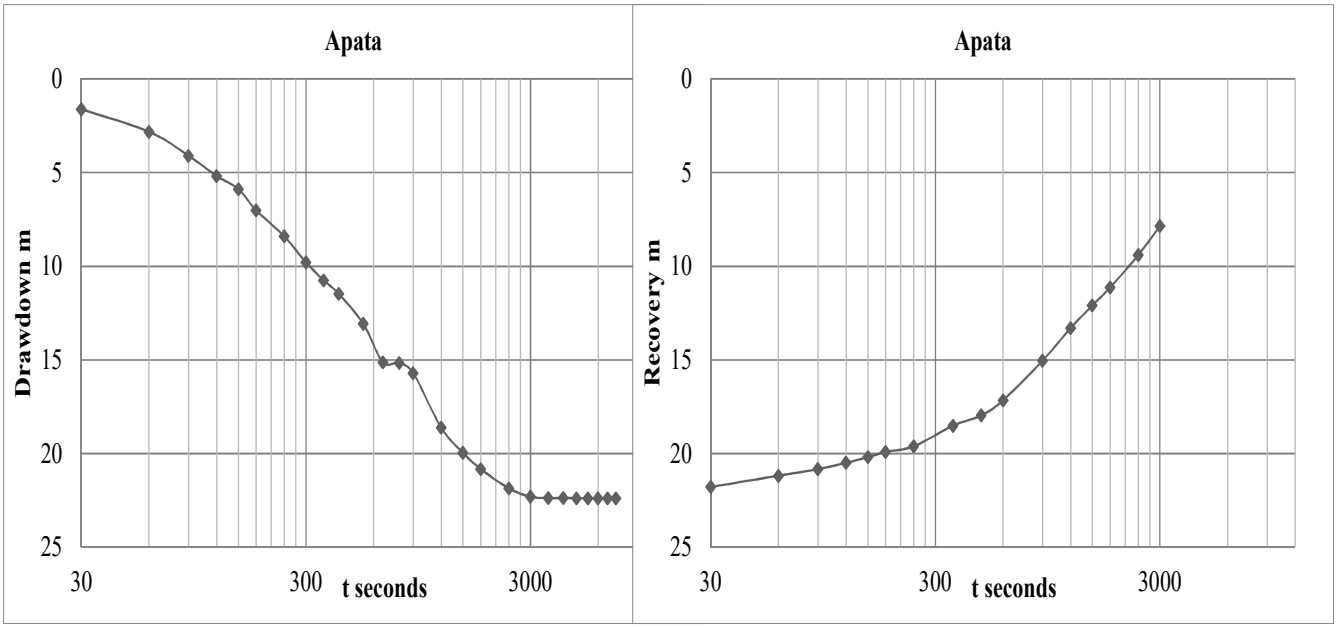
Apata
Drawdown m
0
5
10
15
20
25
30
300
3000
t seconds
Apata
Recovery m
0
5
10
15
20
25
30
300
3000
t seconds

BOREHOLE LOCATION 13: AGBEDE

LONGITUDE: 7 23 57.2
LATITUDE: 3 11 55.0
ELEVATION: 143m
PRE-TEST STATIC WATER LEVEL: 6.42m/6.52m
DEPTH OF WELL: 34.6m/114.2FT
DEPTH OF PUMP INSTALLATION: 25.5m/84FT.

t second	drawdown (m)	t seconds	Recovery m
0	0	0	10.03
30	1.4	30	6.26
60	3	60	4.68
90	4.37	90	3.82
120	5.53	120	3.23
150	6.18	180	2.51
180	6.55	240	2.21
240	7.52	360	1.71
300	8.22	480	1.38
360	8.32	600	1.22
420	8.36		
540	8.64		
660	8.82		
780	8.92		
900	9.02		
1200	9.25		
1500	9.45		
1800	9.56		
2400	9.67		
3000	9.73		
3600	9.80		
4200	9.86		
4800	9.90		
5400	9.95		
6000	9.98		
6600	10.03		
7200	10.03		

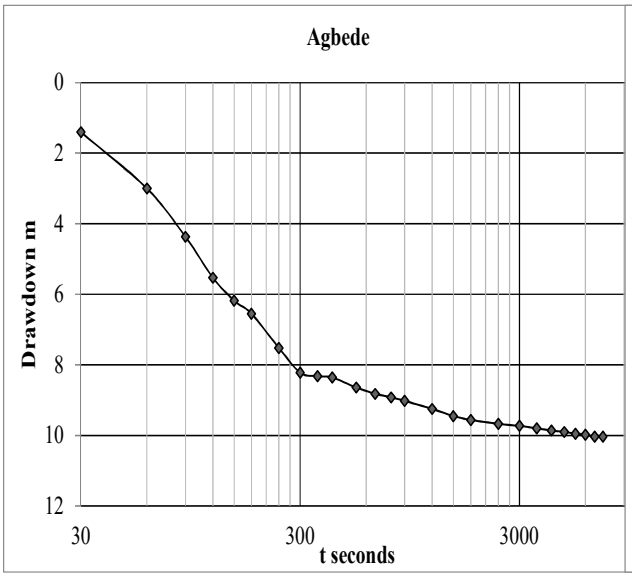

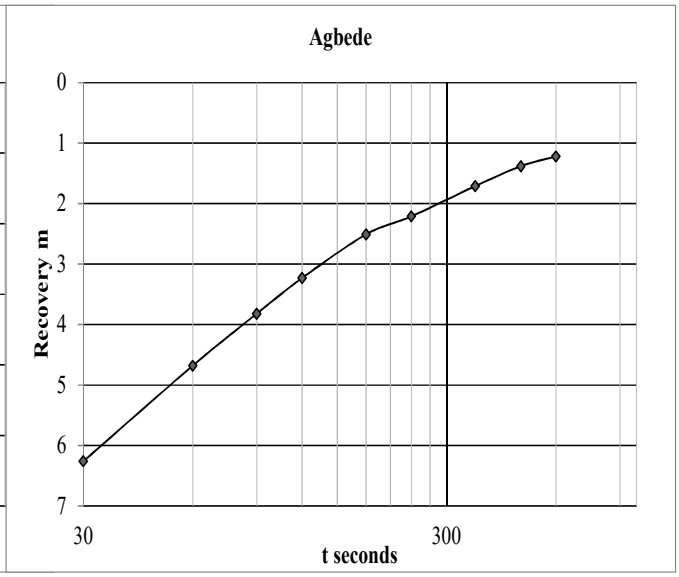

BOREHOLE LOCATION 14: ALABI-OJA

LONGITUDE: 7 35 56.2
LATITUDE: 3 18 07.6
ELEVATION: 188m
PRE-TEST STATIC WATER LEVEL: 3.27m
DEPTH OF WELL: 26.36m/87FT
DEPTH OF PUMP INSTALLATION: 21.8m/72FT.

t seconds	drawdowns m	t seconds	Recovery m
0	0	30	18.63
30	0.88	180	12.57
60	3.53	360	5.6
90	9.11	540	3.46
120	12.28	840	1.76
150	13.86	1140	1.07
180	14.66	1440	0.93
240	16.33	2040	0.6
300	17.53	2640	0.46
360	17.43		
420	17.65		
540	18.43		
660	18.63		
780	18.67		
900	18.63		

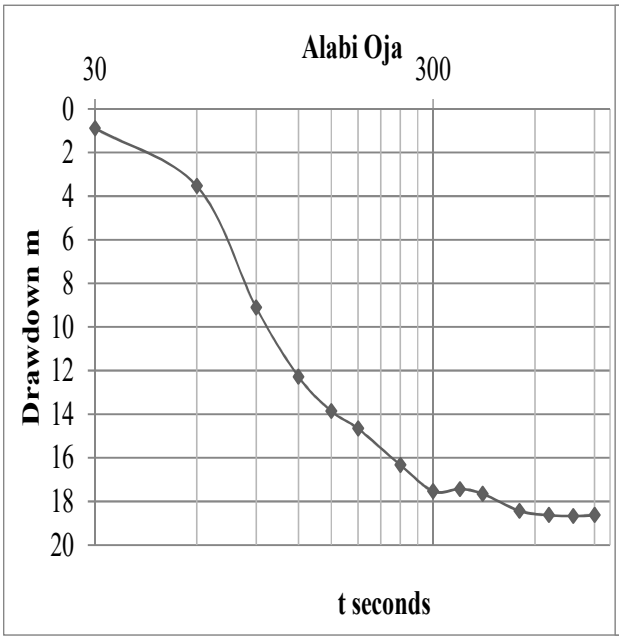

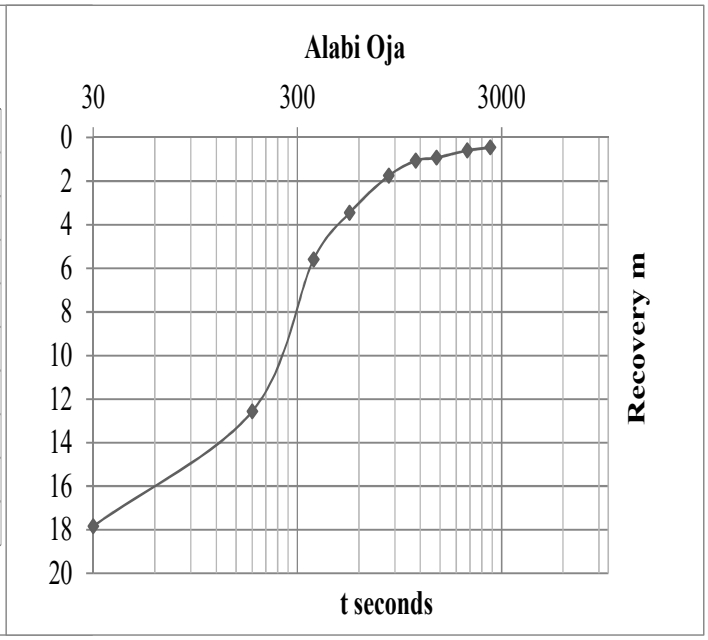

BOREHOLE LOCATION 15: SEKERE- Igboora

LONGITUDE: 7 21 59.0

LATITUDE: 3 18 33.5

ELEVATION: 142m

PRE-TEST STATIC WATER LEVEL: 7.05m

DEPTH OF WELL: 29.1m/96FT

DEPTH OF PUMP INSTALLATION: 25.5m/84FT.

T seconds	Drawdowns m	t seconds	Recovery m
0	0	0	18.7
30	2.2	30	18.2
60	4.5	60	17.7
90	6.7	90	17.1
120	10.0	120	16.6
150	11.9	180	15.9
180	12.8	240	15.3
240	15.8	360	14.4
300	17.9	480	13.8
360	18.7	600	13.4
		900	11.8
		1200	10.0
		1800	7.4
		3600	4.5
		5400	2.7
		7200	1.6

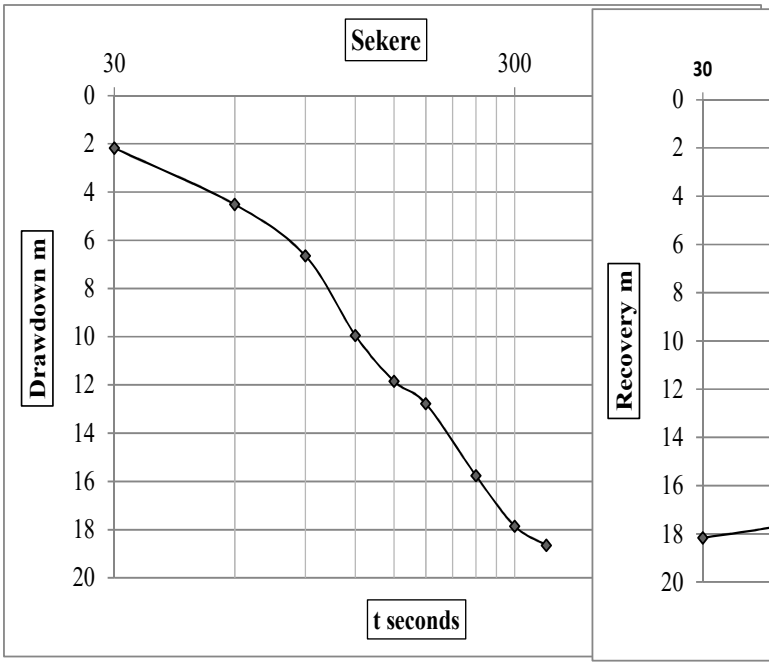

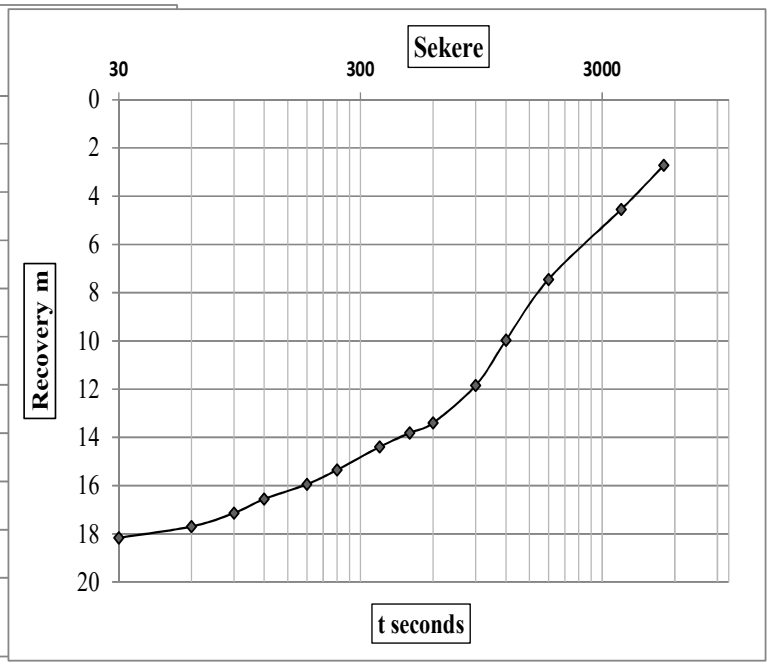

BOREHOLE LOCATION 16: Apata-Faju- Igboora

LONGITUDE: 7 27 23.5
LATITUDE: 3 19 33.3
ELEVATION: 182m
PRE-TEST STATIC WATER LEVEL: 4.2m
DEPTH OF WELL: 29.72m/98FT
DEPTH OF PUMP INSTALLATION: 25.5m/84FT.

t seconds	Drawdowns m	t seconds	Recovery m
0	0	0	21.23
30	5.2	30	20.2
60	6.3	60	19.48
90	7.8	90	18.85
120	9.4	120	18.02
150	11.81	150	17.55
180	13.9	180	16.85
240	16.6	240	15.80
300	19.43	300	14.80
360	21.23	360	13.77
		480	12.69
		600	11.34
		900	8.60
		1200	6.10
		3000	1.65
		4800	0.62
		6600	0.18

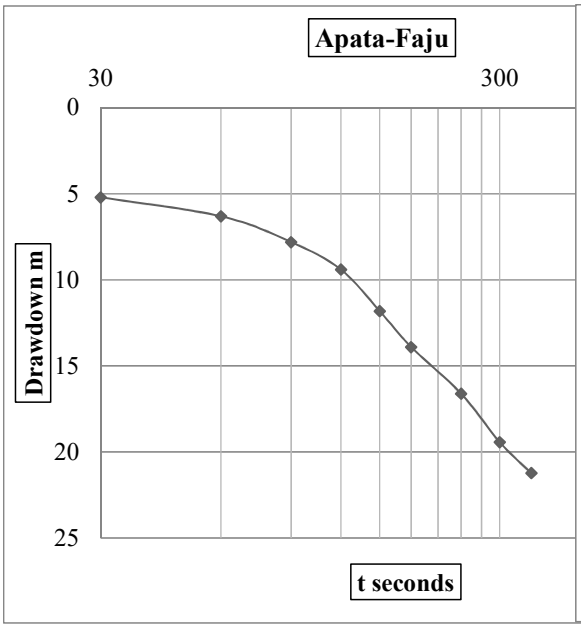

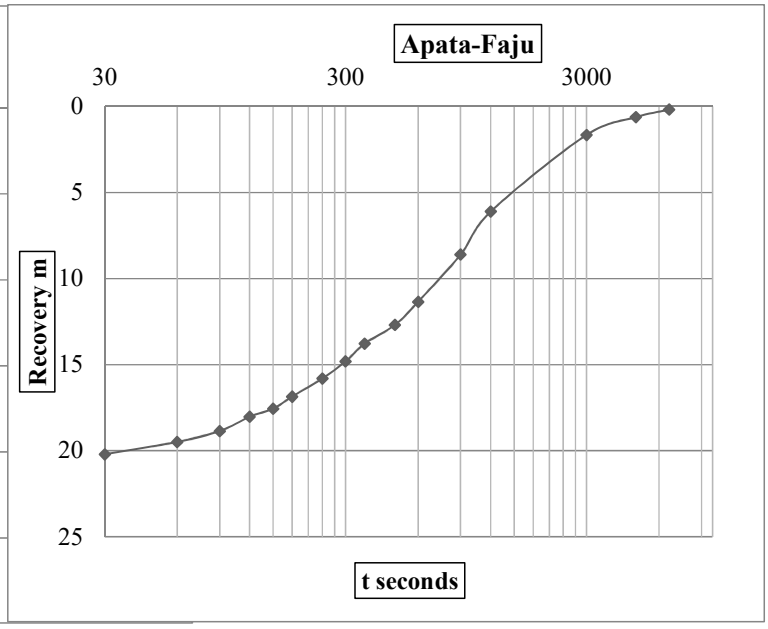

BOREHOLE LOCATION 17: Tobalogbo

LONGITUDE: 7 32 09.0
LATITUDE: 3 16 52.3
ELEVATION: 188m
PRE-TEST STATIC WATER LEVEL: 3.5/2.77m
DEPTH OF WELL: 17.8m/58.7FT
DEPTH OF PUMP INSTALLATION: 14.5m/48FT.

t seconds	Drawdowns m	t seconds	Recovery m
0	0	0	11.49
30	0.58	30	11.28
60	3.73	60	10.62
90	5.32	90	10.41
120	7.24	120	10.13
150	8.5	180	9.74
180	10.83	240	9.30
240	11.49	360	8.65
		480	8.13
		600	7.79
		900	6.63
		1200	5.25
		1800	3.51
		2400	2.23
		3600	0.92

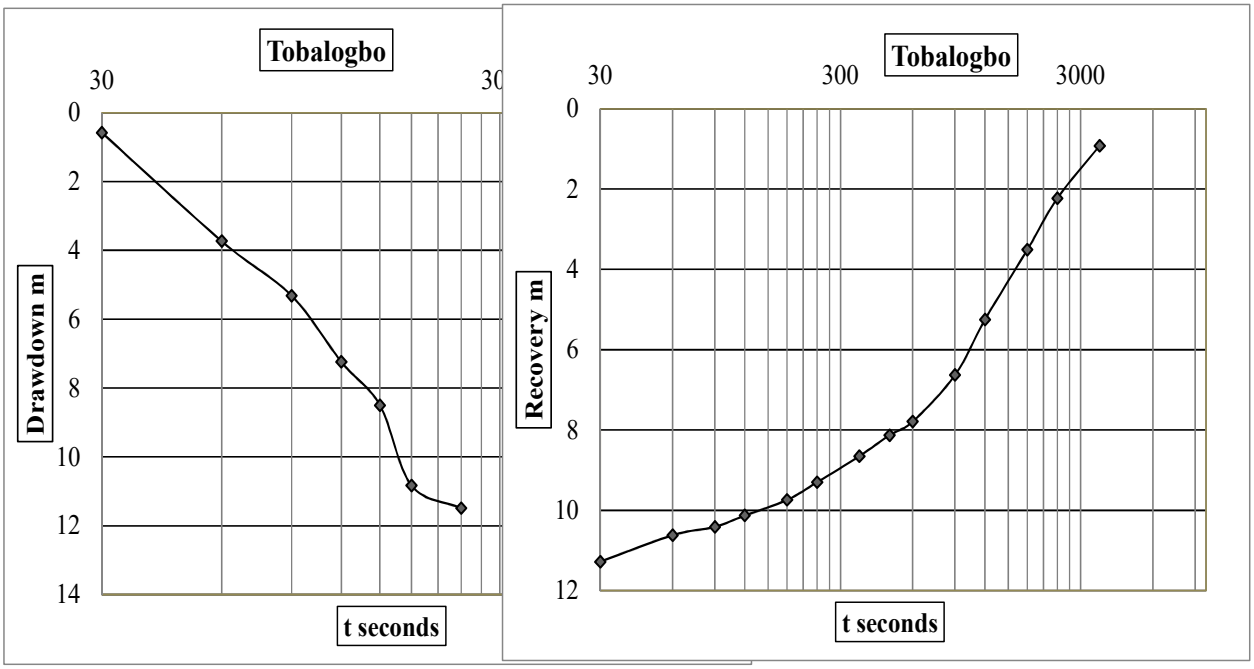

BOREHOLE LOCATION 18: KONDO

LONGITUDE: 7 34 40.6
LATITUDE: 3 18 34.1
ELEVATION: 199m
PRE-TEST STATIC WATER LEVEL:11.83m/10.60m
DEPTH OF WELL: 35.6m/117.5FT
DEPTH OF PUMP INSTALLATION: 29m/96FT.

t seconds	Drawdowns m	t seconds	Recovery m
0	0	0	18.40
30	1.8	30	17.99
60	4.4	60	15.83
90	5.2	90	15.60
120	6.6	120	13.80
150	8.0	180	12.65
180	9.0	240	11.81
240	10.7	360	10.58
300	12.2	480	9.76
360	13.6	600	9.17
420	15.1	900	7.97
540	18.2	1200	7.01
660	18.4	1800	5.53
		2400	4.63
		3000	3.71
		3600	3.63

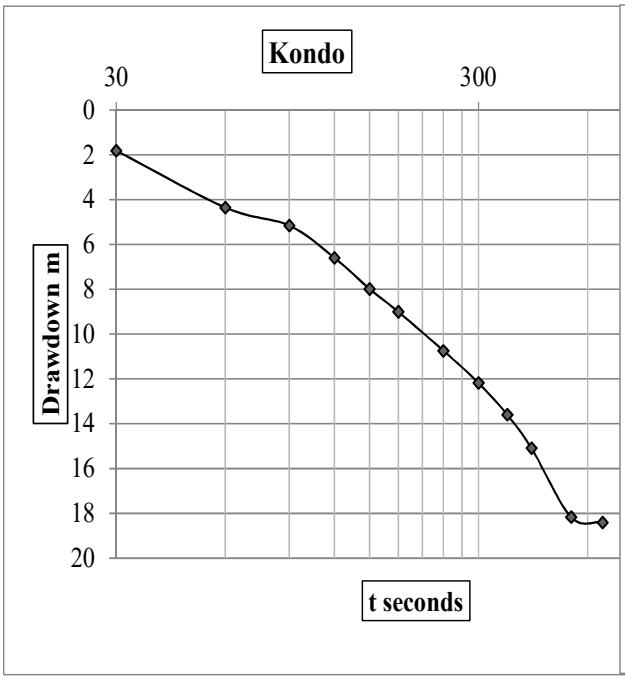

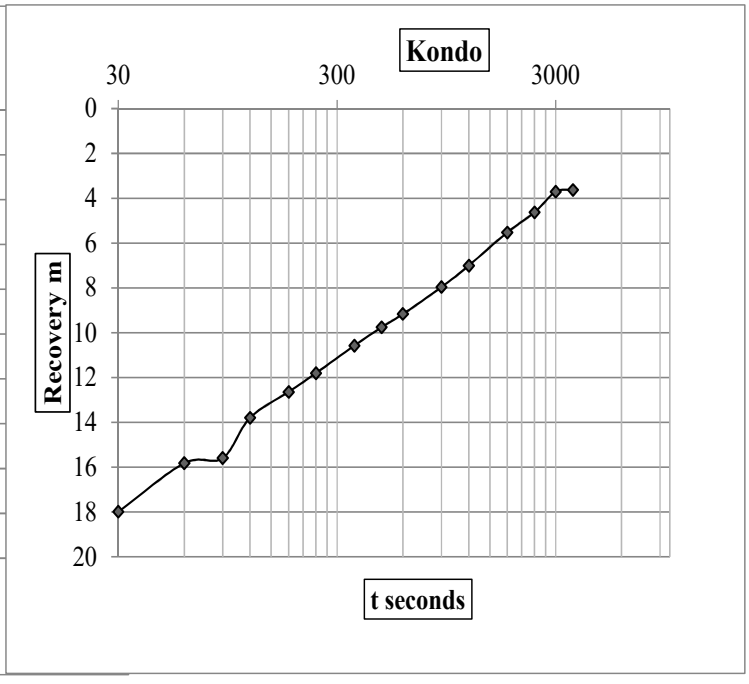

BOREHOLE LOCATION 19: AYETE I

LONGITUDE: 7 32 22.5
LATITUDE: 3 13 18.1
ELEVATION: 141m
PRE-TEST STATIC WATER LEVEL: 1.05m
DEPTH OF WELL: 28m/92FT
DEPTH OF PUMP INSTALLATION: 25.9m/85FT.

t seconds	Drawdowns m	t seconds	Recovery m
0	0	0	19.70
30	0.85	30	18.85
60	1.95	60	16.95
90	2.45	90	16.25
120	2.66	120	15.73
150	3.05	180	14.55
180	3.35	240	13.55
210	3.65	300	12.78
240	3.9	420	11.22
270	4.28	540	10.11
300	4.37	660	9.27
360	5.05	960	7.65
420	5.70	1260	6.60
480	6.16	1560	5.93
540	6.50	2160	4.95
600	6.66	2760	4.05
720	7.85	4560	2.70
840	8.48		
960	8.87		
1080	9.30		
1200	9.65		
1500	11.20		
1800	11.65		
2400	13.13		
3000	13.89		
3600	14.00		
5400	14.70		
7200	15.75		
9000	16.10		
10800	19.70		

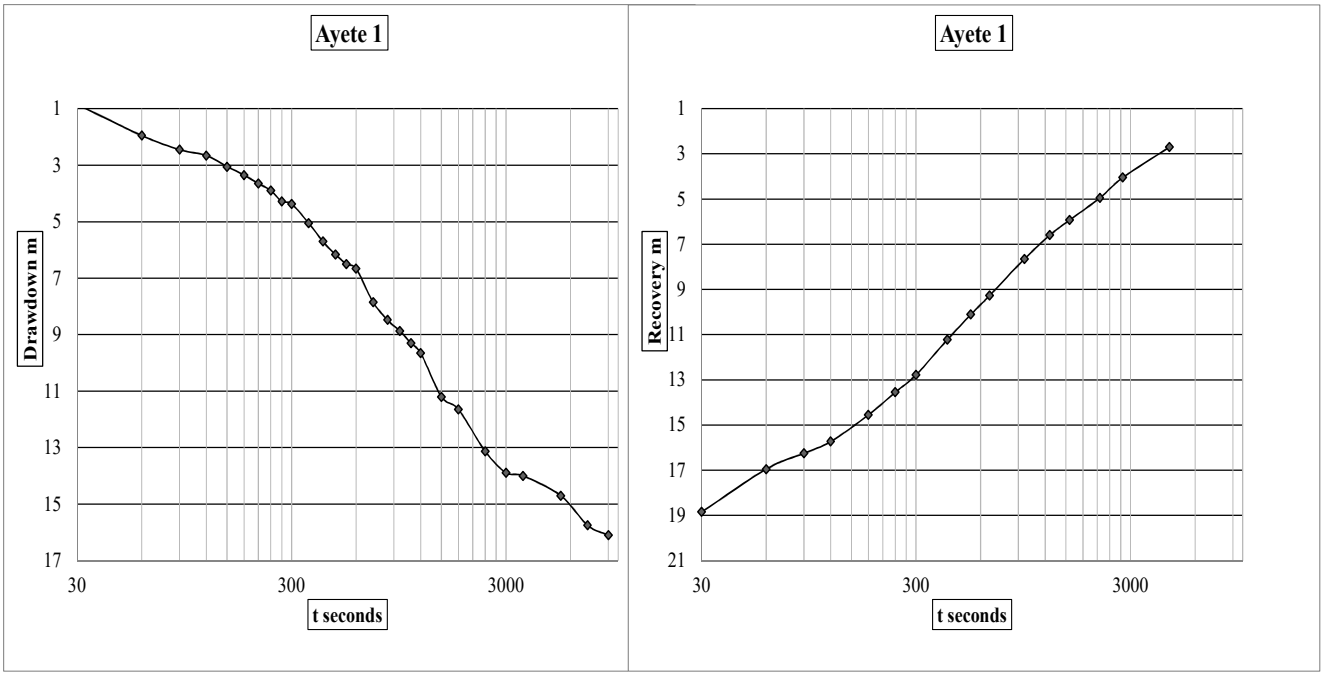
Ayete 1
Drawdown m
1
3
5
7
9
11
13
15
17
30
300
3000
t seconds
Ayete 1
Recovery m
1
3
5
7
9
11
13
15
17
19
21
30
300
3000
t seconds

BOREHOLE LOCATION 20: AYETE II

LONGITUDE: 7 31 55.0
LATITUDE: 3 13 19.8
ELEVATION: 140m
PRE-TEST STATIC WATER LEVEL: 3.65/3.45m
DEPTH OF WELL: 27.85m/92FT
DEPTH OF PUMP INSTALLATION: 23m/77FT.

t seconds	Drawdowns m	t seconds	Recovery m
0	0	0	19.91
30	2.39	30	19.29
60	4.43	60	19.04
90	7.22	90	18.68
120	8.85	120	18.33
180	14.2	180	17.88
240	17.48	240	17.42
300	19.1	360	16.94
360	19.91	480	16.18
		600	15.53
		900	14.02
		1200	12.33
		1800	9.65
		2400	8.46
		3000	7.00
		3600	5.86
		4800	4.01
		6000	2.89
		7200	2.19

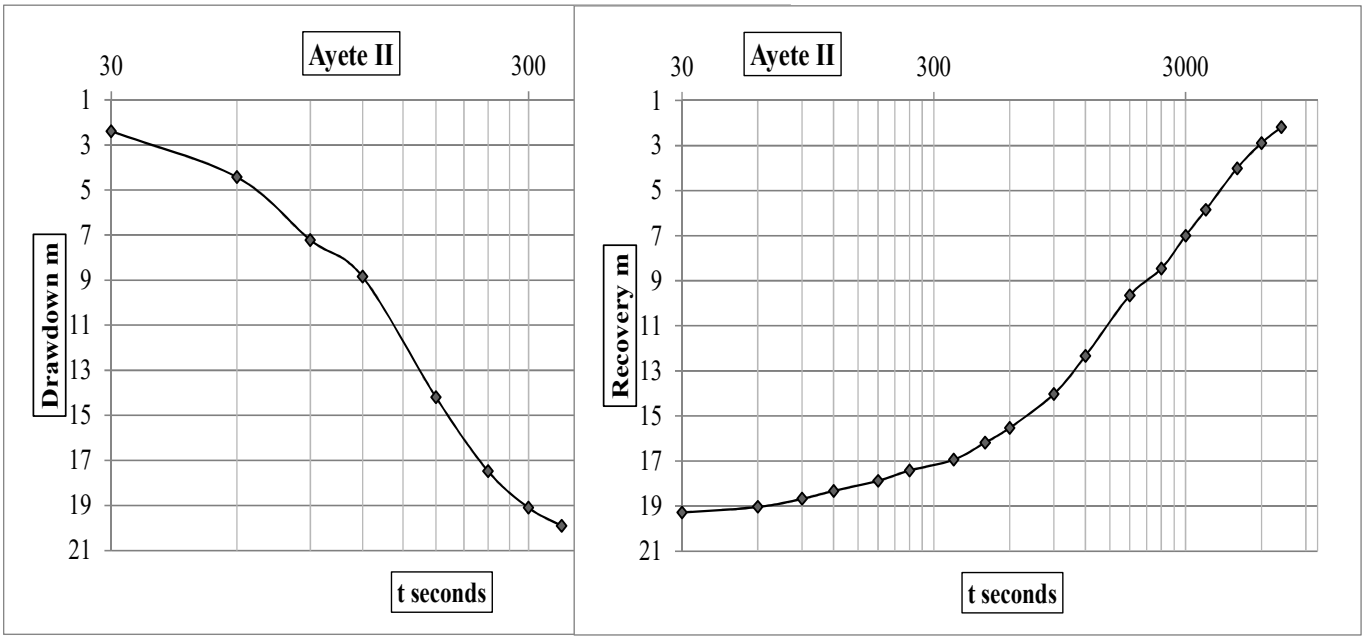

BOREHOLE LOCATION 21: TAPA

LONGITUDE: 7 33 53.1
LATITUDE: 3 13 48.0
ELEVATION: 155m
PRE-TEST STATIC WATER LEVEL: 2.96m
DEPTH OF WELL: 36.5m/120FT
DEPTH OF PUMP INSTALLATION: 25m/84FT.

t seconds	Drawdowns m	t seconds	Recovery m
0	0	0	22.04
30	3.15	30	21.00
60	6.91	180	18.40
90	9.64	240	16.08
120	12.14	300	14.18
150	12.94	360	12.72
180	14.04	480	10.37
210	14.14	600	9.60
240	14.86	900	6.50
270	16.56	1200	4.23
300	20.34	1500	2.87
420	21.54	2100	1.37
540	22.04	3300	0.16

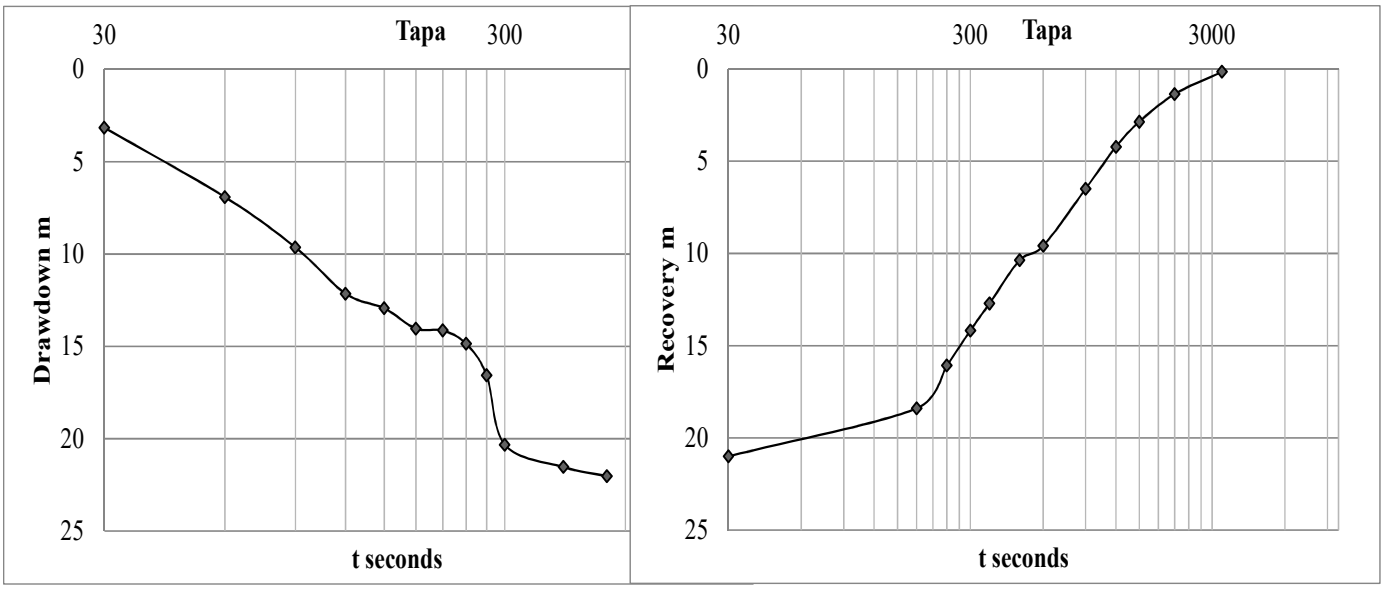

BOREHOLE LOCATION 22: IDERE I

LONGITUDE: 7 29 54.5

LATITUDE: 3 14 24.3

ELEVATION: 215m

PRE-TEST STATIC WATER LEVEL: 5.32m

DEPTH OF WELL: 20.3m

DEPTH OF PUMP INSTALLATION: 14.6m/48FT.

t seconds	Drawdowns m	t seconds	Recovery m
0	0	0	9.27
30	1.63	30	9.07
60	3.05	60	8.9
90	4.42	90	8.75
120	4.88	120	8.64
150	5.33	180	8.39
180	5.78	240	8.13
240	6.33	360	7.83
300	9.27	480	7.56
		600	7.14
		900	6.28
		1200	5.95
		2400	5.37
		3600	4.24
		4800	2.93
		6000	1.91
		7200	1.18

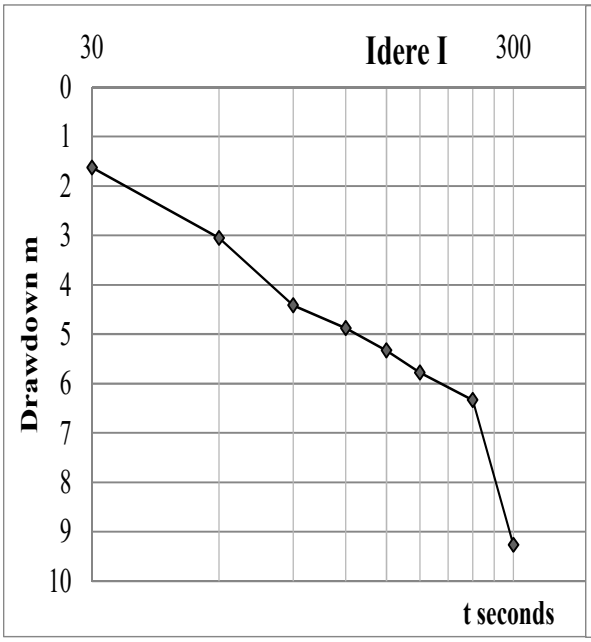

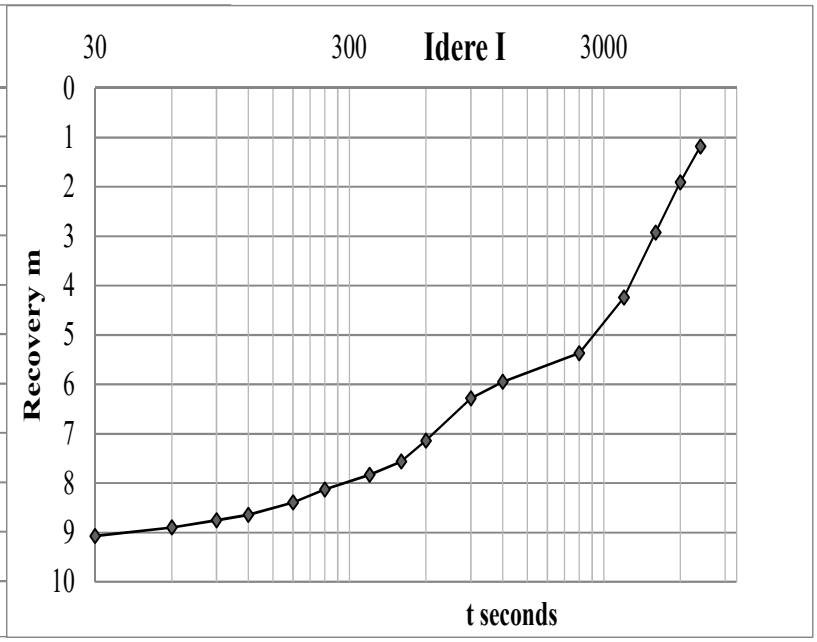

BOREHOLE LOCATION 23: IDERE II

LONGITUDE: 7 29 52.0

LATITUDE: 3 14 22.5

ELEVATION: 209m

PRE-TEST STATIC WATER LEVEL: 6.48m

DEPTH OF WELL: 15.86m

DEPTH OF PUMP INSTALLATION: 11.9m/39FT.

t seconds	Drawdowns m	t seconds	Recovery m
0	0	0	7.00
30	1.7	30	6.58
60	3.3	60	6.28
90	5.3	90	6.27
120	7.0	120	6.12
		180	6.26
		240	4.02
		360	1.77
		480	1.43
		600	1.1
		900	0.52
		1200	0.35
		1800	0.25
		2400	0.2
		3000	0.17